PSYCHEDELIC EFFECTS ON SPATIAL ENCODING IN THE MOUSE RETROSPLENIAL CORTEX

VICTORITA ELENA IVAN
Bachelor of Science, University of Medicine and Pharmacy "Grigore T. Popa", Iasi, Romania, 2013

A thesis submitted
in partial fulfilment of the requirements for the degree of

DOCTOR OF PHILOSOPHY

in

NEUROSCIENCE

Department of Neuroscience
University of Lethbridge
LETHBRIDGE, ALBERTA, CANADA

PSYCHEDELIC EFFECTS ON SPATIAL ENCODING IN THE MOUSE RETROSPLENIAL CORTEX

VICTORITA ELENA IVAN

Date of Defence: 15 August, 2024

Dr. Aaron Gruber Thesis Supervisor	Professor	Ph.D.
Dr. Robert Sutherland Thesis Examination Committee Member	Professor	Ph.D.
Dr. David Euston Thesis Examination Committee Member	Associate Professor	Ph.D.
Dr. Robbin Gibb Internal External Examiner	Professor	Ph.D.
Dr. Matt van der Meer External Examiner Dartmouth College, Hanover, NH, USA	Associate Professor	Ph.D.
Dr. Ian Whishaw Chair, Thesis Examination Committee	Professor	Ph.D.

DEDICATION

To my sister Irina,

The strongest, most amazing woman I know, who always believed I can do anything I set my mind to. This thesis and all the work I did during my graduate journey would not have been possible without her unwavering support.

Multumesc! Te iubesc!

ABSTRACT

Psychedelics are psychoactive substances that evoke a characteristic set of mental phenomena that include altered psychological experiences, unstable moods, and perceptual distortions. These hallucinogens provide a means to study brain function. Analyzing their functional effects on neural activity can provide us with important data about their effects on information encoding. The retrosplenial cortex (RSC) is an excellent target to study the effects of psychoactive drugs because it is a hub that integrates and coordinates the activity of distinct brain regions that mediate cognitive processes. The present work indicates that two different psychedelics (psilocybin and ibogaine) have similar short-term effects on neural encoding of spatial position in the RSC. The data indicate that psychedelics disrupt the brain's process of internally keeping track of position. Furthermore, the RSC exhibited a reduction in the signal to noise ratio of the spatial encoding with chronic amphetamine. Ibogaine administration did not ameliorate this deficit. The data presented in this doctoral thesis are among the first to suggest that cognitive maps are disrupted by psychedelic compounds.

CONTRIBUTIONS OF AUTHORS

The authors and their contributions for the main chapters of this thesis are listed below.

CHAPTER 2: *Psilocybin reduces functional correlation and the encoding of spatial information by neurons in mouse retrosplenial cortex* – submitted to European Journal of Neuroscience, 2024
Authors: Victorita E. Ivan, David P. Tomàs-Cuesta, Ingrid M. Esteves, Artur Luczak, Majid Mohajerani, Bruce L. McNaughton, Aaron J. Gruber
Author Contributions: V.E.I. and A.J.G. designed research, V.E.I. and I.M.E. performed research, M.M. contributed tools, V.E.I., D.P.T-C, and I.M.E. analyzed data, V.E.I., D.P.T-C, A.L., B.L.M., and A.J.G. wrote the paper.

CHAPTER 3: *The non-classic psychedelic ibogaine disrupts cognitive maps* – published in Ivan et al., 2023
Authors: Victorita E. Ivan1, David P. Tomàs-Cuesta1, Ingrid M. Esteves1, Davor Curic, Majid Mohajerani, Bruce L. McNaughton, Joern Davidsen, Aaron J. Gruber
Author Contributions: V.E.I. and A.J.G. designed research, V.E.I. and I.M.E. performed research, M.M. contributed tools, V.E.I., D.P.T-C, and I.M.E. analyzed data, V.E.I., D.P.T-C, A.L., B.L.M., and A.J.G. wrote the paper.

CHAPTER 4: *The spatial encoding in mouse retrosplenial cortex is degraded by repeated amphetamine administration and resistant to psychedelic remediation*
Authors: Victorita E. Ivan, David P. Tomàs-Cuesta, Ingrid M. Esteves, Majid Mohajerani, Bruce L. McNaughton, Aaron J. Gruber
Author Contributions: V.E.I. and A.J.G. designed research, V.E.I. and I.M.E. performed research, M.M. contributed tools, V.E.I., D.P.T-C, and I.M.E. analyzed data, V.E.I., D.P.T-C, B.L.M., and A.J.G. wrote the paper.

ACKNOWLEDGEMENTS

First and foremost, I would like to thank my supervisor, Dr. Aaron Gruber. He has been the best teacher and mentor a graduate student could ask for, and has shaped me into the researcher I am today. Also, my deepest gratitude to the members of my thesis committee, Drs. Rob Sutherland and David Euston, for their invaluable expertise and guidance throughout my PhD program. Additionally, I would like to thank Drs. Gibb, van der Meer and Whishaw for taking the time to be part of my thesis examination committee.

During my research journey (more like an odyssey) I have learned a lot, failed a lot, and accomplished a lot. None of it would have been possible without my colleagues at the Canadian Centre for Behavioural Neuroscience with whom I collaborated, exchanged ideas, and shared information. I particularly would like to thank David Tomas-Cuesta, Dr. Ingrid de Miranda-Esteves, and Dr. Davor Curic, who contributed to the work presented in this thesis.

The members of the Gruber lab (past and present) have always been there for each other, and I appreciate the family we have created, with equal parts scientific collaboration and good-humored teasing. To Scott, Ali, Saeedeh, Afrooz, Ashley, Cecile, thank you for being the best colleagues one could ask for. Over the years, I also worked closely with many members of the McNaughton lab: Adam Neumann, Jen Tarnowski, Dr. HaoRan Chang, Dr. Aubrey Demchuk, Leo Molina, and many others. I would also like to thank Drs. Sergey Chekhov and Edgar Bermudez-Contreras, whose helpful conversations did wonders for both my research and my mental health throughout my graduate program. There are many others that I would like to mention, perhaps too many to count, but I appreciate every single one. A few notable names are

Dr. Hendrik Steenland, Dr. Maurice Needham, and Dr. Michael Eckert, who unselfishly shared their time and knowledge with me when I was a new trainee.

Last but certainly not least I would like to thank my family and my non-academic friends, all of whom have been incredibly supportive of me, even though they thought it was hilarious that I work with rats and mice but have always been afraid of wild ones. I'd also like to thank Alastair for his unwavering moral support and his ability to calm me when I was stressing about my work.

Finally, a big thanks to all the mice that made my research possible.

Funding Acknowledgements: This program was funded by BranchOut Neurological Foundation, institutional scholarships from the University of Lethbridge, and by a number of grants awarded to Dr. Aaron Gruber.

TABLE OF CONTENTS

LIST OF TABLES

LIST OF FIGURES

LIST OF ABBREVIATIONS

5-HT	5-hydroxytryptophan
5-MeO-DMT	5-methoxy-N,N-dimethyltryptamine
AC	trial-to-trial correlation
ACC	anterior cingulate cortex
AMPH	amphetamine
BDNF	brain-derived neurotrophic factor
DAT	dopamine transporter
DLS	dorsolateral striatum
DMN	default-mode network
DMT	N,N-Dimethyltryptamine
DOI	2,5-Dimethoxy-4-iodoamphetamine
EEG	electroencephalography
FC	functional connectivity
fMRI	functional magnetic resonance imaging
FR	firing rate
GDNF	Glial cell line-derived neurotrophic factor
HPC	hippocampus
HSP	heat shock protein
HTR	head-twitch response
IP	intraperitoneal
IM	intramuscular
LD50	median lethal dose
LSD	lysergic acid diethylamide
LTP	long-term potentiation
MDMA	3,4-Methylenedioxymethamphetamine
MEG	magnetoencephalography
MI	mutual information
mPFC	medial prefrontal cortex
nAcc	nucleus accumbens
nAChR	α3β4 nicotinic acetylcholine receptor
NMDA	N-methyl-D-aspartate
PCP	phencyclidine
PFC	prefrontal cortex
rCBF	regional cerebral blood flow
REM	rapid eye movement
ROI	region of interest
RSC	retrosplenial cortex
SERT	serotonin reuptake transporter
SC	subcutaneous
SN	substantia nigra
SNR	signal to noise ratio
VTA	ventral tegmental area

CHAPTER 1: GENERAL INTRODUCTION

Neuroscientists still have much to learn about how the brain encodes and processes information. An important tool of neuroscience is pharmacology. Observing functional changes of the brain, and concomitant changes in behavior, during and after drug administration provides valuable information about information encoding and processing. A series of recent functional magnetic resonance imaging (fMRI) studies in humans have revealed that psychedelic drugs evoke profound changes in patterned brain activity. These changes include a reduction in the normal correlation structure (i.e. functional connectivity) among structures. This has led to claims that psychedelics increase the entropy of the brain and evoke other changes with important ramifications on neural information coding. It is important to note that fMRI signals indirectly reflect changes in activity of large groups of neurons, and cannot resolve the activity of individual neurons. In this thesis, I test whether similar effects manifest among individual neurons using techniques to record large ensembles of neurons in mouse neocortex. Other clinical data suggests that psychedelics can ameliorate addiction and mood disorders for many months after administration. It is speculated that such long-lasting effects involve drug-mediated synaptic changes, but evidence of altered connectivity has never been shown to have functional effects on brain dynamics or information processing. I test for such effects by administering a psychedelic in mice that have previously received chronic administration of amphetamine.

My data indicate that two different psychedelics have similar short-term effects on neural encoding of spatial position in a neocortical region. These changes are largely consistent with the human imaging literature. The data indicate that psychedelics disrupt the brain's process of internally keeping track of position, a process called path-integration. Interestingly, some features

of network dynamics were not affected by the psychedelics, nor was encoding 24 hours after psychedelic administration. Moreover, psychedelic administration did not ameliorate the deficit in spatial encoding evoked by chronic amphetamine treatment. Thus, neocortical representations in mouse revealed by several advanced analytical methods do not reflect processes that could account for months-long remediation of mental disorders, such as addiction and depression, reported in clinical studies.

1.1 PSYCHEDELICS

1.1.1 What is a psychedelic?

The term "psychedelic" in a pharmacological context refers to molecules that evoke a characteristic set of mental phenomena that include altered psychological experiences, unstable moods, and perceptual distortions spanning several modalities including visual, auditory, and somatosensory domains. These molecules can evoke perceptions of stimuli that are not physically present, which is why they are sometimes referred to as "hallucinogens". Psychedelic drugs encompass a variety of molecules with diverse structures and pharmacology. These can be grouped in several ways, and the groups (and individual substances) can differ in their effects on mood, perception, or cognition. For instance, classic psychedelics such as psilocybin, typically evoke strong effects on visual processing, which often causes surrounding colors to appear brighter or clearer, the appearance of fractal or geometric patterns, and static objects becoming dynamic (Aday et al., 2021). Other psychedelics, such as salvinorin A, can evoke profound distortion of space and time perception (Maqueda et al., 2015)

Despite strongly influencing perception and cognition, some aspects of reward processing and decision making appear resistant to modulation by psychedelics. In one study, administration of lysergic acid diethylamide (LSD) to healthy humans did not affect short-term influence of reinforcement on choice; win-stay and lose-shift strategies were not different from controls (Kanen et al., 2022). These subjects did, however, perseverate less after reinforcement contingency shifts. These data indicate that despite intense cognitive effects, humans are able to perform reinforcement-based choice tasks without significant deficits. This is an important consideration for the experiments in this thesis, in which animals perform tasks for reward while under the influence of psychedelics.

1.1.2. Classic versus non-classic psychedelics

Psychedelics have generally been divided into classic and non-classic categories based on their principal mechanism of action. *Classic* psychedelics such as psilocybin, LSD, N,N-Dimethyltryptamine (DMT), 2,5-Dimethoxy-4-iodoamphetamine (DOI), and mescaline act mainly on 5-hydroxytryptophan (5-HT, also known as serotonin) receptors. Classic psychedelics are distinguished by their agonist activity at the 5-HT_{2A} receptor, which appears necessary for psychedelic effects (González-Maeso et al., 2007; Madsen et al., 2019), although they also have affinity for other serotonin receptors. Based on their chemical structure and psychopharmacology, classic psychedelics are divided into tryptamines (e.g. psilocybin, DMT) and phenethylamines (e.g. mescaline, DOI) (Geyer et al., 2009). Lysergamines are a class of tryptamines which include tetracyclic ergolines such as LSD. Classic psychedelics can also be divided into naturally occurring, such as psilocybin and mescaline, and synthetic, including DOI and LSD, but what they

all have in common is the fact that they exert their effects primarily through the serotonergic system (Baumeister et al., 2014). It is worth noting the structural similarity of classic psychedelics with 5-HT (Fig. 1.1).

In contrast to classic psychedelics, substances classified as *non-classic* have primary effects on targets other than 5-HT. Examples of such substances are ibogaine, ketamine, 3,4-Methylenedioxymethamphetamine (MDMA), and salvinorin A. Note that many of these do have some activity at 5-HT receptors directly or indirectly (Helsley et al., 1998; Gigliucci et al., 2013). The present work focuses on psilocybin and ibogaine, two representative substances from each category (Fig. 1.1).

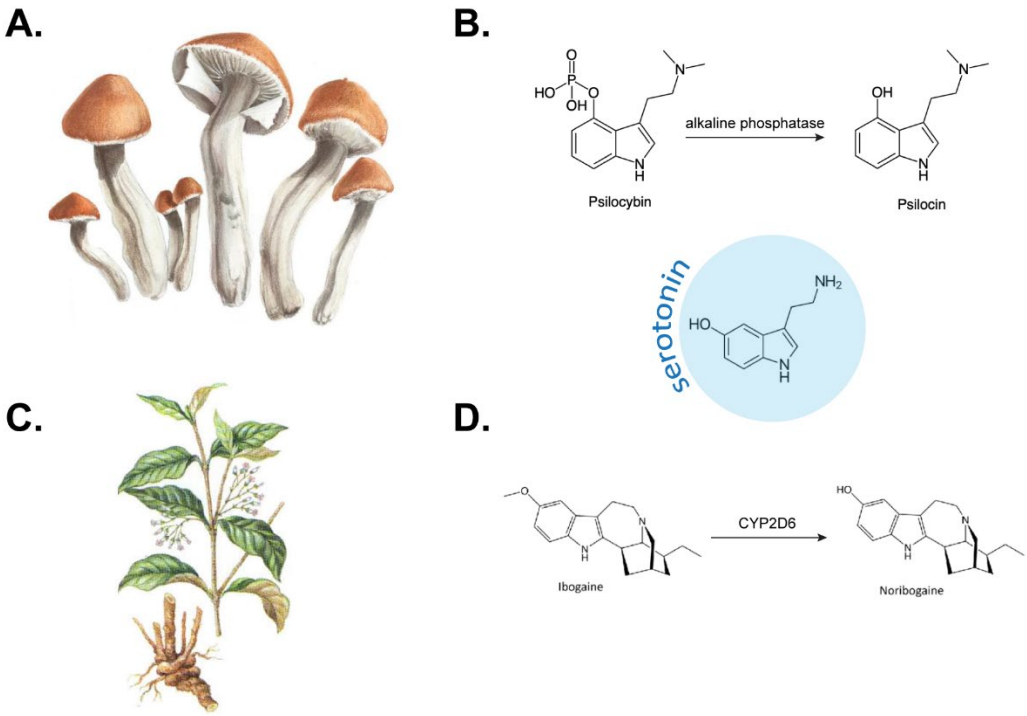

Fig. 1.1: Illustration of the psychedelics and their metabolic pathways. A. Drawing of Psilocybe cubensis, colloquially referred to as "magic mushrooms". Image reproduced with

permission from Hollye Eugenia Maxwell, *Psilocybe cubensis*, 2022, Maxwell Studios, LLC. B. Metabolic pathway of psilocybin adapted form (Nichols, 2020). C. Tabernathe Iboga plant from "Plants of the gods: their sacred, healing, and hallucinogenic powers" (Schultes et al., 2001). D. Metabolic pathway of ibogaine, adapted from (Wasko et al., 2018). The structure of serotonin is shown to illustrate the structural similarity of the exogenous ligands.

1.1.3 Psilocybin (classic psychedelic)

Psychotropic fungi of the genus *Psilocybe* have been used in Europe and the Americas for centuries, largely for spiritual practices (Nichols, 2020). They are best known for their l-tryptophan-derived major natural product, psilocybin. After oral administration, this is metabolized to psilocin, the dephosphorylated metabolite, in the acidic environment of the stomach or by alkaline phosphatase (Fig. 1.1.B) in the intestine and kidneys (Dinis-Oliveira, 2017). Psilocin is a compound that has the ability to cross the brain-blood barrier and acts primarily to agonize the 5-HT_{2A} receptor, thereby impacting perception and consciousness (Madsen et al., 2019). Interestingly, not all 5-HT_{2A} agonists have psychedelic properties (Cao et al., 2022; Cunningham et al., 2023). Rather, psychedelics appear to have modulatory action at this receptor that is important for the psychedelic effect. Classic psychedelics interact with the 5-HT_{2A} receptor to induce a head-twitch response (HTR), a marker of psychedelic state in rodents (Erkizia-Santamaría et al., 2022). In humans, the experience of psilocybin is described as being consistent with that of other classic psychedelics described above. It is characterized by perceptual distortions, space–time awareness alterations, and psychological experiences with spiritual connotations (Griffiths et al., 2006). Some participants report experiencing 'synesthesia', a phenomenon in which the sensory modalities are mixed, enabling the participants to 'see sounds' (Turton et al., 2014). Mood

effects can include a reduction in anxiety, a sense of joy and happiness, and even euphoria (Griffiths et al., 2006).

1.1.4 Ibogaine (non-classic psychedelic)

Ibogaine is an indole alkaloid which is the major psychoactive component of the Tabernanthe Iboga root bark, an Apocynaceous shrub found in West Central Africa, which has long been used in spiritual rituals. Ibogaine is metabolized by cytochrome P4502D6 (CYP2D6) to form its principal metabolite, noribogaine (Fig. 1.1.D) (Obach et al., 1998). The subjective effects of ibogaine, reported by healthy or addicted individuals, differ from that of classic psychedelics (Mash et al., 1998; Schenberg et al., 2014; Glue et al., 2015; Brown and Alper, 2018; Malcolm et al., 2018; Mash et al., 2018; Noller et al., 2018). Most subjects describe strong spiritual experiences, sometimes with negative connotations, heightened memory recollection and prospection of one's own future (Schenberg et al., 2017). The disruption in visual and auditory perception is more often described as a "dream-like state", and the oneiric effects can be accompanied by increased sensitivity to light and sound and ego dissolution (Brown et al., 2019). The immediate experience is followed by an extended period of contemplative state, which can be accompanied by lucid dreaming, autobiographical memories, and introspection. Overall, participants in ibogaine studies do not describe the drug as a pleasant or typical psychedelic experience. Indeed, the majority report having to confront difficult personal past events, such as childhood traumas, overdoses, and strong emotional events, either real or fictitious. Many have posited that this effect on prospection, which appears to be specific to ibogaine, is the key for its ability to produce positive outcomes in addicted patients.

Even though ibogaine does show moderate binding with 5-HT_{2A} (Helsley et al., 1998), it does not produce HTR (González et al., 2018). Ibogaine affects a wide range of neurotransmitters and receptors in the dopamine (Maisonneuve et al., 1991; Sershen et al., 1992b), serotonin (Broderick et al., 1994; Mash et al., 1995), and opioid systems (Codd, 1995; Glick et al., 1997). Ibogaine has a variety of effects: it has a relatively low affinity for κ- and μ-opioid receptors and σ2 receptors; it binds to both serotonin reuptake transporter (SERT) and dopamine transporter (DAT); it is an antagonist to N-methyl-D-aspartate (NMDA) and α3β4 nicotinic acetylcholine (nAChR) receptors; and it is a weak 5-HT_{2A}R agonist (Alper, 2001; Sershen et al., 2001; Bulling et al., 2012; Coleman et al., 2019). The effects of ibogaine could therefore be attributed to a polypharmacological mechanism underpinning the effects on information processing.

In rodents, ibogaine suppresses sleep and promotes wakefulness (González et al., 2018), but this wakeful state has electrophysical properties similar to REM sleep state to such extent that an artificial neural network classified awake ibogaine data as REM sleep (González et al., 2021). This dream-like dissociate state is distinguished by high-power local gamma oscillations that are less complex than in normal wakefulness. These oscillations have been attributed to ibogaine's NMDA receptor antagonism because ketamine (an NMDA antagonist) administration induces similar features (Manduca et al., 2020).

Ibogaine is reported to have long-lasting (up to a week) effects on behavior (Glick et al., 1991; Sershen et al., 1992b; Sershen et al., 1994), and long-term impact on drug abstinence. These effects may be related to its ability to promote the growth of dendritic arbors and spines in rodent cortical neurons (Ly et al., 2018; Cameron et al., 2020). This is similar to other psychedelics that have been shown to induce neuroplasticity, such as DMT (Lima da Cruz et al., 2018), psilocybin

(Shao et al., 2021), ketamine (Pryazhnikov et al., 2018; Treccani et al., 2019; Zhang et al., 2019), and others (Calder and Hasler, 2023). Neuroplastic changes are thought to be the basis of learning and memory and can affect neural dynamics (Yu et al., 2017). These effects inspired ibogaine's classification as a "psychoplastogen". Importantly, no neural correlates of such synaptic reorganization have been reported. Without such data, it remains unclear if synaptic changes are functionally relevant.

1.1.5 Short and long-term mechanisms of psychedelic action in the brain

There are several theories that attempt to explain how psychedelics affect neural processes to produce psychedelic effects (Swanson, 2018). Previous reports on the effects of hallucinogens on human brain activity measured by fMRI are based on mostly classic psychedelics, including psilocybin (Carhart-Harris et al., 2012; Muthukumaraswamy et al., 2013; Tagliazucchi et al., 2014), LSD (Carhart-Harris et al., 2016; Atasoy et al., 2017), ayahuasca and DMT (Alonso et al., 2015; Palhano-Fontes et al., 2015; Riga et al., 2018). Several common denominators emerge throughout the human fMRI literature, such as an increase in connectivity motifs (Tagliazucchi et al., 2014; Atasoy et al., 2017). Complex networks, such as biological systems, can be decomposed into several patterns of connections within the network, which are termed connectivity motifs. The activity dynamics of the network is often dominated by one or a few of these at any one time. These motifs represent potential "processing modes" and can provide insights into the functional properties of a networks (Sporns, 2006). An increase in the number of connectivity motifs can indicate that the network transitioned from highly structured to increasingly homogeneous. Another classic feature of the psychedelic brain is decreased activity

in frontal regions, which is posited to cause a reduction of the top-down control (Carhart-Harris et al., 2012), and increase in the 'entropy' of functional connectivity networks in the neocortex (Carhart-Harris et al., 2014; Girn et al., 2022). Entropy is defined as a dimensionless quantity that is used for measuring of the degree of complexity contained in a system. While entropy is not identical to randomness in all circumstances, the implication is that it reflects the degree of disorder or uncertainty in a system. Psychedelic states are also proposed to cause disruption of information flow between cortical regions in humans (Carhart-Harris et al., 2012; Barnett et al., 2020).

In addition to the short-term effects described above, psychedelics also appear to have effects on cognition and mood that can last for months after an acute dose. One of the best studied is the effect of several individual psychedelics to produce elevated mood and remediate anxiety and depression (Moreno et al., 2006; Griffiths et al., 2016; Rucker et al., 2016; Sanches et al., 2016; Carhart-Harris et al., 2018b). This suggests that psychedelics can promote long-lasting changes in the brain. Most of the attention has been focused on dendrites and spines. Psilocybin has been shown to induce an increase in spine morphology in mice using in vivo 2-photon imaging of layer V pyramidal neurons in the medial frontal cortex (Shao et al., 2021), and Golgi-Cox staining histological assessment in the hippocampus (Du et al., 2023). Similarly, an increase in the spine density was observed in the mouse medial frontal cortex with 5-MeO-DMT treatment (Jefferson et al., 2023). Serotonin itself does not produce psychedelic-like effects on neuronal growth when administered to cortical cultures (Ly et al., 2018). Activation of intracellular 5-HT_{2A} receptors could be an important factor in the neuroplastic changes and antidepressant properties of psychedelic compounds (Vargas et al., 2023), and could explain the persistent effects after the psychedelic is no longer present in the extracellular space. Conversely, plastic changes induced by both psilocin and LSD in mouse HPC and PFC are associated with the high affinity of these

compounds to bind to TrkB, the brain-derived neurotrophic factor (BDNF) receptor, and these neurotrophic effects do not require 5-HT_{2A} activation (Moliner et al., 2023). Some 5-HT_{2A}R ligands can cause behavioral and structural alterations in the absence of hallucinogenic effects (Dunlap et al., 2020; Dong et al., 2021; Cao et al., 2022). However, there are many indications that in humans, the beneficial properties of psychedelics in various conditions are closely linked to their subjective effects (Yaden and Griffiths, 2021). To date, no studies have shown that the neuroplastic changes have functional effects on neural dynamics, memory, or information processing.

1.1.6 Ibogaine as a treatment for addiction

Ibogaine has a long anecdotal history as a treatment for addiction. Proper clinical trials have only been conducted more recently. Ibogaine has been shown to have promising results in treating substance use disorders, particularly for opioid use (Mash et al., 2018; Noller et al., 2018; Köck et al., 2021). Ibogaine thus appears to have some efficacy in attenuating drug taking behavior, but no evidence to date indicates how this is manifested though changes in neural signaling. Ibogaine is effective in reducing measures of drug taking and drug seeking in rodents as well. In rats, it reduces self-administration of cocaine, morphine, and heroin (Glick et al., 1991; Cappendijk and Dzoljic, 1993; Glick et al., 1994; Dworkin et al., 1995). It also reduces alcohol intake (Rezvani et al., 1995; He et al., 2005), and cocaine preference (Sershen et al., 1994).

Of particular interest to this thesis is ibogaine's effect on animal models of addiction to psychostimulants, such as amphetamine. Ibogaine diminishes amphetamine-induced place preference (Moroz et al., 1997), and amphetamine-induced hyper-locomotion (Sershen et al.,

1992b). Amphetamine has been extensively researched in rodents, and its effects on behavior and neural signaling have been described for various dosages, brain regions, and behavioral paradigms. Particularly, prolonged administration of amphetamine has been shown to impair learning and memory (Mandillo et al., 2003; Arroyo-García et al., 2020) and promote patterned behavior such as conditioned place preference, food hoarding, and hyperlocomotion (Creese and Iversen, 1974; Spyraki et al., 1982; Dringenberg et al., 2000). Therefore, using chronic amphetamine administration in rodents in order to observe the interaction between an addictive drug and a psychedelic with anti-addictive properties can reveal important information about the effect of both drugs on neural processing.

Several important features of ibogaine's neural effects remain unresolved. It is still unclear if ibogaine's low affinity for the 5-HT_{2A} receptor has a strong functional relevance, whether the neuroplastic properties are responsible for the long-term effects in treating disorders, and whether the psychedelic experience is germane for its therapeutic effectiveness in humans. While this thesis does not directly address these questions, it does investigate whether it induces long-lasting changes in neural signaling in the cortex in drug-naïve and in chronic drug treated mice, which can help expand our knowledge in the properties of this psychedelic.

1.2 SPATIAL ENCODING & THE RETROSPLENIAL CORTEX

Few studies have reported the effects of psychedelics on information encoding among ensembles of neurons. One has investigated encoding of information in the visual cortex, finding that DOI had a suppressive effect on sensory-driven responses (Michaiel et al., 2019). I am interested in the effects of psychedelics on representations generated internally as well as those

evoked by stimuli. The encoding of spatial position enables such investigation. The location of a rodent is encoded by populations of 'place cells', first described in CA1 of hippocampus (O'Keefe and Dostrovsky, 1971). Each of these cells activates when the animal locomotes through a particular place in the environment. Similar place cells have been reported in the retrosplenial cortex (RSC) (Mao et al., 2017). Intriguingly, rodents can update their estimation of position even in the absence of location cues (such as landmarks) (Cooper et al., 2001). They use a process called 'path integration' to use motion signals in order to update their expected position (Sherrill et al., 2013). This is reflected in the activation of place cells corresponding to the new expected location, and extinguishing activity in place cells corresponding to former locations. The place cells therefore provide a well-understood means to read out a phenomenon dependent on internal neural dynamics (path integration). In general, the representation of the location of the animal and environmental features is termed 'cognitive map' (O'Keefe and Nadel, 1978). It can be mentally navigated to plan and execute navigation.

The rodent retrosplenial cortex occupies the caudal half of the cingulate cortex and is divided in a dorsal dysgranular area (due to the presence of a rudimentary layer IV) and a ventral granular area (van Groen and Wyss, 1992; Vogt and Paxinos, 2014). The two regions are heavily interconnected, both with each other, and with other cortical and subcortical areas (Aggleton et al., 2021). The RSC has been studied in the context of memory research for many decades, but later work has focused on its role in navigation, landmark processing, and direction encoding. Lesion studies in rodents revealed that it can be challenging to identify cognitive functions that depend exclusively on the RSC (Mitchell et al., 2018), but that specific impairments can be observed, particularly in spatial working memory (Sutherland et al., 1988; Cooper and Mizumori, 1999; Whishaw et al., 2001; Vann and Aggleton, 2002; Keene and Bucci, 2009).

The RSC is involved in critical functions such as planning, memory, and navigation (Vann et al., 2009). A large proportion of these functions are due to this brain region's connections to the hippocampus (HPC) (Wyass and Van Groen, 1992; Kobayashi and Amaral, 2003; Sugar et al., 2011; Yamawaki et al., 2019), and the prefrontal cortex (PFC) (Fisk and Wyss, 1999; Shibata et al., 2004; Shibata and Naito, 2008). Rats that learned a spatial navigation task showed an increase in regional cerebral blood flow (rCBF) in the ventral hippocampus, which was positively correlated with activation of the dysgranular RSC (Holschneider et al., 2019). This brain region is therefore well positioned to integrate sensory, mnemonic, and cognitive information by virtue of its strong connectivity with the HPC, which is integral to the processing of contextual memories (Corcoran et al., 2011; Corcoran et al., 2018) and the cortical representation of space (Esteves et al., 2021; Esteves et al., 2023).

As a hub that integrates and coordinates the activity of distinct brain regions that mediate cognitive and emotional processes, the RSC is an excellent target to study the effects of psychoactive drugs. Reports of human perceptual experience is consistent with psychedelic-based disruption of the sense of space and time, causing disorientation and a feeling of spacelessness (Carbonaro et al., 2016; Garcia-Romeu et al., 2016; Smigielski et al., 2019). The loss of spatial boundaries, resulting in a blurring of the distinction between self-representation and external environment was described as an "ego dissolution" (Klee, 1963; Millière et al., 2018; Mason et al., 2020). This dissociative state in which affective responses are uncoupled from sensory percepts is distinguished in mice by slow (1-3 Hz) oscillations in layer V of the RSC, which corresponded with rhythmic coupling with the thalamus (Vesuna et al., 2020). Therefore, it is possible that psychedelic drugs affect information processing in the RSC. The properties of the RSC location-

encoding cells provide a model system to investigate the neural correlates of a drug's effect on navigation and memory. The RSC encodes stable landmarks in an environment (Auger et al., 2012) and the animal's orientation, even when head-fixed (Sit and Goard, 2023). These cells also represent relationships between path elements. In rats traversing a track with a recurrent structure, RSC neurons encode sub-route positions relative to the whole track, further indicating the role of RSC in path integration by the extraction of path sub-spaces (Alexander and Nitz, 2017).

Executive processes that enable behaviors such as decision-making and strategy flexibility depend on contextual representations of space in the PFC, where neurons remap in a novel environment but conserve their tuning in familiar ones (Sauer et al., 2022), and RSC, where contexts are associated with appropriate motor outputs (Franco and Goard, 2021). Furthermore, RSC contextual representations provide information about the reliability of events occurring within them (Auger and Maguire, 2018). RSC may also contribute to the formation of episodic memory by linking sensory stimuli during learning. A study using rats trained in a sensory preconditioning procedure in which a tone and light were paired in the absence of reinforcement, and then paired with food, showed that chemogenetic silencing of RSC neurons during preconditioning prevented the formation of an association between the tone and light (Robinson et al., 2014). The rat RSC also contributes to learning about stimuli that are not explicitly spatial (Robinson et al., 2011; Miller et al., 2014; Nelson et al., 2014; Jiang et al., 2018). These results suggest that in the nonspatial domain, the RSC serves as a comparator between representations from different frames of reference (Nelson et al., 2018).

Drug seeking involves neural processing in networks of brain structures that are essential for navigation, reward processing, and decision making (Dalley et al., 2011). The RSC is important

in drug seeking behavior through its involvement is spatial encoding, path integration, and its role in emotional processes (Maddock, 1999). This brain region contains reward-responsive neurons that encode reward value and preference (Vedder et al., 2017; Hattori et al., 2019). Recent data indicate that reward associations may involve the RSC's connection to the basolateral amygdala (Lefner et al., 2021) and primary sensory cortices (Todd et al., 2016; Fischer et al., 2020). Furthermore, a network of brain regions closely coupled with the RSC, including the ventral tegmental area (VTA), substantia nigra (SN), and hypothalamus, show a strong correlation in response to amphetamine administration (Schwarz et al., 2007). These regions are involved in ethological behaviors (e.g. food foraging), but prolonged exposure to psychostimulants is thought to induce structural and functional changes in order to elicit patterned responses such as drug seeking (Koob and Le Moal, 2001). Furthermore, amphetamine-sensitized rats display increased habit formation and motivation for reinforcement (Nelson and Killcross, 2006; Nordquist et al., 2007; Mendez et al., 2009).

Serotonin plays an important role in the modulation of cortical electrical activity and acts on cortical neurons (Andrade, 2011), which express a variety of receptors for 5-HT (Pazos et al., 1985; Pompeiano et al., 1992; 1994; Beliveau et al., 2017), although the distribution of receptors is typically lower in the RSC. While this brain region does not have a high incidence of 5-HT_{2A} receptors, it is strongly influenced by its connectivity with prefrontal and sensory cortices, which do have a strong expression of 5-HT_{2A}Rs (Andrade and Weber, 2010). Serotonin was found to increase the latency of intracortical synchronous discharges and interhemispheric propagation time in the cingulate (anterior and retrosplenial) cortex of mice, and this effect was simulated by 5-HT_{1B} and 5-HT_{2A} receptor agonists (Rovira and Geijo-Barrientos, 2016). RSC interactions with

other structures thus appear to be modulated by psychedelics. The spatial information encoded in this region provides a means to assess how these psychedelics affect neural information processing at the cellular level.

It is evident from both human studies and animal models that the RSC is involved in various aspects of cognition. Overall, human fMRI studies indicate that psychedelics can temporarily alter the activity and connectivity profile of the RSC (Lebedev et al., 2015; Carhart-Harris et al., 2016). This could be linked to their ability to promote growth of dendritic arbors and spines in rodent cortical neurons (Ly et al., 2018; Cameron et al., 2020; Shao et al., 2021), and therefore inducing structural changes in the cortex. Because structural changes are expected to persist over a long time (months), this should lead to long-lasting changes in functional connectivity. Alternatively, the acute effects observed could be less reliant on anatomical alterations and more on temporary functional changes. As described above, psychedelics promote cortical desynchronization and increase the complexity of the brain activity. The evidence so far points to psychedelic drugs acting upon specific receptors in order to exert their effects. This, in turn, leads to functional and plastic changes which can alter behavior. The work presented in this thesis is one of the first to test psychedelic effects on information processing at the level of neural ensembles in the retrosplenial cortex.

1.3 HYPOTHESES

Based on the literature reviewed above, I have developed 5 primary hypotheses that motivate the thesis experiments.

Hypothesis 1: Psychedelics will corrupt encoding of RSC place encoding, as indicated by reduced signal to noise ratio (SNR). *Rationale:* Humans experience psychedelic-based disruption of the sense of space and time, causing disorientation and a feeling of spacelessness. I expect this to be manifest as loss of signal in place-cell activity in rodents.

Hypothesis 2: Psychedelics will disrupt functional connectivity among single units in RSC. *Rationale:* fMRI studies in humans have shown reduction in functional connectivity among brain regions. I expect that this macroscopic phenomenon will be recapitulated at the cellular level.

Hypothesis 3: Psilocybin and ibogaine will show similar effects on RSC activity despite differences in their molecular structure and pharmacology. *Rationale:* Both psychedelics have similar effects on measures of large-scale activity, such as cortical desynchronization and increased neuroplasticity. I expect the effects on neural dynamics in the RSC will be similar for the two substances.

Hypothesis 4: Chronic amphetamine administration will reduce SNR of place encoding in RSC neurons. *Rationale:* Rodents treated with repeated administration of amphetamine are impaired in spatial tasks. I expect this to be reflected as reduced SNR.

Hypothesis 5: Psychedelics will have long-term effects to improve SNR in rats treated with chronic amphetamine. *Rationale:* Psychedelics appear to remediate depressive symptoms in humans and reduce conditioned place preference for amphetamine in rodents. Moreover, they appear to engage synaptic reorganization. I expect this to remediate deficits in RSC place encoding.

1.4 THESIS ORGANIZATION

Psychedelics provide a fascinating tool to study brain function, such as what neural correlates change and how those are related to reported psychedelic states. Moreover, psychedelics are a potential therapeutic for addiction, depression and other mental illnesses. Their rapid onset and long-lasting efficacy contrast the several weeks or months required for efficacy by traditional treatments. However, we know almost nothing about how psychedelics exert their effects. Testing my theories in a rodent model has significant value because it allows recording of ensemble neural activity with spatiotemporal precision not currently possible in humans. This will likely help develop a much-needed cellular-level model of cognitive phenomena pertinent to psychedelic research.

Clearly defining the precise molecular effects of psychedelics is extremely difficult (Ray, 2010). Analyzing their functional effects on neural activity can provide us with important information about their effects on information encoding, the deviations they cause in healthy and disordered brain, and the therapeutic potential they offer. This will allow us to move forward towards well-controlled, highly regulated, and more successful treatment for a myriad of neurological conditions such as addiction, chronic depression, anxiety, and others.

Furthermore, despite tremendous amount of past research, we still have little knowledge about how information encoding at the single-cell level is affected in addiction. Improving the current treatment options is difficult in the absence of this knowledge. Using chronic amphetamine administration as a rodent model of addiction can provide essential information regarding its effect on the neural activity repertoire.

The present work aimed at investigating several hypotheses related to psychedelic action, which were then tested in three studies I have conducted during my doctoral training, in an attempt to enhance our knowledge on the functional effects of psilocybin and ibogaine on individual neuronal level in the cortex.

Chapter 2: *This experiment provides evidence that psilocybin disrupts cognitive processes (at least those involved in place encoding and/or navigation) in the brain. The spatial information encoded in the RSC provides a means to assess how information processing at the cellular level is altered. I hypothesize that as the head-fixed mice navigate a virtual environment, the spatial representation will become distorted and/or degraded, and I will observe decreased functional connectivity among RSC neurons. Psilocybin exerts its effects mainly through serotonin receptors and therefore blockage of 5-HT_{2A}Rs using an antagonist should counteract these effects.*

Chapter 3: *This experiment provides evidence that ibogaine evokes mental states with psychedelic features in rodents. Despite it having a significantly broader neuropharmacological action than classic psychedelics, I expect to observe a similar phenomenon linked to cognitive maps. This should correspond with a loss of correlation structure, and increased responses to cues, as the sensory signals will be encoded more reliably in the RSC. Together, these data test proposals that compounds with psychedelic properties increase the entropy of neural signaling.*

Chapter 4: *Amphetamine and other drugs of abuse have both short-term and long-lasting effects on brain function, and chronic drug paradigms often result in cognitive impairments. They may also affect the involvement of the RSC in cognitive control. I will test the hypothesis that chronic amphetamine administration degrades the spatial encoding in the RSC. I also aim to determine whether ibogaine can ameliorate amphetamine-induced signaling changes. This hypothesis was inspired by many reports of ibogaine inducing prolonged facilitation of drug cessation in humans with substance use disorders.*

In the following chapters I will describe the experiments conducted to answer the proposed hypotheses. The body of data presented in this doctoral thesis is one of the first to suggest that cognitive maps are disrupted by psychedelic compounds and represents an attempt to contribute to the fields of psychedelic research, path integration, and addiction.

1.5 REFERENCES

Aday, J.S., Wood, J.R., Bloesch, E.K., and Davoli, C.C. (2021). Psychedelic drugs and perception: a narrative review of the first era of research. *Reviews in the Neurosciences* 32(5)**,** 559-571. doi: doi:10.1515/revneuro-2020-0094.

Aggleton, J.P., Yanakieva, S., Sengpiel, F., and Nelson, A.J. (2021). The separate and combined properties of the granular (area 29) and dysgranular (area 30) retrosplenial cortex. *Neurobiology of Learning and Memory* 185**,** 107516. doi: https://doi.org/10.1016/j.nlm.2021.107516.

Alexander, A.S., and Nitz, D.A. (2017). Spatially periodic activation patterns of retrosplenial cortex encode route sub-spaces and distance traveled. *Current Biology* 27(11)**,** 1551-1560.e1554. doi: https://doi.org/10.1016/j.cub.2017.04.036.

Alonso, J.F., Romero, S., Mañanas, M.À., and Riba, J. (2015). Serotonergic psychedelics temporarily modify information transfer in humans. *International Journal of Neuropsychopharmacology* 18(8). doi: 10.1093/ijnp/pyv039.

Alper, K.R. (2001). Chapter 1 Ibogaine: A review. *The Alkaloids: Chemistry and Biology*. Academic Press), 1-38.

Andrade, R. (2011). Serotonergic regulation of neuronal excitability in the prefrontal cortex. *Neuropharmacology* 61(3)**,** 382-386. doi: https://doi.org/10.1016/j.neuropharm.2011.01.015.

Andrade, R., and Weber, E. (2010). Htr2a Gene and 5-HT2A receptor expression in the cerebral cortex studied using genetically modified mice. *Frontiers in Neuroscience* 4(36). doi: 10.3389/fnins.2010.00036.

Arroyo-García, L.E., Tendilla-Beltrán, H., Vázquez-Roque, R.A., Jurado-Tapia, E.E., Díaz, A., Aguilar-Alonso, P., et al. (2020). Amphetamine sensitization alters hippocampal neuronal morphology and memory and learning behaviors. *Molecular Psychiatry*. doi: 10.1038/s41380-020-0809-2.

Atasoy, S., Roseman, L., Kaelen, M., Kringelbach, M.L., Deco, G., and Carhart-Harris, R.L. (2017). Connectome-harmonic decomposition of human brain activity reveals dynamical repertoire re-organization under LSD. *Scientific Reports* 7(1)**,** 17661. doi: 10.1038/s41598-017-17546-0.

Auger, S.D., and Maguire, E.A. (2018). Retrosplenial cortex indexes stability beyond the spatial domain. *Journal of Neuroscience* 38(6)**,** 1472-1481.

Auger, S.D., Mullally, S.L., and Maguire, E.A. (2012). Retrosplenial cortex codes for permanent landmarks. *PloS one* 7(8)**,** e43620. doi: 10.1371/journal.pone.0043620.

Barnett, L., Muthukumaraswamy, S.D., Carhart-Harris, R.L., and Seth, A.K. (2020). Decreased directed functional connectivity in the psychedelic state. *NeuroImage* 209**,** 116462. doi: https://doi.org/10.1016/j.neuroimage.2019.116462.

Baumeister, D., Barnes, G., Giaroli, G., and Tracy, D. (2014). Classical hallucinogens as antidepressants? A review of pharmacodynamics and putative clinical roles. *Therapeutic Advances in Psychopharmacology* 4(4)**,** 156-169.

Beliveau, V., Ganz, M., Feng, L., Ozenne, B., Højgaard, L., Fisher, P.M., et al. (2017). A high-resolution in vivo atlas of the human brain's serotonin system. *Journal of Neuroscience* 37(1)**,** 120-128.

Broderick, P.A., Phelan, F.T., Eng, F., and Wechsler, R.T. (1994). Ibogaine modulates cocaine responses which are altered due to environmental habituation: In vivo microvoltammetric and behavioral studies. *Pharmacology Biochemistry and Behavior* 49(3)**,** 711-728. doi: https://doi.org/10.1016/0091-3057(94)90092-2.

Brown, T.K., and Alper, K. (2018). Treatment of opioid use disorder with ibogaine: detoxification and drug use outcomes. *The American Journal of Drug and Alcohol Abuse* 44(1)**,** 24-36. doi: 10.1080/00952990.2017.1320802.

Brown, T.K., Noller, G.E., and Denenberg, J.O. (2019). Ibogaine and subjective experience: transformative states and psychopharmacotherapy in the treatment of opioid use disorder. *Journal of Psychoactive Drugs* 51(2)**,** 155-165. doi: 10.1080/02791072.2019.1598603.

Bulling, S., Schicker, K., Zhang, Y.-W., Steinkellner, T., Stockner, T., Gruber, C.W., et al. (2012). The mechanistic basis for noncompetitive ibogaine inhibition of serotonin and dopamine transporters. *Journal of Biological Chemistry* 287(22)**,** 18524-18534. doi: https://doi.org/10.1074/jbc.M112.343681.

Calder, A.E., and Hasler, G. (2023). Towards an understanding of psychedelic-induced neuroplasticity. *Neuropsychopharmacology* 48(1)**,** 104-112. doi: 10.1038/s41386-022-01389-z.

Cameron, L.P., Tombari, R.J., Lu, J., Pell, A.J., Hurley, Z.Q., Ehinger, Y., et al. (2020). A non-hallucinogenic psychedelic analogue with therapeutic potential. *Nature*. doi: 10.1038/s41586-020-3008-z.

Cao, D., Yu, J., Wang, H., Luo, Z., Liu, X., He, L., et al. (2022). Structure-based discovery of nonhallucinogenic psychedelic analogs. *Science* 375(6579)**,** 403-411. doi: doi:10.1126/science.abl8615.

Cappendijk, S.L.T., and Dzoljic, M.R. (1993). Inhibitory effects of ibogaine on cocaine self-administration in rats. *European Journal of Pharmacology* 241(2)**,** 261-265. doi: https://doi.org/10.1016/0014-2999(93)90212-Z.

Carbonaro, T.M., Bradstreet, M.P., Barrett, F.S., MacLean, K.A., Jesse, R., Johnson, M.W., et al. (2016). Survey study of challenging experiences after ingesting psilocybin mushrooms: Acute and enduring positive and negative consequences. *Journal of Psychopharmacology* 30(12)**,** 1268-1278. doi: 10.1177/0269881116662634.

Carhart-Harris, R., Leech, R., Hellyer, P., Shanahan, M., Feilding, A., Tagliazucchi, E., et al. (2014). The entropic brain: A theory of conscious states informed by neuroimaging research with psychedelic drugs. *Frontiers in Human Neuroscience* 8**,** 20.

Carhart-Harris, R.L., Bolstridge, M., Day, C.M.J., Rucker, J., Watts, R., Erritzoe, D.E., et al. (2018b). Psilocybin with psychological support for treatment-resistant depression: six-month follow-up. *Psychopharmacology* 235(2)**,** 399-408. doi: 10.1007/s00213-017-4771-x.

Carhart-Harris, R.L., Erritzoe, D., Williams, T., Stone, J.M., Reed, L.J., Colasanti, A., et al. (2012). Neural correlates of the psychedelic state as determined by fMRI studies with psilocybin. *Proceedings of the National Academy of Sciences* 109(6)**,** 2138-2143. doi: 10.1073/pnas.1119598109.

Carhart-Harris, R.L., Muthukumaraswamy, S., Roseman, L., Kaelen, M., Droog, W., Murphy, K., et al. (2016). Neural correlates of the LSD experience revealed by multimodal neuroimaging. *Proceedings of the National Academy of Sciences* 113(17)**,** 4853-4858. doi: 10.1073/pnas.1518377113.

Codd, E.E. (1995). High affinity ibogaine binding to a mu opioid agonist site. *Life Sciences* 57(20), PL315-PL320. doi: https://doi.org/10.1016/0024-3205(95)02171-E.
Coleman, J.A., Yang, D., Zhao, Z., Wen, P.-C., Yoshioka, C., Tajkhorshid, E., et al. (2019). Serotonin transporter–ibogaine complexes illuminate mechanisms of inhibition and transport. *Nature* 569(7754), 141-145. doi: 10.1038/s41586-019-1135-1.
Cooper, B.G., Manka, T.F., and Mizumori, S.J.Y. (2001). Finding your way in the dark: The retrosplenial cortex contributes to spatial memory and navigation without visual cues. *Behavioral Neuroscience* 115(5), 1012-1028. doi: 10.1037/0735-7044.115.5.1012.
Cooper, B.G., and Mizumori, S.J.Y. (1999). Retrosplenial cortex inactivation selectively impairs navigation in darkness. *NeuroReport* 10(3).
Corcoran, K.A., Donnan, M.D., Tronson, N.C., Guzmán, Y.F., Gao, C., Jovasevic, V., et al. (2011). NMDA receptors in retrosplenial cortex are necessary for retrieval of recent and remote context fear memory. *The Journal of Neuroscience* 31(32), 11655. doi: 10.1523/JNEUROSCI.2107-11.2011.
Corcoran, K.A., Yamawaki, N., Leaderbrand, K., and Radulovic, J. (2018). Role of retrosplenial cortex in processing stress-related context memories. *Behavioral Neuroscience* 132(5), 388-395. doi: 10.1037/bne0000223.
Creese, I., and Iversen, S.D. (1974). The role of forebrain dopamine systems in amphetamine induced stereotyped behavior in the rat. *Psychopharmacologia* 39(4), 345-357. doi: 10.1007/BF00422974.
Cunningham, M.J., Bock, H.A., Serrano, I.C., Bechand, B., Vidyadhara, D.J., Bonniwell, E.M., et al. (2023). Pharmacological mechanism of the non-hallucinogenic 5-HT2A agonist ariadne and analogs. *ACS Chemical Neuroscience* 14(1), 119-135. doi: 10.1021/acschemneuro.2c00597.
Dalley, J.W., Everitt, B.J., and Robbins, T.W. (2011). Impulsivity, compulsivity, and top-down cognitive control. *Neuron* 69(4), 680-694. doi: https://doi.org/10.1016/j.neuron.2011.01.020.
Dinis-Oliveira, R.J. (2017). Metabolism of psilocybin and psilocin: Clinical and forensic toxicological relevance. *Drug Metab Rev* 49(1), 84-91. doi: 10.1080/03602532.2016.1278228.
Dong, C., Ly, C., Dunlap, L.E., Vargas, M.V., Sun, J., Hwang, I.-W., et al. (2021). Psychedelic-inspired drug discovery using an engineered biosensor. *Cell* 184(10), 2779-2792. e2718.
Dringenberg, H.C., Wightman, M., and Beninger, R.J. (2000). The effects of amphetamine and raclopride on food transport: Possible relation to defensive behavior in rats. *Behavioural Pharmacology* 11(6).
Du, Y., Li, Y., Zhao, X., Yao, Y., Wang, B., Zhang, L., et al. (2023). Psilocybin facilitates fear extinction in mice by promoting hippocampal neuroplasticity. *Chinese Medical Journal*, 10.1097.
Dunlap, L.E., Azinfar, A., Ly, C., Cameron, L.P., Viswanathan, J., Tombari, R.J., et al. (2020). Identification of psychoplastogenic N,N-Dimethylaminoisotryptamine (isoDMT) analogues through structure–activity relationship studies. *Journal of Medicinal Chemistry* 63(3), 1142-1155. doi: 10.1021/acs.jmedchem.9b01404.
Dworkin, S.I., Gleeson, S., Meloni, D., Koves, T.R., and Martin, T.J. (1995). Effects of ibogaine on responding maintained by food, cocaine and heroin reinforcement in rats. *Psychopharmacology* 117(3), 257-261. doi: 10.1007/BF02246099.

Erkizia-Santamaría, I., Alles-Pascual, R., Horrillo, I., Meana, J.J., and Ortega, J.E. (2022). Serotonin 5-HT2A, 5-HT2c and 5-HT1A receptor involvement in the acute effects of psilocybin in mice. In vitro pharmacological profile and modulation of thermoregulation and head-twich response. *Biomedicine & Pharmacotherapy* 154**,** 113612. doi: https://doi.org/10.1016/j.biopha.2022.113612.

Esteves, I.M., Chang, H., Neumann, A.R., and McNaughton, B.L. (2023). Consolidation of cellular memory representations in superficial neocortex. *Iscience* 26(2).

Esteves, I.M., Chang, H., Neumann, A.R., Sun, J., Mohajerani, M.H., and McNaughton, B.L. (2021). Spatial information encoding across multiple neocortical regions depends on an intact hippocampus. *The Journal of Neuroscience* 41(2)**,** 307. doi: 10.1523/JNEUROSCI.1788-20.2020.

Fischer, L.F., Mojica Soto-Albors, R., Buck, F., and Harnett, M.T. (2020). Representation of visual landmarks in retrosplenial cortex. *eLife* 9**,** e51458. doi: 10.7554/eLife.51458.

Fisk, G.D., and Wyss, J.M. (1999). Associational projections of the anterior midline cortex in the rat: intracingulate and retrosplenial connections. *Brain Research* 825(1)**,** 1-13. doi: https://doi.org/10.1016/S0006-8993(99)01182-8.

Franco, L.M., and Goard, M.J. (2021). A distributed circuit for associating environmental context with motor choice in retrosplenial cortex. *Science Advances* 7(35)**,** eabf9815. doi: doi:10.1126/sciadv.abf9815.

Garcia-Romeu, A., Kersgaard, B., and Addy, P.H. (2016). Clinical applications of hallucinogens: A review. *Experimental and clinical psychopharmacology* 24(4)**,** 229-268. doi: 10.1037/pha0000084.

Geyer, M., Nichols, D., and Vollenweider, F. (2009). Serotonin-related psychedelic drugs. *Encyclopedia of neuroscience***,** 731-738.

Gigliucci, V., O'Dowd, G., Casey, S., Egan, D., Gibney, S., and Harkin, A. (2013). Ketamine elicits sustained antidepressant-like activity via a serotonin-dependent mechanism. *Psychopharmacology* 228(1)**,** 157-166. doi: 10.1007/s00213-013-3024-x.

Girn, M., Roseman, L., Bernhardt, B., Smallwood, J., Carhart-Harris, R., and Nathan Spreng, R. (2022). Serotonergic psychedelic drugs LSD and psilocybin reduce the hierarchical differentiation of unimodal and transmodal cortex. *NeuroImage* 256**,** 119220. doi: https://doi.org/10.1016/j.neuroimage.2022.119220.

Glick, S.D., Kuehne, M.E., Raucci, J., Wilson, T.E., Larson, D., Keller, R.W., et al. (1994). Effects of iboga alkaloids on morphine and cocaine self-administration in rats: relationship to tremorigenic effects and to effects on dopamine release in nucleus accumbens and striatum. *Brain Research* 657(1)**,** 14-22. doi: https://doi.org/10.1016/0006-8993(94)90948-2.

Glick, S.D., Maisonneuve, I.M., and Pearl, S.M. (1997). Evidence for roles of κ-opioid and NMDA receptors in the mechanism of action of ibogaine. *Brain Research* 749(2)**,** 340-343. doi: https://doi.org/10.1016/S0006-8993(96)01414-X.

Glick, S.D., Rossman, K., Steindorf, S., Maisonneuve, I.M., and Carlson, J.N. (1991). Effects and aftereffects of ibogaine on morphine self-administration in rats. *European Journal of Pharmacology* 195(3)**,** 341-345. doi: https://doi.org/10.1016/0014-2999(91)90474-5.

Glue, P., Lockhart, M., Lam, F., Hung, N., Hung, C.-T., and Friedhoff, L. (2015). Ascending-dose study of noribogaine in healthy volunteers: Pharmacokinetics, pharmacodynamics,

safety, and tolerability. *The Journal of Clinical Pharmacology* 55(2)**,** 189-194. doi: https://doi.org/10.1002/jcph.404.

González-Maeso, J., Weisstaub, N.V., Zhou, M., Chan, P., Ivic, L., Ang, R., et al. (2007). Hallucinogens recruit specific cortical 5-HT2A receptor-mediated signaling pathways to affect behavior. *Neuron* 53(3)**,** 439-452. doi: https://doi.org/10.1016/j.neuron.2007.01.008.

González, J., Cavelli, M., Castro-Zaballa, S., Mondino, A., Tort, A.B.L., Rubido, N., et al. (2021). EEG gamma band alterations and REM-like Traits underpin the acute effect of the atypical psychedelic ibogaine in the rat. *ACS Pharmacology & Translational Science* 4(2)**,** 517-525. doi: 10.1021/acsptsci.0c00164.

González, J., Prieto, J.P., Rodríguez, P., Cavelli, M., Benedetto, L., Mondino, A., et al. (2018). Ibogaine acute administration in rats promotes wakefulness, long-lasting REM sleep suppression, and a distinctive motor profile. *Frontiers in Pharmacology* 9(374). doi: 10.3389/fphar.2018.00374.

Griffiths, R.R., Johnson, M.W., Carducci, M.A., Umbricht, A., Richards, W.A., Richards, B.D., et al. (2016). Psilocybin produces substantial and sustained decreases in depression and anxiety in patients with life-threatening cancer: A randomized double-blind trial. *Journal of Psychopharmacology* 30(12)**,** 1181-1197. doi: 10.1177/0269881116675513.

Griffiths, R.R., Richards, W.A., McCann, U., and Jesse, R. (2006). Psilocybin can occasion mystical-type experiences having substantial and sustained personal meaning and spiritual significance. *Psychopharmacology* 187(3)**,** 268-283. doi: 10.1007/s00213-006-0457-5.

Hattori, R., Danskin, B., Babic, Z., Mlynaryk, N., and Komiyama, T. (2019). Area-specificity and plasticity of history-dependent value coding during learning. *Cell* 177(7)**,** 1858-1872.e1815. doi: https://doi.org/10.1016/j.cell.2019.04.027.

He, D.-Y., McGough, N.N.H., Ravindranathan, A., Jeanblanc, J., Logrip, M.L., Phamluong, K., et al. (2005). Glial cell line-derived neurotrophic factor mediates the desirable actions of the anti-addiction drug ibogaine against alcohol consumption. *The Journal of Neuroscience* 25(3)**,** 619. doi: 10.1523/JNEUROSCI.3959-04.2005.

Helsley, S., Fiorella, D., Rabin, R.A., and Winter, J.C. (1998). Behavioral and biochemical evidence for a nonessential 5-ht2a component of the ibogaine-induced discriminative stimulus. *Pharmacology Biochemistry and Behavior* 59(2)**,** 419-425. doi: https://doi.org/10.1016/S0091-3057(97)00451-6.

Holschneider, D.P., Givrad, T.K., Yang, J., Stewart, S.B., Francis, S.R., Wang, Z., et al. (2019). Cerebral perfusion mapping during retrieval of spatial memory in rats. *Behavioural Brain Research* 375**,** 112116. doi: https://doi.org/10.1016/j.bbr.2019.112116.

Jefferson, S.J., Gregg, I., Dibbs, M., Liao, C., Wu, H., Davoudian, P.A., et al. (2023). 5-MeO-DMT modifies innate behaviors and promotes structural neural plasticity in mice. *Neuropsychopharmacology* 48(9)**,** 1257-1266. doi: 10.1038/s41386-023-01572-w.

Jiang, M.Y., DeAngeli, N.E., Bucci, D.J., and Todd, T.P. (2018). Retrosplenial cortex has a time-dependent role in memory for visual stimuli. *Behavioral Neuroscience* 132(5)**,** 396-402. doi: 10.1037/bne0000229.

Kanen, J.W., Luo, Q., Rostami Kandroodi, M., Cardinal, R.N., Robbins, T.W., Nutt, D.J., et al. (2022). Effect of lysergic acid diethylamide (LSD) on reinforcement learning in humans. *Psychological Medicine***,** 1-12. doi: 10.1017/S0033291722002963.

Keene, C.S., and Bucci, D.J. (2009). Damage to the retrosplenial cortex produces specific impairments in spatial working memory. *Neurobiology of Learning and Memory* 91(4), 408-414. doi: https://doi.org/10.1016/j.nlm.2008.10.009.
Klee, G.D. (1963). Lysergic acid diethylamide (LSD-25) and ego functions. *Archives of General Psychiatry* 8(5), 461-474.
Kobayashi, Y., and Amaral, D.G. (2003). Macaque monkey retrosplenial cortex: II. Cortical afferents. *Journal of Comparative Neurology* 466(1), 48-79. doi: https://doi.org/10.1002/cne.10883.
Köck, P., Froelich, K., Walter, M., Lang, U., and Dürsteler, K.M. (2021). A systematic literature review of clinical trials and therapeutic applications of ibogaine. *Journal of Substance Abuse Treatment*, 108717. doi: https://doi.org/10.1016/j.jsat.2021.108717.
Koob, G.F., and Le Moal, M. (2001). Drug addiction, dysregulation of reward, and allostasis. *Neuropsychopharmacology* 24(2), 97-129.
Lebedev, A.V., Lövdén, M., Rosenthal, G., Feilding, A., Nutt, D.J., and Carhart-Harris, R.L. (2015). Finding the self by losing the self: Neural correlates of ego-dissolution under psilocybin. *Human Brain Mapping* 36(8), 3137-3153. doi: https://doi.org/10.1002/hbm.22833.
Lefner, M.J., Magnon, A.P., Gutierrez, J.M., Lopez, M.R., and Wanat, M.J. (2021). Delays to reward delivery enhance the preference for an initially less desirable option: Role for the basolateral amygdala and retrosplenial cortex. *The Journal of Neuroscience* 41(35), 7461. doi: 10.1523/JNEUROSCI.0438-21.2021.
Lima da Cruz, R.V., Moulin, T.C., Petiz, L.L., and Leão, R.N. (2018). A single dose of 5-MeO-DMT stimulates cell proliferation, neuronal survivability, morphological and functional changes in adult mice ventral dentate gyrus. *Frontiers in Molecular Neuroscience* 11(312). doi: 10.3389/fnmol.2018.00312.
Ly, C., Greb, A.C., Cameron, L.P., Wong, J.M., Barragan, E.V., Wilson, P.C., et al. (2018). Psychedelics promote structural and functional neural plasticity. *Cell Reports* 23(11), 3170-3182. doi: https://doi.org/10.1016/j.celrep.2018.05.022.
Maddock, R.J. (1999). The retrosplenial cortex and emotion: New insights from functional neuroimaging of the human brain. *Trends in Neurosciences* 22(7), 310-316. doi: https://doi.org/10.1016/S0166-2236(98)01374-5.
Madsen, M.K., Fisher, P.M., Burmester, D., Dyssegaard, A., Stenbæk, D.S., Kristiansen, S., et al. (2019). Psychedelic effects of psilocybin correlate with serotonin 2A receptor occupancy and plasma psilocin levels. *Neuropsychopharmacology* 44(7), 1328-1334. doi: 10.1038/s41386-019-0324-9.
Maisonneuve, I.M., Keller, R.W., and Glick, S.D. (1991). Interactions between ibogaine, a potential anti-addictive agent, and morphine: an in vivo microdialysis study. *European Journal of Pharmacology* 199(1), 35-42. doi: https://doi.org/10.1016/0014-2999(91)90634-3.
Malcolm, B.J., Polanco, M., and Barsuglia, J.P. (2018). Changes in withdrawal and craving scores in participants undergoing opioid detoxification utilizing ibogaine. *Journal of Psychoactive Drugs* 50(3), 256-265. doi: 10.1080/02791072.2018.1447175.
Mandillo, S., Rinaldi, A., Oliverio, A., and Mele, A. (2003). Repeated administration of phencyclidine, amphetamine and MK-801 selectively impairs spatial learning in mice: a

possible model of psychotomimetic drug-induced cognitive deficits. *Behavioural Pharmacology* 14(7).

Manduca, J.D., Thériault, R.-K., Williams, O.O.F., Rasmussen, D.J., and Perreault, M.L. (2020). Transient dose-dependent effects of ketamine on neural oscillatory activity in Wistar-Kyoto rats. *Neuroscience* 441**,** 161-175. doi: https://doi.org/10.1016/j.neuroscience.2020.05.012.

Mao, D., Kandler, S., McNaughton, B.L., and Bonin, V. (2017). Sparse orthogonal population representation of spatial context in the retrosplenial cortex. *Nature Communications* 8(1)**,** 243. doi: 10.1038/s41467-017-00180-9.

Maqueda, A.E., Valle, M., Addy, P.H., Antonijoan, R.M., Puntes, M., Coimbra, J., et al. (2015). Salvinorin-A induces intense dissociative effects, blocking external sensory perception and modulating interoception and sense of body ownership in humans. *International Journal of Neuropsychopharmacology* 18(12). doi: 10.1093/ijnp/pyv065.

Mash, D.C., Duque, L., Page, B., and Allen-Ferdinand, K. (2018). Ibogaine detoxification transitions opioid and cocaine abusers between dependence and abstinence: Clinical observations and treatment outcomes. *Frontiers in Pharmacology* 9(529). doi: 10.3389/fphar.2018.00529.

Mash, D.C., Kovera, C.A., Buck, B.E., Norenberg, M.D., Shapshak, P., Hearn, W.L., et al. (1998). Medication development of ibogaine as a pharmacotherapy for drug dependence. *Annals of the New York Academy of Sciences* 844(1)**,** 274-292.

Mash, D.C., Staley, J.K., Baumann, M.H., Rothman, R.B., and Lee Hearn, W. (1995). Identification of a primary metabolite of ibogaine that targets serotonin transporters and elevates serotonin. *Life Sciences* 57(3)**,** PL45-PL50. doi: https://doi.org/10.1016/0024-3205(95)00273-9.

Mason, N.L., Kuypers, K.P.C., Müller, F., Reckweg, J., Tse, D.H.Y., Toennes, S.W., et al. (2020). Me, myself, bye: Regional alterations in glutamate and the experience of ego dissolution with psilocybin. *Neuropsychopharmacology* 45(12)**,** 2003-2011. doi: 10.1038/s41386-020-0718-8.

Mendez, I.A., Williams, M.T., Bhavsar, A., Lu, A.P., Bizon, J.L., and Setlow, B. (2009). Long-lasting sensitization of reward-directed behavior by amphetamine. *Behavioural Brain Research* 201(1)**,** 74-79. doi: https://doi.org/10.1016/j.bbr.2009.01.034.

Michaiel, A.M., Parker, P.R.L., and Niell, C.M. (2019). A hallucinogenic serotonin-2A receptor agonist reduces visual response gain and alters temporal dynamics in mouse V1. *Cell Reports* 26(13)**,** 3475-3483.e3474. doi: https://doi.org/10.1016/j.celrep.2019.02.104.

Miller, A.M.P., Vedder, L.C., Law, L.M., and Smith, D.M. (2014). Cues, context, and long-term memory: The role of the retrosplenial cortex in spatial cognition. *Frontiers in Human Neuroscience* 8. doi: 10.3389/fnhum.2014.00586.

Millière, R., Carhart-Harris, R.L., Roseman, L., Trautwein, F.-M., and Berkovich-Ohana, A. (2018). Psychedelics, meditation, and self-consciousness. *Frontiers in Psychology* 9. doi: 10.3389/fpsyg.2018.01475.

Mitchell, A.S., Czajkowski, R., Zhang, N., Jeffery, K., and Nelson, A.J.D. (2018). Retrosplenial cortex and its role in spatial cognition. *Brain and Neuroscience Advances* 2**,** 2398212818757098. doi: 10.1177/2398212818757098.

Moliner, R., Girych, M., Brunello, C.A., Kovaleva, V., Biojone, C., Enkavi, G., et al. (2023). Psychedelics promote plasticity by directly binding to BDNF receptor TrkB. *Nature Neuroscience* 26(6)**,** 1032-1041. doi: 10.1038/s41593-023-01316-5.

Moreno, F.A., Wiegand, C.B., Taitano, E.K., and Delgado, P.L. (2006). Safety, tolerability, and efficacy of psilocybin in 9 patients with obsessive-compulsive disorder. *Journal of Clinical Psychiatry* 67(11)**,** 1735-1740.

Moroz, I., Parker, L.A., and Siegel, S. (1997). Ibogaine interferes with the establishment of amphetamine place preference learning. *Experimental and Clinical Psychopharmacology* 5(2)**,** 119-122. doi: 10.1037/1064-1297.5.2.119.

Muthukumaraswamy, S.D., Carhart-Harris, R.L., Moran, R.J., Brookes, M.J., Williams, T.M., Errtizoe, D., et al. (2013). Broadband cortical desynchronization underlies the human psychedelic state. *The Journal of Neuroscience* 33(38)**,** 15171-15183. doi: 10.1523/jneurosci.2063-13.2013.

Nelson, A., and Killcross, S. (2006). Amphetamine exposure enhances habit formation. *Journal of Neuroscience* 26(14)**,** 3805-3812.

Nelson, A.J., Hindley, E.L., Haddon, J.E., Vann, S.D., and Aggleton, J.P. (2014). A novel role for the rat retrosplenial cortex in cognitive control. *Learning and Memory* 21(2)**,** 90-97. doi: 10.1101/lm.032136.113.

Nelson, A.J.D., Hindley, E.L., Vann, S.D., and Aggleton, J.P. (2018). When is the rat retrosplenial cortex required for stimulus integration? *Behavioral Neuroscience* 132(5)**,** 366-377. doi: 10.1037/bne0000267.

Nichols, D.E. (2020). Psilocybin: from ancient magic to modern medicine. *The Journal of Antibiotics* 73(10)**,** 679-686. doi: 10.1038/s41429-020-0311-8.

Noller, G.E., Frampton, C.M., and Yazar-Klosinski, B. (2018). Ibogaine treatment outcomes for opioid dependence from a twelve-month follow-up observational study. *The American Journal of Drug and Alcohol Abuse* 44(1)**,** 37-46. doi: 10.1080/00952990.2017.1310218.

Nordquist, R.E., Voorn, P., de Mooij-van Malsen, J.G., Joosten, R.N.J.M.A., Pennartz, C.M.A., and Vanderschuren, L.J.M.J. (2007). Augmented reinforcer value and accelerated habit formation after repeated amphetamine treatment. *European Neuropsychopharmacology* 17(8)**,** 532-540. doi: https://doi.org/10.1016/j.euroneuro.2006.12.005.

O'Keefe, J., and Dostrovsky, J. (1971). The hippocampus as a spatial map: Preliminary evidence from unit activity in the freely-moving rat. *Brain Research* 34**,** 171-175. doi: 10.1016/0006-8993(71)90358-1.

O'Keefe, J., and Nadel, L. (1978). *The hippocampus as a cognitive map.* Oxford, Clarendon Press.

Obach, R.S., Pablo, J., and Mash, D.C. (1998). Cytochrome P4502D6 catalyzes the O-demethylation of the psychoactive alkaloid ibogaine to 12-Hydroxyibogamine. *Drug Metabolism and Disposition* 26(8)**,** 764-768.

Palhano-Fontes, F., Andrade, K.C., Tofoli, L.F., Santos, A.C., Crippa, J.A.S., Hallak, J.E.C., et al. (2015). The psychedelic state induced by ayahuasca modulates the activity and connectivity of the default mode network. *PloS one* 10(2)**,** e0118143-e0118143. doi: 10.1371/journal.pone.0118143.

Pazos, A., Cortés, R., and Palacios, J.M. (1985). Quantitative autoradiographic mapping of serotonin receptors in the rat brain. II. Serotonin-2 receptors. *Brain Research* 346(2)**,** 231-249. doi: https://doi.org/10.1016/0006-8993(85)90857-1.

Pompeiano, M., Palacios, J.M., and Mengod, G. (1992). Distribution and cellular localization of mRNA coding for 5-HT1A receptor in the rat brain: correlation with receptor binding. *The Journal of Neuroscience* 12(2)**,** 440. doi: 10.1523/JNEUROSCI.12-02-00440.1992.

Pompeiano, M., Palacios, J.M., and Mengod, G. (1994). Distribution of the serotonin 5-HT2 receptor family mRNAs: comparison between 5-HT2A and 5-HT2C receptors. *Molecular Brain Research* 23(1)**,** 163-178. doi: https://doi.org/10.1016/0169-328X(94)90223-2.

Pryazhnikov, E., Mugantseva, E., Casarotto, P., Kolikova, J., Fred, S.M., Toptunov, D., et al. (2018). Longitudinal two-photon imaging in somatosensory cortex of behaving mice reveals dendritic spine formation enhancement by subchronic administration of low-dose ketamine. *Scientific Reports* 8(1)**,** 6464. doi: 10.1038/s41598-018-24933-8.

Ray, T.S. (2010). Psychedelics and the human receptorome. *PloS one* 5(2)**,** e9019. doi: 10.1371/journal.pone.0009019.

Rezvani, A.H., Overstreet, D.H., and Leef, Y.-W. (1995). Attenuation of alcohol intake by Ibogaine in three strains of alcohol-preferring rats. *Pharmacology Biochemistry and Behavior* 52(3)**,** 615-620. doi: https://doi.org/10.1016/0091-3057(95)00152-M.

Riga, M.S., Lladó-Pelfort, L., Artigas, F., and Celada, P. (2018). The serotonin hallucinogen 5-MeO-DMT alters cortico-thalamic activity in freely moving mice: Regionally-selective involvement of 5-HT1A and 5-HT2A receptors. *Neuropharmacology* 142**,** 219-230. doi: https://doi.org/10.1016/j.neuropharm.2017.11.049.

Robinson, S., Keene, C.S., Iaccarino, H.F., Duan, D., and Bucci, D.J. (2011). Involvement of retrosplenial cortex in forming associations between multiple sensory stimuli. *Behavioral neuroscience* 125(4)**,** 578-587. doi: 10.1037/a0024262.

Robinson, S., Todd, T.P., Pasternak, A.R., Luikart, B.W., Skelton, P.D., Urban, D.J., et al. (2014). Chemogenetic silencing of neurons in retrosplenial cortex disrupts sensory preconditioning. *Journal of Neuroscience* 34(33)**,** 10982-10988.

Rovira, V., and Geijo-Barrientos, E. (2016). Intra- and interhemispheric propagation of electrophysiological synchronous activity and its modulation by serotonin in the cingulate cortex of juvenile mice. *PloS one* 11(3)**,** e0150092. doi: 10.1371/journal.pone.0150092.

Rucker, J.J.H., Jelen, L.A., Flynn, S., Frowde, K.D., and Young, A.H. (2016). Psychedelics in the treatment of unipolar mood disorders: a systematic review. *Journal of Psychopharmacology* 30(12)**,** 1220-1229. doi: 10.1177/0269881116679368.

Sanches, R.F., de Lima Osório, F., dos Santos, R.G., Macedo, L.R.H., Maia-de-Oliveira, J.P., Wichert-Ana, L., et al. (2016). Antidepressant effects of a single dose of ayahuasca in patients with recurrent depression: A SPECT study. *Journal of Clinical Psychopharmacology* 36(1).

Sauer, J.-F., Folschweiller, S., and Bartos, M. (2022). Topographically organized representation of space and context in the medial prefrontal cortex. *Proceedings of the National Academy of Sciences* 119(6)**,** e2117300119. doi: 10.1073/pnas.2117300119.

Schenberg, E.E., de Castro Comis, M.A., Alexandre, J.F.M., Tófoli, L.F., Chaves, B.D.R., and da Silveira, D.X. (2017). A phenomenological analysis of the subjective experience elicited by ibogaine in the context of a drug dependence treatment. *Journal of Psychedelic Studies* 1(2)**,** 74-83. doi: https://doi.org/10.1556/2054.01.2017.007.

Schenberg, E.E., de Castro Comis, M.A., Chaves, B.R., and da Silveira, D.X. (2014). Treating drug dependence with the aid of ibogaine: A retrospective study. *Journal of Psychopharmacology* 28(11)**,** 993-1000. doi: 10.1177/0269881114552713.

Schultes, R.E., Hofmann, A., and Rätsch, C. (2001). *Plants of the Gods: Their Sacred, Healing, and Hallucinogenic Powers.* Inner Traditions/Bear.

Schwarz, A.J., Gozzi, A., Reese, T., and Bifone, A. (2007). Functional connectivity in the pharmacologically activated brain: Resolving networks of correlated responses to d-amphetamine. *Magnetic Resonance in Medicine* 57(4)**,** 704-713. doi: https://doi.org/10.1002/mrm.21179.

Sershen, H., Hashim, A., Harsing, L., and Lajtha, A. (1992). Ibogaine antagonizes cocaine-induced locomotor stimulation in mice. *Life Sciences* 50(15)**,** 1079-1086. doi: https://doi.org/10.1016/0024-3205(92)90344-O.

Sershen, H., Hashim, A., and Lajtha, A. (1994). Ibogaine reduces preference for cocaine consumption in C57BL/6By mice. *Pharmacology Biochemistry and Behavior* 47(1)**,** 13-19. doi: https://doi.org/10.1016/0091-3057(94)90105-8.

Sershen, H., Hashim, A., and Lajtha, A. (2001). Chapter 6 Characterization of multiple sites of action of ibogaine. *The Alkaloids: Chemistry and Biology*. Academic Press, 115-133.

Shao, L.-X., Liao, C., Gregg, I., Davoudian, P.A., Savalia, N.K., Delagarza, K., et al. (2021). Psilocybin induces rapid and persistent growth of dendritic spines in frontal cortex in vivo. *Neuron* 109(16)**,** 2535-2544.e2534. doi: https://doi.org/10.1016/j.neuron.2021.06.008.

Sherrill, K.R., Erdem, U.M., Ross, R.S., Brown, T.I., Hasselmo, M.E., and Stern, C.E. (2013). Hippocampus and retrosplenial cortex combine path integration signals for successful navigation. *The Journal of Neuroscience* 33(49)**,** 19304. doi: 10.1523/JNEUROSCI.1825-13.2013.

Shibata, H., Kondo, S., and Naito, J. (2004). Organization of retrosplenial cortical projections to the anterior cingulate, motor, and prefrontal cortices in the rat. *Neuroscience Research* 49(1)**,** 1-11. doi: https://doi.org/10.1016/j.neures.2004.01.005.

Shibata, H., and Naito, J. (2008). Organization of anterior cingulate and frontal cortical projections to the retrosplenial cortex in the rat. *Journal of Comparative Neurology* 506(1)**,** 30-45. doi: https://doi.org/10.1002/cne.21523.

Sit, K.K., and Goard, M.J. (2023). Coregistration of heading to visual cues in retrosplenial cortex. *Nature Communications* 14(1)**,** 1992. doi: 10.1038/s41467-023-37704-5.

Smigielski, L., Kometer, M., Scheidegger, M., Krähenmann, R., Huber, T., and Vollenweider, F.X. (2019). Characterization and prediction of acute and sustained response to psychedelic psilocybin in a mindfulness group retreat. *Scientific Reports* 9(1)**,** 14914. doi: 10.1038/s41598-019-50612-3.

Sporns, O. (2006). Small-world connectivity, motif composition, and complexity of fractal neuronal connections. *Biosystems* 85(1)**,** 55-64. doi: https://doi.org/10.1016/j.biosystems.2006.02.008.

Spyraki, C., Fibiger, H.C., and Phillips, A.G. (1982). Dopaminergic substrates of amphetamine-induced place preference conditioning. *Brain Research* 253(1)**,** 185-193. doi: https://doi.org/10.1016/0006-8993(82)90685-0.

Sugar, J., Witter, M., van Strien, N., and Cappaert, N. (2011). The retrosplenial cortex: intrinsic connectivity and connections with the (para)hippocampal region in the rat. An interactive connectome. *Frontiers in Neuroinformatics* 5. doi: 10.3389/fninf.2011.00007.

Sutherland, R.J., Whishaw, I.Q., and Kolb, B. (1988). Contributions of cingulate cortex to two forms of spatial learning and memory. *The Journal of Neuroscience* 8(6)**,** 1863. doi: 10.1523/JNEUROSCI.08-06-01863.1988.
Swanson, L.R. (2018). Unifying theories of psychedelic drug effects. *Frontiers in Pharmacology* 9**,** 172.
Tagliazucchi, E., Carhart-Harris, R., Leech, R., Nutt, D., and Chialvo, D.R. (2014). Enhanced repertoire of brain dynamical states during the psychedelic experience. *Human Brain Mapping* 35(11)**,** 5442-5456. doi: 10.1002/hbm.22562.
Todd, T.P., Mehlman, M.L., Keene, C.S., DeAngeli, N.E., and Bucci, D.J. (2016). Retrosplenial cortex is required for the retrieval of remote memory for auditory cues. *Learning & Memory* 23(6)**,** 278-288.
Treccani, G., Ardalan, M., Chen, F., Musazzi, L., Popoli, M., Wegener, G., et al. (2019). S-Ketamine reverses hippocampal dendritic spine deficits in Flinders sensitive line rats within 1 h of administration. *Molecular Neurobiology* 56(11)**,** 7368-7379. doi: 10.1007/s12035-019-1613-3.
Turton, S., Nutt, D.J., and Carhart-Harris, R.L. (2014). A qualitative report on the subjective experience of intravenous psilocybin administered in an fMRI environment. *Current drug abuse reviews* 7(2)**,** 117-127.
van Groen, T., and Wyss, J.M. (1992). Connections of the retrosplenial dysgranular cortex in the rat. *Journal of Comparative Neurology* 315(2)**,** 200-216. doi: https://doi.org/10.1002/cne.903150207.
Vann, S.D., and Aggleton, J.P. (2002). Extensive cytotoxic lesions of the rat retrosplenial cortex reveal consistent deficits on tasks that tax allocentric spatial memory. *Behavioral Neuroscience* 116(1)**,** 85-94. doi: 10.1037/0735-7044.116.1.85.
Vann, S.D., Aggleton, J.P., and Maguire, E.A. (2009). What does the retrosplenial cortex do? *Nature Reviews Neuroscience* 10(11)**,** 792-802. doi: 10.1038/nrn2733.
Vargas, M.V., Dunlap, L.E., Dong, C., Carter, S.J., Tombari, R.J., Jami, S.A., et al. (2023). Psychedelics promote neuroplasticity through the activation of intracellular 5-HT2A receptors. *Science* 379(6633)**,** 700-706. doi: doi:10.1126/science.adf0435.
Vedder, L.C., Miller, A.M.P., Harrison, M.B., and Smith, D.M. (2017). Retrosplenial cortical neurons encode navigational cues, trajectories and reward locations during goal directed navigation. *Cerebral Cortex* 27(7)**,** 3713-3723. doi: 10.1093/cercor/bhw192.
Vesuna, S., Kauvar, I.V., Richman, E., Gore, F., Oskotsky, T., Sava-Segal, C., et al. (2020). Deep posteromedial cortical rhythm in dissociation. *Nature* 586(7827)**,** 87-94. doi: 10.1038/s41586-020-2731-9.
Vogt, B.A., and Paxinos, G. (2014). Cytoarchitecture of mouse and rat cingulate cortex with human homologies. *Brain Structure and Function* 219(1)**,** 185-192. doi: 10.1007/s00429-012-0493-3.
Wasko, M.J., Witt-Enderby, P.A., and Surratt, C.K. (2018). DARK classics in chemical neuroscience: Ibogaine. *ACS Chemical Neuroscience* 9(10)**,** 2475-2483. doi: 10.1021/acschemneuro.8b00294.
Whishaw, I.Q., Maaswinkel, H., Gonzalez, C.L.R., and Kolb, B. (2001). Deficits in allothetic and idiothetic spatial behavior in rats with posterior cingulate cortex lesions. *Behavioural Brain Research* 118(1)**,** 67-76. doi: https://doi.org/10.1016/S0166-4328(00)00312-0.

Wyass, J.M., and Van Groen, T. (1992). Connections between the retrosplenial cortex and the hippocampal formation in the rat: A review. *Hippocampus* 2(1)**,** 1-11. doi: 10.1002/hipo.450020102.

Yaden, D.B., and Griffiths, R.R. (2021). The Subjective Effects of Psychedelics Are Necessary for Their Enduring Therapeutic Effects. *ACS Pharmacology & Translational Science* 4(2)**,** 568-572. doi: 10.1021/acsptsci.0c00194.

Yamawaki, N., Corcoran, K.A., Guedea, A.L., Shepherd, G.M.G., and Radulovic, J. (2019). Differential contributions of glutamatergic hippocampal→retrosplenial cortical projections to the formation and persistence of context memories. *Cerebral Cortex* 29(6)**,** 2728-2736. doi: 10.1093/cercor/bhy142.

Yu, S., Ribeiro, T.L., Meisel, C., Chou, S., Mitz, A., Saunders, R., et al. (2017). Maintained avalanche dynamics during task-induced changes of neuronal activity in nonhuman primates. *eLife* 6**,** e27119. doi: 10.7554/eLife.27119.

Zhang, J., Qu, Y., Chang, L., Pu, Y., and Hashimoto, K. (2019). (R)-Ketamine rapidly ameliorates the decreased spine density in the medial prefrontal cortex and hippocampus of susceptible mice after chronic social defeat stress. *International Journal of Neuropsychopharmacology* 22(10)**,** 675-679. doi: 10.1093/ijnp/pyz048.

CHAPTER 2: PSILOCYBIN REDUCES FUNCTIONAL CORRELATION AND THE ENCODING OF SPATIAL INFORMATION BY NEURONS IN MOUSE RETROSPLENIAL CORTEX

Victorita E. Ivan[1]*, David P. Tomàs-Cuesta[1]*, Ingrid M. Esteves[1], Artur Luczak[1], Majid Mohajerani[1,2], Bruce L. McNaughton[1,3], Aaron J. Gruber[1]✉

[1]Canadian Centre for Behavioural Neuroscience, Department of Neuroscience, University of Lethbridge, Lethbridge, Alberta, Canada

[2]Douglas Research Centre, Department of Psychiatry, McGill University

[3]Center for the Neurobiology of Learning and Memory, University of California Irvine, Irvine, California, USA

*The authors contributed equally.

✉ Aaron J. Gruber

Email: aaron.gruber@uleth.ca

Keywords: retrosplenial cortex, psychedelics, ketanserin, mutual information, serotonin

Submitted to *European Journal of Neuroscience* (Ivan et al., 2024)

2.1 ABSTRACT

Psychedelic drugs have profound effects on perception, cognition, and mood. How psychedelics affect neural signaling to produce these effects remains poorly understood. We investigated the effect of the classic psychedelic psilocybin on neural activity patterns and spatial encoding in the retrosplenial cortex of head-fixed mice navigating on a treadmill. The place specificity of neurons to distinct locations along the belt was reduced by psilocybin. Moreover, the stability of place-related activity across trials decreased. Psilocybin also reduced the functional correlation among simultaneously recorded neurons. The 5-HT_{2A}R (serotonin 2A receptor) antagonist ketanserin blocked these effects. These data are consistent with proposals that psychedelics increase the entropy of neural signaling, and provide a potential neural mechanism contributing to disorientation frequently reported by humans after taking psychedelics.

2.2 INTRODUCTION

Psychedelic drugs have profound acute effects on perception, cognition, and mood. Molecules affecting a variety of neurotransmitter receptor types have psychedelic properties. The serotonin, or hydroxytryptophan (5-HT), 2A receptor has been identified as the primary mediator of the psychedelic effects of classic psychedelics such as psilocybin (Vollenweider et al., 1998; Quednow et al., 2012). 5-HT can modulate neural activity in the brain's neocortex through presynaptic and postsynaptic neuromodulatory effects on cortical neurons (Andrade, 2011), which express a variety of 5-HT receptor types. Several primary effects of psilocybin are blocked by the 5-HT_{2A} antagonist ketanserin (Kometer et al., 2012; Torrado Pacheco et al., 2023). Ketanserin, however, does not block all of its effects (Carter et al., 2005; Hesselgrave et al., 2021). Therefore, non-5-HT_{2A} receptors likely contribute to the effects of psilocybin on mentation.

The effects of psilocybin on neural encoding and brain dynamics have largely been studied using non-invasive imaging in humans (Carhart-Harris et al., 2012; Carhart-Harris et al., 2017b; Daws et al., 2022). This work suggests that the coordination of activity among brain regions becomes less structured (Muthukumaraswamy et al., 2013; Varley et al., 2020). It remains to be determined if this also occurs at the level of neurons, and if this is due more to corruption of the inputs to cortical networks involved in perception, or more due to corruption of the dynamics within these networks. The few existing studies of cellular-level effects in behaving animals report discrepant effects. A recent study of visual cortex showed little effect of a classic psychedelic (2,5-dimethoxy-4-iodoamphetamine; DOI) on responses to visual inputs in mouse primary visual cortex (Michaiel et al., 2019). On the other hand, we reported that the non-classic psychedelic ibogaine significantly degrades the encoding of spatial information in a cortical region called the retrosplenial cortex (RSC) (Ivan et al., 2023). The discrepancy between these studies may involve

differences in brain region and/or the pharmacology of the psychedelic used. Here, we test if the classic psychedelic psilocybin degrades spatial information in RSC similarly to ibogaine, and if this depends on 5-HT_{2A} receptors.

The RSC encodes the spatial state of animals within an environment and supports navigation in freely moving animals (Keene and Bucci, 2009; Alexander and Nitz, 2015). Some RSC neurons activate when an animal traverses specific regions of an environment, similar to 'place cells' in the hippocampus (O'Keefe and Nadel, 1978). RSC neurons generate similar place activity in head-fixed animals navigating virtual environments (Mao et al., 2017; Esteves et al., 2021). The RSC is a key node in a network linking the hippocampus (HPC) with the medial prefrontal cortex (mPFC) (Wyass and Van Groen, 1992; Fisk and Wyss, 1999; Shibata et al., 2004). This network is involved in generating representations of environments via cognitive maps (O'Keefe and Nadel, 1978; Iaria et al., 2007), and navigation decisions to achieve goals. 5-HT appears to affect this processing. Psilocin, psilocybin's active metabolite, causes a decrease in the blood-oxygen-level-dependent (BOLD) signal of rat RSC (Spain et al., 2015). Conversely, resting-state functional magnetic resonance imaging (fMRI) in lightly-anesthetized mice found that psilocybin causes an increase in functional correlation (FC) between the RSC, cingulate cortex, and other structures expressing 5-HT_{2A} receptors, such as the ventral striatum (Grandjean et al., 2021). RSC interactions with other structures thus appears to be modulated by psilocybin, and likely other psychedelic drugs. The spatial information encoded in RSC provides a means to assess how psychedelics affect neural information processing at the cellular level. Here, we quantify how psilocybin, with or without blockage of 5-HT_{2A} receptors, affect spatial representation and neural dynamics of large ensembles of neurons in the agranular RSC of head-fixed mice navigating a virtual environment.

2.3 METHODS

Animals

Adult (4-9 month old) Thy1-GCaMP6s mice (n=10; 2F/8M), weighing 19-28 g, were housed in standard rodent cages, and maintained at 24 °C under a 12 h light/dark cycle. Mice had free access to food and water before training. All experiments were performed during the light cycle (between 7:30 AM and 7:30 PM). Procedures were in accordance with the guidelines established by the Canadian Council on Animal Care, and with protocols approved by the Animal Welfare Committee of the University of Lethbridge.

Surgery

Before surgery, animals received buprenorphine (0.05 mg/kg SC) and dexamethasone (0.2 mg/kg IM). They were then anesthetized with isoflurane (1-1.5%) and head fixed in a stereotaxic frame with body temperature maintained at 37.0 ± 0.5 ◦C with a heating pad. Mice received a 5 mm bilateral craniotomy (AP: +1 to -4; ML: -2.5 to +2.5), which was then covered with three layers of coverslips affixed with optical adhesive (NOA71, Norland). The coverslip was attached to the skull using Vetbond, and a titanium head plate was fixed to the skull using metabond. Post-surgical care included careful weight monitoring and subcutaneous injections of meloxicam (Metacam 1 mg/kg) and enrofloxacin (Baytril, 10 mg/kg) for three days after implant.

Drugs

Psilocybin was obtained from Toronto Research Chemicals, Canada, in powder form and diluted in sterile water in order to achieve a dose of 1.5 or 15 mg/kg in a 0.1 ml volume for each mouse. Ketanserin tartrate salt was obtained from Sigma-Aldrich Canada, in powder form, and dissolved in 20% DMSO, and the stock solutions were stored at −20 °C. The stock solutions were prepared on the day of injection when possible and diluted in saline to achieve a dose of 1 or 5 mg/kg. The control animals received 0.1 ml 0.9% saline solution. All injections were intraperitoneal.

Experimental procedure for behavior

Head-fixed mice were trained to voluntarily run on a treadmill using a positive reinforcement paradigm. They received a drop of 10% sucrose solution on every trial, consisting of one lap of the treadmill belt. Animals were water restricted during training and testing. They had *ad libitum* access to water for up to 30 minutes per day, and their body weight was carefully monitored throughout the experiment to ensure the weight loss did not exceed 15% of their baseline value. The treadmill belt consisted of a Velcro strip that was 150 cm long and 4 cm wide. Three tactile cues with different textures were placed at different locations on the belt. Additionally, we used one auditory cue (1kHz) and one blue light LED cue that each activated at a specific and constant belt position during each trial. An optical encoder attached to the wheel shaft was used to monitor belt movement. A microcontroller was used to monitor the encoder, a licking sensor, and the reward delivery. Training continued in daily sessions until mice performed at least 20 trials in 20 minutes. Mice were trained on one belt and then transferred to a new belt with a different cue configuration for the imaging sessions (see Fig. 1 diagram of cue locations). The training and

testing belts were similar, with the same length, same number of tactile cues, with similar size and texture, placed in different locations along the belt. During testing, the visual cue was delivered on 80% of the trials, while the auditory cue was delivered on 100% of the trials.

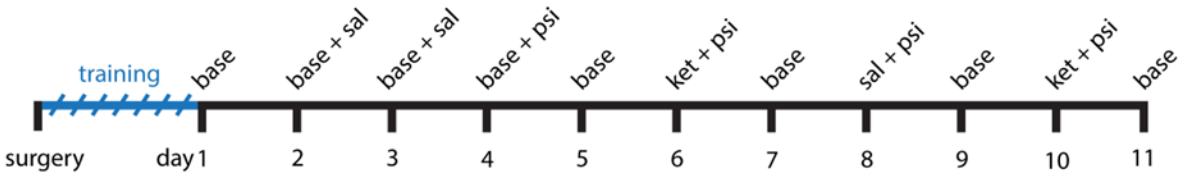

Fig. 2.1: Experimental timeline.

Neural activity was imaged in daily sessions of the task for 15-20 minutes. For drug days, we recorded first a baseline activity for 10 mins in every session. In some sessions, mice (n=7) were injected with either saline or ketanserin before the baseline recording (see Fig. 1). After the 10 minute baseline recording, mice were given an injection of psilocybin or saline. 10 minutes after injection, mice were recorded again for 10 minutes. Recordings were performed starting at 10 minutes after each injection. Each animal was imaged for one session before any injections, for two days of saline injections, and then received 4 days of psilocybin every other day, with or without the ketanserin pretreatment. All experimental animals received 15 mg/kg psilocybin on all 4 days (day 4, 6, 8, and 10). The animals were then assigned to one of two group to receive ketanserin at either low dose (1 mg/kg; n=4) or high dose (5 mg/kg; n=3) before psilocybin. The animals within each group received the same dose of ketanserin pretreatment on both testing days (day 6 and 10). The animals that originally received high dose (n=3) also received 2 doses of low ketanserin paired with low (1.5 mg/kg) psilocybin after day 11. A separate control group (n = 3) received only saline in the same schedule as the treatment group. Statistical tests were performed using GraphPad Prism 10.

Two-Photon Imaging

Neural activity was imaged using a 2-photon microscope (Bergamo II multiphoton microscopy, Thorlabs) through a 16x water-immersion objective lens (NA=0.8, Nikon). Excitation was with a Ti:sapphire pulsed laser (Coherent) tuned to a wavelength of 920 nm, ~80mW power, and controlled by a galvo-resonant X-Y scanner. Images were acquired at depths between 135 μm – 160 μm (layer II/III), from a field of view of 835 x 835 μm. Images were digitized at a sampling rate of 19 Hz, and at a resolution of 800 x 800 pixels. Imaging data from all animals were acquired from one hemisphere of either the left or right RSC (AP: -1 to -3 mm; ML: 0 to +/- 1 mm).

Pre-processing

Automatic image pre-processing was performed using the Suite-2P algorithm (Pachitariu et al., 2017), as previously described (Mao et al., 2017; Mao et al., 2018). The regions of interest (ROIs) detected were inspected manually and labelled as cells or non-cells by experienced users. For each ROI, the ΔF/F time courses were deconvolved using constrained non-negative matrix factorization (Pnevmatikakis et al., 2016), and all subsequent analyses were conducted using the deconvolved time-courses. For injection days, the imaging sequences of both pre- and post-injection intervals were combined during pre-processing so as to acquire the activity of the same set of cells (ROIs) before and after injections.

Computing spatial encoding

In order to identify spatially tuned neurons, we computed the adjusted mutual information (MI) (Vinh et al., 2010) between the firing rate of each neuron and the position of the

mouse in the belt. We first divided the belt into 50 bins (3 cm each). For each bin and trial, we summed the neuron's activity and binned it into 4 levels, giving us the joint bin-activity discrete distribution, which we use to compute the mutual information. The MI used here is an adjustment of mutual information which accounts for the number of trials, which differs among sessions, and thus is appropriate to compare cells from different sessions on the same scale. The MI is upperlimited by 1 and takes an expected value of 0 when the firing and position are independent. Negative values signify that the MI for that cell is lower than the MI one would expect solely due chance.

Unit functional connectivity

The clustering method (Watts and Strogatz, 1998) measures how many of a given neuron's neighbors are themselves neighbors of each other. In our analysis, this corresponds to computing, for a given neuron *i,* how many of the neurons that have high functional correlation with *i* have high functional correlation (FC) between themselves. We chose this measure because it neatly encapsulates the dissolution of the tightly interconnected neuronal clusters.

The clustering is computed as the geometric average of the subgraph edge weights (Onnela et al., 2005):

$$c_u = \frac{1}{\deg(\mathrm{u})\,(deg(\mathrm{u}) - 1))} \sum_{\mathrm{vw}} (\widehat{w}_{uv}\,\widehat{w}_{uw}\widehat{w}_{vw})^{1/3}$$

Where the edge weights $\widehat{w}_{uv}$ are normalized by the maximum network weight:

$$\widehat{w}_{uv} = w_{uv}/max(w)$$

We then took the mean over all the nodes in the network:

$$C = \frac{1}{n} \sum_{v \in G} c_v$$

We used the networkx package (Hagberg et al., 2008) to perform these calculations.

Computing the apparent functional connectivity among neurons involved several steps. First, the spikes underlying the calcium fluorescence traces were inferred using a deconvolution algorithm (Friedrich et al., 2017). Next, the data in which the mouse is slow or not moving (below the 10% quantile of the velocity distribution over the track) is removed. The track is then divided into 50 spatial bins. The trial-averaged activity in each bin is computed for each cell to create a 'tuning curve' over the belt. The Pearson correlation between the tuning curves of all cell pairs is then computed. To visualize clusters in the cells x cells spatial correlation matrix, the columns/rows were ordered so that highly correlated cells are adjacent. For each neuron, a vector of its correlations with all other cells was generated. In order to determine the similarity between the correlation structures, the pairwise euclidean distances between those vectors were calculated. Using the unweighted pair group method with arithmetic mean (UPGMA), a hierarchical clustering on these measures was conducted (Sokal, 1958). To assess the amount of clustering in the spatial correlation matrices, we computed the average clustering coefficient (Saramäki et al., 2007), a measure which quantifies how many cells with similar firing patterns are similar between each other, averaged over all cells; this coefficient is independent of the ordering of rows/columns.

2.4 RESULTS

We used 2-photon imaging to record the activity of ensembles of individual neurons (112-732 simultaneous cells per session; mean = 380.6, STD = 100.1) in the superficial layers (135 – 160 μm; layer II/III) of RSC in head-fixed mice (Fig. 2.2.A). Mice were recorded while running on a treadmill belt that had narrow tactile cues laid across the width of the belt in three positions along its length, as well as one auditory cue and one light cue that each activated at specific places in the virtual environment (i.e. belt position). After running for one full lap of the belt, the animals received a 10% sucrose reward. Mice were injected (i.p.) with saline 10 mins prior to task initiation and neural recordings were performed for a 10-minute baseline ("before") period. They were then injected with either psilocybin (15 mg/kg) or the same volume of saline vehicle 10 mins prior to a second neural recording period. We used both within-session (recording before & after 2nd injection) and within-animal (each received psilocybin or saline on different sessions) controls. We used 2-photon imaging to record the activity of ensembles of individual neurons (112-732 simultaneous cells per session; mean = 380.6, STD = 100.1) in the superficial layers (135 – 160 μm; layer II/III) of RSC in 10 (2F/8M) head-fixed mice (Fig. 2.A). Mice were recorded while running on a treadmill belt that had narrow and distinct tactile cues laid across the width of the belt in three positions along its length, as well as one auditory cue and one light cue that each activated at specific places in the virtual environment (i.e. belt position). After running for one full lap of the belt, the animals received a 10% sucrose reward. Mice were injected (i.p.) with saline 10 mins prior to task initiation and neural recordings were performed for a 10-minute baseline ("before") period. They were then injected with either psilocybin (15 mg/kg) or the same volume of saline vehicle 10 mins prior to a second neural recording period. We used both within-session (recording before & after 2nd injection) and within-animal (each received psilocybin or saline on different

sessions) controls. Statistical inference of drug effect was determined by two-way (session x psilocybin/saline) repeated measures (RM) ANOVA. Unless stated otherwise, the reported source of variation is the main effect of psilocybin computed as percentage change from baseline for each session. If an outlier is identified using robust regression and outlier removal (ROUT; Q = 1%), or a value is missing due to technical error, the RM two-way ANOVA is replaced by a repeated measures mixed effects model with restricted maximum likelihood (REML). This mixed model is a commonly used method when values are missing randomly (Berke et al., 2022).

Psilocybin injection lowered the animals' movement as measured by belt velocity (Fig. 2.B; RM two-way (session x saline/psilocybin) ANOVA; main effect of drug: $F(1, 6) = 12.01$, $p = 0.013$). The psilocybin-induced retardation of locomotion is consistent with previous reports (Halberstadt et al., 2011; Tylš et al., 2016). Psilocybin did not affect the number of trials per minute completed (Fig. 2.C; REML main effect of drug: $F(1, 6) = 2.58$, $p = 0.159$; ROUT (n=1)) or the proportion of time the animals were stationary between the start of a lap and the arrival at the feeder location (stop ratio; Fig. 2.D; RM two-way ANOVA; $F(1, 6) = 0.27$, $p = 0.621$). The average neural activity rate had a non-significant trend to decrease after drug administration (Fig. 2.E; two-way ANOVA; $F(1, 6) = 3.30$, $p = 0.118$). A second cohort of animals that only ever received saline (n=3) showed no significant effect of injection on any of these measures (Supplemental Fig. 1), suggesting that these are effects of the drug.

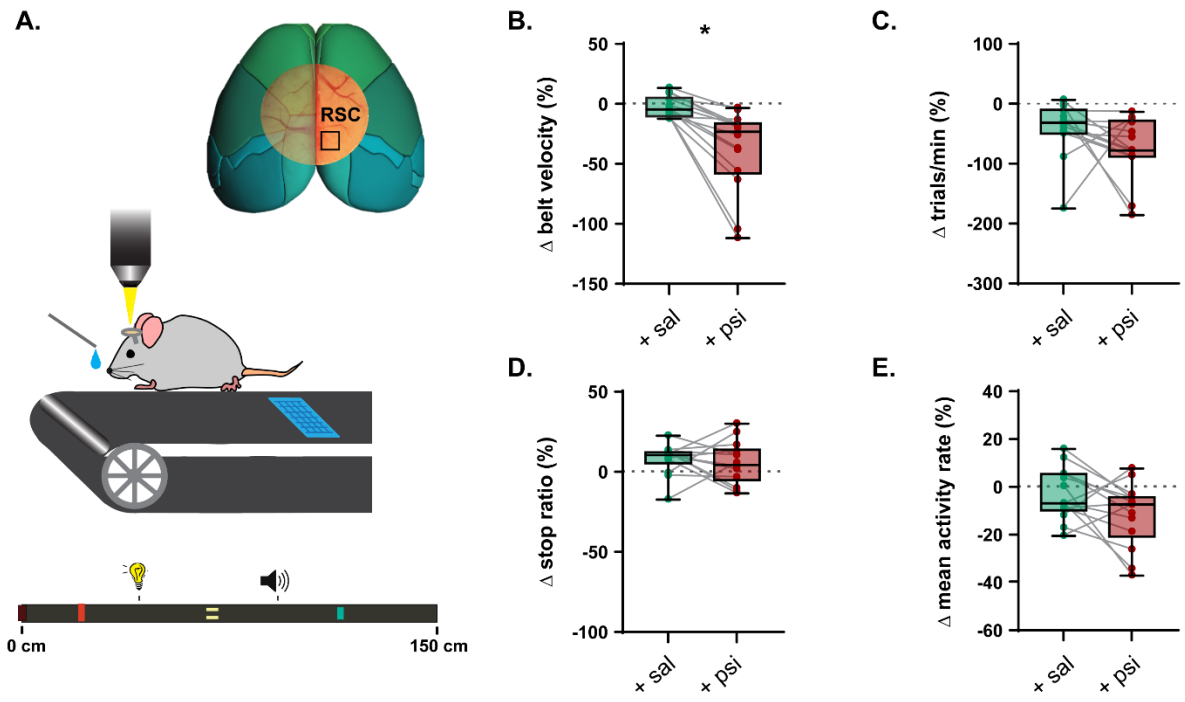

Fig. 2.2: Behavioral effects of psilocybin. A. Illustration of experimental setup and location of the field of view over RSC (inset). Symbols on the treadmill belt indicate approximate locations of tactile cues, as well as locations of visual and auditory cues. B. Box plots and individual session-averaged values of the percentage change of the belt velocity from baseline after saline administration in one session, and after psilocybin administration in another session for the same rats (n=7, two sessions of each condition per subject). C. Percentage change from baseline of the number of trials per minute. D. Percentage change from baseline of the proportion of time that mice were stationary during a trial. E. Percentage change from baseline of the mean activity rate of all neurons recorded simultaneously in a session. Statistical significance ($p<0.05$) is indicated by '*'. Dots are averages from each session.

Many RSC neurons activated at specific locations on the belt during each trial (Fig. 3.A), whereas other cells were not selective to particular positions or have high variability. In order to quantify the amount of spatial information conveyed by each neuron, we computed an adjusted

form of mutual information (MI) between each cell's activity and belt position (details in methods). This metric captures variance of activity along one lap of the belt, as well as variance from trial to trial (Souza et al., 2018). We then restricted analysis of spatial encoding to the cells that were most selective to position (top quartile of MI distribution) in the baseline data. Psilocybin significantly decreased the mean MI of these cells (Fig. 3.B; REML: $F(1, 23) = 6.41$, $p = 0.019$; ROUT (n=1)). We also investigated the average cross correlation of position-dependent cellular activity between trials to assess the stability of spatial tuning. These trial-to-trial correlations (AC) decreased after psilocybin but not saline (Fig. 3.C; REML: $F(1, 23) = 19.51$, $p = 0.0002$; ROUT (n=1)), suggesting less stability of spatial representations after administration of psilocybin as compared to saline.

We next sought to determine if psilocybin affected the functional correlation of activity among cells within the RSC. We computed the pair-wise correlation of activity among all neurons recorded simultaneously during a session, and used hierarchical clustering to order the units so that functionally similar units were adjacent. We applied the same matrix ordering to the activity of the same cells collected after psilocybin administration to visualize any changes in correlation structure (Fig. 3.D; Supplemental Fig. 2 shows an example from every subject). We quantified psychedelic-induced changes in functional correlation patterns by computing the clustering coefficient of the correlation matrix. This coefficient is high when there are multiple clusters, each of which containing functionally-similar units. Psilocybin reduced the clustering coefficient (Fig. 3.E; RM two-way ANOVA; $F(1, 6) = 14.01$, $p = 0.009$), indicating a loss of functional correlation structure. In other words, each neuron is activating more independently from the others. 5-HT_{2A}R is a metabotropic receptor and may thus affect Ca^{2+} dynamics in neurons. This could affect the dynamics of the GCaMP signal and thereby influence metrics such as AC. We therefore analyzed the decay time constant of GCaMP fluorescence signal to assess such possible effects of

psilocybin. Although the mean decay time constant was reduced more following psilocybin than saline, the effect is small relative to the variance of time constants and is therefore unlikely to have a meaningful effect on the AC values (Supplemental Fig. 3).

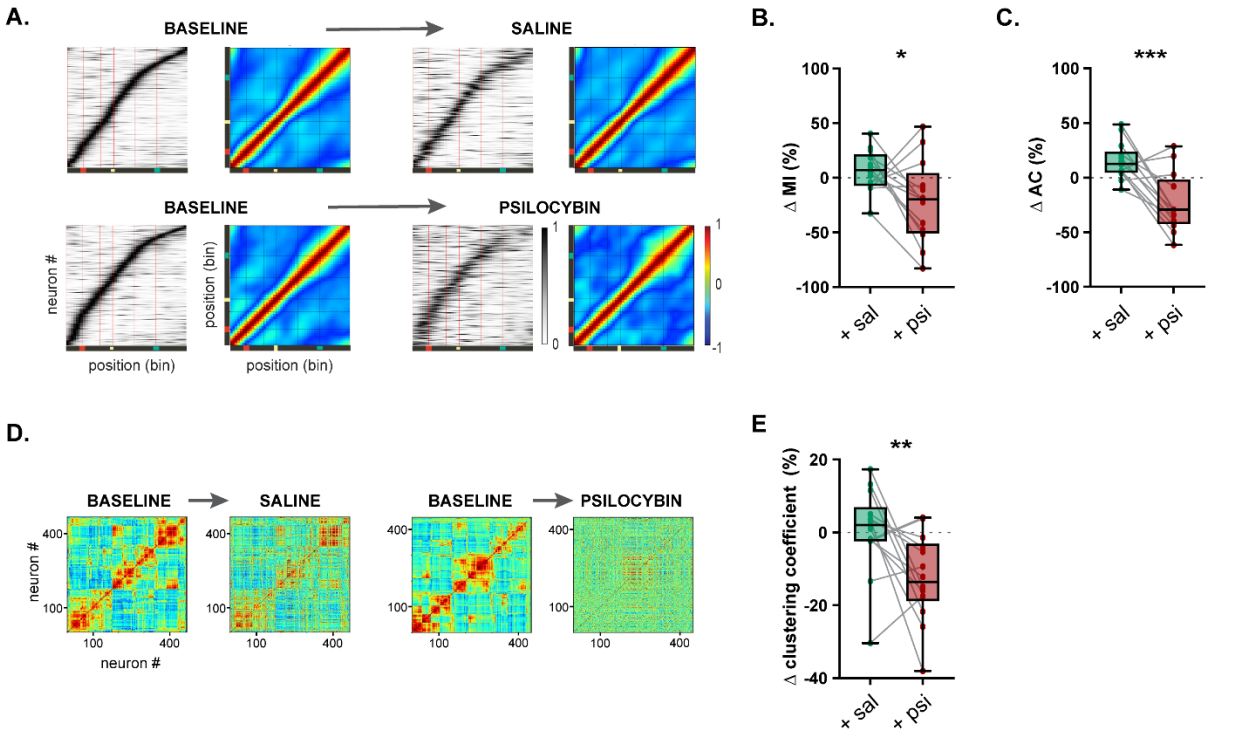

Fig. 2.3: Effects of psilocybin on spatial encoding by neurons in the RSC. A. Leftward panels (black/white) show session-averaged activity of all position-tuned cells ordered by lag to peak activity. The abscissa is treadmill belt position, the ordinate is individual neurons, and shade indicates average normalized activity density of each neuron along the belt. Darker shade is higher activity. Rightward panels (color) shows the mean autocorrelation of activity for the same cells. Grouped panels show aggregated data from the same sessions before (left two panels) and after (right two panels) injection. Sessions testing saline (top) were separate from those testing psilocybin (bottom). The cue zones are indicated by red vertical lines. B. Box plots and individual session-averaged values of percentage change of the mean mutual information (MI) with respect to baseline within each recording session. C. Percentage change of the average trial-to-trial correlation (AC) with respect to baseline within each recording day. D. Pairwise correlation matrices of unit activity in one representative session before/after saline (left) and before/after

psilocybin (right). E. Percentage change of the means correlation coefficients within each recording session. Statistical significance ($p<0.05$) is indicated by '*', ($p<0.01$) is indicated by '**', and ($p<0.001$) is indicated by '***'.

We next investigated if these effects of psilocybin on neural activity were mediated by 5-HT_{2A}R by injecting ketanserin (an antagonist of this receptor) prior to the baseline recording period, and then injecting psilocybin prior to the second recording period. We used a randomized schedule of injection after baseline recordings. Treatments were: low dose ketanserin (k; 1 mg/kg) followed by low dose psilocybin (p; 1.5 mg/kg; n = 3); low dose ketanserin followed by high dose psilocybin (**P**; 15 mg/kg; n = 4); or high dose ketanserin (**K**; 5 mg/kg) followed by high dose psilocybin (n = 3). For each treatment sequence, we recorded the neural activity twice in each animal. One session for the k-**P** group was lost due to technical error. We therefore used the REML model for statistical analysis. Ketanserin blocked the effects of high or low dose psilocybin on all behavioral measures, firing rate, MI, trial-to-trial correlation, and clustering of cross-correlations (Fig. 4. A-G), as reported by the percentage change in psilocybin from the ketanserin pretreatment. REML main effect of drug for: belt velocity: $F(2, 7) = 1.05$, $p = 0.39$; number of trials per minute: $F(2, 7) = 0.62$, $p = 0.56$; stop probability: $F(2, 7) = 0.94$, $p = 0.43$; mean activity rate: $F(2, 7) = 1.65$, $p = 0.25$; MI: $F(2, 7) = 1.71$, $p = 0.24$; AC: $F(2, 7) = 0.33$, $p = 0.72$; clustering coefficient: $F(2, 7) = 0.43$, $p = 0.66$. The high dose ketanserin appears to be less successful at blocking the effects of high psilocybin on MI or firing rate (Fig. 4. D-E), but these trends do not reach statistical significance. Nonetheless, it appears that ketanserin blocks or reduces the effects of psilocybin on both behavior and neural activity, suggesting that 5-HT_{2A}R are involved in the phenomena.

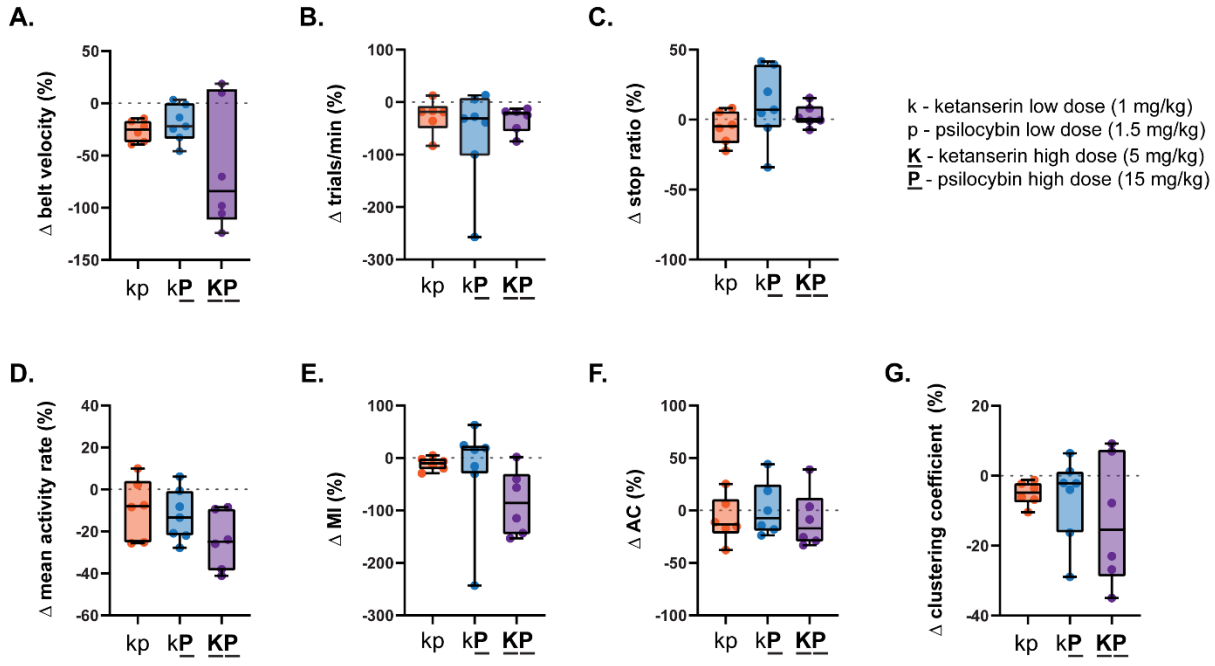

Fig. 2.4. Effects of ketanserin pretreatment on psilocybin-mediated changes in RSC spatial encoding. A. Box plots and individual values of percentage change from baseline in belt velocity for the different dose combinations with either low (k; 1 mg/kg) or high (**K**; 5 mg/kg) ketanserin pretreatment and low (p; 1.5 mg/kg) or high (**P**; 15 mg/kg) psilocybin administration. B. Percentage change in number of trials per minute for each group. C. Percentage change in the time the mice were stationary during a trial. D. Box plots and individual values of percentage change in average firing rates for each group. E. Percentage change in adjusted mutual information (MI). F. Percentage change in mean trial-to-trial correlations (AC). G. Percentage change in mean correlation coefficients.

2.5 DISCUSSION

In this study, psilocybin reduced locomotion, decreased spatial information encoded by RSC cells, and decreased functional correlation among RSC neurons in the agranular region. The 5-HT_{2A} antagonist ketanserin blocked the behavioral effects and prevented the loss of spatial

information. Unexpectedly, the higher dose of ketanserin (5 mg/kg) had a diminished effect on blocking the psilocybin effects on firing rate and MI. Nonetheless, the preponderance of evidence suggests that the effects of psilocybin in this study are primarily mediated by 5-HT_{2A}R. Treatment effects were sufficiently strong as to overcome potential variance of sex and age. It is possible that these independent factors play a role in effect magnitudes, but we do not have sufficient statistical power in the present sample to robustly test for them.

The administration of psilocybin reduced locomotion speed in the present data, consistent with previous reports (Halberstadt et al., 2011; Tylš et al., 2016). Psilocybin also showed a trend to decrease the mean activity rate of RSC neurons in this study, which contrasts the increase in RSC activity rate by the non-classic psychedelic ibogaine in our previous study using the same experimental apparatus (Ivan et al., 2023). We are unaware of other prior studies examining effects of psychedelics on single unit activity of RSC neurons. Some indirect evidence is consistent with our finding. Psilocybin's active metabolite, psilocin, caused a decrease in the BOLD signal relative to baseline in rat RSC (Spain et al., 2015). This paper also reported a decrease in the anterior cingulate cortex (ACC), which contrasts other reports. Lower doses of psilocybin (2 mg/kg) increased the firing rate of ACC neurons in head-fixed mice running on a treadmill (Golden and Chadderton, 2022). Similarly, 5-methoxy-N,N-dimethyltryptamine (5-MeO-DMT) also increased activity rates in a majority of neurons recorded in layer V of ACC in anesthetized rats (Riga et al., 2014). 5-MeO-DMT and psilocybin increase excitatory post-synaptic currents of pyramidal neurons in brain slices of prefrontal cortex (Shao et al., 2021; Vargas et al., 2023). In contrast, a psilocybin-containing extract decreased neuronal spiking in the majority of CA1 pyramidal neurons in brain-slices of HPC (Moldavan et al., 2000). It is unclear if these discrepant effects of psychedelics on firing rate is due to dose, brain structure, locomotion, or other factors.

Psilocybin caused a large-scale reorganization of the relationship of activity among RSC neurons. After psilocybin administration, the dominant motifs of pair-wise correlation structure are dispersed, indicating that the most common patterns of RSC activity during baseline largely vanish. This response is consistent across sessions and animals, indicating that acute psilocybin causes a restructuring of functional correlation (FC) among neurons. This effect can be partially explained by the destabilization of positional signaling. In human fMRI studies, psychedelic drugs have been generally reported to increase the distribution of activity covariance motifs among brain regions (Tagliazucchi et al., 2014; Atasoy et al., 2017), and promote cortical desynchronization (Muthukumaraswamy et al., 2013; Riga et al., 2018). Psilocybin has been shown to particularly affect the FC within the default-mode network (DMN), which includes RSC (Carhart-Harris et al., 2012; Roseman et al., 2014; Daws et al., 2022). The psychedelic-associated loss of functional correlation is often associated with ego-dissolution, which was shown to correlate with decreased functional correlation between the parahippocampal and retrosplenial cortex (Carhart-Harris et al., 2016; Lebedev et al., 2016). Both psilocybin and LSD significantly increase the 'complexity' of functional correlation networks in the neocortex (Varley et al., 2020; Girn et al., 2022). Our results are consistent with these reports, and demonstrate similar dynamical changes at the cellular level within the RSC. It is worth noting that 5-HT_{2A}R, as with nearly all neuromodulatory receptors, affect Ca^{2+} signaling. It is therefore possible that the fluorescent signaling is somehow degraded by psilocybin via modulation of intracellular Ca^{2+}. We examined features of fluorescent transients to assess this possibility (Supplemental Fig. 3). The time constant of GCaMP decay is lower after injection of either saline or psilocybin. The effect for psilocybin is stronger than saline but it is small compared to the natural variance. It is therefore unlikely that reduced FC in the present report is due to degradation of the GCaMP signal.

Acute psilocybin administration decreased the stability of RSC neuron encoding of position, shown by the reduced mutual information and trial-to-trial correlation of individual neurons. Many RSC cells encoded specific locations on the belt before psychedelic administration, as shown previously (Mao et al., 2017), but these cells are destabilized by psilocybin, similar to the effect of the non-classic psychedelic ibogaine (Ivan et al., 2023). However, despite the high dosage of psilocybin used here, the changes in spatial encoding were surprisingly weak as compared to those evoked by a moderate dose of ibogaine (Ivan et al., 2023). Multiple regions in the neocortex encode position, environmental cues, and spatial information (Mashhoori et al., 2018; Esteves et al., 2021), which can provide a framework for navigation and context-dependent learning (Gruber and McDonald, 2012b; Chang et al., 2020). Reports of human perceptual experience is consistent with psychedelic-based disruption of this information. Psychedelics often disrupt the sense of space and time, causing disorientation and a feeling of spacelessness (Carbonaro et al., 2016; Garcia-Romeu et al., 2016; Smigielski et al., 2019). It is unclear if the altered encoding of space in RSC is more due to the direct action of psilocybin in RSC, or to alterations of afferent information. RSC positional information relies on hippocampal processing (Esteves et al., 2021) in order to form and maintain the cognitive map (McNaughton et al., 2006). Psilocybin not only affects 5-HT receptors, but also alters glutamate levels in both the mPFC and the HPC (Mason et al., 2020). Interestingly, higher glutamate in mPFC correlated with negative experiences, whereas lower glutamate in HPC was associated with a pleasant state of ego dissolution. Rodent studies have likewise found that psilocybin or its active form psilocin can affect dopamine, serotonin, glutamate, and gamma-aminobutyric acid (GABA) levels in the frontal cortex and/or striatum (Sakashita et al., 2015; Wojtas et al., 2022). These data suggest that the

effect of psilocybin on RSC activity could involve modulation of several neurotransmitter systems in RSC and afferent structures.

It is possible that the motoric slowing under the drug affected spatial encoding, even though we normalized firing by belt position rather than time in order to minimize artifacts of altered motoric output. We explicitly tested if belt velocity (a readout of motoric output) was related to encoding of space and neural dynamics (Supplemental Fig. 4). We did not find that belt velocity affected spatial encoding quality (MI) or the cluster coefficient in control animals, suggesting that the degraded spatial encoding was not a second order effect of the motoric slowing we observed in animals with psilocybin on board. Furthermore, while the belt velocity was decreased with psilocybin administration, the distributions of velocity are similar for saline and psilocybin (Supplemental Fig. 5.A). We note that the animals have extensive training on the apparatus prior to imaging. Moreover, the cues convey little novel data about the task. It is therefore likely the animals do not attend much to the cues. For instance, motoric output was not different during cue traverses as compared to non-cue regions of the belt (Supplemental Fig. 5.B). The distribution of MI over cells (Supplemental Fig. 5.C) reveals that there is not a high incidence of cells that completely lose their place specificity.

Despite affecting several neurotransmitter systems, psilocybin exerts its psychoactive effects primarily through the 5-HT_{2A} receptor. The occupancy of these receptors in the neocortex relates closely to the intensity of the psychedelic effect (Madsen et al., 2019; Kringelbach et al., 2020). We found that blocking these receptors with ketanserin reduced the majority of the behavioral and neural activity effects caused by psilocybin. Interestingly, the low dose fully blocked the effects of high dose psilocybin, whereas the high dose of ketanserin was less effective, although not statistically significant. After the end of the experiment (the data presented in the

paper), we ran a saline-ketanserin experiment. Mice (n=4) received a high ketanserin dose after baseline. The motoric output of the animals was reduced, but no other measures were affected (Supplementary Fig. 6). Prior rodent work has similarly shown only partial blockade of psilocybin effects at behavioral and synaptic levels with ketensarin or closely related molecules (Moldavan et al., 2000; Hesselgrave et al., 2021; Torrado Pacheco et al., 2023). Indeed, other 5-HT receptors are involved in modulating behavior. For instance, 5-HT_{1A} and 5-HT_{2C} receptors also contribute significantly the suppressing effect of psilocin on locomotion and investigatory behavior in rats (Tylš et al., 2016) and mice (Halberstadt et al., 2011). Moreover, the effects of 5-HT blockade depend on cellular physiology and/or phenotype. For instance, systemic administration of ketanserin reduced conditioned freezing in rats bred to display enhanced freezing, but exerted the opposite effect in low-freezing animals (León et al., 2017). Besides the possible involvement of multiple 5-HT receptor subtypes, it is also possible that the pharmacodynamics contributed to the inability of ketanserin to fully block effects of psilocybin on spatial encoding in the present data, as psilocybin was administered 30 min after the antagonist. In previous reports, ketanserin pretreatment only partially reduced psilocybin-induced head-twitch behavior when administered 1h before the psychedelic (Hesselgrave et al., 2021), but abolished it when administered 10 minutes before psilocybin (Shao et al., 2021). In sum, our data are consistent with prior studies in that they suggest some involvement of 5-HT_{2A} receptors in the effects of psilocybin, but do not rule out contributions of other neurotransmitter systems.

We used a dose of psilocybin (15 mg/kg) that is higher than the dose needed for behavioral effects such as head twitch. We wanted to avoid a false negative result due to low dose on the acute effects as well as any lasting effects that persisted for days after administration. Higher doses have stronger effects on neurotransmitter release in the prefrontal cortex (Wojtas et al.,

2022). Higher doses also have stronger effects on plasticity-related genes (Jefsen et al., 2021). These may affect either acute or long-lasting effects (i.e. over days or weeks) of psilocybin on information processing and neural dynamics. Although we found strong evidence for the former, we found no evidence for the latter.

2.6 CONCLUSION

Although several fMRI studies in humans and rodents have indicated that psychedelics alter mesoscale brain activity levels and cross-regional coordination, little is known about how these drugs affect information representation and processing at the cellular level. The present data suggest that activity of individual RSC neurons become discoordinated from one another. These data are consistent with mesoscale effects reported in fMRI studies. Despite the discoordination among neurons, the representation of spatial position by individual neurons was only mildly impaired. This was surprising because of the high dose of psilocybin administered (15 mg/kg), which in humans would evoke profound changes in mentation. We therefore speculate that either psychedelics effects are manifested by subtle changes to neural encoding that are difficult to identify in the present experimental design or the disruption of the agranular RSC activity is not a major contributor to the classic effects of psilocybin on human mentation.

Acknowledgments

We would like to thank Adam Neumann for technical support and Dr. HaoRan Chang for helpful discussions. Funding provided by: Natural Sciences and Engineering Council of Canada, New Frontiers Research Fund, Alberta Innovates, Beswick Fellowship, Canadian Institute of Health Research.

Author Contributions: V.E.I. and A.J.G. designed research, V.E.I. and I.M.E. performed research, M.M. contributed tools, V.E.I., D.P.T-C, and I.M.E. analyzed data, V.E.I., D.P.T-C, A.L., B.L.M., and A.J.G. wrote the paper.

Competing Interest Statement: The authors declare no competing interests.

Data availability statement: Access to the datasets and analysis code for the work presented in this paper will be granted to members of the research community. Requests to access the datasets and code used in this paper should be directed to aaron.gruber@uleth.ca

2.7 REFERENCES

Alexander, A.S., and Nitz, D.A. (2015). Retrosplenial cortex maps the conjunction of internal and external spaces. *Nature Neuroscience* 18(8)**,** 1143-1151. doi: 10.1038/nn.4058.

Andrade, R. (2011). Serotonergic regulation of neuronal excitability in the prefrontal cortex. *Neuropharmacology* 61(3)**,** 382-386. doi: https://doi.org/10.1016/j.neuropharm.2011.01.015.

Atasoy, S., Roseman, L., Kaelen, M., Kringelbach, M.L., Deco, G., and Carhart-Harris, R.L. (2017). Connectome-harmonic decomposition of human brain activity reveals dynamical repertoire re-organization under LSD. *Scientific Reports* 7(1)**,** 17661. doi: 10.1038/s41598-017-17546-0.

Carbonaro, T.M., Bradstreet, M.P., Barrett, F.S., MacLean, K.A., Jesse, R., Johnson, M.W., et al. (2016). Survey study of challenging experiences after ingesting psilocybin mushrooms: Acute and enduring positive and negative consequences. *Journal of Psychopharmacology* 30(12)**,** 1268-1278. doi: 10.1177/0269881116662634.

Carhart-Harris, R.L., Erritzoe, D., Williams, T., Stone, J.M., Reed, L.J., Colasanti, A., et al. (2012). Neural correlates of the psychedelic state as determined by fMRI studies with psilocybin. *Proceedings of the National Academy of Sciences* 109(6)**,** 2138-2143. doi: 10.1073/pnas.1119598109.

Carhart-Harris, R.L., Muthukumaraswamy, S., Roseman, L., Kaelen, M., Droog, W., Murphy, K., et al. (2016). Neural correlates of the LSD experience revealed by multimodal neuroimaging. *Proceedings of the National Academy of Sciences* 113(17)**,** 4853-4858. doi: 10.1073/pnas.1518377113.

Carhart-Harris, R.L., Roseman, L., Bolstridge, M., Demetriou, L., Pannekoek, J.N., Wall, M.B., et al. (2017b). Psilocybin for treatment-resistant depression: fMRI-measured brain mechanisms. *Scientific reports* 7(1)**,** 1-11.

Carter, O.L., Burr, D.C., Pettigrew, J.D., Wallis, G.M., Hasler, F., and Vollenweider, F.X. (2005). Using psilocybin to investigate the relationship between attention, working memory, and the serotonin 1A and 2A receptors. *Journal of Cognitive neuroscience* 17(10)**,** 1497-1508.

Chang, H., Esteves, I.M., Neumann, A.R., Sun, J., Mohajerani, M.H., and McNaughton, B.L. (2020). Coordinated activities of retrosplenial ensembles during resting-state encode spatial landmarks. *Philosophical Transactions of the Royal Society B: Biological Sciences* 375(1799)**,** 20190228. doi: doi:10.1098/rstb.2019.0228.

Daws, R.E., Timmermann, C., Giribaldi, B., Sexton, J.D., Wall, M.B., Erritzoe, D., et al. (2022). Increased global integration in the brain after psilocybin therapy for depression. *Nature Medicine* 28(4)**,** 844-851. doi: 10.1038/s41591-022-01744-z.

Esteves, I.M., Chang, H., Neumann, A.R., Sun, J., Mohajerani, M.H., and McNaughton, B.L. (2021). Spatial information encoding across multiple neocortical regions depends on an intact hippocampus. *The Journal of Neuroscience* 41(2)**,** 307. doi: 10.1523/JNEUROSCI.1788-20.2020.

Fisk, G.D., and Wyss, J.M. (1999). Associational projections of the anterior midline cortex in the rat: intracingulate and retrosplenial connections. *Brain Research* 825(1)**,** 1-13. doi: https://doi.org/10.1016/S0006-8993(99)01182-8.

Friedrich, J., Zhou, P., and Paninski, L. (2017). Fast online deconvolution of calcium imaging data. *PLOS Computational Biology* 13(3)**,** e1005423. doi: 10.1371/journal.pcbi.1005423.

Garcia-Romeu, A., Kersgaard, B., and Addy, P.H. (2016). Clinical applications of hallucinogens: A review. *Experimental and clinical psychopharmacology* 24(4)**,** 229-268. doi: 10.1037/pha0000084.

Girn, M., Roseman, L., Bernhardt, B., Smallwood, J., Carhart-Harris, R., and Nathan Spreng, R. (2022). Serotonergic psychedelic drugs LSD and psilocybin reduce the hierarchical differentiation of unimodal and transmodal cortex. *NeuroImage* 256**,** 119220. doi: https://doi.org/10.1016/j.neuroimage.2022.119220.

Golden, C.T., and Chadderton, P. (2022). Psilocybin reduces low frequency oscillatory power and neuronal phase-locking in the anterior cingulate cortex of awake rodents. *Scientific Reports* 12(1)**,** 12702. doi: 10.1038/s41598-022-16325-w.

Grandjean, J., Buehlmann, D., Buerge, M., Sigrist, H., Seifritz, E., Vollenweider, F.X., et al. (2021). Psilocybin exerts distinct effects on resting state networks associated with serotonin and dopamine in mice. *NeuroImage* 225**,** 117456. doi: https://doi.org/10.1016/j.neuroimage.2020.117456.

Gruber, A.J., and McDonald, R.J. (2012). Context, emotion, and the strategic pursuit of goals: interactions among multiple brain systems controlling motivated behavior. *Frontiers Behavioral Neuroscience* 6(50)**,** 50. doi: 10.3389/fnbeh.2012.00050.

Halberstadt, A.L., Koedood, L., Powell, S.B., and Geyer, M.A. (2011). Differential contributions of serotonin receptors to the behavioral effects of indoleamine hallucinogens in mice. *Journal of Psychopharmacology* 25(11)**,** 1548-1561.

Hesselgrave, N., Troppoli, T.A., Wulff, A.B., Cole, A.B., and Thompson, S.M. (2021). Harnessing psilocybin: antidepressant-like behavioral and synaptic actions of psilocybin are independent of 5-HT2R activation in mice. *Proceedings of the National Academy of Sciences* 118(17)**,** e2022489118. doi: 10.1073/pnas.2022489118.

Iaria, G., Chen, J.-K., Guariglia, C., Ptito, A., and Petrides, M. (2007). Retrosplenial and hippocampal brain regions in human navigation: complementary functional contributions to the formation and use of cognitive maps. *European Journal of Neuroscience* 25(3)**,** 890-899. doi: https://doi.org/10.1111/j.1460-9568.2007.05371.x.

Ivan, V.E., Tomàs-Cuesta, D.P., Esteves, I.M., Curic, D., Mohajerani, M., McNaughton, B.L., et al. (2023). The non-classic psychedelic ibogaine disrupts cognitive maps. *Biological Psychiatry Global Open Science*. doi: https://doi.org/10.1016/j.bpsgos.2023.07.008.

Keene, C.S., and Bucci, D.J. (2009). Damage to the retrosplenial cortex produces specific impairments in spatial working memory. *Neurobiology of Learning and Memory* 91(4)**,** 408-414. doi: https://doi.org/10.1016/j.nlm.2008.10.009.

Kometer, M., Schmidt, A., Bachmann, R., Studerus, E., Seifritz, E., and Vollenweider, F.X. (2012). Psilocybin biases facial recognition, goal-directed behavior, and mood state toward positive relative to negative emotions through different serotonergic subreceptors. *Biological Psychiatry* 72(11)**,** 898-906. doi: https://doi.org/10.1016/j.biopsych.2012.04.005.

Kringelbach, M.L., Cruzat, J., Cabral, J., Knudsen, G.M., Carhart-Harris, R., Whybrow, P.C., et al. (2020). Dynamic coupling of whole-brain neuronal and neurotransmitter systems. *Proceedings of the National Academy of Sciences* 117(17)**,** 9566-9576. doi: 10.1073/pnas.1921475117.

Lebedev, A.V., Kaelen, M., Lövdén, M., Nilsson, J., Feilding, A., Nutt, D.J., et al. (2016). LSD-induced entropic brain activity predicts subsequent personality change. *Human Brain Mapping* 37(9)**,** 3203-3213. doi: https://doi.org/10.1002/hbm.23234.

León, L.A., Castro-Gomes, V., Zárate-Guerrero, S., Corredor, K., Mello Cruz, A.P., Brandão, M.L., et al. (2017). Behavioral effects of systemic, infralimbic and prelimbic injections of a serotonin 5-HT2A antagonist in Carioca high- and low-conditioned freezing rats. *Frontiers in Behavioral Neuroscience* 11. doi: 10.3389/fnbeh.2017.00117.

Madsen, M.K., Fisher, P.M., Burmester, D., Dyssegaard, A., Stenbæk, D.S., Kristiansen, S., et al. (2019). Psychedelic effects of psilocybin correlate with serotonin 2A receptor occupancy and plasma psilocin levels. *Neuropsychopharmacology* 44(7)**,** 1328-1334. doi: 10.1038/s41386-019-0324-9.

Mao, D., Kandler, S., McNaughton, B.L., and Bonin, V. (2017). Sparse orthogonal population representation of spatial context in the retrosplenial cortex. *Nature Communications* 8(1)**,** 243. doi: 10.1038/s41467-017-00180-9.

Mao, D., Neumann, A.R., Sun, J., Bonin, V., Mohajerani, M.H., and McNaughton, B.L. (2018). Hippocampus-dependent emergence of spatial sequence coding in retrosplenial cortex. *Proceedings of the National Academy of Sciences* 115(31)**,** 8015. doi: 10.1073/pnas.1803224115.

Mashhoori, A., Hashemnia, S., McNaughton, B.L., Euston, D.R., and Gruber, A.J. (2018). Rat anterior cingulate cortex recalls features of remote reward locations after disfavoured reinforcements. *eLife* 7**,** e29793. doi: 10.7554/eLife.29793.

Mason, N.L., Kuypers, K.P.C., Müller, F., Reckweg, J., Tse, D.H.Y., Toennes, S.W., et al. (2020). Me, myself, bye: Regional alterations in glutamate and the experience of ego dissolution with psilocybin. *Neuropsychopharmacology* 45(12)**,** 2003-2011. doi: 10.1038/s41386-020-0718-8.

McNaughton, B.L., Battaglia, F.P., Jensen, O., Moser, E.I., and Moser, M.-B. (2006). Path integration and the neural basis of the 'cognitive map'. *Nature Reviews Neuroscience* 7(8)**,** 663-678. doi: 10.1038/nrn1932.

Michaiel, A.M., Parker, P.R.L., and Niell, C.M. (2019). A hallucinogenic Serotonin-2A receptor agonist reduces visual response gain and alters temporal dynamics in mouse V1. *Cell Reports* 26(13)**,** 3475-3483.e3474. doi: https://doi.org/10.1016/j.celrep.2019.02.104.

Moldavan, M., Solomko, E.F., Grodzinskaya, A.A., Storozhuk, V.M., and Lomberg, M.L. (2000). Neurotropic effect of extracts from the hallucinogenic mushroom Psilocybe cubensis (Earle) Sing.(Agaricomycetideae). In Vitro Studies. *International Journal of Medicinal Mushrooms* 2(4).

Muthukumaraswamy, S.D., Carhart-Harris, R.L., Moran, R.J., Brookes, M.J., Williams, T.M., Errtizoe, D., et al. (2013). Broadband cortical desynchronization underlies the human psychedelic state. *The Journal of Neuroscience* 33(38)**,** 15171-15183. doi: 10.1523/jneurosci.2063-13.2013.

O'Keefe, J., and Nadel, L. (1978). *The Hippocampus as a Cognitive Map.* Oxford: Clarendon Press.

Pachitariu, M., Stringer, C., Dipoppa, M., Schröder, S., Rossi, L.F., Dalgleish, H., et al. (2017). Suite2p: beyond 10,000 neurons with standard two-photon microscopy. *Biorxiv*.

Pnevmatikakis, Eftychios A., Soudry, D., Gao, Y., Machado, T.A., Merel, J., Pfau, D., et al. (2016). Simultaneous denoising, deconvolution, and demixing of calcium imaging data. *Neuron* 89(2)**,** 285-299. doi: https://doi.org/10.1016/j.neuron.2015.11.037.

Quednow, B.B., Kometer, M., Geyer, M.A., and Vollenweider, F.X. (2012). Psilocybin-induced deficits in automatic and controlled inhibition are attenuated by ketanserin in healthy

human volunteers. *Neuropsychopharmacology* 37(3), 630-640. doi: 10.1038/npp.2011.228.
Riga, M.S., Lladó-Pelfort, L., Artigas, F., and Celada, P. (2018). The serotonin hallucinogen 5-MeO-DMT alters cortico-thalamic activity in freely moving mice: Regionally-selective involvement of 5-HT1A and 5-HT2A receptors. *Neuropharmacology* 142, 219-230. doi: https://doi.org/10.1016/j.neuropharm.2017.11.049.
Riga, M.S., Soria, G., Tudela, R., Artigas, F., and Celada, P. (2014). The natural hallucinogen 5-MeO-DMT, component of Ayahuasca, disrupts cortical function in rats: Reversal by antipsychotic drugs. *International Journal of Neuropsychopharmacology* 17(8), 1269-1282. doi: 10.1017/S1461145714000261.
Roseman, L., Leech, R., Feilding, A., Nutt, D.J., and Carhart-Harris, R.L. (2014). The effects of psilocybin and MDMA on between-network resting state functional connectivity in healthy volunteers. *Frontiers in Human Neuroscience* 8. doi: 10.3389/fnhum.2014.00204.
Sakashita, Y., Abe, K., Katagiri, N., Kambe, T., Saitoh, T., Utsunomiya, I., et al. (2015). Effect of psilocin on extracellular dopamine and serotonin levels in the mesoaccumbens and mesocortical pathway in awake rats. *Biological and Pharmaceutical Bulletin* 38(1), 134-138.
Saramäki, J., Kivelä, M., Onnela, J.-P., Kaski, K., and Kertész, J. (2007). Generalizations of the clustering coefficient to weighted complex networks. *Physical Review E* 75(2), 027105. doi: 10.1103/PhysRevE.75.027105.
Shao, L.-X., Liao, C., Gregg, I., Davoudian, P.A., Savalia, N.K., Delagarza, K., et al. (2021). Psilocybin induces rapid and persistent growth of dendritic spines in frontal cortex in vivo. *Neuron* 109(16), 2535-2544.e2534. doi: https://doi.org/10.1016/j.neuron.2021.06.008.
Shibata, H., Kondo, S., and Naito, J. (2004). Organization of retrosplenial cortical projections to the anterior cingulate, motor, and prefrontal cortices in the rat. *Neuroscience Research* 49(1), 1-11. doi: https://doi.org/10.1016/j.neures.2004.01.005.
Smigielski, L., Kometer, M., Scheidegger, M., Krähenmann, R., Huber, T., and Vollenweider, F.X. (2019). Characterization and prediction of acute and sustained response to psychedelic psilocybin in a mindfulness group retreat. *Scientific Reports* 9(1), 14914. doi: 10.1038/s41598-019-50612-3.
Sokal, R.R. (1958). A statistical method for evaluating systematic relationships. *Univ. Kansas, Sci. Bull.* 38, 1409-1438.
Souza, B.C., Pavão, R., Belchior, H., and Tort, A.B.L. (2018). On information metrics for spatial coding. *Neuroscience* 375, 62-73. doi: https://doi.org/10.1016/j.neuroscience.2018.01.066.
Spain, A., Howarth, C., Khrapitchev, A.A., Sharp, T., Sibson, N.R., and Martin, C. (2015). Neurovascular and neuroimaging effects of the hallucinogenic serotonin receptor agonist psilocin in the rat brain. *Neuropharmacology* 99, 210-220. doi: https://doi.org/10.1016/j.neuropharm.2015.07.018.
Tagliazucchi, E., Carhart-Harris, R., Leech, R., Nutt, D., and Chialvo, D.R. (2014). Enhanced repertoire of brain dynamical states during the psychedelic experience. *Human Brain Mapping* 35(11), 5442-5456. doi: 10.1002/hbm.22562.
Torrado Pacheco, A., Olson, R.J., Garza, G., and Moghaddam, B. (2023). Acute psilocybin enhances cognitive flexibility in rats. *Neuropsychopharmacology : official publication of the American College of Neuropsychopharmacology*. doi: 10.1038/s41386-023-01545-z.

Tylš, F., Páleníček, T., Kadeřábek, L., Lipski, M., Kubešová, A., and Horáček, J. (2016). Sex differences and serotonergic mechanisms in the behavioural effects of psilocin. *Behavioural Pharmacology* 27(4)**,** 309-320.

Vargas, M.V., Dunlap, L.E., Dong, C., Carter, S.J., Tombari, R.J., Jami, S.A., et al. (2023). Psychedelics promote neuroplasticity through the activation of intracellular 5-HT2A receptors. *Science* 379(6633)**,** 700-706. doi: doi:10.1126/science.adf0435.

Varley, T.F., Carhart-Harris, R., Roseman, L., Menon, D.K., and Stamatakis, E.A. (2020). Serotonergic psychedelics LSD & psilocybin increase the fractal dimension of cortical brain activity in spatial and temporal domains. *NeuroImage* 220**,** 117049. doi: https://doi.org/10.1016/j.neuroimage.2020.117049.

Vinh, N.X., Epps, J., and Bailey, J. (2010). Information theoretic measures for clusterings comparison: Variants, properties, normalization and correction for chance. *The Journal of Machine Learning Research* 11**,** 2837-2854.

Vollenweider, F.X., Vollenweider-Scherpenhuyzen, M.F.I., Bäbler, A., Vogel, H., and Hell, D. (1998). Psilocybin induces schizophrenia-like psychosis in humans via a serotonin-2 agonist action. *NeuroReport* 9(17).

Wojtas, A., Bysiek, A., Wawrzczak-Bargiela, A., Szych, Z., Majcher-Maślanka, I., Herian, M., et al. 2022. Effect of psilocybin and ketamine on brain neurotransmitters, glutamate receptors, DNA and rat behavior. *International Journal of Molecular Sciences* [Online], 23(12).

Wyass, J.M., and Van Groen, T. (1992). Connections between the retrosplenial cortex and the hippocampal formation in the rat: A review. *Hippocampus* 2(1)**,** 1-11. doi: 10.1002/hipo.450020102.

2.8 SUPPLEMENTARY INFORMATION

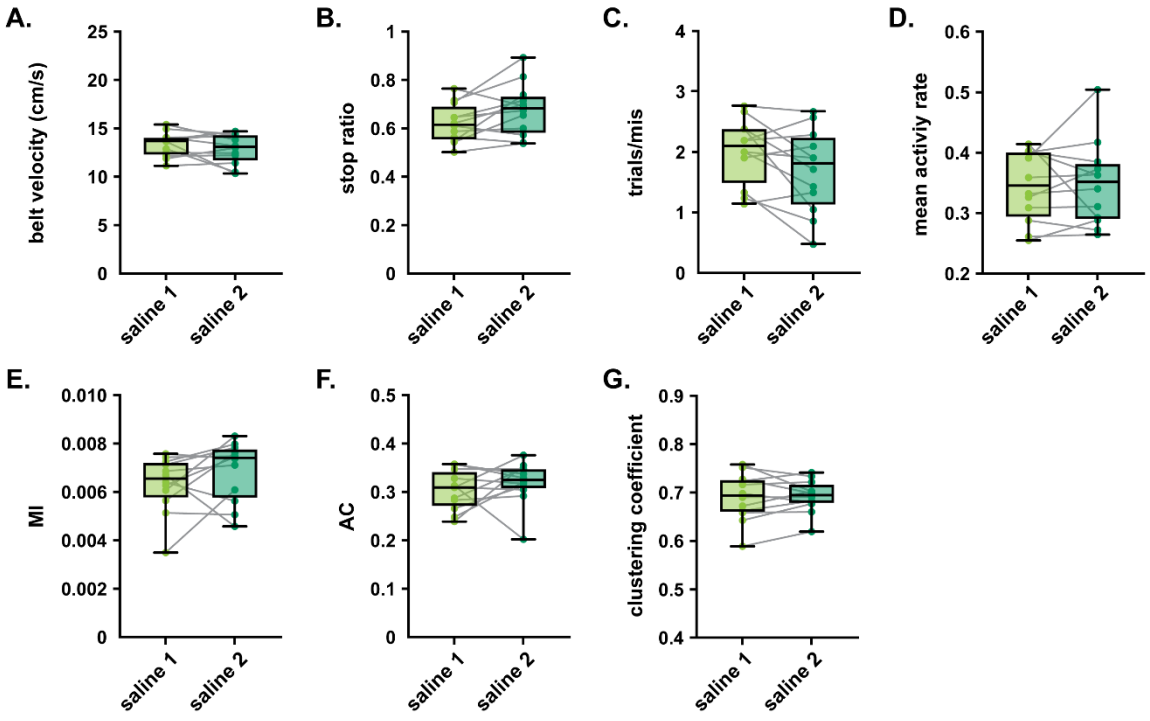

Supplemental Fig. 2.5: Effects of saline on behavior and neural activity in a second cohort of animals (n=3) that only received saline. Box plots and individual session-averaged values (dots) of behavioral and neural measures. A. Belt velocity; $F(1, 2) = 2.501$, $p = 0.255$; B. Fraction of time that mice were stationary during a trial; $F(1, 2) = 9.480$, $p = 0.091$; C. Number of trials per minute; $F(1, 2) = 5.172$, $p = 0.151$. D. Mean activity rate of all neurons in each session; $F(1, 2) = 0.083$, $p = 0.801$. E. Mean mutual information (MI); $F(1, 2) = 15.92$, $p = 0.057$; F. Average trial-to-trial correlation (AC); $F(1, 2) = 3.211$, $p = 0.215$. G. Clustering coefficients within each recording session; $F(1, 2) = 0.023$, $p = 0.894$.

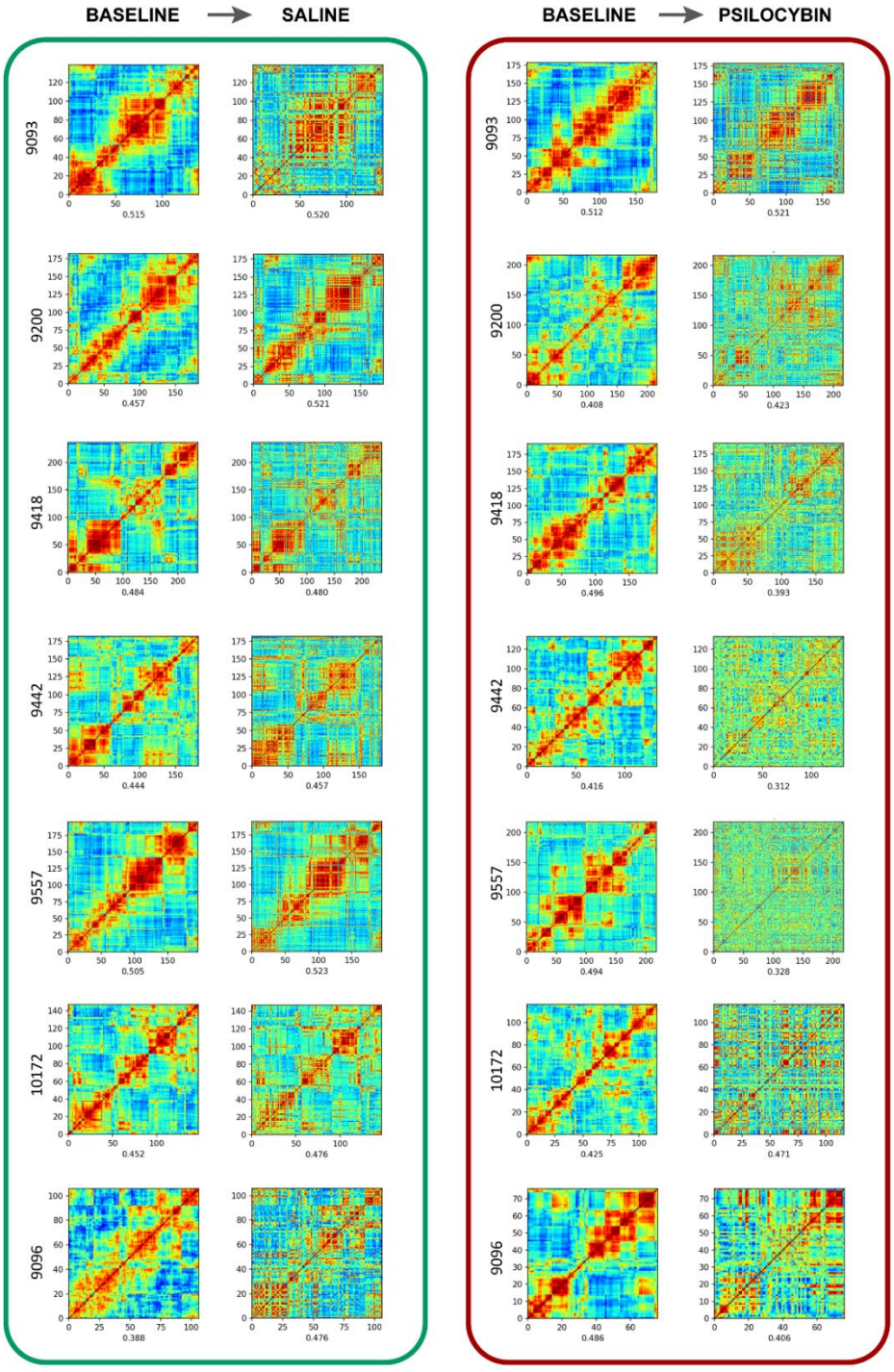

Supplemental Fig. 2.6: Correlation matrices of unit activity in one representative session of saline injection (left) and psilocybin injection (right) for each animal in the study (n=7). The sorting of rows/columns is the same for each pair of plots.

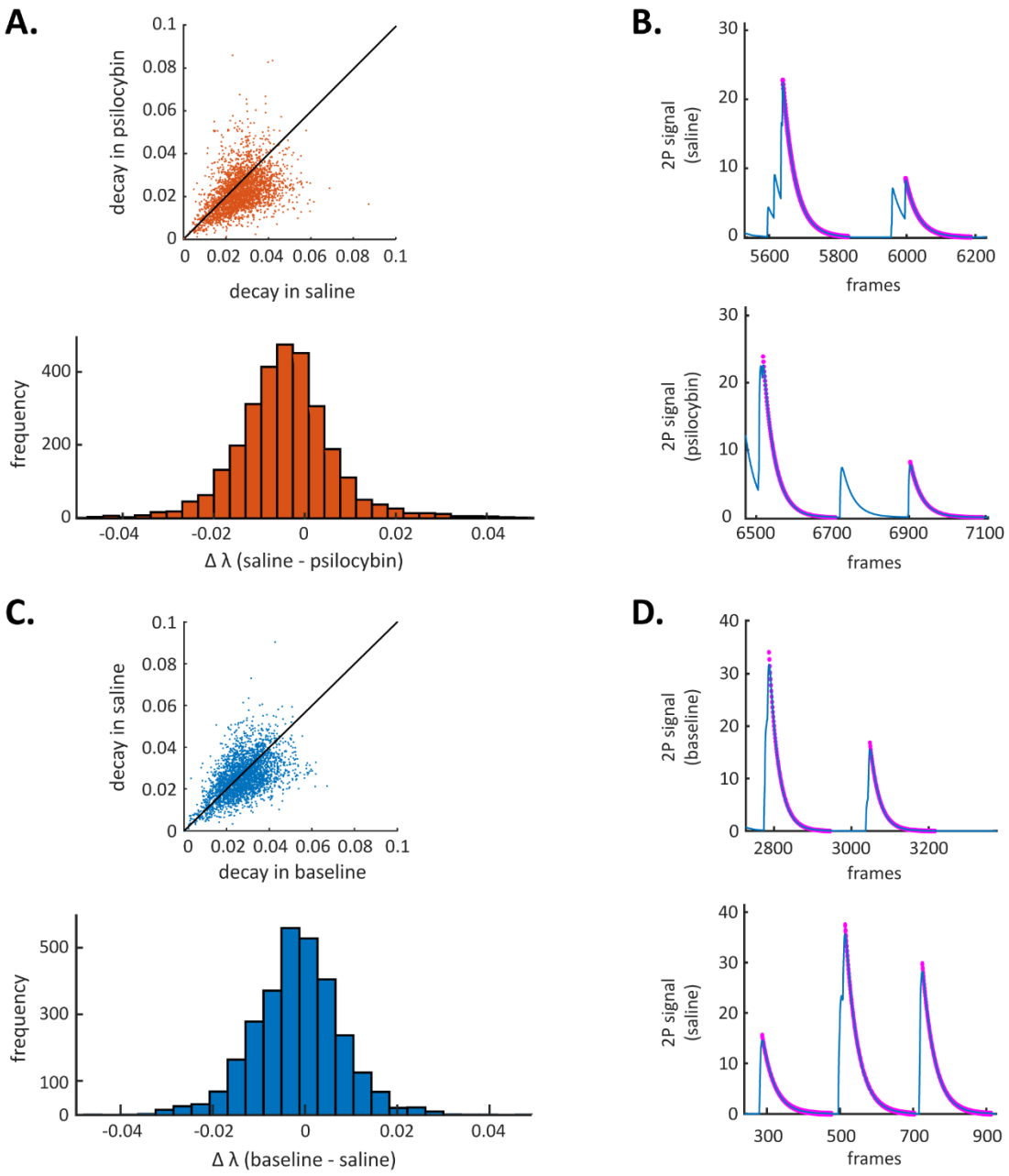

Supplemental Fig. 2.7: Analysis of the decay of the fluorescence signal. A. Top: Scatter plot of the decay time constant before (horizontal axis) and after (vertical axis) psilocybin for each cell with good fit, based on root mean squared error (RMSE). Some neurons (< 4%) could not be well fit because their high activity rate did not provide a sufficient number of decay events of at least

200 ms that were not interrupted by a subsequent Ca2+ spike. Correlation coefficient R = 0.409; Bottom: change in decay time constant λ for all cells from baseline (saline) to psilocybin. Mean = -0.004, STD = 0.010; test if mean is different from 0: t(2897) = -21.12, p = 3.14 e-92; B. Example of the signal trace (blue) and exponential fit (magenta) for a cell before (top) and after (bottom) psilocybin. C. Top: Scatter plot of the decay time constant before and after saline for each cell with good fit (R = 0.538); Bottom: change in decay time constant for all cells from baseline to saline. Mean = -0.001, STD = 0.009; test if mean is different from 0: t(2925) = - 9.62, p = 1.25 e-21; D. Example of the signal trace and exponential fit for a cell before (top) and after (bottom) saline.

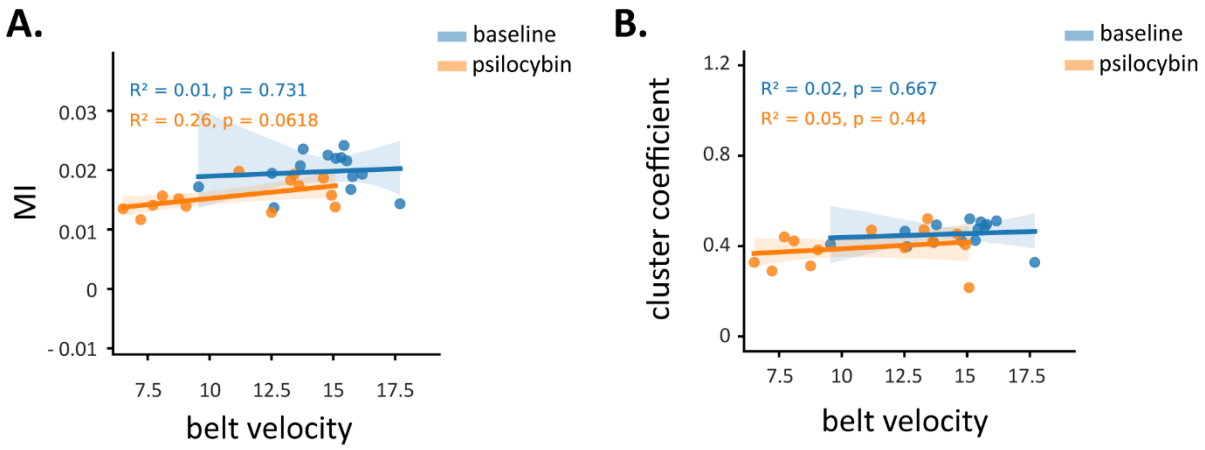

Supplemental Fig. 2.8: Effect of belt velocity on neural encoding and dynamics. Correlation of belt velocity with MI (A) and cluster coefficient (B) for before (blue) and after (orange) psilocybin. Dots represent averages from each session, and shaded region represents 95% confidence interval.

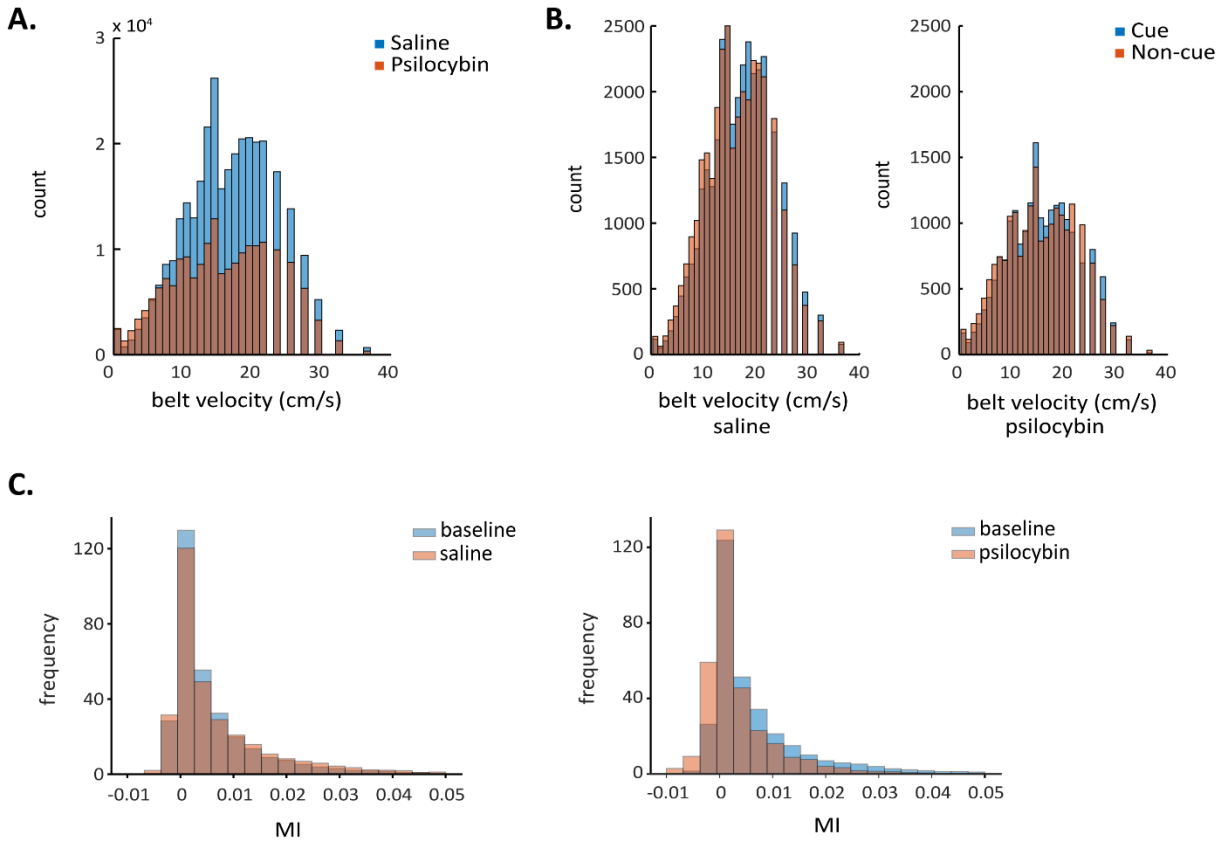

Supplemental Fig. 2.9: Velocity and MI distributions. A. Belt velocity distributions for saline (blue) and psilocybin (orange) groups. B. Belt velocity distributions for saline (left) and psilocybin (right) when animals are traversing a cue (blue) or non-cue (orange) containing portion of the treadmill belt. C. Distribution of MI over cells for saline (left) or psilocybin (right) as compared to baseline.

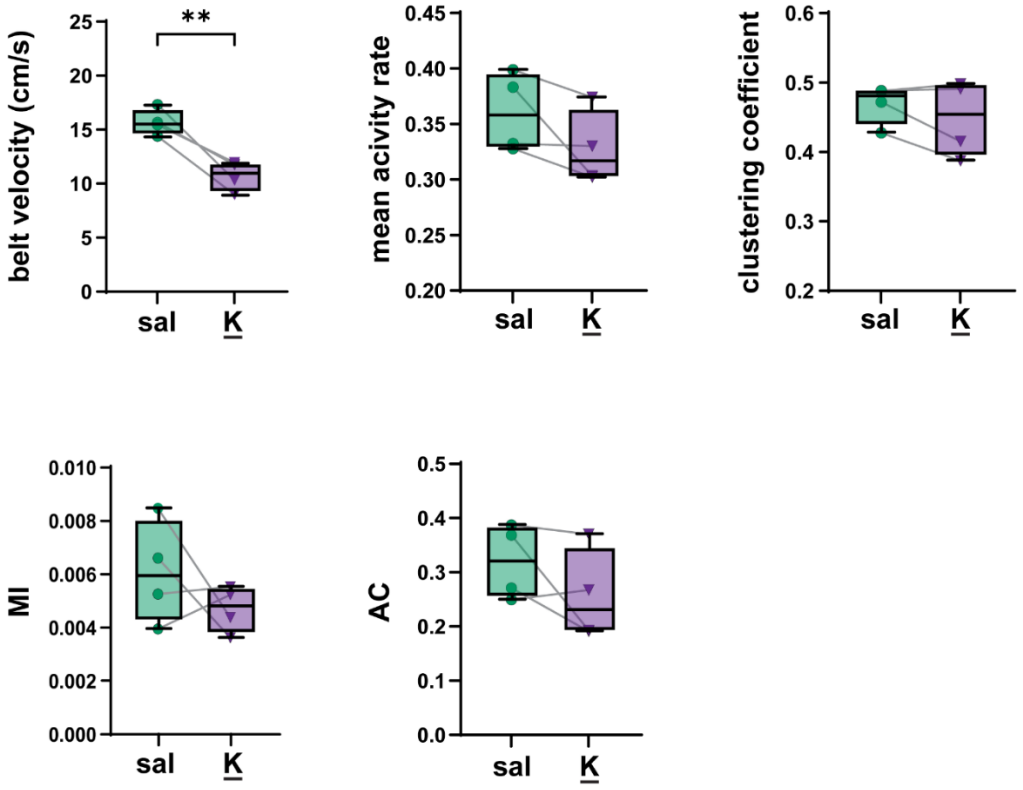

Supplemental Fig. 2.10: Effect of ketanserin on behavior and neural activity. The animals (n = 4) received an injection of saline before a high dose (5 mg/kg) of ketanserin. While the animals were slower ($t(3) = 6.276$, $p = 0.008$), the other factors were not affected by ketanserin (p values range 0.14 - 0.36). Each dot is one session from 4 animals after saline injection but before ketanserin (labeled 'sal') and after high dose ketanserin (**K**).

CHAPTER 3: THE NON-CLASSIC PSYCHEDELIC IBOGAINE DISRUPTS COGNITIVE MAPS

Victorita E. Ivan[1]*, David P. Tomàs-Cuesta[1]*, Ingrid M. Esteves[1]*, Davor Curic[2], Majid Mohajerani[1], Bruce L. McNaughton[1,3], Joern Davidsen[2], Aaron J. Gruber[1]✉

[1]Canadian Centre for Behavioural Neuroscience, Department of Neuroscience, University of Lethbridge, Lethbridge, Alberta, Canada

[2]Department of Physics and Astronomy, University of Calgary, Calgary, Alberta, Canada

[3]Center for the Neurobiology of Learning and Memory, University of California Irvine, Irvine, California, USA

*The authors contributed equally.

✉ Aaron J. Gruber

Email: aaron.gruber@uleth.ca

Keywords: retrosplenial cortex, path integration, neuronal avalanches, psychedelics

Published in *Biological Psychiatry Global Open Science* (Ivan et al., 2023)

3.1 ABSTRACT

Background: The ability of psychedelic compounds to profoundly alter mental function has been long known, but the underlying changes in cellular-level information encoding remain poorly understood. **Methods:** We used 2-photon microscopy to record from the retrosplenial cortex (RSC) in head-fixed mice running on a treadmill before and after injection of the non-classic psychedelic ibogaine (40 mg/kg i.p.). **Results:** We found that the cognitive map, formed by the representation of position encoded by ensembles of individual neurons in the RSC, was destabilized by ibogaine when mice had to infer position between tactile landmarks. This corresponded with increased neural activity rates, loss of correlation structure, and increased responses to cues. Ibogaine had surprisingly little effect on the size-frequency distribution of network activity events, suggesting that signal propagation within RSC was largely unaffected. **Conclusion:** Together, these data support proposals that compounds with psychedelic properties disrupt representations important for constraining neocortical activity, thereby increasing the entropy of neural signaling. Furthermore, the loss of expected position encoding between landmarks recapitulated effects of hippocampal impairment, suggesting that disruption of cognitive maps or other hippocampal processing may be a contributing mechanism of discoordinated neocortical activity in psychedelic states.

3.2 INTRODUCTION

The retrosplenial cortex (RSC) is well positioned to integrate sensory, mnemonic, motivational, and cognitive information by virtue of its strong connectivity with the hippocampus (Kobayashi and Amaral, 2003), medial prefrontal cortex (Shibata and Naito, 2008), and primary sensory

cortices (Todd et al., 2016; Fischer et al., 2020). The normal covariation of activity among these structures revealed by fMRI in humans is disrupted by classic psychedelics such as LSD and psilocybin (Carhart-Harris et al., 2016; Preller et al., 2019). Here we test if coordination of activity among individual neurons within RSC is disrupted, and how this impacts information encoding.

Many neurons in the rodent RSC encode spatial position (Alexander and Nitz, 2015). In head-fixed mice, such RSC neurons encode the virtual position of the animal on a treadmill by activating reliably at specific belt positions (Mao et al., 2017). These neurons therefore have signaling properties similar to place cells in the hippocampus, which appear to represent a 'cognitive map' of space (O'Keefe and Nadel, 1978; Behrens et al., 2018) and may provide a contextual/'index' code to bind together attributes of experience represented in neocortex (Teyler and DiScenna, 1985; Teyler and Rudy, 2007). The present position of an animal is encoded by the activity state of place cells comprising the cognitive map for a given environment. As an animal locomotes, it uses an estimate of the distance and direction of movement to update the ensemble activity according to the cognitive map, in order to reflect the new expected position (McNaughton et al., 2006). This process is called path integration. Animals can correct for accumulated errors of path integration when familiar landmarks are encountered (Jayakumar et al., 2019).

Head-fixed mice running on a treadmill belt are able to engage these systems. In this preparation, RSC place cells have activity that is stable over multiple laps of the belt, even in the absence of landmarks other than a start location (Mao et al., 2017). This suggests that head-fixed mice are capable of using path integration to update the cognitive map to infer the virtual position on a treadmill belt. Both RSC and hippocampus appear to be involved in this process. Inactivation of hippocampus disrupts RSC place cell stability (Esteves et al., 2021), and RSC inactivation impairs

path integration in freely moving animals (Cooper et al., 2001). Regardless of the relative roles of these structures in the underlying computations, the positional signal in RSC provides a window into the brain's ability to maintain a cognitive map and update it appropriately to infer position between landmarks. Here, we test the effects of ibogaine on the encoding of positional inference and the associated coordination of neural firing in RSC as a means to test the theory that drugs with psychedelic effects disrupt the brain's ability to generate predictions and regulate neural activity (Carhart-Harris and Friston, 2019).

Ibogaine evokes mental states with psychedelic features in humans (Kohek et al., 2020). It is considered a non-classic psychedelic because it has significantly broader neuropharmacological action than classic psychedelics (Sershen et al., 2001). Nonetheless, both classes affect phenomena linked to cognitive maps, including navigation (Kesner et al., 1995; Rambousek et al., 2014) and mood disorders (Johnson et al., 2019; Köck et al., 2021; Maxim and Brown, 2023). The present work focuses on navigation because it is much better understood than mood regulation in animal models.

3.3 METHODS

Animals

Adult (9-11 month old) Thy1-GCaMP6s mice (n=8; 3F/5M), weighing 30-35g, were housed in standard rodent cages, and maintained at 24 °C under a 12 h light/dark cycle. Mice had free access to food and water before training. All experiments were performed during the light cycle (between 7:30 AM and 7:30 PM). Procedures were in accordance with the guidelines

established by the Canadian Council on Animal Care, and with protocols approved by the Animal Welfare Committee of the University of Lethbridge.

Surgery

The mice received a 5 mm bilateral craniotomy (AP: +1 to -4; ML: -2.5 to +2.5), which was then covered with a coverslip, and a titanium head plate was fixed to the skull for head fixation. Full description of the surgical procedure can be found in the Supplementary Methods.

Drugs

Ibogaine HCl was obtained from Toronto Research Chemicals, Canada, in powder form and diluted in sterile water to a concentration of 10-12 mg/ml, in order to achieve a dose of 40 mg/kg in a 0.1 ml volume for each mouse (intraperitoneal administration). This dose is based on previous reports (Blackburn and Szumlinski, 1997; Szumlinski et al., 2001; Marton et al., 2019). Our pilot studies indicate that this concentration produced moderate levels of behavioral indicators typical of psychedelics (tremors, ataxia) while allowing animals to complete trials of the task. The control animals received 0.1 ml 0.9% saline solution. We chose saline instead of water for the control at the recommendation of the University's Animal Care Staff, to minimize any potential issues with the IP injections.

Experimental procedure for behavior

Head-fixed mice were trained to run on a treadmill using a positive reinforcement paradigm. They received a drop of 10% sucrose solution on every trial, consisting of one lap of the treadmill belt. Animals were water restricted during the training and testing. They had *ad*

libitum access to water for up to 30 minutes per day, and their body weight was carefully monitored throughout the experiment to ensure the weight loss did not exceed 15% of their baseline value. The treadmill belt consisted of a Velcro strip that was 150 cm long and 4 cm wide. Three tactile cues were placed in different locations on the belt. Licking behavior was recorded using a capacitive sensor connected to the lick spout. An optical encoder attached to the wheel shaft was used to monitor belt movement. A microcontroller was used to monitor the encoder, licking sensor, and the reward delivery.

Neural activity was imaged in daily sessions of the task. There were three 10-minute epochs of recording while mice performed the task; one before drug or saline, and two afterward. This allowed us to control for day-to-day variance in performance, and to test the effects of injections on a well-isolated population of neurons. The first 10 min epoch in every session was the baseline condition before injection. Mice were then given an injection of ibogaine or saline, and waited 10 mins (while still head-fixed) for the drug to take effect. The second epoch of task and recording began again for 10 minutes (minutes 20-30 of the experiment). The third 10-minute recording epoch began 30 minutes after injection. All analyses were performed at the two post-injection epochs independently. Remarkably, every analysis was consistent among these epochs. For compactness and to reduce the complexity of figures, we therefore present only analysis of the first 10-minute epoch in the main text. The supplemental figures show data at both time points. Each animal was imaged in one session before any injections (Pre-drug day 1), for two days of saline injections, and then either 3 days (Test day 1-3) of ibogaine HCl (40 mg/kg; n=6) or 3 days of saline (n=2). The control group consists of the two animals that received only saline, and the initial injection of saline in the six animals that later received ibogaine, for a total of 18 sessions.

Neural Activity Analysis

Full description for the methods used for imaging, pre-processing, computing spatial encoding, decoding error, and unit functional connectivity, along with the neuronal avalanche analysis methods are provided in Supplementary Methods.

3.4 RESULTS

We used 2-photon imaging to record the activity of ensembles of individual RSC neurons (153-702 simultaneous cells per session) in head-fixed mice (Fig. 3.1.A). Mice were placed on a treadmill belt that had narrow tactile cues in three positions along its length. Mice received a liquid reward on every lap of the belt. A within-session design was used in order to test drug effects relative to baseline conditions in the same populations of neurons (Supplemental Fig. 3.4).

Ibogaine disrupts encoding of inferred position

Prior to any injections, some RSC cells activated at a specific position of the belt during each trial (Fig. 3.1.B). Other cells were not selective to position, or were inconsistent from trial-to-trial. We therefore computed the adjusted mutual information (MI) between activity and belt position, which captures both sources of variance (Souza et al., 2018), to restrict analysis to those cells that were most selective to position. The injection of ibogaine (40 mg/kg, i.p.) destabilized the place firing of these RSC cells, and correspondingly led to a significant decrease in mean MI relative to baseline (Fig. 3.1.B; Supplemental Fig. 3.5; Paired t-test, $t(16)=5.135$, $p=9.978e-05$). In contrast, there was a slight increase in mean MI following saline ($t(10)=-2.86$, $p=0.017$). The distribution of position fields among the population of high-MI cells (top quartile) extended over the entire belt prior to injections (Fig. 3.1.C).

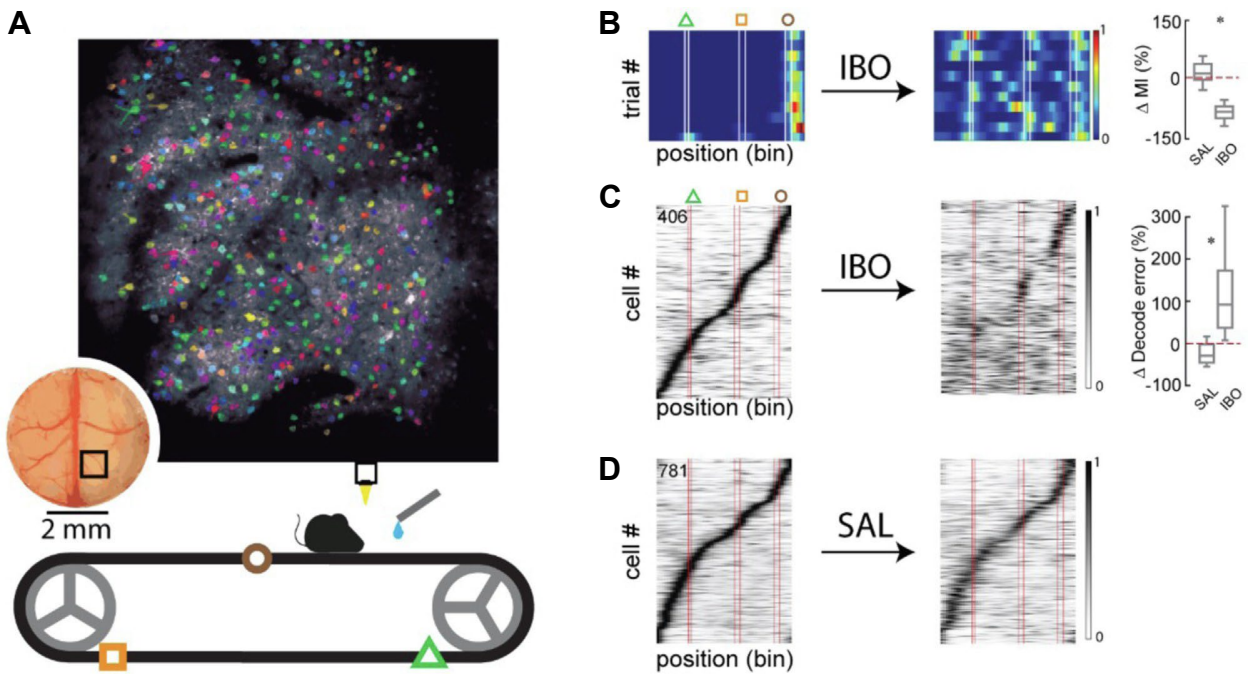

Fig. 3.1: Ibogaine disrupts encoding of virtual position. A. Illustration of experimental setup (bottom) and sample image showing segmented neurons (indicated by colored patches) within the field of view over the retrosplenial cortex (inset). Symbols on the treadmill belt indicate approximate locations of tactile cues. B. Activity of 1 neuron as a function of position on the belt for several consecutive trials. Vertical lines indicate locations of tactile cues. The neuron selectively activates at one position prior to ibogaine but loses location specificity after injection. The right panel shows the change in session-averaged adjusted MI from baseline for all sessions (n = 17). C. Session-averaged activity of position-tuned cells before (left panel) and after (center panel) injection of ibogaine for all sessions. Cells in both panels are ordered by a lag to peak activity before injection. The right panel shows the change in decoding error after injection of ibogaine. D. The same as C, but for saline injection. *p, .001. IBO, ibogaine; MI, mutual information; SAL, saline.

We next evaluated whether RSC encoded a map of the virtual location on the belt by testing whether the belt position at any instant could be decoded from ensemble RSC activity. Indeed, position was decodable with far less error than expected by chance (Paired t-test, t(27)=11.724, p=4.218e-12), consistent with previous reports (Mao et al., 2017). Ibogaine

disrupted the map encoded by ensembles, and led to significantly greater decoding error by a classifier trained on baseline data (Fig. 3.1.C; Supplemental Fig. 3.6; Paired t-test, t(16)=-8.456, p=2.683e-07), whereas saline did not (Fig. 3.1.D; Paired t-test, t(10)=-0.23, p=0.823). Unsurprisingly, the increase in decoder error was proportional to the decrease of mean MI values (Supplemental Fig. 3.7). Interestingly, the disruption by ibogaine was more prominent in the ambiguous regions of the belt between the tactile cues. This is evident in the persistence of place fields by some cells at the cue regions (Fig. 3.1.C). We tested this by comparing the MI of cells responding at cue locations to those responding at positions between the cues. A rank-order analysis of the top quartile of MI values in the four conditions (saline/ibogaine x cue/inter-cue) revealed a significant interaction of cue and ibogaine on MI (Kruskal-Wallis t(7)=235.978, p=2.66e-47; Supplemental Fig. 3.8). The MI values of cells was not different between cue and non-cue locations prior to ibogaine (Nemenyi post-hoc; p=0.355), but there were more highly informative cells at cue locations than non-cue locations after ibogaine (p=3.34e-03). Saline did not produce this difference among cue and non-cue locations (p=0.556). Note that the MI of *cue-location* cells did not decrease after ibogaine (p=0.265), whereas the *non-cue* cells did decrease after ibogaine (p=1.44e-09). These results indicate that ibogaine impairs signaling of position more drastically at the ambiguous regions between cues, when position estimates depend on path integration and cognitive maps. Despite the disruption of the cognitive map, mice continued to perform the task after ibogaine with only moderate decreases in movement velocity and other metrics (Supplemental Fig. 3.4). Lastly, we tested whether a new map of space forms after ibogaine, by training a new classifier on the post-ibogaine data. The error of this classifier tested on post-ibogaine data (cross-validated) was significantly higher than the error of the classifier trained and tested on baseline data prior to injection (Paired t-test, t(16)=-7.119, p=2.436e-06),

indicating that there had not been a remapping of position. Rather, it appears that there was no stable mapping of non-cue positions after ibogaine.

The mean activity rate during the task increased following ibogaine ($t(16)=-5.112$, $p=1.044e-04$), but not saline ($t(10)=1.345$, $p=0.208$). Sensory inputs are proposed to become disinhibited under psychedelics (Carhart-Harris and Friston, 2019) so we expected proportionally greater increases of firing rate during traverses of the tactile cue patches than at positions between the cues. Indeed, we found evidence for this prediction. On the cells with the MI in the 4th quartile, we computed the ratio between the cue and non-cue location activity of each cell. This ratio increased after ibogaine (Paired t-test, $t(16)=-2.983$, $p=0.009$), but not saline (Paired t-test, $t(10)=-0.468$, $p=0.65$). This indicates that the increased activity was greater during cue traverses than non-cue regions of the belt.

Ibogaine reduces functional connectivity

Studies in humans show that covariance of activity among brain regions is reorganized by psychedelic compounds so as to attenuate dominant motifs (Muthukumaraswamy et al., 2013; Barnett et al., 2020). We therefore tested whether a similar reorganization occurs at the cellular level. We computed the correlation of activity among all neurons recorded simultaneously during a session before injection, and used hierarchical clustering to order the units so that functionally similar units were adjacent. This matrix defines the functional connectivity. We applied the same matrix ordering to the data collected after injection, so as to visualize changes in correlation structure. Injection of ibogaine drastically changed the correlation structure, whereas saline appeared to reduce the amplitude of correlations but preserve the overall pattern (Fig. 3.2.A-B). We quantified injection-related changes by computing the clustering coefficient of all pair-wise

correlations, which indicates how distinct clusters of correlated units are from one another (Fig. 3.2.C). Saline had no effect ($t(10)=-0.794$, $p=0.446$), but ibogaine significantly reduced the clustering coefficient (Paired t-test, $t(16)=6.477$, $p=7.639e-06$). This analysis of pairwise correlations indicates that the network has become functionally more homogeneous. We next investigated covariance among larger groups of cells using principal component analysis to decompose neural activity into a reduced space. In baseline sessions, the top 6 factors accounted for 72.9 +/- 4.7% of the explained variance. After ibogaine administration, a new decomposition revealed that the explained variance of the top 6 factors dropped significantly to 64.8 +/- 2.6% (Fig. 3.2.D; Supplemental Fig. 3.9; Anova-RM, $t(1,32)=21.86$, $p=5.096e-05$). Saline did not have this effect (EV = 76.5 +/- 4.1 %; Anova-RM, $t(1, 20)=0.099$, $p=0.755$). This indicates a significant reduction in the covariance of activity among groups of cells, such that activity is more independent among units after ibogaine. These data suggest that functional connectivity is reduced after ibogaine administration.

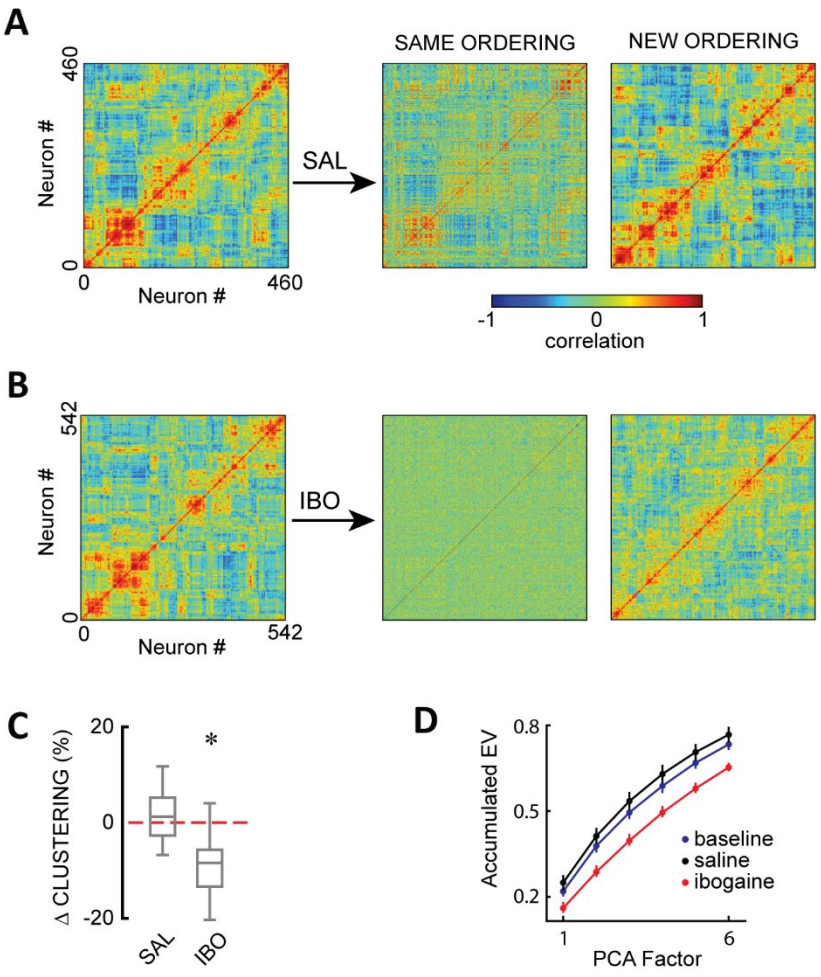

Fig. 3.2: Population covariance. Population covariance. A. Pairwise correlation of unit activity in 1 representative session prior to injection (left panel) and after saline injection. The middle panel has the same ordering as the left panel, and the right panel shows a reclustering of correlation patterns. B. Pairwise correlation before and after injection of ibogaine in 1 session, showing that functional connectivity is reorganized and becomes less structured (fewer large blocks of high correlation) after injection. C. Box plot of the change in clustering coefficient of the correlation matrices from baseline. The reduced clustering after ibogaine reflects a loss of dominant functional connectivity motifs. D. Cumulative explained variance as a function of principal component factors, showing that signaling among neurons becomes more independent after ibogaine. *p, .0001. EV, explained variance; IBO, ibogaine; PCA, principal component analysis; SAL, saline.

Higher order statistics

The loss of spatial information could arise from disruption of processing within the RSC, or from disruption of structured input to the RSC, such as from hippocampus. To shed light on which is more likely, we next sought to determine how ibogaine affected the propagation of signals within RSC. One approach to quantify such dynamics is to assess the size and duration of activity burst events in the network, which are often called information cascades or neuronal avalanches (Beggs and Plenz, 2003). The relationship between the size and duration follows power-law statistics (Lombardi et al., 2016; Yaghoubi et al., 2018), which are characteristic of physical systems near a critical state separating distinct dynamical regimes. The brain is proposed to be 'self-tuned' to lie at the boundary between an ordered and disordered phase that supports self-sustained activity. Further, recent fMRI data suggests that brain networks shift toward criticality (e.g. more disorganized) under psychedelics (Atasoy et al., 2017). We next tested if ibogaine has a similar effect at the cellular level.

Avalanche events and quiescent periods between events were detected according to previous work (Curic et al., 2021) (Fig. 3.3.A; see Supplemental Methods). Briefly, activity was binned and summed across all units. Each excursion of summed activity over a threshold is a neural 'avalanche'. The duration of the avalanche is the number of consecutive bins the summed activity exceeds the threshold, and the duration of quiescent periods is the time between the end of one avalanche and the start of the next one. The avalanche size is the area under the curve between the summed activity and threshold. The distributions of normalized avalanche size, avalanche duration, and the quiescent duration all exhibit hallmark features of near-critical systems (Fig. 3.3.B). Specifically, there is an approximately linear regime in the log-log plot, which then

transitions at a cutoff point to a rapid decline as magnitude increases. The linear regime in the log-log plot is referred to as a power-law, wherein the frequency of observing an event is inversely proportional to its magnitude.

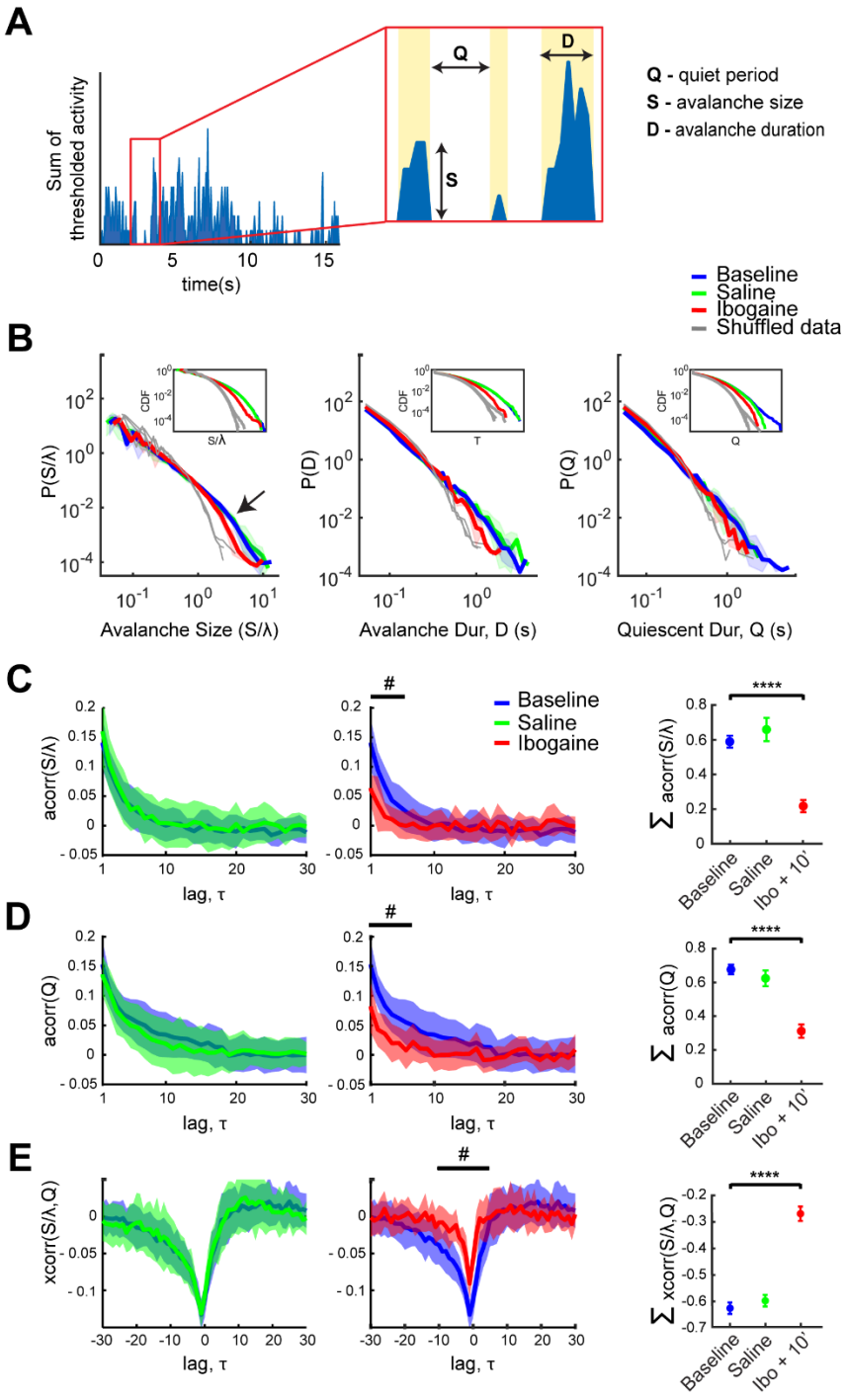

Fig. 3.3: Neural avalanches. A. Diagram showing parametrization of avalanche size, duration, and quiescent period duration from the sum of thresholded activity among simultaneously recorded cells (blue trace). Λ is a scaling factor applied to each recording prior to generating grand averages over recordings. It is the product of the number of neurons and the mean firing rate of the population in the recording. B. Frequency distributions of normalized avalanche size (left panel), avalanche duration (center panel), and quiet period duration (right panel) for baseline, saline administration, and ibogaine administration. Data in all plots show mean ± 1 SD computed over all sessions of each type. The arrow indicates the cutoff point for baseline. Insets show cumulative densities from large to small values. C. Correlations among the size of an avalanche and the size of future avalanches. Right-side panel shows mean and standard deviation for successive avalanches in a window including the past 3 and future 3 events. D. Correlation among duration of an avalanche and the duration of future quiescent periods. E. Cross-correlation of avalanche size and the duration of past/current quiescent periods. These data show that ibogaine reduced correlation structure among events, but the properties of the events themselves (e.g., power-law slope of size, duration, and quiescent periods) were not affected much. This suggests that ibogaine had little effect on the propagation of network activity within the retrosplenial cortex. #p, .05 (statistical significance of correlation values). ****p, .0001 (statistical difference of means). acorr, autocorrelation; CDF, cumulative distribution function; Ibo, ibogaine; xcorr, cross-correlation.

Changes in the slope of the power-law or cutoff point are indicative of specific shifts in the underlying dynamics. The slope of the linear portion of the size distribution was 1.8 ± 0.1 at baseline, and was not different after ibogaine (one-way ANOVA: $F(2, 19) = 0.1190$, $p = 0.88$; Tukey post hoc for ibogaine, $p = 0.88$, and for saline $p = 0.98$). The cutoff point, on the other hand, was shifted following ibogaine (one-way ANOVA: $F(2, 19) = 10.24$, $p = 0.001$; Tukey post hoc for ibogaine, $p = 0.003$, and for saline $p = 0.92$). Under ibogaine, the network generated fewer large events, despite the increase in activity rate. This indicates that the additional activity occurs outside of the large information cascade events.

The first order avalanche statistics above do not provide information about the temporal relationships between bursts of neuronal activity. To quantify these relationships, we computed correlations among and between successive avalanche sizes and quiescent durations (see Supplemental Methods). Avalanches tended to be followed by avalanches of similar size in the baseline condition, and this tendency was weakened by ibogaine (Fig. 3.3.C; RM ANOVA: $F(29, 1189) = 10.32$, $p < 0.001$) but not saline (RM ANOVA $F(29, 1218) = 0.8484$, $p = 0.69$). This effect was even more striking when averaging the autocorrelation over the past 3 and future 3 avalanches (right-hand panel in Fig. 3.3.C). This window-averaged avalanche autocorrelation was affected by ibogaine (one way ANOVA: $F(2, 56) = 22.94$, $p < 0.0001$; Tukey post hoc for ibogaine, $p < 0.0001$), but not after saline ($p = 0.50$). Similarly, quiescent periods of similar duration tended to follow one another in both baseline and saline conditions (Fig. 3.3.D; RM ANOVA: $F(29, 1218) = 1.030$, $p = 0.42$), but this trend was diminished by ibogaine (RM ANOVA: $F(29, 1189) = 7.754$, $p < 0.0001$). This was recapitulated in the window-averaged values; ibogaine decreased the autocorrelation (one way ANOVA: $F(2, 56) = 26.01$, $p < 0.0001$; Tukey post hoc for ibogaine, $p < 0.0001$), while saline did not ($p = 0.56$). We reliably obtained these results for many different binarizing threshold values, and even when a random cell sub-sampling method was implemented.

The cross-correlation between avalanche sizes and subsequent quiescent-times was negative, indicating that large avalanches tend to be followed by short quiescent periods, and short avalanches are followed by long quiescent-times (Fig. 3.3.E). This relationship was not different between baseline and saline conditions (Fig. 3.3.E; RM ANOVA: $F(60, 2520) = 0.8442$, $p = 0.79$). In contrast, ibogaine decreased the negative correlation (RM ANOVA: $F(60, 2460) = 9.872$, $p < 0.0001$). This, again, was even more striking when averaging over the window of 3 previous and

3 future events; the cross-correlation was significantly reduced following ibogaine (main effect injection ANOVA: $F(2, 56) = 59.77$, $p < 0.0001$; Tukey post hoc for ibogaine, $p < 0.0001$), but not saline ($p = 0.67$). In sum, the temporal extent of all tested correlations was reduced after ibogaine. It thus appears that ibogaine is shortening the temporal window over which signals are integrated in RSC.

3.5 DISCUSSION

In this study, the non-classic psychedelic ibogaine destabilized the linkage between RSC neuron activity and location on a treadmill belt, which significantly reduced the ability to decode position from ensemble activity. Many RSC cells encoded positions between cues prior to ibogaine, as shown previously (Mao et al., 2017). Ibogaine administration reduced the position-related MI of individual RSC cells in the non-cue regions, and impaired position decoding from the population. This indicates that RSC either cannot properly process positional information, or more likely, that afferent positional information is corrupted. RSC positional information depends on intact hippocampal processing (Esteves et al., 2021), and hippocampal place cells have long been known to encode position in the absence of detectable landmarks, which involves using path integration to update the cognitive map (McNaughton et al., 2006). The loss of positional information between landmarks in RSC may therefore reflect ibogaine-mediated impairment of path integration and/or instability of the cognitive map. Interestingly, cells that activated upon traversal of the tactile cues were less affected by the drug than those activating at locations between these cues. This could possibly reflect preservation of somatosensory signals to RSC, or re-stabilization of the cognitive map upon traversing landmarks. The loss of spatial information under

ibogaine may explain previous reports that ibogaine impairs spatial learning in rats (Kesner et al., 1995).

Previous reports on the effects of psychedelic compounds on brain function are largely based on human imaging using drugs such as psilocybin (Carhart-Harris et al., 2012; Muthukumaraswamy et al., 2013; Tagliazucchi et al., 2014), LSD (Carhart-Harris et al., 2016; Atasoy et al., 2017), and ayahuasca/DMT (Alonso et al., 2015; Palhano-Fontes et al., 2015; Riga et al., 2018). The psychedelic actions of these drugs are due to agonism of the 5-HT_{2A} receptor (Smith et al., 1998; Madsen et al., 2019). In humans, these drugs generally increase the distribution of activity covariance motifs among brain regions (Tagliazucchi et al., 2014; Atasoy et al., 2017), and promote cortical desynchronization (Muthukumaraswamy et al., 2013; Riga et al., 2018). The present data suggest similar effects at the cellular level. Note that although ibogaine agonizes 5-HT2a, it has broader effects on 5-HT signaling and other neuromodulators than do classic psychedelics (Bulling et al., 2012; Coleman et al., 2019). We cannot rule out the possibility that these latter effects contribute to the loss of spatial information and discoordination of neural activity. If these do contribute, then the effect might not be specific to psychedelics, and may be produced by other psychoactive drugs. Correlation analysis showed that the dominant motifs were abolished by ibogaine, and the newly emergent motifs were less distinct from one another. Moreover, the explained variance of the top PCA factors was reduced, indicating that the neurons became more functionally independent from one another. At least part of these effect can be explained by the deterioration of positional signaling, meaning that cells with overlapping position fields will exhibit covariation, which will be reduced by the destabilization of position fields by ibogaine. The avalanche analysis, on the other hand, is more independent of information encoding. Nonetheless, it likewise revealed a reduction in the timescale of correlations among bursting/pause

events. In sum, these analyses show a loss of structure among units, and across time such that causal relationships are diminished.

A recent report of the psychedelic 2,5-dimethoxy-4-iodoamphetamine (DOI), revealed a decrease in the neuronal responses to visual stimuli in layer II/III of visual cortex (Michaiel et al., 2019). Other features such as tuning properties and retinotopic organization were not disrupted. The authors propose that these results suggest a *reduction* of bottom-up sensory drive, which causes the system to rely more on top-down expectations. There are several possible explanations for the discrepancy with our finding. First, DOI is a selective 5-HT_{2A}R agonists, whereas ibogaine affects a wider variety of neurotransmitters, such as dopamine (Maisonneuve et al., 1991; Sershen et al., 1992a), serotonin (Broderick et al., 1994; Mash et al., 1995), and the opioid system (Codd, 1995; Glick et al., 1997). The effects of ibogaine could therefore depend on complex interactions of these neuromodulators on neural activity. Secondly, the afferents to RSC and visual cortex differ. It is possible that primary inputs to RSC, such as hippocampal formation or anterior cingulate region of medial prefrontal cortex, are more affected than the primary inputs to visual cortex.

Some recent analysis of functional connectivity in fMRI data suggests that brain networks shift toward criticality under psychedelics (Atasoy et al., 2017). This is based on the interaction between brain regions, whereas the present data are at the level of individual neurons within a brain structure. We found that ibogaine had surprisingly little effect on network criticality, as indicated by a lack of change in the slope of the size-frequency relationship of neural activity. This suggests that the drug did not much affect the propagation of information within the RSC network, at least in the superficial layers that were the target of the present recordings. This

supports the notion that the disruption of positional encoding between landmarks arises from the loss of structured input, such as the hippocampal cognitive map, rather than a change in RSC processing. Indeed, the ibogaine-mediated disruption is strikingly similar to the effects of hippocampal lesions on encoding of space in RSC (Esteves et al., 2021). They both degrade positional encoding when animals are between landmarks. A recent study has shown that place fields of hippocampal CA1 cells were relatively stable under high-dose LSD in a navigation task that did not require path integration (Domenico et al., 2021). This supports our interpretation of the present data that it is the processes needed for path integration, either the sensory inputs or the cognitive map, that are affected by ibogaine. Regardless of the neural circuits involved, the present data are consistent with proposals that psychedelics disrupt top-down predictions about future inputs (Clark, 2013; Pink-Hashkes et al., 2017), which diminishes the inhibition of 'bottom-up' sensory information leading to increased entropy of neural activity (Friston, 2010; Muthukumaraswamy et al., 2013). Here, firing rates during cue traverses increases proportionally more than non-cue regions, consistent with disinhibition, and neural activity became disordered, consistent with increased entropy.

Ibogaine somewhat reduced motivation and motoric output in the present study. Although such changes could in principle modulate the firing rates of place cells (McNaughton et al., 2006), no evidence suggests they could cause the severe degradation of place encoding observed here. Spatial representation was not remapped as could be explained by modulation of place cell firing rates, but was rather lost.

Positional signaling is widespread throughout the rodent neocortex (Mashhoori et al., 2018; Esteves et al., 2021), and may serve as a framework for associative learning to impart context

(Gruber and McDonald, 2012a; Mashhoori et al., 2018; Chang et al., 2020). Therefore, disruption of positional signaling may have widespread effects on other sensory modalities as well as cognitive function. Psychedelics often evoke disorientation (Garcia-Romeu et al., 2016), suggesting that they disrupt positional signaling. The hippocampus, in particular, has been proposed to bind together attributes of experience represented in neocortex (Teyler and Rudy, 2007). Disruption of this process by psychedelic drugs could provide a mechanism accounting for their effects on perception and discoordination of neocortical activation, and should be included in revised theories.

Acknowledgments

We would like to thank Adam Neumann for technical support and HaoRan Chang for helpful discussions. Funding provided by: Natural Sciences and Engineering Council of Canada, New Frontiers Research Fund, Alberta Innovates, Branch out Neurological Foundation, Beswick Fellowship, Canadian Institute of Health Research.

Author Contributions: V.E.I. and A.J.G. designed research, V.E.I. and I.M.E. performed research, M.M. contributed tools, V.E.I., D.P.T-C, I.M.E., D.C., and J.D. analyzed data, V.E.I., D.P.T-C, B.L.M., and A.J.G. wrote the paper.

Competing Interest Statement: The authors declare no competing interests.

3.6 REFERENCES

Alexander, A. S., & Nitz, D. A. (2015). Retrosplenial cortex maps the conjunction of internal and external spaces. *Nature Neuroscience, 18*(8), 1143-1151. doi:10.1038/nn.4058

Alonso, J. F., Romero, S., Mañanas, M. À., & Riba, J. (2015). Serotonergic psychedelics temporarily modify information transfer in humans. *International Journal of Neuropsychopharmacology, 18*(8). doi:10.1093/ijnp/pyv039

Atasoy, S., Roseman, L., Kaelen, M., Kringelbach, M. L., Deco, G., & Carhart-Harris, R. L. (2017). Connectome-harmonic decomposition of human brain activity reveals dynamical repertoire re-organization under LSD. *Scientific Reports, 7*(1), 17661. doi:10.1038/s41598-017-17546-0

Barnett, L., Muthukumaraswamy, S. D., Carhart-Harris, R. L., & Seth, A. K. (2020). Decreased directed functional connectivity in the psychedelic state. *NeuroImage, 209*, 116462. doi:https://doi.org/10.1016/j.neuroimage.2019.116462

Beggs, J. M., & Plenz, D. (2003). Neuronal Avalanches in Neocortical Circuits. *The Journal of Neuroscience, 23*(35), 11167. doi:10.1523/JNEUROSCI.23-35-11167.2003

Behrens, T. E. J., Muller, T. H., Whittington, J. C. R., Mark, S., Baram, A. B., Stachenfeld, K. L., & Kurth-Nelson, Z. (2018). What Is a Cognitive Map? Organizing Knowledge for Flexible Behavior. *Neuron, 100*(2), 490-509. doi:https://doi.org/10.1016/j.neuron.2018.10.002

Blackburn, J. R., & Szumlinski, K. K. (1997). Ibogaine effects on sweet preference and amphetamine induced locomotion: implications for drug addiction. *Behavioural Brain Research, 89*(1), 99-106. doi:https://doi.org/10.1016/S0166-4328(97)00050-8

Broderick, P. A., Phelan, F. T., Eng, F., & Wechsler, R. T. (1994). Ibogaine modulates cocaine responses which are altered due to environmental habituation: In vivo microvoltammetric and behavioral studies. *Pharmacology Biochemistry and Behavior, 49*(3), 711-728. doi:https://doi.org/10.1016/0091-3057(94)90092-2

Bulling, S., Schicker, K., Zhang, Y.-W., Steinkellner, T., Stockner, T., Gruber, C. W., . . . Sandtner, W. (2012). The mechanistic basis for noncompetitive ibogaine inhibition of serotonin and dopamine transporters. *Journal of Biological Chemistry, 287*(22), 18524-18534. doi:https://doi.org/10.1074/jbc.M112.343681

Carhart-Harris, R. L., Erritzoe, D., Williams, T., Stone, J. M., Reed, L. J., Colasanti, A., . . . Nutt, D. J. (2012). Neural correlates of the psychedelic state as determined by fMRI studies with psilocybin. *Proceedings of the National Academy of Sciences, 109*(6), 2138-2143. doi:10.1073/pnas.1119598109

Carhart-Harris, R. L., & Friston, K. J. (2019). REBUS and the anarchic brain: Toward a unified model of the brain action of psychedelics. *Pharmacological reviews, 71*(3), 316. doi:10.1124/pr.118.017160

Carhart-Harris, R. L., Muthukumaraswamy, S., Roseman, L., Kaelen, M., Droog, W., Murphy, K., . . . Nutt, D. J. (2016). Neural correlates of the LSD experience revealed by multimodal neuroimaging. *Proceedings of the National Academy of Sciences, 113*(17), 4853-4858. doi:10.1073/pnas.1518377113

Chang, H., Esteves, I. M., Neumann, A. R., Sun, J., Mohajerani, M. H., & McNaughton, B. L. (2020). Coordinated activities of retrosplenial ensembles during resting-state encode

spatial landmarks. *Philosophical Transactions of the Royal Society B, 375*(1799), 20190228.
Clark, A. (2013). Whatever next? Predictive brains, situated agents, and the future of cognitive science. *Behavioral and Brain Sciences, 36*(3), 181-204. doi:10.1017/S0140525X12000477
Codd, E. E. (1995). High affinity ibogaine binding to a mu opioid agonist site. *Life Sciences, 57*(20), PL315-PL320. doi:https://doi.org/10.1016/0024-3205(95)02171-E
Coleman, J. A., Yang, D., Zhao, Z., Wen, P.-C., Yoshioka, C., Tajkhorshid, E., & Gouaux, E. (2019). Serotonin transporter–ibogaine complexes illuminate mechanisms of inhibition and transport. *Nature, 569*(7754), 141-145. doi:10.1038/s41586-019-1135-1
Cooper, B. G., Manka, T. F., & Mizumori, S. J. Y. (2001). Finding your way in the dark: The retrosplenial cortex contributes to spatial memory and navigation without visual cues. *Behavioral neuroscience, 115*(5), 1012-1028. doi:10.1037/0735-7044.115.5.1012
Curic, D., Ivan, V. E., Cuesta, D. T., Esteves, I. M., Mohajerani, M. H., Gruber, A. J., & Davidsen, J. (2021). Deconstructing scale-free neuronal avalanches: behavioral transitions and neuronal response. *Journal of Physics: Complexity, 2*(4), 045010. doi:10.1088/2632-072X/ac35b4
Domenico, C., Haggerty, D., Mou, X., & Ji, D. (2021). LSD degrades hippocampal spatial representations and suppresses hippocampal-visual cortical interactions. *Cell Reports, 36*(11). doi:10.1016/j.celrep.2021.109714
Esteves, I. M., Chang, H., Neumann, A. R., Sun, J., Mohajerani, M. H., & McNaughton, B. L. (2021). Spatial information encoding across multiple neocortical regions depends on an intact hippocampus. *The Journal of Neuroscience, 41*(2), 307. doi:10.1523/JNEUROSCI.1788-20.2020
Fischer, L. F., Mojica Soto-Albors, R., Buck, F., & Harnett, M. T. (2020). Representation of visual landmarks in retrosplenial cortex. *eLife, 9*, e51458. doi:10.7554/eLife.51458
Friston, K. (2010). The free-energy principle: a unified brain theory? *Nature Reviews Neuroscience, 11*(2), 127-138. doi:10.1038/nrn2787
Garcia-Romeu, A., Kersgaard, B., & Addy, P. H. (2016). Clinical applications of hallucinogens: A review. *Experimental and Clinical Psychopharmacology, 24*(4), 229-268. doi:10.1037/pha0000084
Glick, S. D., Maisonneuve, I. M., & Pearl, S. M. (1997). Evidence for roles of κ-opioid and NMDA receptors in the mechanism of action of ibogaine. *Brain Research, 749*(2), 340-343. doi:https://doi.org/10.1016/S0006-8993(96)01414-X
Gruber, A., & McDonald, R. (2012). Context, emotion, and the strategic pursuit of goals: interactions among multiple brain systems controlling motivated behavior. *Frontiers in Behavioral Neuroscience, 6*(50). doi:10.3389/fnbeh.2012.00050
Jayakumar, R. P., Madhav, M. S., Savelli, F., Blair, H. T., Cowan, N. J., & Knierim, J. J. (2019). Recalibration of path integration in hippocampal place cells. *Nature, 566*(7745), 533-537. doi:10.1038/s41586-019-0939-3
Johnson, M. W., Hendricks, P. S., Barrett, F. S., & Griffiths, R. R. (2019). Classic psychedelics: An integrative review of epidemiology, therapeutics, mystical experience, and brain network function. *Pharmacology & Therapeutics, 197*, 83-102. doi:https://doi.org/10.1016/j.pharmthera.2018.11.010

Kesner, R. P., Jackson-Smith, P., Henry, C., & Amann, K. (1995). Effects of ibogaine on sensory-motor function, activity, and spatial learning in rats. *Pharmacology Biochemistry and Behavior, 51*(1), 103-109. doi:https://doi.org/10.1016/0091-3057(94)00367-R

Kobayashi, Y., & Amaral, D. G. (2003). Macaque monkey retrosplenial cortex: II. Cortical afferents. *Journal of Comparative Neurology, 466*(1), 48-79. doi:https://doi.org/10.1002/cne.10883

Köck, P., Froelich, K., Walter, M., Lang, U., & Dürsteler, K. M. (2021). A systematic literature review of clinical trials and therapeutic applications of ibogaine. *Journal of Substance Abuse Treatment*, 108717. doi:https://doi.org/10.1016/j.jsat.2021.108717

Kohek, M., Ohren, M., Hornby, P., Alcázar-Córcoles, M. Á., & Bouso, J. C. (2020). The ibogaine experience: A qualitative study on the acute subjective effects of ibogaine. *Anthropology of Consciousness, 31*(1), 91-119. doi:https://doi.org/10.1111/anoc.12119

Lombardi, F., Herrmann, H. J., Plenz, D., & de Arcangelis, L. (2016). Temporal correlations in neuronal avalanche occurrence. *Scientific Reports, 6*(1), 24690. doi:10.1038/srep24690

Madsen, M. K., Fisher, P. M., Burmester, D., Dyssegaard, A., Stenbæk, D. S., Kristiansen, S., . . . Knudsen, G. M. (2019). Psychedelic effects of psilocybin correlate with serotonin 2A receptor occupancy and plasma psilocin levels. *Neuropsychopharmacology, 44*(7), 1328-1334. doi:10.1038/s41386-019-0324-9

Maisonneuve, I. M., Keller, R. W., & Glick, S. D. (1991). Interactions between ibogaine, a potential anti-addictive agent, and morphine: An in vivo microdialysis study. *European Journal of Pharmacology, 199*(1), 35-42. doi:https://doi.org/10.1016/0014-2999(91)90634-3

Mao, D., Kandler, S., McNaughton, B. L., & Bonin, V. (2017). Sparse orthogonal population representation of spatial context in the retrosplenial cortex. *Nature Communications, 8*(1), 243. doi:10.1038/s41467-017-00180-9

Marton, S., González, B., Rodríguez-Bottero, S., Miquel, E., Martínez-Palma, L., Pazos, M., . . . Carrera, I. (2019). Ibogaine administration modifies GDNF and BDNF expression in brain regions involved in mesocorticolimbic and nigral dopaminergic circuits. *Frontiers in Pharmacology, 10*(193). doi:10.3389/fphar.2019.00193

Mash, D. C., Staley, J. K., Baumann, M. H., Rothman, R. B., & Lee Hearn, W. (1995). Identification of a primary metabolite of ibogaine that targets serotonin transporters and elevates serotonin. *Life Sciences, 57*(3), PL45-PL50. doi:https://doi.org/10.1016/0024-3205(95)00273-9

Mashhoori, A., Hashemnia, S., McNaughton, B. L., Euston, D. R., & Gruber, A. J. (2018). Rat anterior cingulate cortex recalls features of remote reward locations after disfavoured reinforcements. *eLife, 7*, e29793. doi:10.7554/eLife.29793

Maxim, P., & Brown, T. I. (2023). Toward an understanding of cognitive mapping ability through manipulations and measurement of schemas and stress. *Topics in Cognitive Science, 15*(1), 75-101. doi:https://doi.org/10.1111/tops.12576

McNaughton, B. L., Battaglia, F. P., Jensen, O., Moser, E. I., & Moser, M.-B. (2006). Path integration and the neural basis of the 'cognitive map'. *Nature Reviews Neuroscience, 7*(8), 663-678. doi:10.1038/nrn1932

Michaiel, A. M., Parker, P. R. L., & Niell, C. M. (2019). A hallucinogenic Serotonin-2A receptor agonist reduces visual response gain and alters temporal dynamics in mouse V1. *Cell Reports, 26*(13), 3475-3483.e3474. doi:https://doi.org/10.1016/j.celrep.2019.02.104

Muthukumaraswamy, S. D., Carhart-Harris, R. L., Moran, R. J., Brookes, M. J., Williams, T. M., Errtizoe, D., . . . Nutt, D. J. (2013). Broadband cortical desynchronization underlies the human psychedelic state. *The Journal of Neuroscience, 33*(38), 15171-15183. doi:10.1523/jneurosci.2063-13.2013

O'Keefe, J., & Nadel, L. (1978). *The Hippocampus as a Cognitive Map*: Oxford: Clarendon Press.

Palhano-Fontes, F., Andrade, K. C., Tofoli, L. F., Santos, A. C., Crippa, J. A. S., Hallak, J. E. C., . . . de Araujo, D. B. (2015). The psychedelic state induced by ayahuasca modulates the activity and connectivity of the default mode network. *PloS one, 10*(2), e0118143-e0118143. doi:10.1371/journal.pone.0118143

Pink-Hashkes, S., van Rooij, I., & Kwisthout, J. (2017). *Perception is in the Details: A Predictive Coding Account of the Psychedelic Phenomenon.* Paper presented at the CogSci.

Preller, K. H., Razi, A., Zeidman, P., Stämpfli, P., Friston, K. J., & Vollenweider, F. X. (2019). Effective connectivity changes in LSD-induced altered states of consciousness in humans. *Proceedings of the National Academy of Sciences, 116*(7), 2743. doi:10.1073/pnas.1815129116

Rambousek, L., Palenicek, T., Vales, K., & Stuchlik, A. (2014). The effect of psilocin on memory acquisition, retrieval, and consolidation in the rat. *Frontiers in Behavioral Neuroscience, 8*. doi:10.3389/fnbeh.2014.00180

Riga, M. S., Lladó-Pelfort, L., Artigas, F., & Celada, P. (2018). The serotonin hallucinogen 5-MeO-DMT alters cortico-thalamic activity in freely moving mice: Regionally-selective involvement of 5-HT1A and 5-HT2A receptors. *Neuropharmacology, 142*, 219-230. doi:https://doi.org/10.1016/j.neuropharm.2017.11.049

Sershen, H., Harsing, L. G., Hashim, A., & Lajtha, A. (1992). Ibogaine reduces amphetamine-induced locomotor stimulation in C57BL/6By mice, but stimulates locomotor activity in rats. *Life Sciences, 51*(13), 1003-1011. doi: https://doi.org/10.1016/0024-3205(92)90498-E

Sershen, H., Hashim, A., & Lajtha, A. (2001). Chapter 6 Characterization of multiple sites of action of ibogaine. *The Alkaloids: Chemistry and Biology* (Vol. 56, pp. 115-133): Academic Press.

Shibata, H., & Naito, J. (2008). Organization of anterior cingulate and frontal cortical projections to the retrosplenial cortex in the rat. *Journal of Comparative Neurology, 506*(1), 30-45. doi:https://doi.org/10.1002/cne.21523

Smith, R. L., Canton, H., Barrett, R. J., & Sanders-Bush, E. (1998). Agonist properties of N,N-Dimethyltryptamine at serotonin 5-HT2A and 5-HT2C receptors. *Pharmacology Biochemistry and Behavior, 61*(3), 323-330. doi:https://doi.org/10.1016/S0091-3057(98)00110-5

Souza, B. C., Pavão, R., Belchior, H., & Tort, A. B. L. (2018). On Information Metrics for Spatial Coding. *Neuroscience, 375*, 62-73. doi:https://doi.org/10.1016/j.neuroscience.2018.01.066

Szumlinski, K. K., Haskew, R. E., Balogun, M. Y., Maisonneuve, I. M., & Glick, S. D. (2001). Iboga compounds reverse the behavioural disinhibiting and corticosterone effects of acute methamphetamine: Implications for their antiaddictive properties. *Pharmacology Biochemistry and Behavior, 69*(3), 485-491. doi:https://doi.org/10.1016/S0091-3057(01)00564-0

Tagliazucchi, E., Carhart-Harris, R., Leech, R., Nutt, D., & Chialvo, D. R. (2014). Enhanced repertoire of brain dynamical states during the psychedelic experience. *Human Brain Mapping, 35*(11), 5442-5456. doi:10.1002/hbm.22562

Teyler, T. J., & DiScenna, P. (1985). The role of hippocampus in memory: A hypothesis. *Neuroscience & Biobehavioral Reviews, 9*(3), 377-389. doi:https://doi.org/10.1016/0149-7634(85)90016-8

Teyler, T. J., & Rudy, J. W. (2007). The hippocampal indexing theory and episodic memory: Updating the index. *Hippocampus, 17*(12), 1158-1169. doi:https://doi.org/10.1002/hipo.20350

Todd, T. P., Mehlman, M. L., Keene, C. S., DeAngeli, N. E., & Bucci, D. J. (2016). Retrosplenial cortex is required for the retrieval of remote memory for auditory cues. *Learning & Memory, 23*(6), 278-288.

Yaghoubi, M., de Graaf, T., Orlandi, J. G., Girotto, F., Colicos, M. A., & Davidsen, J. (2018). Neuronal avalanche dynamics indicates different universality classes in neuronal cultures. *Scientific Reports, 8*(1), 3417. doi:10.1038/s41598-018-21730-1

3.7 SUPPLEMENTARY INFORMATION

A.

	Pre-drug day 1	Saline day 1	Saline day 2	Test day 1	Test day 2	Test day 3
Baseline	20 min	15 min	15 min	6-10 min	6-10 min	6-10 min
10 min after injection		15 min	15 min	10 min	10 min	10 min
30 min after injection				10 min	10 min	10 min

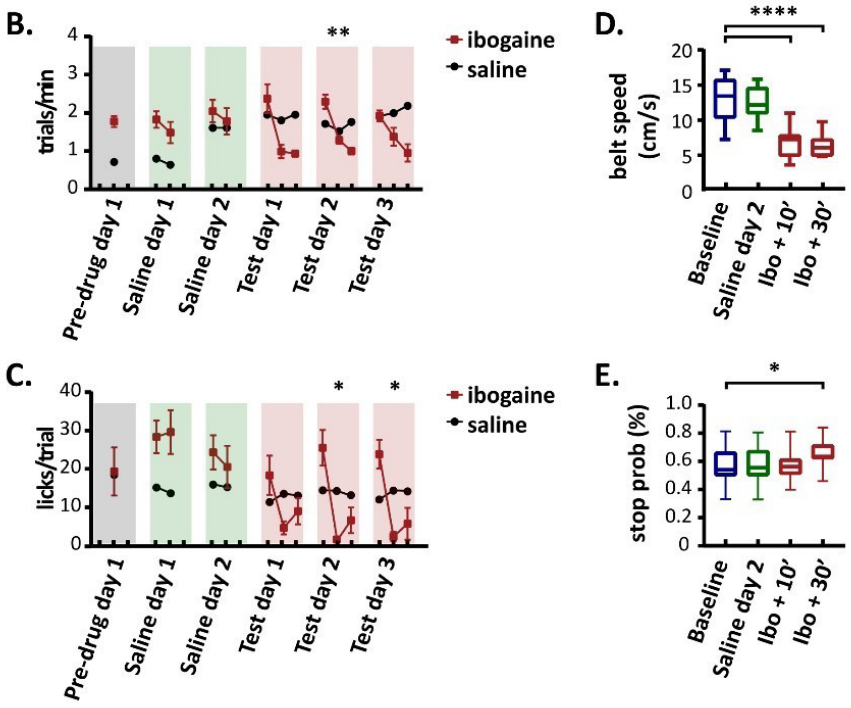

Supplemental Fig. 3.4: Experimental design and behavioral measures. A. Testing procedure. We recorded RSC activity as mice performed trials on the task for 6-20 minutes before any injection to serve as a baseline epoch for each session. We then injected either saline or ibogaine, paused behavior for 10 minutes, and then recorded for 10-15 minutes as the animal resumed the task. For ibogaine sessions, we added a third epoch by again pausing the behavior, and then recording during trials for 10 minutes starting at 30 minutes after injection. B. Rate of trial completion for each testing epoch during the session (baseline, 10', 30'). Each day had either one,

two, or three epochs, which are plotted by connected dots within each daily block. Data represent mean and SEM computed over all animals. Saline did not significantly alter trial completion rate, whereas ibogaine did. Black markers indicate two animals that received saline on testing days. Red dots are the six animals that received ibogaine on the test days. C. Average number of spout licks for each epoch in the sessions. D. Average running speed. E. Probability that mice stopped running between start of a lap, and arrival at the feeder-active position. Asterisks indicate statistical significance at $p<0.05$ (*), $p<0.01$ (**), and $p<0.0001$ (****).

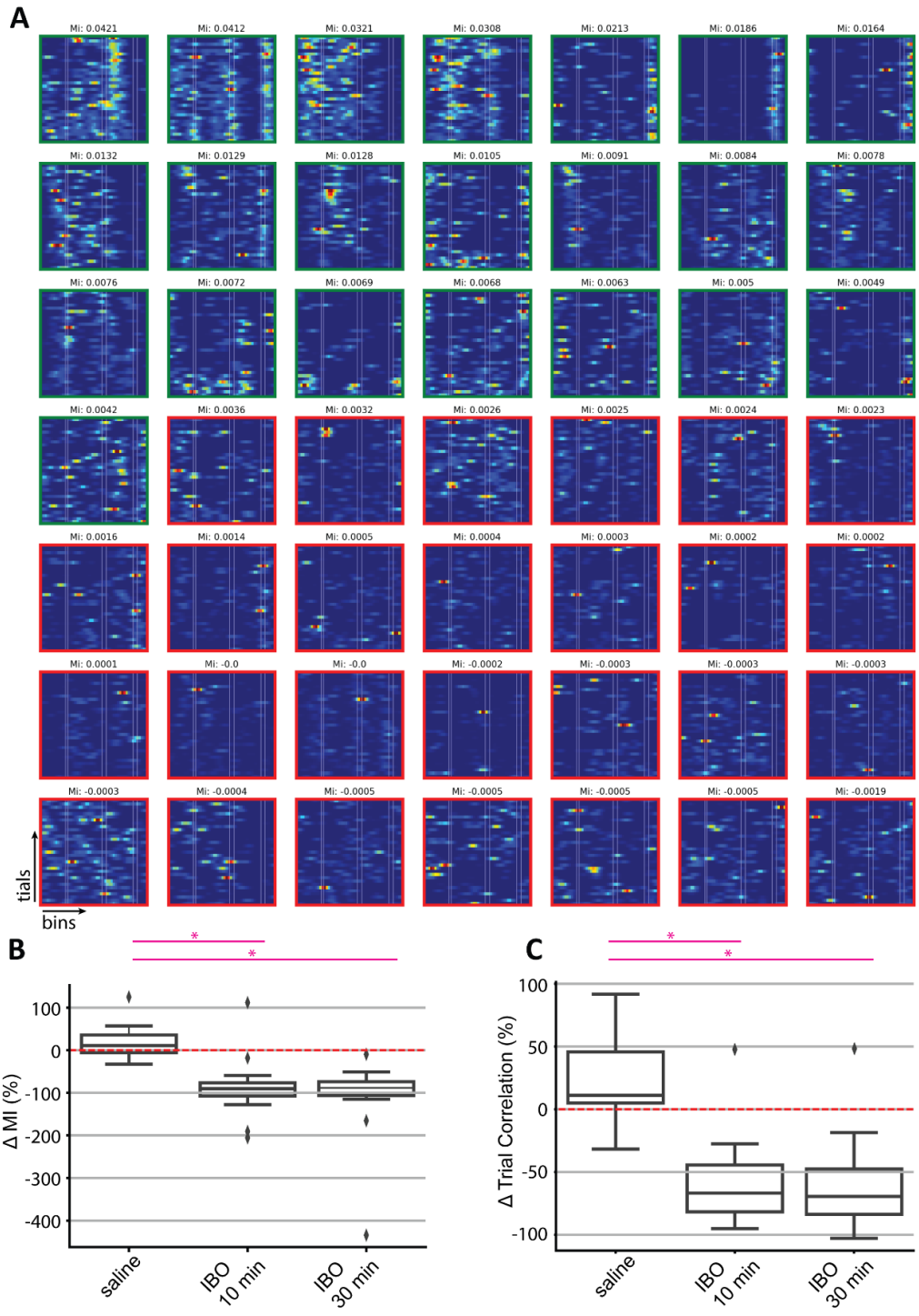

Supplemental Fig. 3.5: Adjusted Mutual Information. A. Trial-based activity of randomly sampled example cells. Each panel contains the normalized activity counts of a given cell in each of the spatial bins (horizontal axis) and trials (vertical axis). Cells are sorted from highest to lowest

MI. Cells in the upper quartile are highlighted with a green border, while other cells are shown with a red border. As expected, high MI cells activate in one or more bins consistently across multiple trials, and thus are informative of position. B. Percentage change of the mean MI after injection, with respect to the baseline within each recording day. The average MI significantly drops when ibogaine is on board, indicating a decrease in position dependent firing. We observed this 10 minutes after IBO injection, (see text), as well as in separate trials collected 30 min after IBO injection. Statistical tests:

Sal - IBO10: One-sided t-test, $t(26)=4.589$, $p=9.946e-05$

Sal - IBO30: One-sided t-test, $t(24)=4.077$, $p=4.337e-04$

IBO10 – IBO30: Two-sided t-test, $t(30)=0.734$, $p=0.469$

C. Percentage change of the mean trial to trial correlation of each cell after injection, with respect to the baseline within each recording day. As expected from the decrease in MI, the average cross correlation between trials, a measure of similarity of spatial firing patterns across different trials, significantly decreases 10 and 30 minutes after ibogaine injection as compared to saline. Statistical tests:

Sal - IBO10 One-sided t-test, $t(26)=5.938$, $p=2.887e-06$

Sal - IBO30 One-sided t-test, $t(24)=5.694$, $p=7.266e-06$

IBO10 – IBO30 Two-sided t-test, $t(30)=0.156$, $p=0.877$

Asterisks indicate statistical significance at $p < 0.01$.

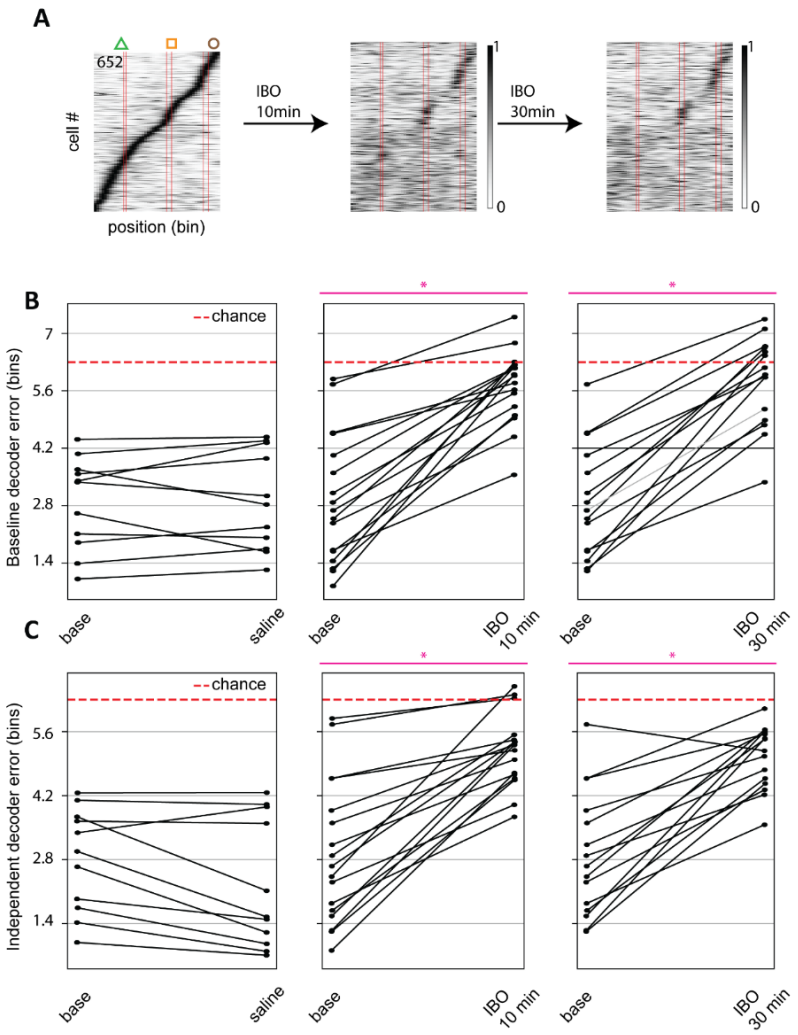

Supplemental Fig. 3.6: Population decoding at 10 and 30 minutes after injection, showing persistence of ibogaine effects. A. Trial average activity of the upper quartile of cells ordered by MI in baseline (left), after 10 min of IBO injection (middle), and after 30 min of IBO injection (right), ordered by lag to peak in baseline. As described in the text, neurons mostly lose their spatial tuning. Cells in the cue zones (indicated by red vertical lines) are less affected. This effect persists 30 min after injection.

B. Position decoder error when training a decoder using the baseline data for each session, and using it to decode position at baseline and after injection. The error increases towards chance at both 10 and 30 minutes after injection of ibogaine. The saline control shows no significant

decrease, showing that the encoding of baseline is preserved in the absence of IBO. Statistical tests:

Sal: Paired t-test, t(10)=-0.969, p=0.355

IBO10: Paired t-test, t(16)=-8.583, p=2.202e-07

IBO30: Paired t-test, t(14)=-11.39, p=1.821e-08

C. Position decoder error when training independent decoders for baseline and post-injection data for each session. As reported in the manuscript, the average errors increase after 10 min of ibogaine injection, indicating a decrease in the encoded spatial information. This effect is observed 30 min after IBO injection, but not after saline. Statistical tests:

Sal: Paired t-test, t(10)=2.963, p=0.014

IBO10: Paired t-test, t(16)=-7.058, p=2.707e-06

IBO30: Paired t-test, t(14)=-6.353, p=1.789e-05

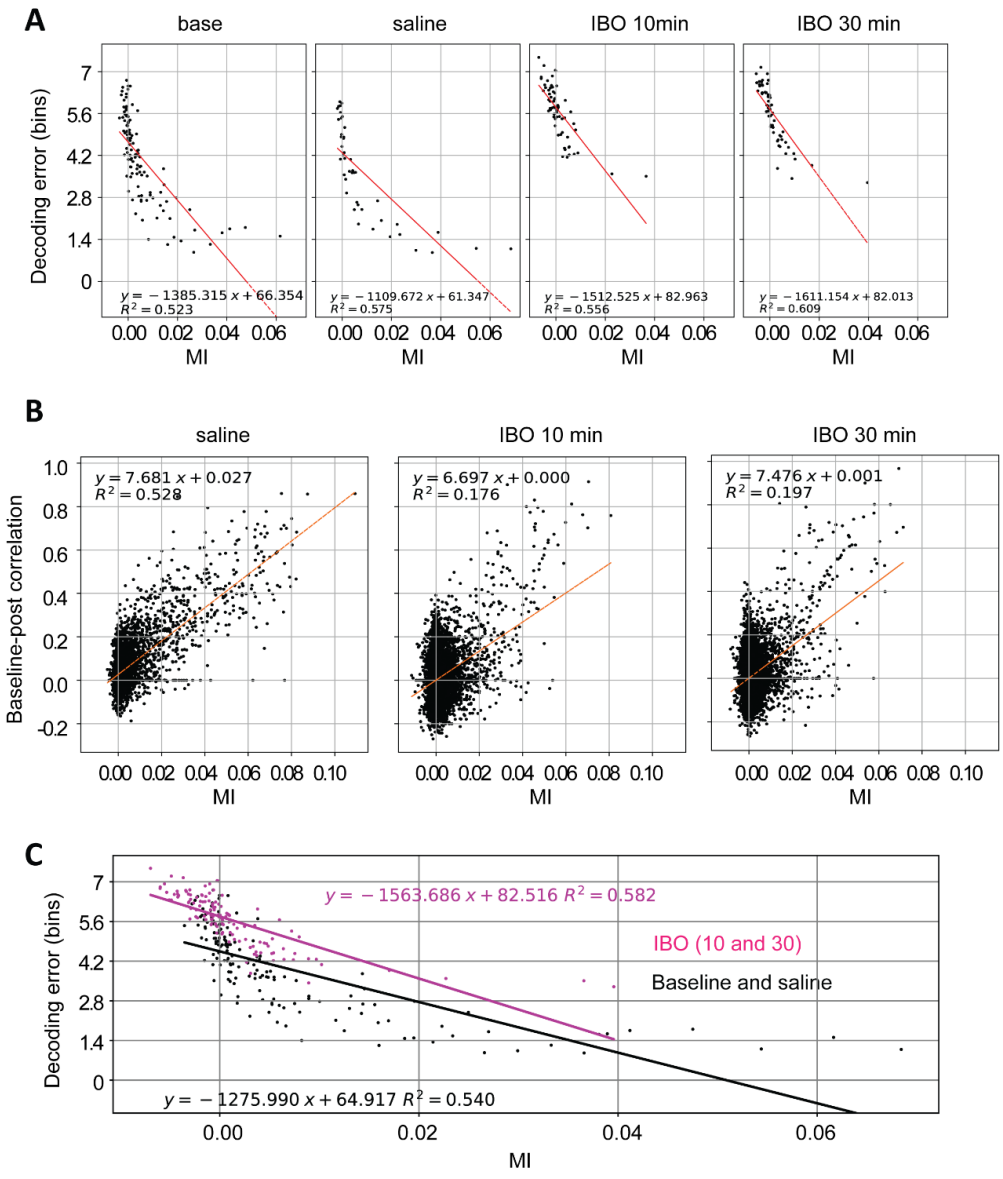

Supplemental Fig. 3.7: Relationship of MI, decoding error, and trial-by-trial correlation. A. Position decoding error as a function of the average MI of the cell partition (decile of MI values). For each recording session, neurons are divided into 10 deciles according to their MI, and the decoding error of each quartile and the mean MI of the cells in the quartile is computed. As expected, decoding error is negatively correlated with MI in each condition. There are fewer high-MI cells after ibogaine at 10 and 30 minutes, reducing the correlation values. B. Correlation of average unit activity before and after injection, as a function of its MI. For each neuron, its average activity correlation between the baseline trials and the subsequent post-injection trials is positively

correlated with the average MI of the neuron in both epochs. This relationship still holds after ibogaine, indicating that highly position-informative neurons tend to preserve their activity profile. C. Position decoding error as a function of the average MI of the cell partition, showing a negative correlation. The relationship is shifted upward after ibogaine, indicating higher decoding error even when the average MI is similar to a baseline/saline condition. In other words, even when controlling for average MI, sessions under IBO tend to have a higher decoding error. This suggests differences in the encoding of the position at the cell population level, and/or a disproportionate effect of very high-MI cells on position decoding.

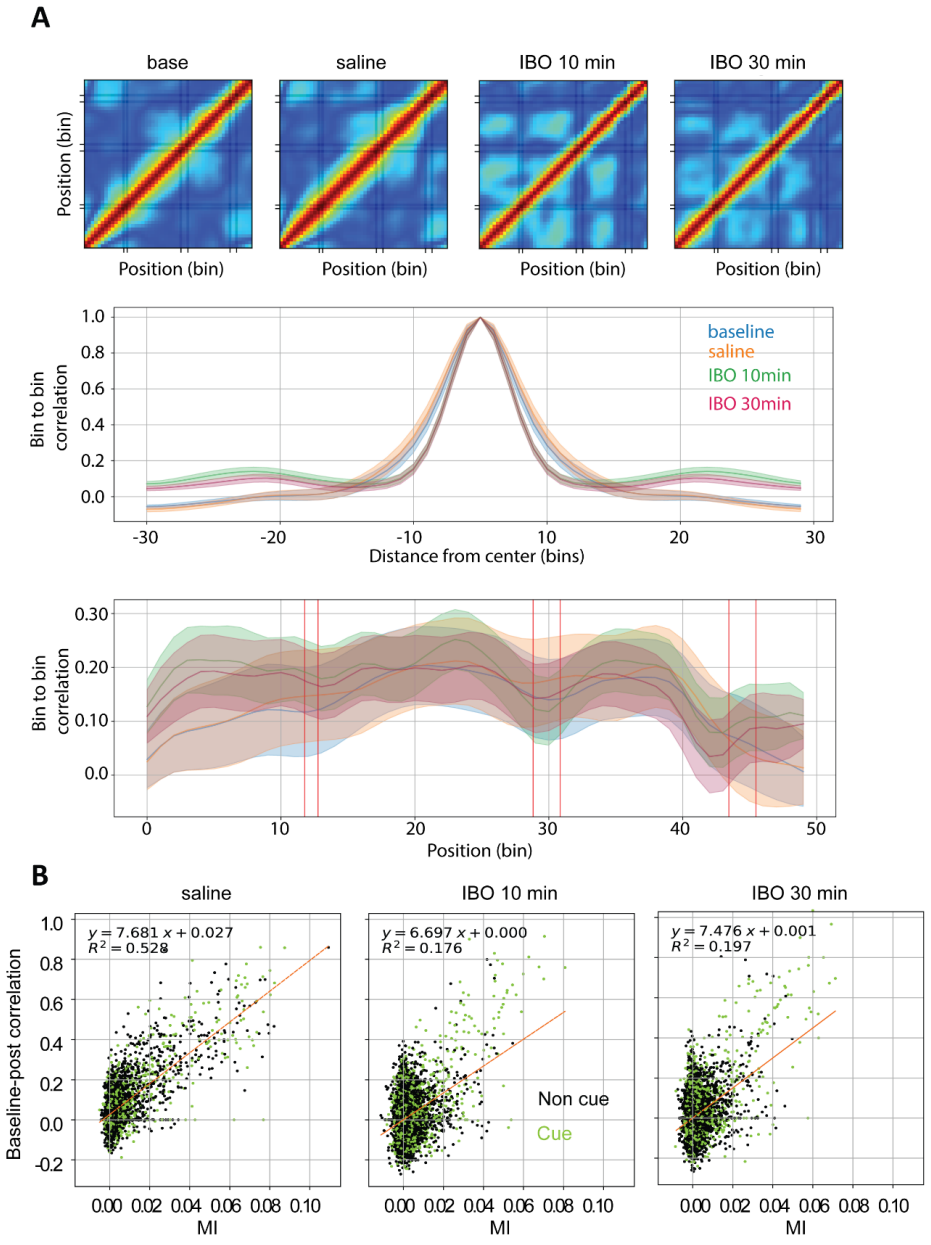

Supplemental Fig. 3.8: Autocorrelation of ensemble activity. A. We constructed cell x position vectors of average cell activity for each spatial bin (n=50) of the track. The cell order in the columns is arranged by lag to peak activity. We then computed correlations across the vectors (trial-averaged neuron activity) between each bin pair in the track (top row of plots). At baseline and after saline, this autocorrelation shows a diagonal band with little off-diagonal activity. This indicates that the ensemble creates a pattern of activity in each band that has some similarity to the

neighboring bins, but is distinct from distant bins. After ibogaine, off-diagonal correlations emerge in the non-cue locations, indicating a loss of position specificity in these regions. Moreover, ibogaine narrows the center band (middle panel). Lastly, the correlation of ensemble activity appears to dip near the cue locations, particularly at the latter two (bottom panel). This persists after ibogaine and indicates that the ensemble patterns of activity at each cue is more unique from other positions, as compared to the uniqueness of patterns at inter-cue locations. These data suggest a shift from a map initially tiled across the belt towards a map that retains accuracy mostly at the cue locations after ibogaine. B. Baseline to post-activity correlations as a function of the average MI for each cell. Each neuron is colored according to whether its activity peaks on a cue (green) or not (black). For any given neuron, its average activity correlation between the baseline trials and the subsequent session's is positively correlated with the average MI of the neuron. This still holds after ibogaine, indicating that highly position-informative neurons tend to preserve their activity profile. As shown in the manuscript, there are fewer high-MI cells (black dots) at non-cue locations after ibogaine, whereas the cue cells (green) are preserved.

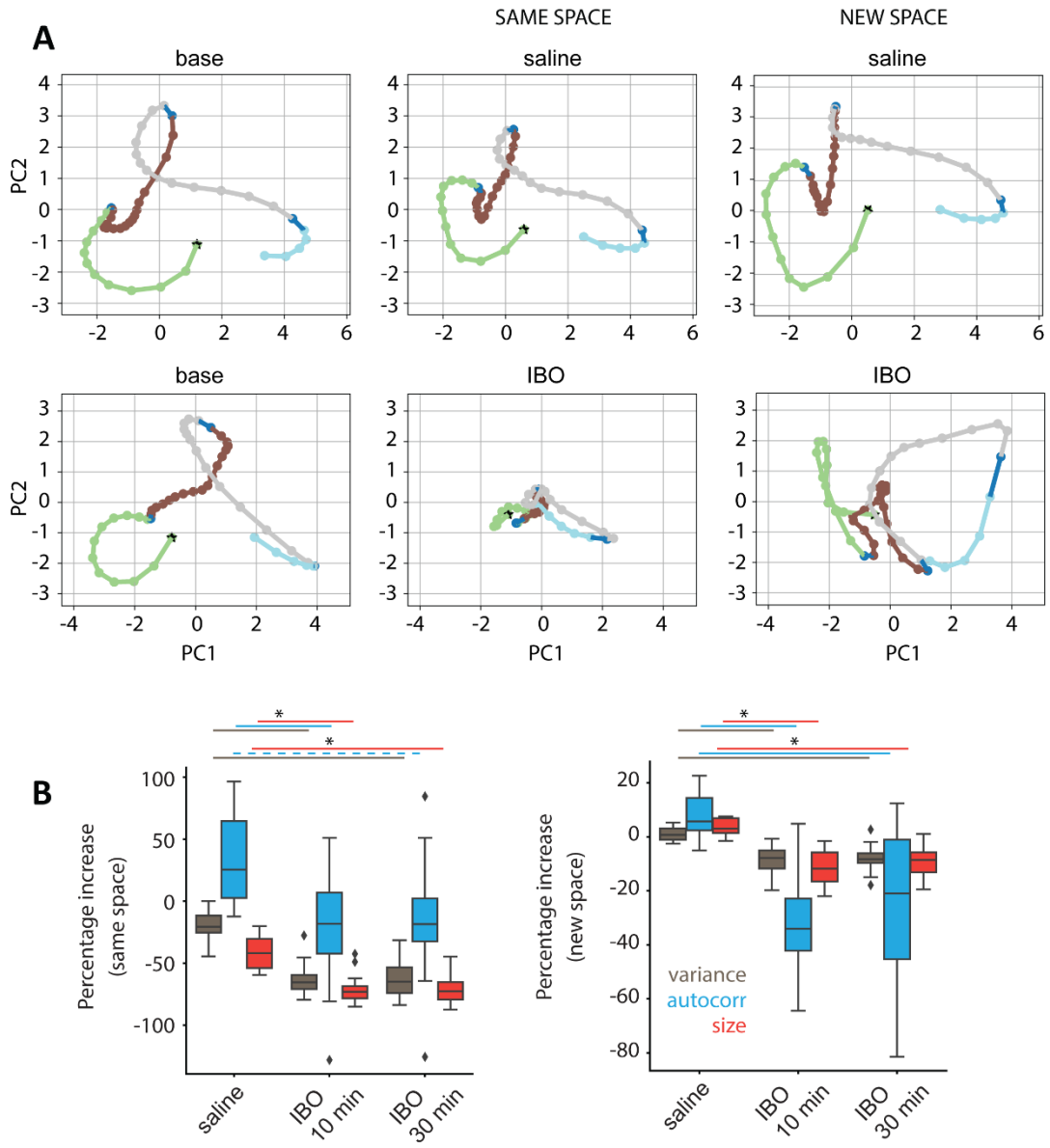

Supplemental Fig. 3.9: Effects of ibogaine on state space. A. State space formed by the two first principal components (PC) of the average neural activity during the trial. Left: Baseline session decomposition. Middle: The subsequent epoch (post-injection) PC projected to the same space as baseline. While the trajectory in state space remains similar to baseline after saline, the trajectory after ibogaine is markedly different. Right: Same activity as in the middle panel, but using a new PCA projection on this data. Again, saline remains similar to baseline, whereas the topology changes markedly after ibogaine. This is consistent with the changes in population correlation. B. We next quantified the trajectories formed by the first 6 PCA factors. We computed

the explained variance, decay parameter of an exponential fit to measure autocorrelation, and volume enclosed by the trajectories, and computed the changes from baseline. We did this for projections into the same space (left panel), and for independent decompositions for baseline and post-injection (right panel). When using the same decomposition as for baseline, saline caused a slight reduction in size and variance, but an increase in autocorrelation. Ibogaine, on the other hand, produces a pronounced collapse in the space. Note that the dark blue regions in Panel A indicate the cue regions, which are still separate in the space. Using a projection into a new space after injection (right panels), the trajectory for post-saline is inverted in the horizontal axis, but otherwise similar to baseline. The post-ibogaine data shows a more erratic trajectory in the space. All three derived metrics of the trajectories tended to decrease in both decomposition schemes. This indicates a loss of covariance of unit activity after ibogaine. Asterisks '*' and horizontal lines indicate statistically significant difference of means by t-test after Bonferroni correction of $p < 0.001$ (solid line), or $p < 0.025$ (dashed line).

Supplementary Methods

Surgery

Before surgery, animals received buprenorphine (0.05 mg/kg SC) and dexamethasone (0.2 mg/kg IM). They were then anesthetized with isoflurane (1-1.5%) and head fixed in a stereotaxic frame with body temperature maintained at 37.0 ± 0.5 ◦C with a heating pad. Mice received a 5 mm bilateral craniotomy (AP: +1 to -4; ML: -2.5 to +2.5), which was then covered with three layers of coverslips affixed with optical adhesive (NOA71, Norland). The coverslip was attached to the skull using Vetbond, and a titanium head plate was fixed to the skull using dental acrylic. Post-surgical care included careful weight monitoring and subcutaneous injections of meloxicam (Metacam 1 mg/kg) and enrofloxacin (Baytril, 10 mg/kg) for three days after implant.

Two-Photon Imaging

Neural activity was imaged using a 2-photon microscope (Bergamo II multiphoton microscopy, Thorlabs) through a 16x water-immersion objective lens (NA=0.8, Nikon). Excitation was with a Ti:sapphire pulsed laser (Coherent) tuned to a wavelength of 920 nm, ~80mW power, and controlled by a galvo-resonant X-Y scanner. Images were acquired at depths between 135 μm – 170 μm (layer II/III), from a field of view of 835 x 835 μm. Images were digitized at a sampling rate of 19 Hz, and at a resolution of 800 x 800 pixels. Imaging data from all animals were acquired from one hemisphere of either the left or right RSC (AP: -1 to -3; ML: 0 to +/- 1).

Pre-processing

Automatic image pre-processing was performed using the Suite-2P algorithm (Pachitariu et al., 2017) for MATLAB (MathWorks), as previously described (Mao et al., 2017). The regions of

interest (ROIs) detected were inspected manually and labelled as cells or non-cells by experienced users. For each ROI, the ΔF/F time courses were deconvolved using constrained non-negative matrix factorization (Pnevmatikakis et al., 2016), and all subsequent analyses were conducted using the deconvolved time-courses. For injection days, the imaging sequences of both pre- and post-injection intervals were combined during pre-processing so as to acquire the activity of the same set of cells (ROIs) before and after injections.

Computing spatial encoding

In order to identify spatially tuned neurons, we computed the adjusted mutual information (MI) (Vinh et al., 2010) between the firing rate of each neuron and the position of the mouse in the belt. We first divided the belt into 50 bins (3 cm each). For each bin and trial, we summed the neuron's activity and binned it into 4 levels, giving us the joint bin-activity discrete distribution, which we use to compute the mutual information. The MI used here is an adjustment of mutual information which accounts for the number of trials, which differs number among session, and thus is appropriate to compare cells from different sessions on the same scale. The MI is upperlimited by 1 and takes an expected value of 0 when the firing and position are independent. Negative values signify that the MI for that cell is lower than the MI one would expect solely due chance. Visually, the MI is a convincing measure of how predictive a neuron's firing is of a particular position (Supplementary Fig S2.1) and strongly correlates with decoding accuracy (Supplementary Fig S2.3).

Computing decoding error

Recordings of the daily session from each mouse are comprised of several epochs, such as the baseline recording prior to injection, and the recording 10 minutes after injection. To compute the decoding errors, we first bin and concatenate all trials in a given recording epoch (e.g. prior to injection), yielding with a matrix of cells x bins, in which bins is the resolution of spatial binning for one lap (25 for this analysis) multiplied by the number of trials completed in the epoch. To accurately compare between epochs with different number of trials, we crop all epochs to the minimum number of laps in any epoch for each mouse in the comparison set. We then do 10-fold cross-validation by training and testing a decoder to predict in which of 25 bins was the animal located given the vector of binned cell activities. We use a logistic regression for our decoder, and the error is represented as the minimum distance on the unit circle between the bins. This is done to correct for the label discontinuity of the boundary between the 25^{th} and 1^{st} bins. The reported decoding error is the root mean of the squared differences between the predicted and correct bins, averaged over the 10 folds.

Unit functional connectivity

Computing the apparent functional connectivity among neurons involved several steps. First, the spikes underlying the calcium fluorescence traces were inferred using a deconvolution algorithm (Friedrich et al., 2017). Next, the data in which the mouse is slow or not moving (below the 10% quantile of the velocity distribution over the track) is removed. The track is then divided into 50 spatial bins. The trial-averaged activity in each bin is computed for each cell to create a 'tuning curve' over the belt. The Pearson correlation between the tuning curves of all cell pairs is then computed. To visualize clusters in the cells x cells spatial correlation matrix, the columns/rows were ordered so that highly correlated cells are adjacent. For each neuron, a vector of its

correlations with all other cells was generated. In order to determine the similarity between the correlation structures, the pairwise euclidean distances between those vectors were calculated. Using the unweighted pair group method with arithmetic mean (UPGMA), a hierarchical clustering on these measures was conducted (Sokal, 1958). To assess the amount of clustering in the spatial correlation matrices, we computed the average clustering coefficient (Saramäki et al., 2007), a measure which quantifies how many cells with similar firing patterns are similar between each other, averaged over all cells; this coefficient is independent of the ordering of rows/columns.

Quantifying neuronal avalanches

Neuronal avalanches are typically defined as successive time bins of non-zero neural activity, delineated by at least one quiescent time bin between avalanches (Beggs and Plenz, 2003). When the neural activity is high relative to the sampling rate of the data acquisition system, periods of quiescence become rare, and so a non-zero threshold is typically employed. We take this approach by using a threshold to binarize the deconvolved calcium signal. This approach was chosen because the binarized signal has a more straightforward interpretation – an above threshold signal indicates a probable firing event within that time bin. The size (S) of the avalanche is the number of neuron firing events that contributed to the avalanche. Following the analysis in (Bellay et al., 2015), we normalize the avalanche size by Λ, the product of the number of neurons in an individual recording and the firing rate averaged over the total population. This allows for comparisons across recordings with variable cell numbers and population activity. The duration (D) is the number of consecutive frames of above-threshold activity, divided by the sampling rate. Similarly, we can define the quiet period (Q), to be duration of the quiescent intervals between two avalanches.

Avalanche detection depends on our choice of the duration of a single time bin, and the threshold. For this study, the time-bin (52.6 ms) is the minimum afforded by the scanning rate of the imaging system (19 Hz). We follow a previously-described method (Priesemann et al., 2013; Bowen et al., 2019) to set the threshold for each recording. The number, and size distribution of the avalanches (as well as the quiet periods) depends on the threshold chosen. As the threshold λ is increased from zero, the number of avalanches initially increases because long events become segmented into multiple shorter ones. If the threshold becomes very high, the number of avalanches decreases as less of the global activity signal $I(t)$ is above the threshold. This implies there exists a threshold λ_{max} that maximizes the number of avalanches. From the de-convolved calcium signals, we find $I_i(t; \lambda)$, i.e., the binarized signal of the i-th neuron, given the threshold λ. We then calculate the time-varying intensity of the population $I(t; \lambda) = \sum_i I_i(t; \lambda)$. From $I(t; \lambda)$ we find the number of resulting avalanches, and iterate this procedure to find λ_{max} (Bellay et al., 2015). Typical values of λ_{max} are greater than the 95-th percentile of the variable spike data, which mean they are more likely to correspond to actual neuronal events, rather than noise. This process is repeated for each recording. Avalanche surrogates (shuffled data) were generated by independent random cyclic shuffling of individual neuronal time series - which preserve autocorrelation but not cross-correlation structure between neurons (gray curves in Fig. 3.B). Thresholds were recalculated for the surrogate raster's and the subsequent avalanche analysis was performed in the same manner as described above.

We determined the slope of the size distribution by maximum likelihood estimation. We determined the cutoff by the customary technique of manual inspection (Miller et al., 2019). To reduce bias, cutoff identification was done in a blind manner in which the distribution from each session was scored in ignorance of the experimental condition (baseline, saline, ibogaine).

Avalanche Correlation Analysis

As avalanches can be ordered chronologically, we define a list (S_1, S_2, … , S_M) of avalanche sizes, where S_i is the size of the *i*-th avalanche. Similarly, we can also define a list of 'quiet' periods (Q_1, Q_2, … , Q_M) with activity below the threshold, where Q_i is the duration of the quiet period following the *i*-th avalanche. Correlations were computed by either calculating the auto-correlation functions of the ordered avalanche sizes or quiet periods, or by calculating cross-correlation functions between avalanche sizes and quiet periods.

Supplemental References

Beggs, J. M., & Plenz, D. (2003). Neuronal avalanches in neocortical circuits. *The Journal of Neuroscience, 23*(35), 11167. doi:10.1523/JNEUROSCI.23-35-11167.2003

Bellay, T., Klaus, A., Seshadri, S., & Plenz, D. (2015). Irregular spiking of pyramidal neurons organizes as scale-invariant neuronal avalanches in the awake state. *eLife, 4*, e07224. doi:10.7554/eLife.07224

Bowen, Z., Winkowski, D. E., Seshadri, S., Plenz, D., & Kanold, P. O. (2019). Neuronal avalanches in input and associative layers of auditory cortex. *Frontiers in Systems Neuroscience, 13*, 45. Retrieved from https://www.frontiersin.org/article/10.3389/fnsys.2019.00045

Friedrich, J., Zhou, P., & Paninski, L. (2017). Fast online deconvolution of calcium imaging data. *PLOS Computational Biology, 13*(3), e1005423. doi:10.1371/journal.pcbi.1005423

Mao, D., Kandler, S., McNaughton, B. L., & Bonin, V. (2017). Sparse orthogonal population representation of spatial context in the retrosplenial cortex. *Nature Communications, 8*(1), 243. doi:10.1038/s41467-017-00180-9

Miller, S. R., Yu, S., & Plenz, D. (2019). The scale-invariant, temporal profile of neuronal avalanches in relation to cortical γ–oscillations. *Scientific Reports, 9*(1), 16403. doi:10.1038/s41598-019-52326-y

Pachitariu, M., Stringer, C., Dipoppa, M., Schröder, S., Rossi, L. F., Dalgleish, H., . . . Harris, K. D. (2017). Suite2p: beyond 10,000 neurons with standard two-photon microscopy. *Biorxiv*.

Pnevmatikakis, Eftychios A., Soudry, D., Gao, Y., Machado, T. A., Merel, J., Pfau, D., . . . Paninski, L. (2016). Simultaneous denoising, deconvolution, and demixing of calcium imaging data. *Neuron, 89*(2), 285-299. doi:https://doi.org/10.1016/j.neuron.2015.11.037

Priesemann, V., Valderrama, M., Wibral, M., & Le Van Quyen, M. (2013). Neuronal avalanches differ from wakefulness to deep sleep – evidence from intracranial depth recordings in humans. *PLOS Computational Biology, 9*(3), e1002985. doi:10.1371/journal.pcbi.1002985

Saramäki, J., Kivelä, M., Onnela, J.-P., Kaski, K., & Kertész, J. (2007). Generalizations of the clustering coefficient to weighted complex networks. *Physical Review E, 75*(2), 027105. doi:10.1103/PhysRevE.75.027105

Sokal, R. R. (1958). A statistical method for evaluating systematic relationships. *Univ. Kansas, Sci. Bull., 38*, 1409-1438. Retrieved from https://ci.nii.ac.jp/naid/10004143217/en/

Vinh, N. X., Epps, J., & Bailey, J. (2010). Information theoretic measures for clusterings comparison: Variants, properties, normalization and correction for chance. *The Journal of Machine Learning Research, 11*, 2837-2854.

CHAPTER 4: THE SPATIAL ENCODING IN MOUSE RETROSPLENIAL CORTEX IS DEGRADED BY REPEATED AMPHETAMINE ADMINISTRATION AND RESISTANT TO PSYCHEDELIC REMEDIATION

Victorita E. Ivan[1]*, David P. Tomàs-Cuesta[1]*, Ingrid M. Esteves[1], Majid Mohajerani[1], Bruce L. McNaughton[1,2], Aaron J. Gruber[1]✉

[1]Canadian Centre for Behavioural Neuroscience, Department of Neuroscience, University of Lethbridge, Lethbridge, Alberta, Canada

[2]Center for the Neurobiology of Learning and Memory, University of California Irvine, Irvine, California, USA

*The authors contributed equally.

✉ Aaron J. Gruber

Email: aaron.gruber@uleth.ca

Keywords: retrosplenial cortex, psychedelics, chronic amphetamine,

4.1 ABSTRACT

Repeated administration of abused drugs causes structural and functional changes in the brain. The effect of these changes on the neural activity mediating neural functions, such as goal-directed navigation based on cognitive maps, is not well understood. We investigated this by using 2-photon microscopy to longitudinally record spatial encoding in the retrosplenial cortex (RSC) of head-fixed mice navigating a virtual environment before, during, and after a 10-day course of escalating amphetamine (AMPH) administration (0.5 – 2 mg/kg). We found that amphetamine degrades spatial information and reduces signaling stability both when amphetamine was ON board (1h after injection) and 24 hours later when AMPH was OFF board. We subsequently administered ibogaine, a non-classic psychedelic used to treat drug addiction, to test its ability to remediate the impaired spatial encoding. Ibogaine (40 mg/kg) acutely reduced spatial encoding and correlation of activity among RSC neurons, but there was no effect observed 24 hours later in mice that had previously received amphetamine. Interestingly, control animals that had previously received saline instead of amphetamine showed enhanced spatial encoding the day after ibogaine administration. In sum, chronic amphetamine persistently reduced the signal-to-noise ratio of spatial encoding by RSC neurons, and ibogaine did not remediate these effects.

4.2 INTRODUCTION

Drug addiction has been conceptualized as a disorder defined by an addiction cycle involving intoxication, withdrawal, and craving (Koob and Le Moal, 2001). This cycle promotes drug seeking behavior, which appears to be mediated primarily by neural systems that control ethological behaviors such as resource foraging (Everitt et al., 2001; Milton, 2023). These systems involve brain structures mediating navigation, reward processing, and decision making (Dalley et al., 2011). Some investigators have proposed that drug abuse can be conceptualized as a disorder of learning and memory (Milton and Everitt, 2012). Indeed, chronic administration of amphetamine (AMPH) at high doses has been shown to impair learning and memory in a variety of tasks, such as novel spatial and object recognition (Mandillo et al., 2003; Arroyo-García et al., 2020) and attentional set-shifting (Featherstone et al., 2008). These behavioral effects may be in some part attributed to changes in synapses and/or cholinergic transmission. It also attenuates attentional task-related increases of acetylcholine release in rat prefrontal cortex (Kozak et al., 2007). It remains to be determined how such changes affect neural processing in brain networks that encode environmental space and guide goal-directed navigation.

One important node of the navigation network is the retrosplenial cortex (RSC), which encodes the state of the animal in an environment and supports navigational choices (Keene and Bucci, 2009; Alexander and Nitz, 2015). Many RSC cells encode the location of the animal in a virtual environment by activating at a particular location, similar to hippocampal place cells (Mao et al., 2017). The properties of these cortical place cells thus provide a means to quantify how information is affected by drug administration. Furthermore, the RSC is anatomically connected to the hippocampus (HPC) (Wyass and Van Groen, 1992), the medial prefrontal cortex (PFC)

(Fisk and Wyss, 1999; Shibata et al., 2004), and other related structures that regulate emotion, memory, and spatial encoding (Corcoran et al., 2016). It is therefore well integrated into brain networks known to be affected by psychostimulants and other drugs with abuse potential.

Mental representations of the environment allow animals to navigate and achieve goals. This representation is often referred to as a cognitive map (O'Keefe and Nadel, 1978). The RSC is involved in both the formation and the use of cognitive maps, and its contribution is comparable to the HPC (Wolbers and Büchel, 2005; Iaria et al., 2007). The cognitive map is updated using path integration, in which signals related to movement are used to update a mental estimate of the animal's position in an environment. The RSC works in conjunction with the HPC and other structures for path integration in goal-directed spatial tasks (Sherrill et al., 2013). The location-encoding RSC cells reflect this process (Mao et al., 2017). Here, we tested if repeated amphetamine impairs the encoding of space by RSC cells, which may help account for the deficits in novel spatial and object recognition after repeated AMPH administration (Mandillo et al., 2003; Arroyo-García et al., 2020).

Both recent clinical and animal studies suggest that an acute treatment of psychedelics provide long-term efficacy in reducing substance abuse. The psychoactive alkaloid, ibogaine, has been particularly of interest, as it is purported to disrupt the addiction cycle in humans (dos Santos et al., 2017; Noller et al., 2018; Köck et al., 2021). Research in rodents likewise shows efficacy in ameliorating cocaine, morphine, and heroin self-administration (Glick et al., 1994; Dworkin et al., 1995; Havel et al., 2021), and to reduce the rewarding effect of a morphine, amphetamine, or alcohol in rodents (Parker et al., 1995; Moroz et al., 1997; Henriques et al., 2021). Little is known about how such treatment affects cognitive function. We therefore tested the effect of the non-

classic psychedelic ibogaine on RSC spatial encoding in mice that have been exposed to repeated AMPH treatment, and to controls.

4.3 RESULTS

We used 2-photon imaging to record the activity of ensembles of individual neurons (133-786 simultaneous cells per session) in the superficial layers (~ 150 nm deep) of RSC in head-fixed mice (Fig. 4.1.A). Mice were placed on a treadmill belt that had narrow tactile cues in three positions along its length. Mice received a liquid reward on every lap. We used an amphetamine (AMPH) x ibogaine (IBO) design with saline (SAL) as negative control. In the first phase of the experiment, one group of mice (n=8) received escalating daily injections of amphetamine (0.5 to 2 mg/kg) over 10 days, and another group (n=6) received daily injections of saline. In order to discriminate acute effects of AMPH on neural signaling from adaptations of signaling due to repeated administration, we alternated the order of drug administration and recording among successive recording days. This allows us to compare neural signaling effects when animals have amphetamine on-board (ON; injection 1h before recording) or off-board (OFF; injections 10 mins after recording).

4.3.1 Amphetamine

We observed no overall behavioral differences between the amphetamine and control groups during the 10 days of chronic drug administration. These include animals' speed, the probability that the mice stopped running between the start of a lap and the arrival at the feeder position, and the rate of trial completion, all reported as two-way ANOVA: Group (AMPH/SAL) x injection (ON/OFF) (Fig. 4.1. B-D; belt velocity: $F(3, 126) = 0.720$, $p = 0.542$; stop probability: $F(3, 126) = 1.541$, $p = 0.207$; trials/min: $F(3, 126) = 0.799$, $p = 0.497$). When amphetamine was

ON board, the overall firing rate of the neurons in the RSC was decreased (Fig. 4.1.E; two-way ANOVA: $F(3, 126) = 13.91$, $p < 0.0001$), as compared to both SAL ON (Tukey post hoc test, $p = 0.0003$) and AMPH OFF (Tukey post hoc test, $p < 0.0001$) groups, but the mean activity rate was not different between the two groups during the OFF condition (Tukey post hoc test, $p = 0.622$). This is consistent with previous reports of AMPH-induced reduction of activity in other cortical regions of behaving animals (Homayoun and Moghaddam, 2006; Hashemnia et al., 2020), although some groups of neurons exhibit an increase depending on dose and length of treatment.

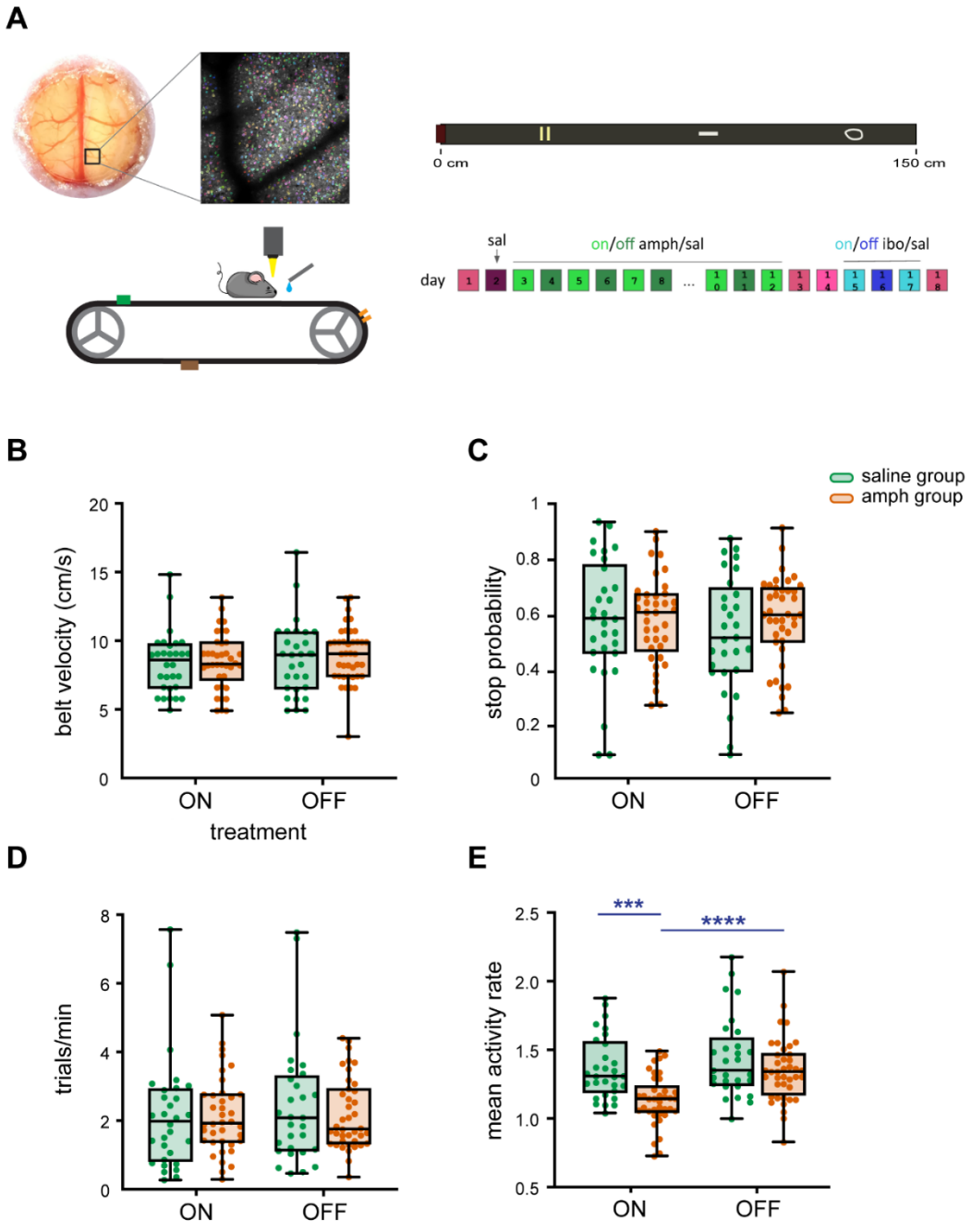

Fig. 4.1: Effects of amphetamine on behavior and neural activity rate. A. Experimental setup. In each animal, we recorded RSC while the animal was running on a treadmill with tactile cues for rewards. B. Box plots and individual values of the animals' speed with either saline or amphetamine ON or OFF board. C. Box plots and individual values of the stop probability. D. Box plots and individual values for the number of trials per minute. E. Box plots and individual values

for the mean activity rate of all neurons during each condition. Statistical significance ($p<0.001$) is indicated by '***', and ($p<0.0001$) is indicated by '****'.

We next sought to determine the effect of amphetamine on neural signaling. Many RSC neurons have place-specific activity (Mao et al., 2017), activating at specific locations on the belt during each trial (Fig. 4.2.A). Other cells do not activate at particular positions, or activate at inconsistent positions from trial-to-trial. We computed an adjusted form of mutual information (MI) between activity and belt position, which captures both sources of variance (Souza et al., 2018). The AMPH-treated animals had significantly lower MI relative to the saline-treated animals (Fig. 4.2.B; two-way ANOVA: $F(3, 126) = 6.186$, $p = 0.0006$), in both ON (Tukey post hoc test, $p = 0.008$) and OFF conditions (Tukey post hoc test, $p = 0.015$). In other words, the encoding of spatial position by neurons was reduced when AMPH was ON- or OFF-board.

The average correlation of each units' activity over trials, a measure of signaling stability, was also lower in amphetamine animals in both ON and OFF conditions (Fig. 4.2.C; two-way ANOVA: $F(3, 126) = 6.296$, $p = 0.0005$; ON: Tukey post hoc test, $p = 0.021$; OFF: Tukey post hoc test, $p = 0.005$). We previously found that the non-classic psychedelic ibogaine degraded spatial representations in RSC when the mouse was between tactile cues on the belt, but not when the animal traversed tactile cues (Ivan et al., 2023). This suggests that the presence of somatosensory input overshadowed drug effects on spatial encoding in RSC. In the present experiment, we did not observe such an effect. We tested this by computing the fraction of high-information cells (those in the top quartile of MI) that encoded cue locations as compared to non-cue locations. The ratio of cue and non-cue locations of these high-information cells was not different between SAL and AMPH groups (Fig. 4.2. D; two-way ANOVA: $F(3, 126) = 0.852$, p

= 0.468). This suggests that AMPH effects are not selective to non-cue locations, wherein animals must rely on path integration to estimate position. In sum, the rate of activity was reduced when AMPH was on board, and this corresponded with reduced location information, measured both by MI and correlation. Although activity rate was no longer suppressed in AMPH-treated mice when the drug was off, spatial encoding was still impaired.

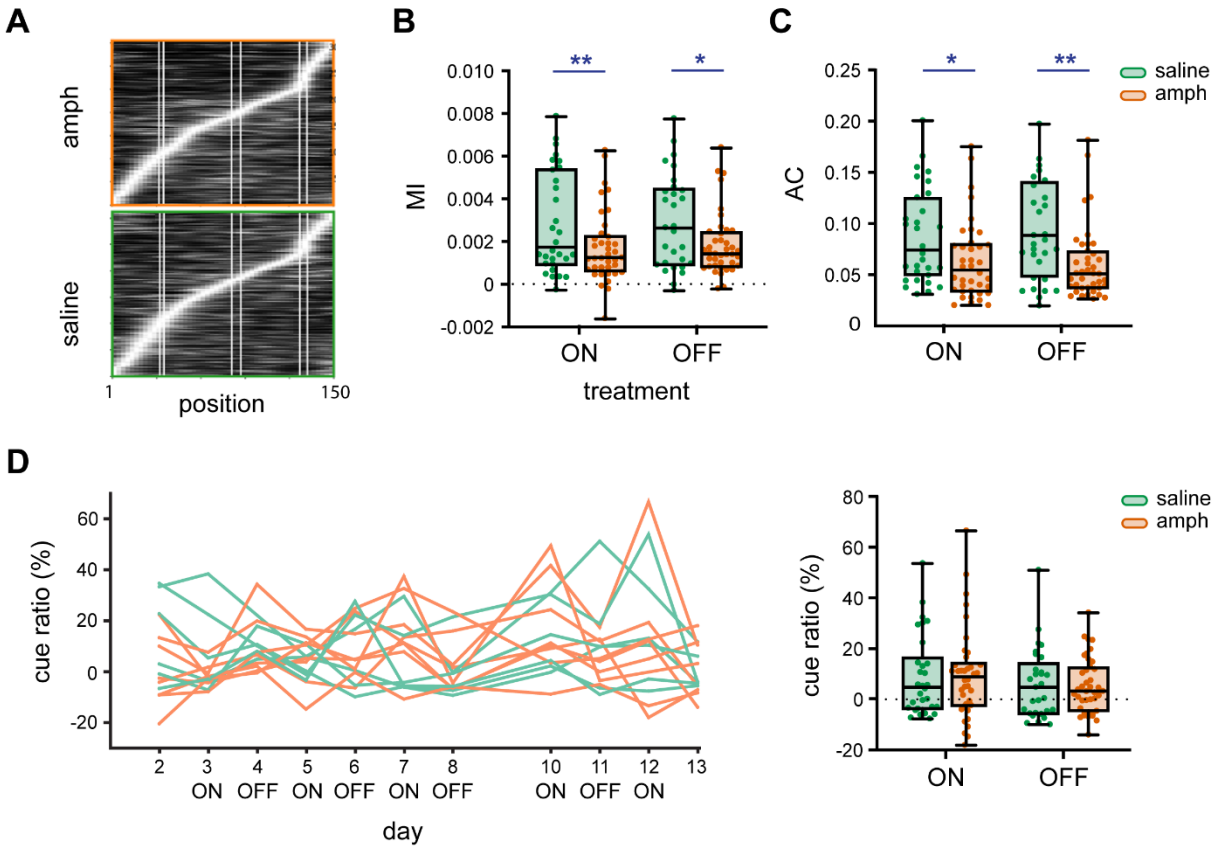

Fig. 4.2: Effects of amphetamine on mutual information. A. Session-averaged activity of position tuned cells under amphetamine (top) or saline (bottom) for all sessions. Cells in both panels are ordered by lag to peak activity. B. Box plots and individual values of mean mutual information (MI). The average MI significantly drops in the amphetamine group. C. Average trial-to-trial correlation (AC) for each session. D. Average of ratios between cue and non-cue location encoding of cells across days (left) and box plots and individual values (right). Statistical significance ($p<0.05$) is indicated by '*', and ($p<0.01$) is indicated by '**'.

Amphetamine affects catecholaminergic transmission throughout the brain, which may have complex effects manifesting in the relationship of activity between cells. To assess this, we first computed the pair-wise correlation of activity among all neurons recorded simultaneously during a session. We then used hierarchical clustering to order the units so that functionally similar units were adjacent (Fig. 4.3.A), and computed the clustering coefficient, which indicates how distinct clusters of correlated units are from one another (Fig. 4.3.B). There was no significant difference in the clustering coefficients, either between the AMPH/SAL groups or ON/OFF condition (two-way ANOVA: $F(3, 126) = 0.063$, $p = 0.979$), which suggests the functional connectivity revealed by neural activity covariance was not affected by amphetamine.

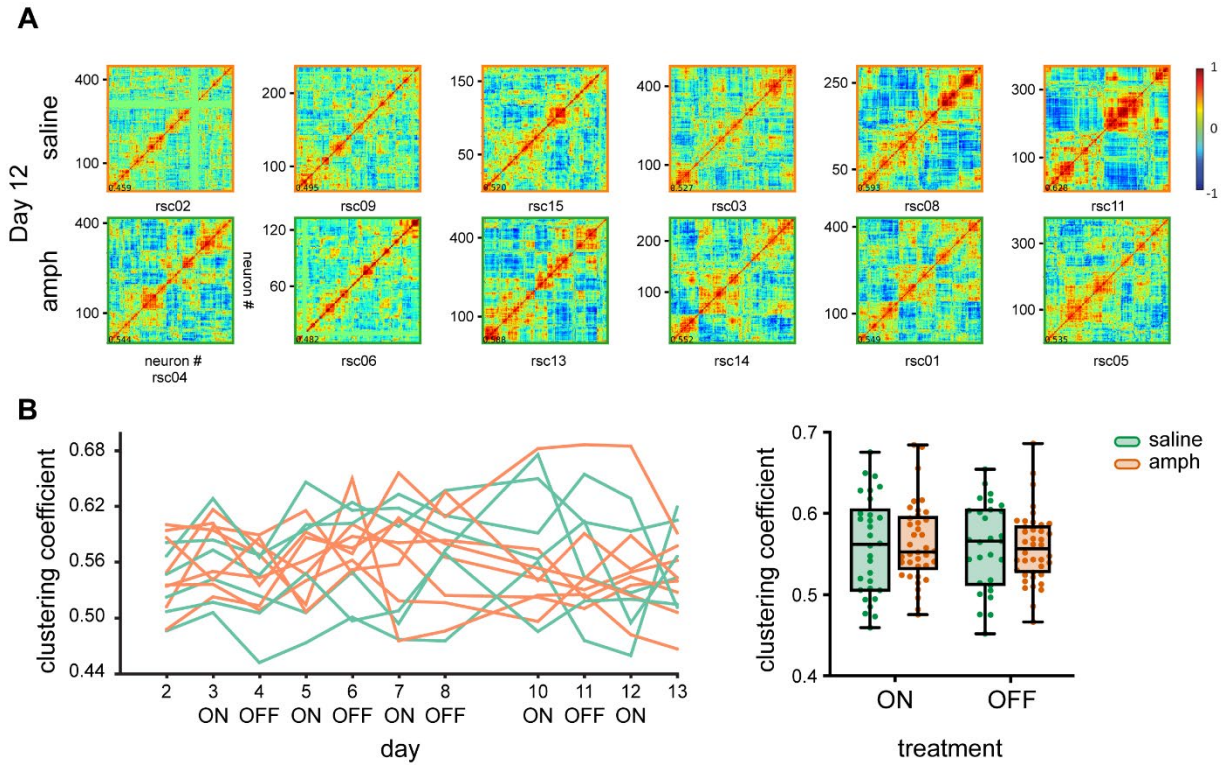

Fig. 4.3. Effects of amphetamine on connectivity. A. Pairwise correlation matrices of unit activity in one representative session (day 12) for saline (top row) and amphetamine (bottom row) animals. The diagonal represents the autocorrelation coefficients. B. Connectivity coefficients

across days (left) and box plots and individual values of the means for the 10 days of drug administration. The results indicate that amphetamine does not affect the correlation structure.

4.3.2 Ibogaine

We previously showed that the non-classic psychedelic ibogaine acutely reduced spatial coding by RSC position-coding cells (Ivan et al., 2023). We next investigated if ibogaine administration affected RSC neural encoding differently in animals that previously received amphetamine as compared to those receiving only saline injections. Ibogaine thus serves as a perturbation to test differences in the stability of cognitive maps in treated animals, and if ibogaine could exert a long-term amelioration of the degraded spatial encoding in animals treated with chronic AMPH, as suggested by behavioral data indicating its efficacy in reducing drug seeking (Moroz et al., 1997; Alper et al., 1999). To distinguish acute effects of ibogaine from lasting effects, we alternated recording days ON drug (recorded 1h after ibogaine injection) and OFF ibogaine (~24 hours later). Half of the AMPH-treated and SAL-treated mice received ibogaine, starting 72h after the last dose of AMPH (or SAL).

When ibogaine was ON board, the mice were significantly slower, regardless of whether they were pretreated with saline (Fig. 4.4.A; two-way RM ANOVA: $F(1, 4) = 20.63$, $p = 0.011$), or amphetamine ($F(1, 6) = 64.14$, $p = 0.0002$). This effect was absent 24h later ($F(1,4) = 1.660$, $p = 0.267$; $F(1,6) = 0.038$, $p = 0.852$). Ibogaine administration did not affect the proportion of time animals were stationary. There was, however, a difference the day after ibogaine (OFF condition) between the SAL-IBO and AMPH-IBO groups (Fig. 4.4.B; two-way RM ANOVA: $F(1, 5) = 13.86$, $p = 0.014$). The lower belt velocity when ibogaine was ON board led to a reduced rate of trial completion (Fig. 4.4.C; two-way RM ANOVA; saline: $F(1, 4) = 8.506$, $p = 0.043$; amphetamine: $F(1, 6) = 7.558$, $p = 0.033$). Neural activity rate was higher in AMPH-naïve mice

after ibogaine than when these mice were given saline (Fig. 4.4.D; two-way RM ANOVA: F (1, 4) = 7.943, p = 0.048). This reproduces our previous results of acute ibogaine effects on drug-naïve animals (Ivan et al., 2023). In the present study however, ibogaine administration did not affect firing rate relative to the off condition. The activity rate in the AMPH-naïve mice that were administered ibogaine was similar when the psychedelic was ON and OFF board (two-way RM ANOVA; saline: F (1, 4) = 1.501, p = 0.288). In contrast to these effects in the AMPH-naïve mice, ibogaine did not increase the activity rate in mice previously given AMPH (two-way RM ANOVA: ibogaine ON, F (1, 6) = 0.415, p = 0.543; ibogaine OFF, F (1, 6) = 0.041, p = 0.845).

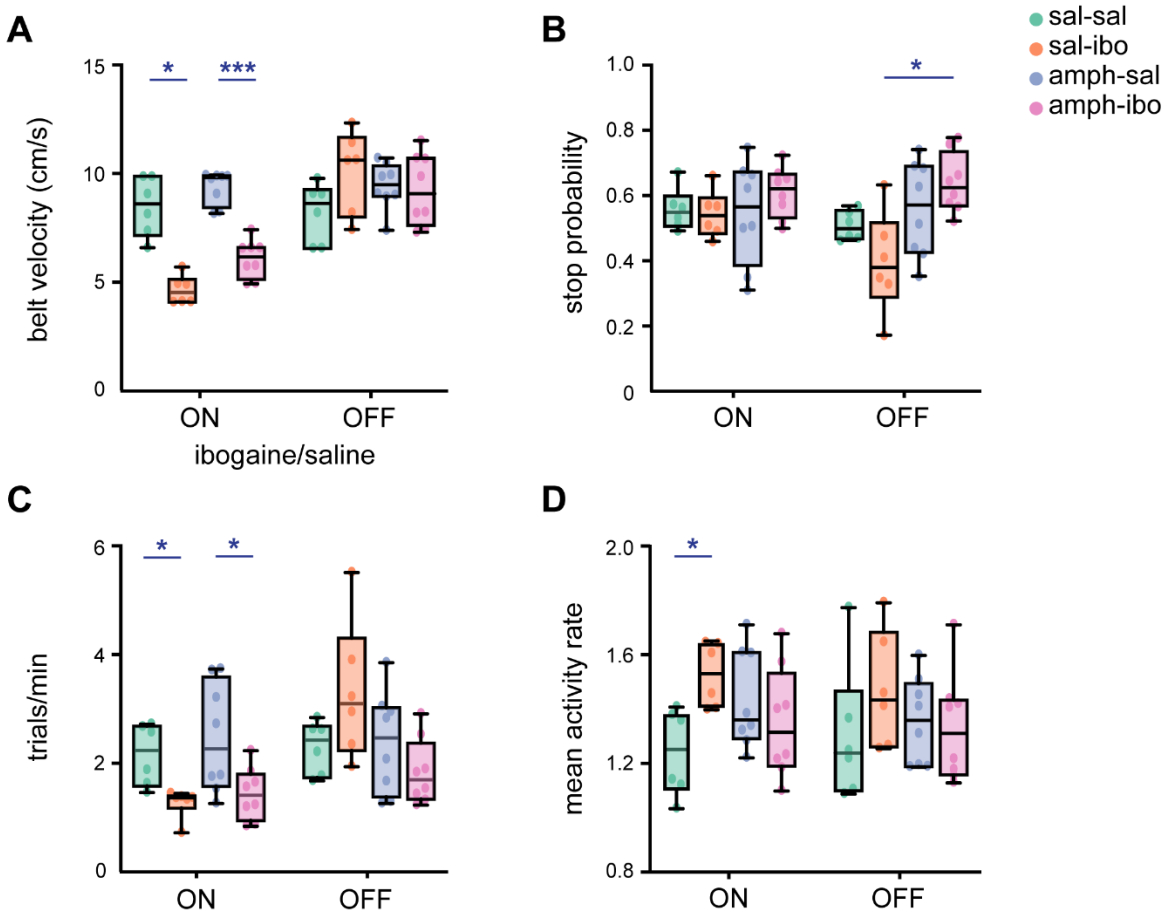

Fig. 4.4. Effects of ibogaine on behavioral measures in AMPH-treated and AMPH-naïve mice. A. Box plots and individual values of median moving speed with either saline or ibogaine ON or OFF board for the 4 different experimental groups. B. Probability that animals were not locomoting the belt. C. Rate of trial completion. D. Mean activity rate. Statistical significance ($p<0.05$) is indicated by '*', ($p<0.001$) is indicated by '***'.

We previously showed that acute ibogaine decreased place encoding in RSC (Ivan et al., 2023), and so expected a similar effect here. Although administration of ibogaine did indeed appear to lower MI for some treatment groups, the effect was not consistent in the full statistical model (Fig. 4.5.A; two-way RM ANOVA; saline: $F(1, 4) = 0.676$, $p = 0.457$; amphetamine: $F(1, 6) = 2.124$, $p = 0.195$). A similar phenomenon occurred for the stability of place cell firing over trials, measured by trial-to-trial correlation (Fig. 4.5.B; two-way RM ANOVA; saline: $F(1, 4) = 2.068$, $p = 0.224$; amphetamine: $F(1, 6) = 2.147$, $p = 0.193$). We noted two possible technical issues with this analysis. First, the variance of SAL-SAL animals is higher than other groups for both measures. Secondly, there may be a floor effect, particularly in the MI for AMPH-treated animals (Fig. 4.5.A, AMPH-IBO ON condition). We therefore performed a within-group comparison to determine if ibogaine ON/OFF had an effect on the amphetamine animals, and found that while there is no significant effect on MI (two-way RM ANOVA; $F(1, 3) = 5.060$, $p = 0.11$), we can detect a difference in the trial-to-trial correlations (AC; $F(1, 3) = 31.49$, $p = 0.011$). Of course, this evidence should be discounted by the negative result in the full model. In contrast, there was a strong effect in both measures for the SAL-IBO group (two-way RM ANOVA; MI: $F(1, 2) = 1130$, $p = 0.001$; AC: $F(1, 2) = 182.6$, $p = 0.005$). Note the 'rebound' effect of ibogaine in AMPH-naïve animals in the OFF condition. In other words, control animals appear to have higher MI and AC in the days after ibogaine (Supplemental Fig. 4.7).

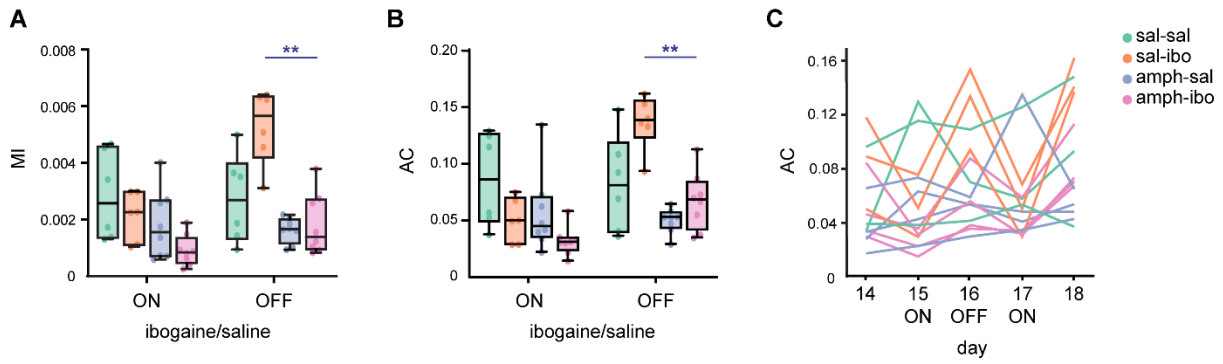

Fig. 4.5. Effects of ibogaine on mutual information. A. Mean mutual MI. B. Trial-to-trial correlations (AC) of session mean values. C. AC plotted across days for each group. Statistical significance ($p < 0.01$) is indicated by '**'.

Ibogaine administration reduced the clustering coefficients in the amphetamine group (Fig. 4.6.B; REML: $F(1, 6) = 52.22$, $p = 0.0004$; ROUT (Q = 1%; n=1)). This effect occurred only in the ON, and not the OFF condition (two-way RM ANOVA: $F(1, 6) = 0.805$, $p = 0.404$). It thus appears to be an acute effect only. Likewise, ibogaine administration decreased the clustering coefficient of AMPH-treated animals relative to the OFF condition (two-way RM ANOVA: $F(1, 3) = 11.6$, $p = 0.042$). This again may be a rebound effect by which the values are higher because of receiving ibogaine the previous day. Similar to the MI analysis above, the variance of the AMPH-naive animals is high, which may compromise statistical power. A within-group analysis shows that ibogaine ON-board also reduces the clustering coefficient in SAL animals (two-way RM ANOVA: $F(1, 2) = 117.9$, $p = 0.008$).

The SAL-IBO group has a higher coefficient when the psychedelic is OFF board, particularly when compared to the AMPH-IBO group (two-way RM ANOVA: $F(1, 5) = 18.51$, $p = 0.008$), which correlates with the increase in MI, suggesting that amphetamine blocks the

increase in connectivity associated with the prolonged effects of the psychedelic. The decrease in connectivity when ibogaine is ON board in the SAL-IBO animals as compared to the SAL-SAL group does not reach statistical significance (two-way RM ANOVA: F (1, 4) = 1.915, p = 0.239), but the results are similar with previous reports from our lab (Ivan et al., 2023).

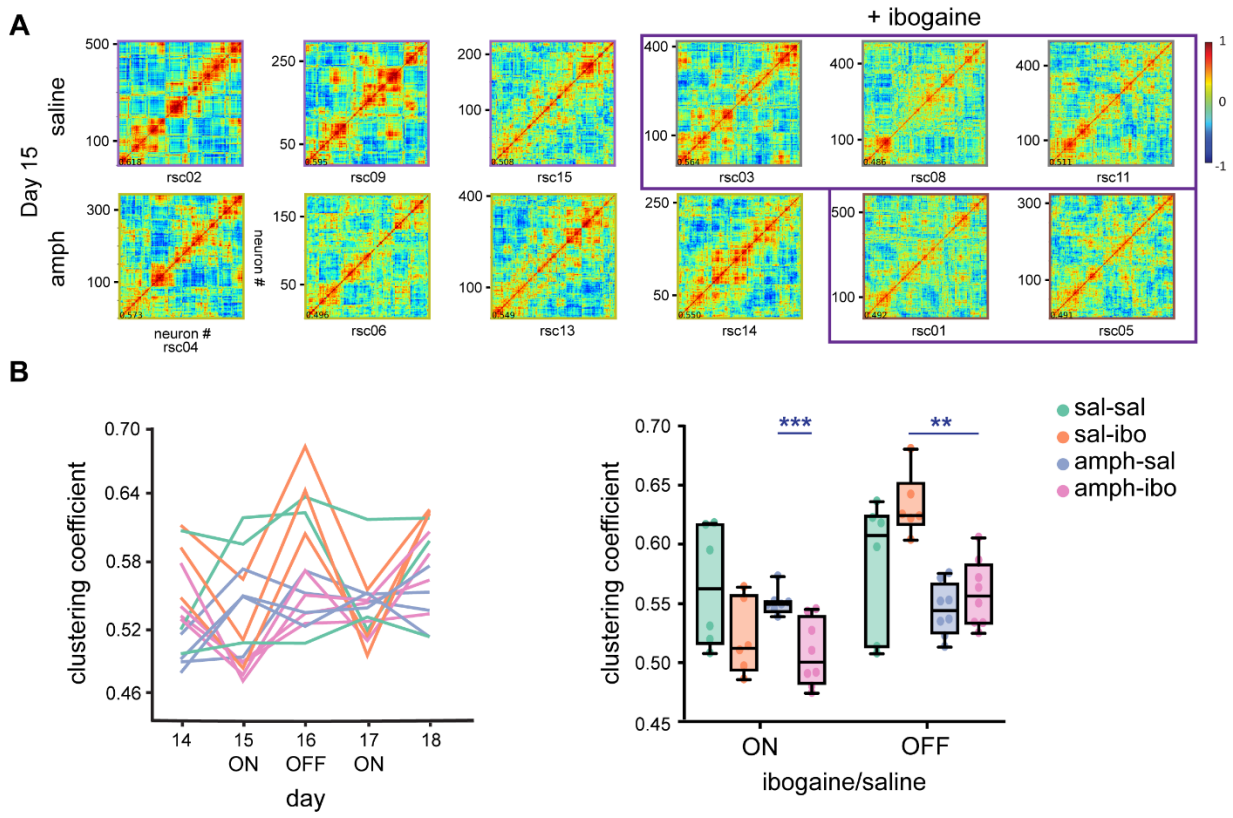

Fig. 4.6. Effects of ibogaine on functional connectivity. A. Correlation matrices of unit activity in representative sessions (day 15) for saline (top row) and amphetamine (bottom row) animals. Ibogaine sessions are indicated by the purple outline. B. Connectivity coefficients across days (left) and box plots and individual values of the means for the ibogaine and post-ibogaine days (right). Statistical significance ($p<0.01$) is indicated by '**', ($p<0.001$) is indicated by '***'.

4.4 DISCUSSION

We used 2-photon imaging to record the changes in activity of mouse RSC neurons associated with a 10-day course of escalating amphetamine administration. Despite having no strong behavioral effect, amphetamine degrades spatial encoding by RSC neurons, but not functional connectivity. This appears to be a long-lasting change because we observe it when AMPH is not on board. In contrast, ibogaine tends to degrade spatial encoding when it is on board, although the effect does not reach statistical significance. We found evidence that ibogaine may produce a 'rebound' effect in which the encoding and functional connectivity are enhanced 24 hours after administration in AMPH-naïve animals.

Amphetamine reduced the overall activity rate in the RSC when the drug is ON board. To our knowledge, this is the first report on the effects of amphetamine in the RSC at the cellular level. Amphetamine can have dose-dependent effects on the firing rate of cortical neurons. Most previous work on AMPH effects has targeted the prefrontal cortex (PFC). AMPH can increase firing rates of some PFC neurons and reduce that of others (Wood et al., 2012). Acute low-dose amphetamine tends to cause excitation (Homayoun and Moghaddam, 2006; Lapish et al., 2015), whereas repeated high-dose administration is more likely to suppress firing rates (Homayoun and Moghaddam, 2006; Gulley and Stanis, 2010). The chronic exposure effects in the prefrontal cortex are consistent with our findings in the RSC. These differences can sometimes be attributed to the effects of movements and the variability in running speed but, this is unlikely for the present data because we did not observe any behavioral differences between AMPH-treated and AMPH-naïve mice. We conclude the reduced neural activity is likely due to the direct effect of the drug on the brain, rather than a byproduct of altered motoric output.

Modulation of neural activity by monoamine neurotransmitters is thought to play an essential role in shaping computations in the neocortex (Seamans and Yang, 2004; Gruber and McDonald, 2012a; Lesch and Waider, 2012). Amphetamine and other drugs of abuse have both short-term and long-lasting effects on brain function, and chronic drug paradigms often result in chronic impairments in behavior. Acute low-dose AMPH can enhance memory in some situation (Krivanek and McGaugh, 1969; McGaugh, 1973; Soetens et al., 1993). On the other hand, chronic high-dose paradigms (such as psychostimulant sensitization) have been shown to impair learning and memory (Mandillo et al., 2003; Arroyo-García et al., 2020).

The RSC is relevant to drug seeking behavior because of its roles in spatial encoding (Mao et al., 2017; Chang et al., 2020), path integration (Cooper and Mizumori, 1999), and emotional processes (Maddock, 1999). A rodent pharmacological MRI study (Schwarz et al., 2007) showed that the relative cerebral blood volume response to d-amphetamine can be resolved into different groups of brain structures forming different networks. These groups exhibit a strong within-group covariance in their response to the drug. One of these groups is consistent with primary projections of the mesolimbic dopamine system and closely coupled with the RSC; this network includes the ventral tegmental area (VTA), substantia nigra (SN), and hypothalamus. These regions are important in arousal, motivation and navigation, which are engaged in ethological behaviors such as food foraging. Psychostimulants, such as amphetamine, modify the functions of these structures to promote patterned behavior such as conditioned place preference, food hoarding, and hyperlocomotion (Creese and Iversen, 1974; Spyraki et al., 1982; Dringenberg et al., 2000). Prolonged exposure is thought to convert these behaviors to drug seeking and drug taking (Koob and Le Moal, 2001), as habit formation and motivation for reinforcement are increased in amphetamine-sensitized rats (Nelson and Killcross, 2006; Nordquist et al., 2007). The

increase in expression of stimulus-response over goal-directed actions have been associated with a shift of cognitive control to sensorimotor areas (Everitt and Robbins, 2005; Lucantonio et al., 2014), particularly the dorsolateral striatum (DLS) (Everitt and Robbins, 2013). This transition of may be produced by plastic changes in the striatum, as amphetamine sensitization increases dendritic spine density and branching in the DLS (Jedynak et al., 2007; Wong et al., 2016). This may also affect the involvement of the RSC in cognitive control, as this area supports the use of contextual cues in response conflict, as shown by lesion studies in rats (Nelson et al., 2014).

The changes in RSC spatial encoding observed in the present study may reflect a component of this process. Our data revealed that 1h after administration (when the drug is ON board), amphetamine reduces spatial information and trial-to-trial correlation of single unit activity. One possible explanation is that the mice are not engaging the navigation systems as much, due to the shift of control towards the sensorimotor system. Animals can use allocentric ('goal-directed') or egocentric ('habit') navigation when exposed to spatial tasks. The predominance of the habit system associated with prolonged psychostimulant exposure means that the allocentric system is less engaged. The role of the RSC in allocentric navigation and path integration has been well established (Vann and Aggleton, 2002; Holschneider et al., 2019), although recently its ability to integrate both allo- and egocentric information to support navigation has been emphasized (Hindley et al., 2014; Alexander and Nitz, 2015; Stacho and Manahan-Vaughan, 2022; Alexander et al., 2023b). The shift towards a more egocentric system is reflected in the lower MI and AC values associated with amphetamine administration, as the encoding of spatial information in the RSC is diminished. This is not likely simply due to decreased firing rates because the MI and AC remain at the same decreased levels in the OFF condition even though the firing rates are significantly higher.

Another possible explanation for the observed effect on spatial encoding may rely on a loss of motivation for sucrose. Repeated and escalating AMPH may reduce the salience of the reward in the present task, which may affect the fidelity of the navigational systems to acquire it. AMPH is well known to reduce motivation for natural rewards (Koob and Volkow, 2010) and this is contaminant with reduced encoding of reward in medial PFC (Hashemnia et al., 2020). AMPH can also increase the salience of cues for sucrose reward, but not necessarily the hedonic reaction associated with reward consumption (Wyvell and Berridge, 2000; Wyvell and Berridge, 2001). In other words, it is possible that the altered spatial encoding is due to changes in motivational states. An alternative explanation to our findings is that the chronic treatment altered intracellular physiology, as AMPH and related compounds cause oxidative stress and inhibition of LTP in the hippocampus (Chen et al., 2021). This could mean that the decrease in spatial encoding can be attributed to a lower signal to noise ratio (SNR), rather than remodeling of synaptic networks, and would account for both the lower activity rates and the preservation of functional connectivity. This is consistent with previous data showing lower SNR at similar (1.5 mg/kg) doses (Hashemnia et al., 2020). Indeed, AMPH did not affect the clustering among RSC neurons, suggesting the absence of large-scale synaptic remodeling.

An aim of this study was to determine whether ibogaine could ameliorate AMPH-induced signaling changes. This hypothesis was inspired by many reports of ibogaine inducing prolonged facilitation of drug cessation by reducing craving and drug seeking behavior in humans with substance use disorders (Köck et al., 2021). Although we did observe a rebound effect (24 hours after IBO) of increased place signaling and functional connectivity in AMPH-naïve animals, we did not observe such an effect in AMPH-treated animals. There are several potential explanations for this. It could be associated with a change in the motivational state, but there were no significant

changes in behavioral output, which renders this explanation unlikely. This could also be a spurious effect, given the variability between animals but, as the MI correlates with increased trial-to-trial correlation, it indicates that the heightened spatial neural encoding stability is due to the psychedelic effect. Alternatively, these effects could be related to ibogaine and other analogues' ability to promote growth of dendritic arbors and spines in rodent cortical neurons (Ly et al., 2018; Cameron et al., 2020). The changes in physiology associated with chronic amphetamine could render the RSC less susceptible to the ibogaine-induced neuroplasticity alterations. This premise is supported by the fact that the MI values remain similar for day 7 and day 12 post-ibogaine (Supplemental Fig. 4.7). This could mean that the increase in MI and AC we observe in drug-naïve animals in the OFF-board condition is a result of the cortical reorganization enabled by the psychedelic, a reorganization that is rendered ineffective by prolonged exposure to amphetamine. These possibilities are not necessarily independent from one another. When ON-board, psychedelics have also been shown to cause an "ego dissolution", induce a feeling of loss of spatial self-location (Millière et al., 2018; Mason et al., 2020), and sensory inputs are proposed to become disinhibited (Carhart-Harris and Friston, 2019). In the current data set, this may reflect the trend toward lower MI under acute (ON) ibogaine administration, similar to our previous results (Ivan et al., 2023).

Ibogaine increased activity rate in saline animals when the drug is on board, similar to previous results (Ivan et al., 2023), but not in the amphetamine treated mice. Other psychedelics with strong 5-HT_{2A}R affinity such as TCB-2 and DOI can both up- and down-regulate neural activity in the PFC (Dearnley et al., 2023), and visual cortex (Michaiel et al., 2019). In the present data, ibogaine could have similarly bidirectionally modulated individual neurons, but the overall population activity is increased. However, once the psychedelic was OFF board, the higher mean

activity rate dissipates. It is therefore likely due to a short-term modulatory effect, rather than long-term change in connectivity or cellular metabolism.

Classic psychedelics, such as LSD, ketamine and psilocybin cause an increase in spontaneous signal complexity and entropy of humans brain activity recorded via magnetoencephalography (Schartner et al., 2017), electroencephalography (Li and Mashour, 2019; Farnes et al., 2020), and fMRI (Herzog et al., 2023). In the present data, ibogaine appears to lower the functional connectivity in the amphetamine animals when ON board, and increase it at 24h after the last administration in saline animals. The biphasic effect suggests that the reduced clustering after ibogaine reflects a stronger loss of functional connectivity motifs in amphetamine animals, but the long-term rebound effect of ibogaine in drug-naïve animals is also revealed in the connectivity within the RSC. This response correlates with the effects on spatial encoding, linking the correlation of activity among all neurons with the position information encoded at cellular level.

4.5 CONCLUSION

The present data suggest that chronic amphetamine administration degrades the spatial encoding in the RSC and decreases the signal-to-noise ratio, but does not affect the functional connectivity among the recorded neurons. This may reflect physiological changes in the RSC, or possibly a shift of behavioral control to sensory motor (e.g. habit) systems such that the animal relies less on cognitive maps during the task. Whatever the mechanism, the brain's adaptation to repeated amphetamine attenuates the neurophysiological effects of the non-classic psychedelic ibogaine.

Acknowledgments

We would like to thank Adam Neumann for technical support and Dr. HaoRan Chang for helpful discussions. Funding provided by: Natural Sciences and Engineering Council of Canada, New Frontiers Research Fund, Alberta Innovates, Branch out Neurological Foundation, Beswick Fellowship, Canadian Institute of Health Research.

Author Contributions: V.E.I. and A.J.G. designed research, V.E.I. and I.M.E. performed research, M.M. contributed tools, V.E.I., D.P.T-C, and I.M.E. analyzed data, V.E.I., D.P.T-C, B.L.M., and A.J.G. wrote the paper.

Competing Interest Statement: The authors declare no competing interests.

4.6 METHODS

Animals

Adult (4 - 6 month old) Thy1-GCaMP6s mice (n=14; 11M/3F), weighing 30-35g, were housed in standard rodent cages, and maintained at 24 °C under a 12 h light/dark cycle. Mice had free access to food and water before training. All experiments were performed during the light cycle (between 2:00 PM and 2:00 AM). Procedures were in accordance with the guidelines established by the Canadian Council on Animal Care, and with protocols approved by the Animal Welfare Committee of the University of Lethbridge.

Surgery

Before surgery, animals received buprenorphine (0.05 mg/kg SC) and dexamethasone (0.2 mg/kg IM). They were then anesthetized with isoflurane (1-1.5%) and head fixed in a stereotaxic frame with body temperature maintained at 37.0 ± 0.5 ◦C with a heating pad with a closed-loop control system. Once the skull was exposed, a titanium head-plate was fixed to the skull using adhesive cement (Metabond, Parkell) and dental acrylic. Mice received a 5 mm bilateral craniotomy (AP: +1 to -4; ML: -2.5 to +2.5), which was then covered with three layers of coverslips affixed with optical adhesive (NOA71, Norland). The coverslip was attached to the skull using Vetbond, and a rubber ring was fixed over the head-plate to form a well to hold water between the imaging region and the immersion objective. Post-surgical care included careful weight monitoring and subcutaneous (SC) injections of meloxicam (Metacam 1 mg/kg) and enrofloxacin (Baytril, 10 mg/kg) for three days after implant.

Drugs

For the chronic amphetamine administration, we diluted d-Amphetamine sulfate (Sigma Aldrich) in 0.9% saline solution. We used an escalated dose paradigm, in which each AMPH animal (n = 8) received a volume of 0.1 ml SC of solution in a schedule of 2 days of 0.5 mg/kg, 2 days of 1 mg/kg, and 6 days of 2 mg/kg. The amphetamine was administered subcutaneously at the University of Lethbridge's veterinarian recommendation, to minimize possible side effects due to multiple IP injections (e.g. peritonitis). The control animals (n = 6) received the same volume of saline. Ibogaine HCl was obtained from Toronto Research Chemicals, Canada, in powder form and diluted in sterile water to a concentration of 10-12 mg/ml. The stock concentration was determined so that each animal (n = 7) received 0.1 ml IP and received the appropriate dosage per weight. IP route has been shown to be preferable to IV administration, as it results in higher bloodstream concentrations of noribogaine (Baumann et al., 2001). The control animals (n = 7) received 0.1 ml 0.9% saline solution.

Experimental procedure for behavior

Head-fixed mice were trained to run on a treadmill using a positive reinforcement paradigm. They received a drop of 10% sucrose solution on every trial, consisting of one lap of the treadmill belt. Animals were water restricted during the training and testing. They had *ad libitum* access to water for up to 30 minutes per day, and their body weight was carefully monitored throughout the experiment to ensure the weight loss did not exceed 15% of their baseline value. The treadmill belt consisted of a Velcro strip that was 150 cm long and 4 cm wide. Three tactile cues were placed in different locations on the belt. Licking behavior was recorded using a capacitive sensor connected to the lick spout. An optical encoder attached to the wheel shaft was

used to monitor belt movement. A microcontroller was used to monitor the encoder, licking sensor, and the reward delivery.

Training continued in daily sessions until mice performed at least 20 trials in 20 minutes. Neural activity was imaged in either the left (n=6) or the right (n=8) RSC in subsequent daily sessions of the task for 23-28 minutes (recording schedule shown in table 1). Mice were trained on one belt and then the imaging sessions were recorded while they ran on a new belt.

Supplemental table 4. 1: Experimental protocol.

Day	Drug protocol	Imaging protocol
Day 1	baseline	IMG 28’
Day 2	Saline SC	IMG 28’
Day 3	AMPH 0.5 mg/kg OR Saline	IMG drug ON 23’
Day 4	AMPH 0.5 mg/kg OR Saline	IMG drug OFF 23’
Day 5	AMPH 1 mg/kg OR Saline	IMG drug ON 23’
Day 6	AMPH 1 mg/kg OR Saline	IMG drug OFF 23’
Day 7	AMPH 2 mg/kg OR Saline	IMG drug ON 23’
Day 8	AMPH 2 mg/kg OR Saline	IMG drug OFF 23’
Day 9	AMPH 2 mg/kg OR Saline	No IMG
Day 10	AMPH 2 mg/kg OR Saline	IMG drug ON 23’
Day 11	AMPH 2 mg/kg OR Saline	IMG drug OFF 23’
Day 12	AMPH 2 mg/kg OR Saline	IMG drug ON 23’
Day 13	baseline	IMG 23’
Day 15	Ibo 40mg/kg OR Saline	IMG drug ON 23’
Day 16	Ibo 40mg/kg OR Saline	IMG drug OFF 23’
Day 17	Ibo 40mg/kg OR Saline	IMG drug ON 23’
Day 18	baseline	IMG 23’
Day 33	perfusion	

Based on the drug protocol used, the animals were randomly assigned one of 4 groups: AMPH – SAL (n = 4), AMPH – IBO (n = 4), SAL – SAL (n = 3), SAL – IBO (n = 3). The imaging sessions during drug administration were performed either one hour after the injection (IMG drug ON), or 24h after the last injection (IMG drug OFF).

Two-Photon Imaging

Neural activity was imaged using a 2-photon microscope (Bergamo II multiphoton microscopy, Thorlabs) through a 16x water-immersion objective lens (NA=0.8, Nikon). Excitation was with a Ti:sapphire pulsed laser (Coherent) tuned to a wavelength of 920 nm, ~80mW power, and controlled by a galvo-resonant X-Y scanner. Images were acquired at depths between 135 μm – 170 μm (layer II/III), from a field of view of 835 x 835 μm. Images were digitized at a sampling rate of 19 Hz, and at a resolution of 800 x 800 pixels. Imaging data from all animals were acquired from one hemisphere of either the left or right RSC (AP: -1 to -3; ML: 0 to +/- 1).

Neural Activity Analysis

Pre-processing

Automatic image pre-processing was performed using the Suite-2P (Pachitariu et al., 2017) algorithm, as previously described (Mao et al., 2017). The regions of interest (ROIs) detected were inspected manually and labelled as cells or non-cells by experienced users. For each ROI, the ΔF/F time courses were deconvolved using constrained non-negative matrix factorization (Pnevmatikakis et al., 2016), and all subsequent analyses were conducted using the deconvolved time-courses. For injection days, the imaging sequences of both pre- and post-injection intervals were combined during pre-processing so as to acquire the activity of the same set of cells (ROIs) before and after injections.

Computing spatial encoding

In order to identify spatially tuned neurons, we computed the adjusted mutual information (MI) (Vinh et al., 2010) between the firing rate of each neuron and the position of the mouse in the belt. We first divided the belt into 50 bins (3 cm each). For each bin and trial, we summed the neuron's activity and binned it into 4 levels, giving us the joint bin-activity discrete distribution, which we use to compute the mutual information. The MI used here is an adjustment of mutual information which accounts for the number of trials, which differs number among session, and thus is appropriate to compare cells from different sessions on the same scale. The MI is upperlimited by 1 and takes an expected value of 0 when the firing and position are independent. Negative values signify that the MI for that cell is lower than the MI one would expect solely due chance. Visually, the MI is a convincing measure of how predictive a neuron's firing is of a particular position and strongly correlates with decoding accuracy. For trial-to-trial correlations we computed for each neuron its average activity correlation between the baseline trials and the subsequent post-injection trials is positively correlated with the average MI of the neuron in both epochs.

Unit functional connectivity

Computing the apparent functional connectivity among neurons involved several steps. First, the spikes underlying the calcium fluorescence traces were inferred using a deconvolution algorithm (Friedrich et al., 2017). Next, the data in which the mouse is slow or not moving (below the 10% quantile of the velocity distribution over the track) is removed. The track is then divided into 50 spatial bins. The trial-averaged activity in each bin is computed for each cell to create a 'tuning curve' over the belt. The Pearson correlation between the tuning curves of all cell pairs is

then computed. To visualize clusters in the cells x cells spatial correlation matrix, the columns/rows were ordered so that highly correlated cells are adjacent. For each neuron, a vector of its correlations with all other cells was generated. In order to determine the similarity between the correlation structures, the pairwise euclidean distances between those vectors were calculated. Using the unweighted pair group method with arithmetic mean (UPGMA), a hierarchical clustering on these measures was conducted (Sokal, 1958). To assess the amount of clustering in the spatial correlation matrices, we computed the average clustering coefficient (Saramäki et al., 2007), a measure which quantifies how many cells with similar firing patterns are similar between each other, averaged over all cells; this coefficient is independent of the ordering of rows/columns.

Statistical tests

Due to technical difficulties during the recordings, we are missing 2 sessions in the amphetamine ON group and one session in the saline OFF group, and we were therefore unable to employ Repeated Measure ANOVAs to compare the effects of chronic exposure to amphetamine. Ordinary two-way ANOVA was used to detect the main effects of the drugs, with Tukey post-hoc multiple comparison test. For the ibogaine administration we used a RM two-way ANOVA design for each comparison.

4.7 REFERENCES

Alexander, A.S., and Nitz, D.A. (2015). Retrosplenial cortex maps the conjunction of internal and external spaces. *Nature Neuroscience* 18(8)**,** 1143-1151. doi: 10.1038/nn.4058.

Alexander, A.S., Robinson, J.C., Stern, C.E., and Hasselmo, M.E. (2023). Gated transformations from egocentric to allocentric reference frames involving retrosplenial cortex, entorhinal cortex, and hippocampus. *Hippocampus* 33(5)**,** 465-487. doi: https://doi.org/10.1002/hipo.23513.

Alper, R., Lotsof, H.S., Frenken G.M.N., Luciano, D.J., Bastiaans, J.K. (1999). Treatment of acute opioid withdrawal with ibogaine. *American Journal on Addictions*, *8*(3), 234-242.

Arroyo-García, L.E., Tendilla-Beltrán, H., Vázquez-Roque, R.A., Jurado-Tapia, E.E., Díaz, A., Aguilar-Alonso, P., et al. (2020). Amphetamine sensitization alters hippocampal neuronal morphology and memory and learning behaviors. *Molecular Psychiatry*. doi: 10.1038/s41380-020-0809-2.

Baumann, M.H., Rothman, R.B., Pablo, J.P., and Mash, D.C. (2001). In vivo neurobiological effects of ibogaine and its O-Desmethyl metabolite, 12-Hydroxyibogamine (noribogaine), in rats. *Journal of Pharmacology and Experimental Therapeutics* 297(2)**,** 531-539.

Cameron, L.P., Tombari, R.J., Lu, J., Pell, A.J., Hurley, Z.Q., Ehinger, Y., et al. (2020). A non-hallucinogenic psychedelic analogue with therapeutic potential. *Nature*. doi: 10.1038/s41586-020-3008-z.

Carhart-Harris, R.L., and Friston, K.J. (2019). REBUS and the anarchic brain: Toward a unified model of the brain action of psychedelics. *Pharmacological Reviews* 71(3)**,** 316. doi: 10.1124/pr.118.017160.

Chang, H., Esteves, I.M., Neumann, A.R., Sun, J., Mohajerani, M.H., and McNaughton, B.L. (2020). Coordinated activities of retrosplenial ensembles during resting-state encode spatial landmarks. *Philosophical Transactions of the Royal Society B* 375(1799)**,** 20190228.

Chen, G., Wei, X., Xu, X., Yu, G., Yong, Z., Su, R., et al. (2021). Methamphetamine inhibits long-term memory acquisition and synaptic plasticity by evoking endoplasmic reticulum stress. *Frontiers in Neuroscience* 14. doi: 10.3389/fnins.2020.630713.

Cooper, B.G., and Mizumori, S.J.Y. (1999). Retrosplenial cortex inactivation selectively impairs navigation in darkness. *NeuroReport* 10(3).

Corcoran, K.A., Frick, B.J., Radulovic, J., and Kay, L.M. (2016). Analysis of coherent activity between retrosplenial cortex, hippocampus, thalamus, and anterior cingulate cortex during retrieval of recent and remote context fear memory. *Neurobiology of Learning and Memory* 127**,** 93-101. doi: https://doi.org/10.1016/j.nlm.2015.11.019.

Creese, I., and Iversen, S.D. (1974). The role of forebrain dopamine systems in amphetamine induced stereotyped behavior in the rat. *Psychopharmacologia* 39(4)**,** 345-357. doi: 10.1007/BF00422974.

Dalley, Jeffrey W., Everitt, Barry J., and Robbins, Trevor W. (2011). Impulsivity, compulsivity, and top-down cognitive control. *Neuron* 69(4)**,** 680-694. doi: https://doi.org/10.1016/j.neuron.2011.01.020.

Dearnley, B., Jones, M., Dervinis, M., and Okun, M. (2023). Brain state transitions primarily impact the spontaneous rate of slow-firing neurons. *Cell Reports* 42(10).

dos Santos, R.G., Bouso, J.C., and Hallak, J.E.C. (2017). The antiaddictive effects of ibogaine: A systematic literature review of human studies. *Journal of Psychedelic Studies* 1(1)**,** 20-28. doi: 10.1556/2054.01.2016.001.

Dringenberg, H.C., Wightman, M., and Beninger, R.J. (2000). The effects of amphetamine and raclopride on food transport: possible relation to defensive behavior in rats. *Behavioural Pharmacology* 11(6).

Dworkin, S.I., Gleeson, S., Meloni, D., Koves, T.R., and Martin, T.J. (1995). Effects of ibogaine on responding maintained by food, cocaine and heroin reinforcement in rats. *Psychopharmacology* 117(3)**,** 257-261. doi: 10.1007/BF02246099.

Everitt, B.J., Dickinson, A., and Robbins, T.W. (2001). The neuropsychological basis of addictive behaviour. *Brain Research Reviews* 36(2)**,** 129-138. doi: https://doi.org/10.1016/S0165-0173(01)00088-1.

Everitt, B.J., and Robbins, T.W. (2005). Neural systems of reinforcement for drug addiction: from actions to habits to compulsion. *Nature Neuroscience* 8(11)**,** 1481-1489. doi: 10.1038/nn1579.

Everitt, B.J., and Robbins, T.W. (2013). From the ventral to the dorsal striatum: Devolving views of their roles in drug addiction. *Neuroscience & Biobehavioral Reviews* 37(9, Part A)**,** 1946-1954. doi: https://doi.org/10.1016/j.neubiorev.2013.02.010.

Farnes, N., Juel, B.E., Nilsen, A.S., Romundstad, L.G., and Storm, J.F. (2020). Increased signal diversity/complexity of spontaneous EEG, but not evoked EEG responses, in ketamine-induced psychedelic state in humans. *PloS one* 15(11)**,** e0242056. doi: 10.1371/journal.pone.0242056.

Featherstone, R.E., Rizos, Z., Kapur, S., and Fletcher, P.J. (2008). A sensitizing regimen of amphetamine that disrupts attentional set-shifting does not disrupt working or long-term memory. *Behavioural Brain Research* 189(1)**,** 170-179. doi: https://doi.org/10.1016/j.bbr.2007.12.032.

Fisk, G.D., and Wyss, J.M. (1999). Associational projections of the anterior midline cortex in the rat: intracingulate and retrosplenial connections. *Brain Research* 825(1)**,** 1-13. doi: https://doi.org/10.1016/S0006-8993(99)01182-8.

Friedrich, J., Zhou, P., and Paninski, L. (2017). Fast online deconvolution of calcium imaging data. *PLOS Computational Biology* 13(3)**,** e1005423. doi: 10.1371/journal.pcbi.1005423.

Glick, S.D., Kuehne, M.E., Raucci, J., Wilson, T.E., Larson, D., Keller, R.W., et al. (1994). Effects of iboga alkaloids on morphine and cocaine self-administration in rats: relationship to tremorigenic effects and to effects on dopamine release in nucleus accumbens and striatum. *Brain Research* 657(1)**,** 14-22. doi: https://doi.org/10.1016/0006-8993(94)90948-2.

Gruber, A., and McDonald, R. (2012). Context, emotion, and the strategic pursuit of goals: interactions among multiple brain systems controlling motivated behavior. *Frontiers in Behavioral Neuroscience* 6(50). doi: 10.3389/fnbeh.2012.00050.

Gulley, J.M., and Stanis, J.J. (2010). Adaptations in medial prefrontal cortex function associated with amphetamine-induced behavioral sensitization. *Neuroscience* 166(2)**,** 615-624. doi: https://doi.org/10.1016/j.neuroscience.2009.12.044.

Hashemnia, S., Euston, D.R., and Gruber, A.J. (2020). Amphetamine reduces reward encoding and stabilizes neural dynamics in rat anterior cingulate cortex. *eLife* 9**,** e56755. doi: 10.7554/eLife.56755.

Havel, V., Kruegel, A.C., Bechand, B., McIntosh, S., Stallings, L., Hodges, A., et al. (2021). Novel class of psychedelic iboga alkaloids disrupts opioid addiction states. *bioRxiv*, 2021. 07.453441. doi: 10.1101/2021.07.22.453441.

Henriques, G.M., Anjos-Santos, A., Rodrigues, I.R.S., Nascimento-Rocha, V., Reis, H.S., Libarino-Santos, M., et al. (2021). Ibogaine blocks cue- and drug-induced reinstatement of conditioned place preference to ethanol in male mice. *Frontiers in Pharmacology* 12. doi: 10.3389/fphar.2021.739012.

Herzog, R., Mediano, P.A.M., Rosas, F.E., Lodder, P., Carhart-Harris, R., Perl, Y.S., et al. (2023). A whole-brain model of the neural entropy increase elicited by psychedelic drugs. *Scientific Reports* 13(1), 6244. doi: 10.1038/s41598-023-32649-7.

Hindley, E.L., Nelson, A.J.D., Aggleton, J.P., and Vann, S.D. (2014). The rat retrosplenial cortex is required when visual cues are used flexibly to determine location. *Behavioural Brain Research* 263, 98-107. doi: https://doi.org/10.1016/j.bbr.2014.01.028.

Holschneider, D.P., Givrad, T.K., Yang, J., Stewart, S.B., Francis, S.R., Wang, Z., et al. (2019). Cerebral perfusion mapping during retrieval of spatial memory in rats. *Behavioural Brain Research* 375, 112116. doi: https://doi.org/10.1016/j.bbr.2019.112116.

Homayoun, H., and Moghaddam, B. (2006). Progression of Cellular Adaptations in Medial Prefrontal and Orbitofrontal Cortex in Response to Repeated Amphetamine. *The Journal of Neuroscience* 26(31), 8025. doi: 10.1523/JNEUROSCI.0842-06.2006.

Iaria, G., Chen, J.-K., Guariglia, C., Ptito, A., and Petrides, M. (2007). Retrosplenial and hippocampal brain regions in human navigation: complementary functional contributions to the formation and use of cognitive maps. *European Journal of Neuroscience* 25(3), 890-899. doi: https://doi.org/10.1111/j.1460-9568.2007.05371.x.

Ivan, V.E., Tomàs-Cuesta, D.P., Esteves, I.M., Curic, D., Mohajerani, M., McNaughton, B.L., et al. (2023). The non-classic psychedelic ibogaine disrupts cognitive maps. *Biological Psychiatry Global Open Science*. doi: https://doi.org/10.1016/j.bpsgos.2023.07.008.

Jedynak, J.P., Uslaner, J.M., Esteban, J.A., and Robinson, T.E. (2007). Methamphetamine-induced structural plasticity in the dorsal striatum. *European Journal of Neuroscience* 25(3), 847-853. doi: https://doi.org/10.1111/j.1460-9568.2007.05316.x.

Jentsch, J.D., Olausson, P., De La Garza, R., and Taylor, J.R. (2002). Impairments of reversal learning and response perseveration after repeated, intermittent cocaine administrations to monkeys. *Neuropsychopharmacology* 26(2), 183-190. doi: https://doi.org/10.1016/S0893-133X(01)00355-4.

Keene, C.S., and Bucci, D.J. (2009). Damage to the retrosplenial cortex produces specific impairments in spatial working memory. *Neurobiology of Learning and Memory* 91(4), 408-414. doi: https://doi.org/10.1016/j.nlm.2008.10.009.

Köck, P., Froelich, K., Walter, M., Lang, U., and Dürsteler, K.M. (2021). A systematic literature review of clinical trials and therapeutic applications of ibogaine. *Journal of Substance Abuse Treatment*, 108717. doi: https://doi.org/10.1016/j.jsat.2021.108717.

Koob, G.F., and Le Moal, M. (2001). Drug addiction, dysregulation of reward, and allostasis. *Neuropsychopharmacology* 24(2), 97-129.

Koob, G.F., and Volkow, N.D. (2010). Neurocircuitry of Addiction. *Neuropsychopharmacology* 35(1), 217-238. doi: 10.1038/npp.2009.110.

Kozak, R., Martinez, V., Young, D., Brown, H., Bruno, J.P., and Sarter, M. (2007). Toward a neuro-cognitive animal model of the cognitive symptoms of schizophrenia: Disruption of cortical cholinergic neurotransmission following repeated amphetamine exposure in

attentional task-performing, but not non-performing, rats. *Neuropsychopharmacology* 32(10), 2074-2086. doi: 10.1038/sj.npp.1301352.
Krivanek, J.A., and McGaugh, J.L. (1969). Facilitating effects of pre- and posttrial amphetamine administration on discrimination learning in mice. *Agents and Actions* 1(2), 36-42. doi: 10.1007/BF01977664.
Lapish, C.C., Balaguer-Ballester, E., Seamans, J.K., Phillips, A.G., and Durstewitz, D. (2015). Amphetamine exerts dose-dependent changes in prefrontal cortex attractor dynamics during working memory. *The Journal of Neuroscience* 35(28), 10172. doi: 10.1523/JNEUROSCI.2421-14.2015.
Lesch, K.-P., and Waider, J. (2012). Serotonin in the modulation of neural plasticity and networks: Implications for neurodevelopmental disorders. *Neuron* 76(1), 175-191. doi: https://doi.org/10.1016/j.neuron.2012.09.013.
Li, D., and Mashour, G.A. (2019). Cortical dynamics during psychedelic and anesthetized states induced by ketamine. *NeuroImage* 196, 32-40. doi: https://doi.org/10.1016/j.neuroimage.2019.03.076.
Lucantonio, F., Caprioli, D., and Schoenbaum, G. (2014). Transition from 'model-based' to 'model-free' behavioral control in addiction: Involvement of the orbitofrontal cortex and dorsolateral striatum. *Neuropharmacology* 76, 407-415. doi: https://doi.org/10.1016/j.neuropharm.2013.05.033.
Ly, C., Greb, A.C., Cameron, L.P., Wong, J.M., Barragan, E.V., Wilson, P.C., et al. (2018). Psychedelics promote structural and functional neural plasticity. *Cell Reports* 23(11), 3170-3182. doi: https://doi.org/10.1016/j.celrep.2018.05.022.
Maddock, R.J. (1999). The retrosplenial cortex and emotion: new insights from functional neuroimaging of the human brain. *Trends in Neurosciences* 22(7), 310-316. doi: https://doi.org/10.1016/S0166-2236(98)01374-5.
Mandillo, S., Rinaldi, A., Oliverio, A., and Mele, A. (2003). Repeated administration of phencyclidine, amphetamine and MK-801 selectively impairs spatial learning in mice: a possible model of psychotomimetic drug-induced cognitive deficits. *Behavioural Pharmacology* 14(7).
Mao, D., Kandler, S., McNaughton, B.L., and Bonin, V. (2017). Sparse orthogonal population representation of spatial context in the retrosplenial cortex. *Nature Communications* 8(1), 243. doi: 10.1038/s41467-017-00180-9.
Marton, S., González, B., Rodríguez-Bottero, S., Miquel, E., Martínez-Palma, L., Pazos, M., et al. (2019). Ibogaine administration modifies GDNF and BDNF expression in brain regions involved in mesocorticolimbic and nigral dopaminergic circuits. *Frontiers in Pharmacology* 10(193). doi: 10.3389/fphar.2019.00193.
Mason, N.L., Kuypers, K.P.C., Müller, F., Reckweg, J., Tse, D.H.Y., Toennes, S.W., et al. (2020). Me, myself, bye: regional alterations in glutamate and the experience of ego dissolution with psilocybin. *Neuropsychopharmacology* 45(12), 2003-2011. doi: 10.1038/s41386-020-0718-8.
McGaugh, J.L. (1973). Drug facilitation of learning and memory. *Annual review of pharmacology* 13(1), 229-241.
Michaiel, A.M., Parker, P.R.L., and Niell, C.M. (2019). A hallucinogenic Serotonin-2A receptor agonist reduces visual response gain and alters temporal dynamics in mouse V1. *Cell Reports* 26(13), 3475-3483.e3474. doi: https://doi.org/10.1016/j.celrep.2019.02.104.

Millière, R., Carhart-Harris, R.L., Roseman, L., Trautwein, F.-M., and Berkovich-Ohana, A. (2018). Psychedelics, meditation, and self-consciousness. *Frontiers in Psychology* 9. doi: 10.3389/fpsyg.2018.01475.
Milton, A.L. (2023). Drug memory reconsolidation: From molecular mechanisms to the clinical context. *Translational Psychiatry* 13(1)**,** 370. doi: 10.1038/s41398-023-02666-1.
Milton, A.L., and Everitt, B.J. (2012). The persistence of maladaptive memory: Addiction, drug memories and anti-relapse treatments. *Neuroscience & Biobehavioral Reviews* 36(4)**,** 1119-1139. doi: https://doi.org/10.1016/j.neubiorev.2012.01.002.
Moroz, I., Parker, L.A., and Siegel, S. (1997). Ibogaine interferes with the establishment of amphetamine place preference learning. *Experimental and Clinical Psychopharmacology* 5(2)**,** 119-122. doi: 10.1037/1064-1297.5.2.119.
Nelson, A., and Killcross, S. (2006). Amphetamine exposure enhances habit formation. *Journal of Neuroscience* 26(14)**,** 3805-3812.
Nelson, A.J., Hindley, E.L., Haddon, J.E., Vann, S.D., and Aggleton, J.P. (2014). A novel role for the rat retrosplenial cortex in cognitive control. *Learn Mem* 21(2)**,** 90-97. doi: 10.1101/lm.032136.113.
Noller, G.E., Frampton, C.M., and Yazar-Klosinski, B. (2018). Ibogaine treatment outcomes for opioid dependence from a twelve-month follow-up observational study. *The American Journal of Drug and Alcohol Abuse* 44(1)**,** 37-46. doi: 10.1080/00952990.2017.1310218.
Nordquist, R.E., Voorn, P., de Mooij-van Malsen, J.G., Joosten, R.N.J.M.A., Pennartz, C.M.A., and Vanderschuren, L.J.M.J. (2007). Augmented reinforcer value and accelerated habit formation after repeated amphetamine treatment. *European Neuropsychopharmacology* 17(8)**,** 532-540. doi: https://doi.org/10.1016/j.euroneuro.2006.12.005.
North, A., Swant, J., Salvatore, M.F., Gamble-george, J., Prins, P., Butler, B., et al. (2013). Chronic methamphetamine exposure produces a delayed, long-lasting memory deficit. *Synapse* 67(5)**,** 245-257. doi: https://doi.org/10.1002/syn.21635.
O'Keefe, J., and Nadel, L. (1978). *The Hippocampus as a Cognitive Map.* Oxford: Clarendon Press.
Pachitariu, M., Stringer, C., Dipoppa, M., Schröder, S., Rossi, L.F., Dalgleish, H., et al. (2017). Suite2p: beyond 10,000 neurons with standard two-photon microscopy. *Biorxiv*.
Parker, L.A., Siegel, S., and Luxton, T. (1995). Ibogaine attenuates morphine-induced conditioned place preference. *Experimental and Clinical Psychopharmacology* 3(4)**,** 344-348. doi: 10.1037/1064-1297.3.4.344.
Pnevmatikakis, Eftychios A., Soudry, D., Gao, Y., Machado, T.A., Merel, J., Pfau, D., et al. (2016). Simultaneous denoising, deconvolution, and demixing of calcium imaging data. *Neuron* 89(2)**,** 285-299. doi: https://doi.org/10.1016/j.neuron.2015.11.037.
Saramäki, J., Kivelä, M., Onnela, J.-P., Kaski, K., and Kertész, J. (2007). Generalizations of the clustering coefficient to weighted complex networks. *Physical Review E* 75(2)**,** 027105. doi: 10.1103/PhysRevE.75.027105.
Schartner, M.M., Carhart-Harris, R.L., Barrett, A.B., Seth, A.K., and Muthukumaraswamy, S.D. (2017). Increased spontaneous MEG signal diversity for psychoactive doses of ketamine, LSD and psilocybin. *Scientific Reports* 7(1)**,** 46421. doi: 10.1038/srep46421.
Schoenbaum, G., Saddoris, M.P., Ramus, S.J., Shaham, Y., and Setlow, B. (2004). Cocaine-experienced rats exhibit learning deficits in a task sensitive to orbitofrontal cortex lesions. *European Journal of Neuroscience* 19(7)**,** 1997-2002. doi: https://doi.org/10.1111/j.1460-9568.2004.03274.x.

Schwarz, A.J., Gozzi, A., Reese, T., and Bifone, A. (2007). Functional connectivity in the pharmacologically activated brain: Resolving networks of correlated responses to d-amphetamine. *Magnetic Resonance in Medicine* 57(4), 704-713. doi: https://doi.org/10.1002/mrm.21179.

Seamans, J.K., and Yang, C.R. (2004). The principal features and mechanisms of dopamine modulation in the prefrontal cortex. *Progress in Neurobiology* 74(1), 1-58. doi: https://doi.org/10.1016/j.pneurobio.2004.05.006.

Sherrill, K.R., Erdem, U.M., Ross, R.S., Brown, T.I., Hasselmo, M.E., and Stern, C.E. (2013). Hippocampus and retrosplenial cortex combine path integration signals for successful navigation. *The Journal of Neuroscience* 33(49), 19304. doi: 10.1523/JNEUROSCI.1825-13.2013.

Shibata, H., Kondo, S., and Naito, J. (2004). Organization of retrosplenial cortical projections to the anterior cingulate, motor, and prefrontal cortices in the rat. *Neuroscience Research* 49(1), 1-11. doi: https://doi.org/10.1016/j.neures.2004.01.005.

Soetens, E., D'Hooge, R., and Hueting, J.E. (1993). Amphetamine enhances human-memory consolidation. *Neuroscience Letters* 161(1), 9-12. doi: https://doi.org/10.1016/0304-3940(93)90127-7.

Sokal, R.R. (1958). A statistical method for evaluating systematic relationships. *Univ. Kansas, Sci. Bull.* 38, 1409-1438.

Souza, B.C., Pavão, R., Belchior, H., and Tort, A.B.L. (2018). On information metrics for spatial coding. *Neuroscience* 375, 62-73. doi: https://doi.org/10.1016/j.neuroscience.2018.01.066.

Spyraki, C., Fibiger, H.C., and Phillips, A.G. (1982). Dopaminergic substrates of amphetamine-induced place preference conditioning. *Brain Research* 253(1), 185-193. doi: https://doi.org/10.1016/0006-8993(82)90685-0.

Stacho, M., and Manahan-Vaughan, D. (2022). Mechanistic flexibility of the retrosplenial cortex enables its contribution to spatial cognition. *Trends in Neurosciences* 45(4), 284-296. doi: https://doi.org/10.1016/j.tins.2022.01.007.

Vann, S.D., and Aggleton, J.P. (2002). Extensive cytotoxic lesions of the rat retrosplenial cortex reveal consistent deficits on tasks that tax allocentric spatial memory. *Behavioral Neuroscience* 116(1), 85-94. doi: 10.1037/0735-7044.116.1.85.

Vinh, N.X., Epps, J., and Bailey, J. (2010). Information theoretic measures for clusterings comparison: Variants, properties, normalization and correction for chance. *The Journal of Machine Learning Research* 11, 2837-2854.

Wolbers, T., and Büchel, C. (2005). Dissociable retrosplenial and hippocampal contributions to successful formation of survey representations. *Journal of Neuroscience* 25(13), 3333-3340.

Wong, S.A., Thapa, R., Badenhorst, C.A., Briggs, A.R., Sawada, J.A., and Gruber, A.J. (2016). Opposing effects of acute and chronic d-amphetamine on decision-making in rats. *Neuroscience*. doi: http://dx.doi.org/10.1016/j.neuroscience.2016.04.021.

Wood, J., Kim, Y., and Moghaddam, B. (2012). Disruption of prefrontal cortex large scale neuronal activity by different classes of psychotomimetic drugs. *The Journal of Neuroscience* 32(9), 3022-3031. doi: 10.1523/jneurosci.6377-11.2012.

Wyass, J.M., and Van Groen, T. (1992). Connections between the retrosplenial cortex and the hippocampal formation in the rat: A review. *Hippocampus* 2(1), 1-11. doi: 10.1002/hipo.450020102.

Wyvell, C.L., and Berridge, K.C. (2000). Intra-accumbens amphetamine increases the conditioned incentive salience of sucrose reward: enhancement of reward "wanting" without enhanced "liking" or response reinforcement. *Journal of Neuroscience* 20(21)**,** 8122-8130.

Wyvell, C.L., and Berridge, K.C. (2001). Incentive sensitization by previous amphetamine exposure: Increased cue-triggered "wanting" for sucrose reward. *The Journal of Neuroscience* 21(19)**,** 7831. doi: 10.1523/JNEUROSCI.21-19-07831.2001.

4.8 SUPPLEMENTARY INFORMATION

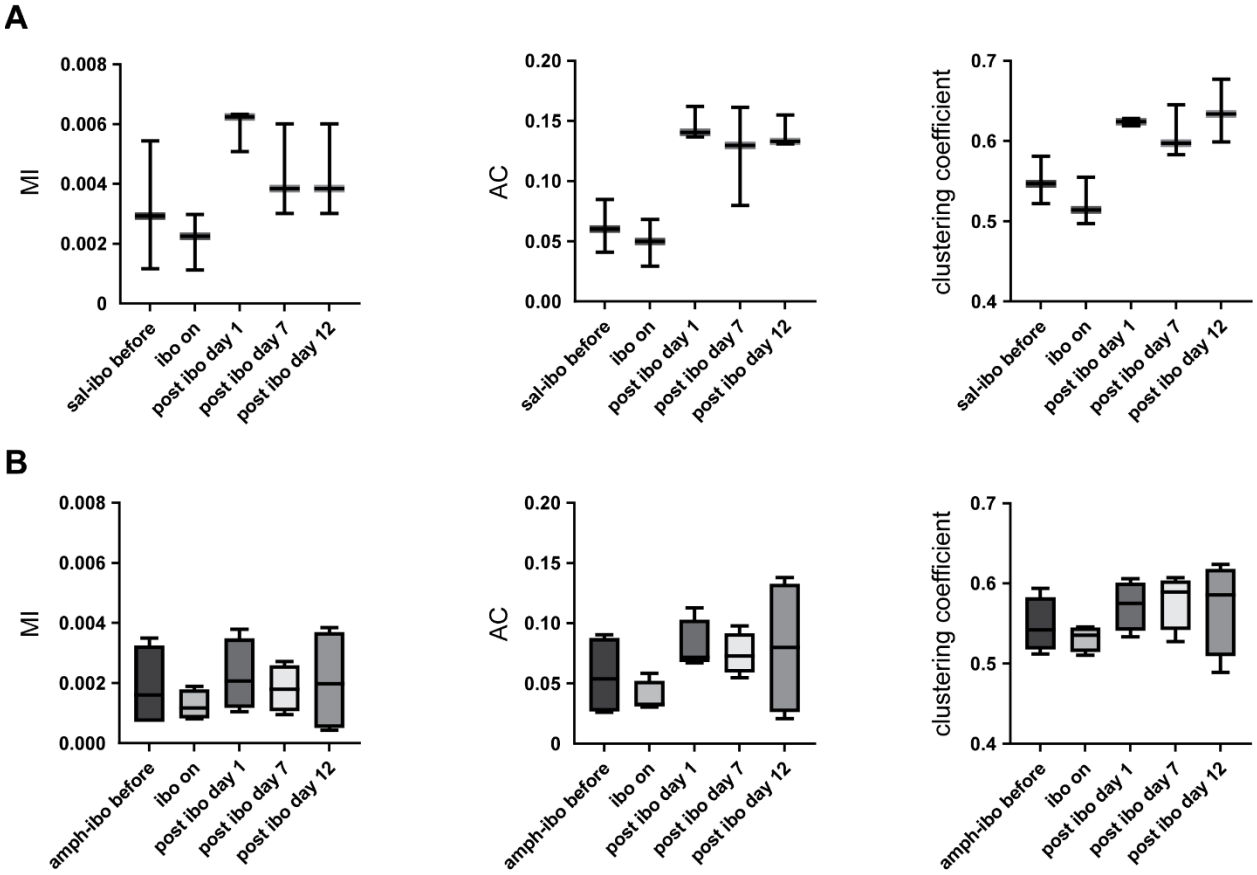

Supplemental Fig. 4.7. Long-term effects of ibogaine on information encoding. A. Mean mutual information (MI), trial-to-trial correlations (AC), and clustering coefficient in SAL-IBO group before, during, and after ibogaine administration B. Mean mutual information (MI), trial-to-trial correlations (AC), and clustering coefficient in AMPH-IBO group before, during, and after ibogaine administration.

CHAPTER 5: GENERAL DISCUSSION

In order to identify common neural features of psychedelics with varied pharmacological effects (i.e., receptor binding profiles), I chose to test the effects of the classic psychedelic psilocybin and the non-classic psychedelic ibogaine. I recorded the activity of individual neurons in the superficial layers of the agranular retrosplenial cortex in head-fixed mice running on a treadmill with tactile cues. My thesis aimed to determine if the psychedelic compounds degraded location encoding and functional connectivity of neural ensembles. Additionally, I tested the hypothesis that ibogaine administration will have long term effects to help recover the loss of spatial information in mice chronically administered amphetamine. Throughout the 3 experiments presented, common denominators for both psychedelics emerged. The data indicate that the two psychedelics have similar short-term effects on neural encoding of spatial position in the retrosplenial cortex. The psychedelics disrupt the brain's ability to maintain the integrity of the cognitive map by interfering with path-integration, a process used to keep track of the position in an environment. These effects dissipate 24 hours after psychedelic administration, and I did not find a meaningful interaction between chronic amphetamine and ibogaine. The results I obtained complement the research in humans, and also raise interesting new questions for future research. In the following sections I will discuss my key findings in a broader context than in previous chapters in order to synthesize a better understanding of psychedelic action on the brain.

5.1 WHAT ARE COGNITIVE MAPS?

The concept of "cognitive maps" was first introduced in 1948 by Edward Tolman (Tolman, 1948) as a systematic organization of knowledge of the environment which determines behavioral responses. This term has evolved to encompass mental representation employed to

acquire, recall, and decode information about the relative locations and attributes of phenomena in the environment. The maps are used to form 'schemas', abstractions and inferences that are separate from sensory representations and therefore generalize across different events (Behrens et al., 2018). There are many parallels between acquiring non-spatial and spatial information. The encoding of spatial information is much better understood, so I chose this system to assess the effects of psychedelics on information encoding. Cognitive maps have strongly influenced research of spatial navigation (O'Keefe and Nadel, 1978). It has been found that animals (and humans) use path integration to constantly update the cognitive map during movement. This is achieved by tracking the starting point, using contextual cues, and registering active movement to update expected location (Chrastil et al., 2015; Mao et al., 2020). The retrosplenial cortex (RSC) has long been implicated in path integration (Takahashi et al., 1997; Cho and Sharp, 2001; Wolbers and Büchel, 2005), along with the hippocampus (HPC) and prefrontal cortex (PFC) (Wolbers et al., 2007; Sherrill et al., 2013). These regions work in conjunction to support navigational choices. Although their function may overlap, it has been shown that: (1) the PFC is important for goal tracking, adapting behavior to new contingencies, and record the abstract location within the task constraints (Yu et al., 2018; Patai and Spiers, 2021); (2) the hippocampal place cells encode the actual position within the environment (Wilson and McNaughton, 1993); and (3) the RSC serves as an information bridge between PFC and hippocampus important for tracking direction, movement correlates, and integrating inputs from sensory and motor cortices in order to update the cognitive map (van Groen and Wyss, 1992; 2003; Iaria et al., 2007; Hindley et al., 2014).

Psychedelic drugs have demonstrable effects on mentation, but the neural correlates are poorly understood. Human fMRI studies suggest that these substances cause a reduction of functional connectivity between brain structures involved in the construction and maintenance of

cognitive maps. The cognitive map can therefore be used as a system to understand the effects of psychedelics on information encoding.

5.2 PSYCHEDELIC EFFECTS ON SPATIAL ENCODING AND NEURAL FUNCTIONAL CONNECTIVITY

The identification of place-cells in the CA1 of hippocampus of freely moving animals is relatively straight-forward because these cells have a large signal-to-noise profile. They have a low background firing rate when outside of the place field, but reliably increase firing substantially while traversing the place field. I found more variability in our experimental design, which used head-fixed mice and neural recording in RSC. In particular, neurons that had a clear place field on most trials, would fail to fire on other trials. I therefore searched the literature for a method that would quantify this variance and other sources of variance such as spatial selectivity (place field width). An adjusted version of mutual information (MI) captures both sources (Vinh et al., 2010). MI is a computational method used to identify spatially tuned neurons. Using the firing rate of each neuron and the position of the mouse on the belt for each trial, I was able to determine which cells respond to a specific location. This method has been validated, and can also be used for identifying hippocampal place cells from calcium imaging data (Gobbo et al., 2022). The MI reveals changes in the accuracy and stability of spatial information encoding when the system is perturbed, such as when administering neural dynamics-altering substances.

In the present data both psychedelics reduced the position-related MI of individual RSC neurons while the drugs were on board, reflecting an impairment of the path integration stability. Interestingly, in the case of ibogaine, this effect was stronger for the non-cue regions. The RSC provides an anchoring to fixed landmarks for the cognitive map (Epstein et al., 2017), and therefore this effect could reflect a preservation of sensory signals to RSC, indicating a potential mechanism

for stabilizing the cognitive map. Other hallucinogens that are selective 5-HT_{2A}R agonists did not alter previously established CA1 place cells (Zhang et al., 2017), and therefore this may be a RSC-specific effect. It is important to note that the decrease in MI was a transient effect because it was absent when testing 24 hours after injection.

Psilocybin and ibogaine caused a decrease in the clustering coefficient of the correlation matrix. This coefficient was calculated from the hierarchical clustering of the Pearson correlation matrices of all cell-pairs recorded in a session, a method previously described for assessing the similarity between the population activity structure (Chang et al., 2020). This method differs slightly from functional connectivity as described in fMRI literature, which determines temporal correlations between the blood-oxygen-level-dependent (BOLD) signals from different brain regions. If two or more brain areas show synchronized activity over time they are described as functionally connected. The functional connectivity described in these studies shows a similar analysis at cellular level, with the caveat that the activity of each neuron is averaged across all trials to create the 'tuning curve' over the belt. Therefore, the animals' position is factored in when generating the correlation matrices. This is an important step for this type of data, in which the behavior and movement of the mouse must be considered. High correlation between two neurons indicates similar activity profiles, which suggests they are functionally connected. After the psychedelic administration, the correlation structure exhibits fewer dominant motifs, indicating that the neurons became more functionally disconnected from one another. Saline administration appeared to slightly reduce the amplitude of correlations but preserve the overall pattern. The minor decrease in amplitude could be due to a reduction in motivation or as an effect of the injection itself.

The cortical desynchronization and increase in the entropy of functional connectivity has been previously reported in humans using fMRI and magnetoencephalography (MEG) (Muthukumaraswamy et al., 2013; Tagliazucchi et al., 2014; Girn et al., 2022). The data presented here is one of the first to show a similar effect at neuronal level. The decoupling between the RSC and the parahippocampal gyrus has been particularly implicated in the psychedelic-induced loss of functional connectivity in fMRI studies (Carhart-Harris et al., 2016; Lebedev et al., 2016), and our results are consistent with these findings. The decrease of the clustering coefficient can be partly explained by the destabilization of positional signaling, but the avalanche analysis performed in Chapter 3 is independent from the neuronal information encoding, and showed a decrease in the correlation between bursting/pause events, indicating a loss of structure among units and across time. Human imaging data suggests that brain networks shift toward criticality under psychedelics (Atasoy et al., 2017). The concept of criticality refers to a state where a complex dynamical system operates at the boundary between order and disorder. Because the brain is a complex system, the criticality framework has been heavily featured in psychedelic brain theories, which propose that under the influence of psychedelic drugs the complexity of brain states increases, bringing the system closer to a critical point. Such systems often display critical phenomena, such as power-law distributions of network properties, self-organized criticality, and activity bursts (avalanches) of network events that can occur spontaneously (Beggs and Plenz, 2003). Analyzing neuronal avalanches can provide information into the system's intrinsic memory. Despite its prominent role, there are few studies directly investigating psychedelic effects as they relate to a critical neural system. One such study from Varley et. al. used fMRI data from participants under the influence of psilocybin and LSD to show that both psychedelics increase the complexity of cortical functional connectivity networks, bringing the system closer to a critical

point (Varley et al., 2020). Functional MRI is an indirect measure of neural activity over spatial scales much larger than individual neurons and it was undetermined if a similar shift toward criticality would occur among neural ensembles. Ibogaine did not affects the slope of the power-law distributions or the cutoff point, which would indicate a shift in the underlying dynamics. However, the psychedelic did cause the network of neurons to generate increased activity outside of large avalanche events, suggesting a reduction in the temporal window during which signals are integrated in the RSC. The present data provide important information for the critical brain state theory, but further work is required in order to determine specific transition states.

The results discussed in this section reveal that psilocybin and ibogaine have similar acute effects on information processing and network dynamics in the RSC in freely behaving mice, despite heterogeneous receptor binding profiles. These effects were absent upon testing 24h later, and we were unable to find any prolonged effects at day 7 and 10 post-administration for either psychedelic. These (null) results indicate that the long-term effects of the psychedelics might not encompass changes in the RSC cognitive map or that they might not be distinguishable within the current experimental design. In particular, the design did not include paradigms, such as fear conditioning or drug self-administration, reported to be affected days after psychedelic administration.

5.3 PSYCHEDELIC EFFECTS ON NEURAL ACTIVITY RATE

The acute effects on neural encoding and functional connectivity are similar for the two psychedelics investigated, despite divergent effects on neuronal firing rates. Ibogaine increased the activity rate in drug-naïve animals when the drug is on board, whereas psilocybin decreased it. There are no prior studies examining effects of psychedelics on RSC neuron activity, but there are

some limited data in functionally related brain structures. The majority of the hallucinogens investigated, such as PCP, MK-801, and 5-MeO-DMT cause an overall increase in population activity in the PFC (Suzuki et al., 2002; Wood et al., 2012; Lladó-Pelfort et al., 2018). Lower doses of psilocybin (2 mg/kg) have a similar enhancing effect (Golden and Chadderton, 2022), which differs from our findings in the RSC. However, different psychedelics can also have divergent effects on mean activity rates in the PFC. Some studies showed that DOI causes a decrease in spiking activity in the mPFC (Wood et al., 2012; Rangel-Barajas et al., 2017; Brys et al., 2023). Other work has found that DOI has a bidirectional modulatory effect on firing rate in the PFC (Dearnley et al., 2023) and visual cortex (Michaiel et al., 2019). In contrast, in vitro studies showed that psilocybin can decrease neuronal spiking in hippocampal pyramidal neurons (Moldavan et al., 2000). In the present data, the psychedelics could have bidirectionally modulated individual neurons, but the overall population activity is increased with ibogaine and decreased by high doses of psilocybin. The discrepancies between the effects of psilocybin on firing rate in the present data and previous studies could be due to dose differences, physiological variations between the RSC and PFC, and/or functional connectivity variance for the two cortical regions. At the 24h point, the changes in mean activity rate dissipate, indicating that the effects are transitory.

Despite divergent effects on mean activity rates, both ibogaine and psilocybin slowed behavioral output while the drugs were on board. The mice continued to perform the task after the psychedelic administration with only moderate decreases in movement velocity and other metrics. The reduced locomotion in the present data is similar to previous reports (Halberstadt et al., 2011; Tylš et al., 2016). However, the changes in behavior are not solely responsible for the effects I observed in the neural information processing measures. This is primary because the measures are

binned by position, not time. Furthermore, the adjusted MI method used to assess the spatial encoding controls for the difference in number of trials.

5.4 THEORIES OF PSYCHEDELICS

The brain appears to have some hierarchical organization of information processing in which sensory data is transmitted through so-called 'lower-level' inputs and more complex information processing occurs in 'higher-level' systems (Gilbert and Sigman, 2007; Wacongne et al., 2011). I will use these terms because they are prevalent in the literature. The higher-level systems are associated with cognition. There are many theories that attempt to explain different aspects of cognition and, particularly relevant for the body of work presented in this doctoral thesis, how psychedelics affect the neural processes (Swanson, 2018). The leading framework of psychedelic action has been proposed by Carhart-Harris and Friston and has been termed the REBUS (RElaxed Beliefs Under pSychedelics) model (Carhart-Harris and Friston, 2019) and is based on the predictive coding theory (Friston, 2010). This theory is predicated on the notion that the neocortex is organized in a hierarchical manner, in which top levels produce a prediction about upcoming events, which propagates down the hierarchy. These top-down predictions constrain the bottom-up propagation of sensory information. Thus, if events are fully expected, the sensory-related perturbation to ongoing brain dynamics is small. Hallucinogenic drugs are proposed to disrupt the balance between the top-down/bottom-up information flow. Psychedelics are proposed to impair the top-level predictions such that sensory inputs cause large perturbations of neural activity, thereby increasing the entropy of neural signaling (Carhart-Harris and Friston, 2019). Psychedelic states are associated with disruption of information flow between cortical regions in humans (Carhart-Harris et al., 2012; Barnett et al., 2020). This is particularly evident in brain regions involved in the default mode network (DMN), which regulates mental processes when

subjects are not engaged in tasks (Palhano-Fontes et al., 2015). While these proposals generally agree that psychedelics disrupt the top-down control, it is still unclear whether this is due to a reduction of precision of high-level predictions, thereby liberating bottom-up information flow (Carhart-Harris and Friston, 2019), or if the top-down activity is increased due to a pharmacological hyperactivation of top-down synaptic transmission (Muthukumaraswamy et al., 2013). The REBUS model indicates the bottom-up signaling originates in the limbic system, including the hippocampus and the parahippocampal gyrus, among other structures. In this state, the mismatch between predictions and sensory information causes an increase in the prediction errors (Pink-Hashkes et al., 2017), which generates many of the symptoms associated with the psychedelic state (e.g. hallucinations). For example, a classic feature of the psychedelic experience is perceiving static objects as moving, such as walls breathing or colors in motion. Carhart-Harris and Friston argue that this could be viewed as a loss of high-level constraint (walls don't usually breathe) on visual perception, which is driven by heightened sensory signaling.

If we consider the present data through this framework, it could explain the modulation of spatial encoding. The theory has focused on sensory processing and the interaction with high-level association regions, such as the DMN. The effect on navigation and spatial information encoding has not been fully explored but certain inferences can be made. The RSC is an association cortex within the DMN and has been posited to be central to generating top-down signals predicting perceptual information to guide behavior (for review see (Alexander et al., 2023a)). The predictive coding theory posits that deep layers of association cortices encode expectations of upcoming sensory states, and the expectation inhibits sensory inputs in the superficial layers. Psychedelics are proposed to impair the top-level predictions. Because many psychedelics affect the serotonergic system, the effects are purported to stem from a 5-HT_{2A} receptor-mediated

hyperactivation of the pyramidal cells in layer V (Muthukumaraswamy et al., 2013), which cause an increase in the number (and details) of the predictions in the system. It is possible that the dysregulated predictions in layer V fail to properly counteract inputs to superficial layers from other cortical regions, causing an increase in prediction errors. Therefore, the decrease in the spatial encoding could reflect an impairment in generating accurate predictions for the position of the animal on the belt and the associated increase in prediction errors in the superficial layers of the RSC. This proposal is still speculative and requires additional testing but fits within the literature, although some studies have shown a psychedelic-induced reduction in sensory inputs in the visual cortex (Michaiel et al., 2019). Additionally, in psychopathologies such as depression, it has been proposed that high-level priors are overweighted and biased toward negative expectations (Kiang et al., 2017). This can cause a suppression of bottom-up signaling, and a "rigid" system (Carhart-Harris and Friston, 2019). Consistent with this proposal, depression has been showed to cause a decrease in frontal activity and a lack of reward-related prediction errors (Ubl et al., 2015). Administration of several psychedelics has been reported to decrease the negative bias (Palhano-Fontes et al., 2019; Zeifman et al., 2020). Mechanistically, weaker top-down signals should be observed. Although the on-board data are consistent with this theory, the longitudinal data showed no effect.

5.5 MORPHOLOGICAL EFFECTS OF PSYCHEDELICS

A central idea associated with psychedelic action is the fact that many psychedelics can induce plastic changes in the brain. Although this thesis does not directly assess plasticity, the correlation structure of cellular activity can be used to generate inferences on the overarching theory. Various psychedelics have been posited to alter spine and dendritic morphology, such as DMT (Lima da Cruz et al., 2018), ketamine (Pryazhnikov et al., 2018; Treccani et al., 2019; Zhang

et al., 2019), and others (Calder and Hasler, 2023). At a cellular level, structural plasticity includes dendritic and synaptic plasticity, and possibly neurogenesis (in hippocampus). Both psilocybin (Shao et al., 2021) and ibogaine (Ly et al., 2018; Cameron et al., 2020) have been shown to promote structural markers of synaptic plasticity, particularly in cortical neurons. It is important to note that it is not yet clear if the anatomical evidence of synaptogenesis has functional consequences. In other words, it is not known if new synapses play a functional role in information processing. Some neurological conditions such as depression are associated with atrophy of neurons and a loss of synapses in the frontal cortex (Liu et al., 2017; Holmes et al., 2019). The therapeutic effects of psychedelics can last for up to 6 months after administration (Andersen et al., 2021) and therefore it has been posited that these effects could be linked to their synaptic effects in the neocortex. A direct, conclusive correlation has yet to be demonstrated. To our knowledge, no psychedelic studies have investigated synaptic alterations in the RSC, but the HPC also appears to be a target for increased structural neuroplasticity (Du et al., 2023). However, psilocybin can also have an inhibitory effect on hippocampal neurogenesis (Catlow et al., 2013), an effect that does not correlate to behavioral effects on fear extinction.

At a molecular level, neuroplasticity encompasses changes in gene and protein expression, which trigger morphological changes. Studies in rats have shown that psilocybin causes dose- and region- dependent transcriptional regulation of genes that have been linked to synaptic plasticity (e.g. Arc, Egr2), with a general trend of lower levels found in the HPC, and increased levels in the PFC (Jefsen et al., 2021). A single dose of psilocybin can alter the expression of several genes associated with plasticity and cognition (e.g. neuroplastin, brain derived neurotrophic factor) in the mouse PFC (Fadahunsi et al., 2022). Conversely, diminished BDNF levels have been found in pathological populations suffering from depression (Karege et

al., 2002). Similar results have been shown with ibogaine. Glial cell derived neurotrophic factor (GDNF) and BDNF are neurotrophic factors that promote the growth, synaptogenesis, and survival of neurons. They have been shown to mediate neuronal processes that occur during drug-seeking behavior in animal models (Ghitza et al., 2010; Koskela et al., 2017). One interesting study showed that in rodents, ibogaine increased the expression of GDNF in the ventral tegmental area (VTA), which correlated with reduced ethanol self-administration (He et al., 2005). An iboga synthetic analog was shown to induce the release of GDNF in cell culture systems (Gassaway et al., 2016). A more recent study demonstrated that ibogaine causes a site and dose-specific upregulation of BDNF and GDNF transcripts in several brain regions implicated in addiction, such as the VTA, PFC, nucleus accumbens (NAcc), and substantia nigra 24h after administration, particularly at a dose of 40 mg/kg (Marton et al., 2019). These observations led to the idea that the ibogaine-induced GDNF expression may persist beyond the elimination of the drug which can be the mechanism of action underlying the anti-addictive effect of ibogaine. Few studies directly investigate if structural changes lead to behavioral outcomes and therefore a causal inference is difficult to assess.

Synaptic changes would purportedly also correlate with alterations in neural dynamics. In the data presented in this thesis I did not find such psychedelic-induced long-term effect on spatial encoding. Several hypotheses could explain this discrepancy. The changes in neural encoding that result from increased synaptic plasticity might not be reflected in the RSC cognitive map. While that is certainly possible, I argue the RSC's strong reciprocal connections with the PFC and HPC should reveal meaningful effects on RSC spatial encoding via synaptic changes in these other structures, which have been repeatedly reported. Alternatively, perhaps new spines might not be integrated quickly enough to reveal changes in the present study. Clinical data,

however, reveals a rapid (within 24h) onset of positive cognitive effects associated with psychedelic administration. Moreover, I tested at several timepoints post-treatment: 1, 3, 7, and 10 days (data not shown). It is therefore unlikely that the duration of the investigation relative to psychedelics synaptogenic actions accounts for the negative finding. Another possibility is that the synaptogenesis hypothesis might not fully explain the prolonged behavioral and neural effects. In mice treated with psilocybin, the rate of dendritic spine formation in dopaminergic areas was elevated for the first 3 days and returned to baseline by day 5 post-administration (Shao et al., 2021). Note that the ibogaine-induced increase in neurotrophic factors in dopaminergic areas (VTA, NAcc) might not be particularly relevant in the current task. The dopaminergic signaling might not affect the path integration systems in the present study because the mice are well trained and complete trials without engaging the goal-directed systems.

If plastic changes would be the driving force of the long-term effects that last days-to-months after treatment, I would expect that the neural encoding and/or dynamics will be more strongly affected after the drug is cleared, but that was not the case for the present data. The only prolonged (>24h) effect detected is the increase in the information encoding indicators in the control animals that were administered ibogaine in Chapter 4. This finding is singular to this group and was not observed in the first ibogaine study (Chapter 3). Such long-lasting effects may involve psychedelic-induced synaptic changes. However, the low number of animals in this group and lack of replicability make it difficult to determine if morphological changes are the primary cause for this result. They could be the result of a different, unobserved factor. No such effect was found in the amphetamine-treated mice. Overall, the absence of discernible long-term alterations reinforces the interpretation that the psychedelic effects observed in these experiments are more likely caused by the functional changes in network dynamics, rather than structural effects on neuronal synapses.

5.6 PSYCHEDELIC PHARMACOKINETICS

The selected epochs for the neural recordings were chosen based on the pharmacokinetics of ibogaine and psilocybin. The 'on-board' epoch (20-60 mins after i.p injection) occurred when the psychoactive metabolites noribogaine and psilocin are above concentration thresholds in blood plasma for psychoactive effect (Baumann et al., 2001; Sakashita et al., 2015; Rodríguez et al., 2020). The second 'off-board' epoch was at 24 h post administration, when no significant amounts of the psychedelic compounds would be present in the system. This allowed us to record both the acute and long-term effects elicited by the drugs. At 40 mg/kg i.p. administration of ibogaine in rats, its blood half-life is slightly less than 2h (Baumann et al., 2001) and both ibogaine and noribogaine are present at highest concentration (18-22 μM) levels in the rat brain within this window (Rodríguez et al., 2020). Because ibogaine is metabolized quickly, the long-term effects are likely due to the prolonged presence of noribogaine in the brain (Mash et al., 2000).

There are reports that acute, high doses (100 mg/kg) of ibogaine have a toxic effect on the Purkinje cells in the cerebellum (O'Hearn and Molliver, 1993). This effect is not evident with lower doses of 40 or 10 mg/kg (Molinari et al., 1996; Helsley et al., 1997). The dose investigated in the current work (40 mg/kg i.p.) is the standard used in rodent literature because: (1) it exerts psychomimetic effects; (2) does not show changes in heart rate or blood pressure (Glick et al., 2000); (3) does not cause cerebellar degeneration, and (4) is much lower than ibogaine's LD_{50} of 145-175 mg/kg (Schep et al., 2016). The investigation of the effects of a higher (15 mg/kg) dose of psilocybin was motivated by reports showing that higher doses have stronger effects on plasticity-related genes (Jefsen et al., 2021) and on neurotransmitter release in the prefrontal cortex (Wojtas et al., 2022), while not causing any toxic effects. Psilocybin's LD_{50} is 285-293 mg/kg (Gable, 2004; Zhuk et al., 2015).

5.7 AMPHETAMINE EFFECTS ON SPATIAL ENCODING

The effects of amphetamine on the brain have been researched extensively, but the majority of this work is beyond the scope of my thesis. I will focus this discussion on evidence regarding its effect on information encoding in the neocortex. Prolonged exposure to amphetamine can impair learning and memory in a variety of spatial tasks (Mandillo et al., 2003; North et al., 2013; Arroyo-García et al., 2020). The RSC has been shown to have a prominent role in path integration and spatial encoding (Cooper and Mizumori, 1999; Chang et al., 2020). Furthermore, this cortical region is likely implicated in the transition from ethological behavior to the patterned behavior associated with drug taking and seeking (Koob and Le Moal, 2001). Chronic amphetamine increases habit formation and motivation for reinforcement (Nelson and Killcross, 2006; Nordquist et al., 2007), and the RSC is likely susceptible to changes in neural activity and information encoding associated with the drug.

In the experiment in Chapter 4, an escalating dose of amphetamine was administered daily for 10 days, replicating proven chronic exposure to amphetamine paradigms shown to induce long-lasting changes in neocortical physiology (McDonald et al., 2021; McDonald et al., 2023). I chose a higher peak dose (2 mg/kg) because it was shown that it increases locomotion without inducing stereotypy in mice (Yates et al., 2007) and it induces withdrawal symptoms (Fukushiro et al., 2011). I escalated the dose over time, from 0.5 mg/kg to 2 mg/kg per day to habituate the animals gradually to the drug. Our data revealed that amphetamine reduces spatial information and trial-to-trial correlation of single unit activity. There are several possible explanations for the observed effect, such as loss of motivation for sucrose, or a shift of control towards the sensorimotor system. However, the most likely explanation, is that the chronic treatment altered intracellular physiology, causing a lower signal to noise ratio (SNR), similar to

electrophysiological data from the rat PFC from our lab (Hashemnia et al., 2020). However, amphetamine did not affect the clustering of activity covariance among RSC neurons, suggesting the lower spatial encoding is not caused by a large-scale synaptic remodeling. Additionally, this effect persisted in the OFF condition, at 24h after the last i.p. injection, but that did not correlate with a lower locomotion speed, or a lower mean activity rate of the neurons, suggesting the loss of positional information is due to the effect of the drug and not to movement or other features.

Based on the results, I speculate that chronic amphetamine did not alter RSC morphology sufficiently to cause a persistent remodeling of information. However, it is possible that structural changes in other brain regions could impact the spatial encoding in the RSC. Amphetamine is known to increase dendritic length and spine density in various brain regions important for learning and memory, such as PFC, striatum, NAcc, and caudate putamen, (Robinson and Kolb, 1999; Li et al., 2003; Crombag et al., 2005; Wong et al., 2016). It also modulates neuronal and spine density in the HPC (Arroyo-García et al., 2020; McDonald et al., 2021) and causes inhibition of long-term potentiation (LTP) in the HPC (Chen et al., 2021). These regions have strong connections with the RSC and could indirectly modulate the integrity of the cognitive map in this cortical area. However, the preservation of neuronal functional connectivity and the decrease in the activity rate suggests that the system has the same dynamical capacity, but the information encoded is diminished. Whether this is a local effect in the RSC or due to changes in afferent regions is difficult to establish with the present data set.

5.8 LIMITATIONS AND CAVEATS

Regarding the present data, a few caveats need to be acknowledged. Firstly, the high dose of psilocybin is higher than what other behavioral rodent studies have employed. In rodents, high doses of drugs such as ketamine and phencyclidine (PCP), have been shown to cause neuronal damage in the RSC and the expression of the heat shock protein HSP70 (Sharp et al., 1992; Tian et al., 2018). There are no reports of such damage associated with psilocybin. In fact, one study failed to detect any HSP70-positive neurons in the rat RSC, even at doses as high as 20 mg/kg (Iorgu et al., 2023). Nonetheless, I checked the integrity of the RSC in the animals administered high doses of psilocybin using Nissl staining (Fig. 5.1; Supplemental Fig. 5.2-5.3) and found no evidence of neuronal damage.

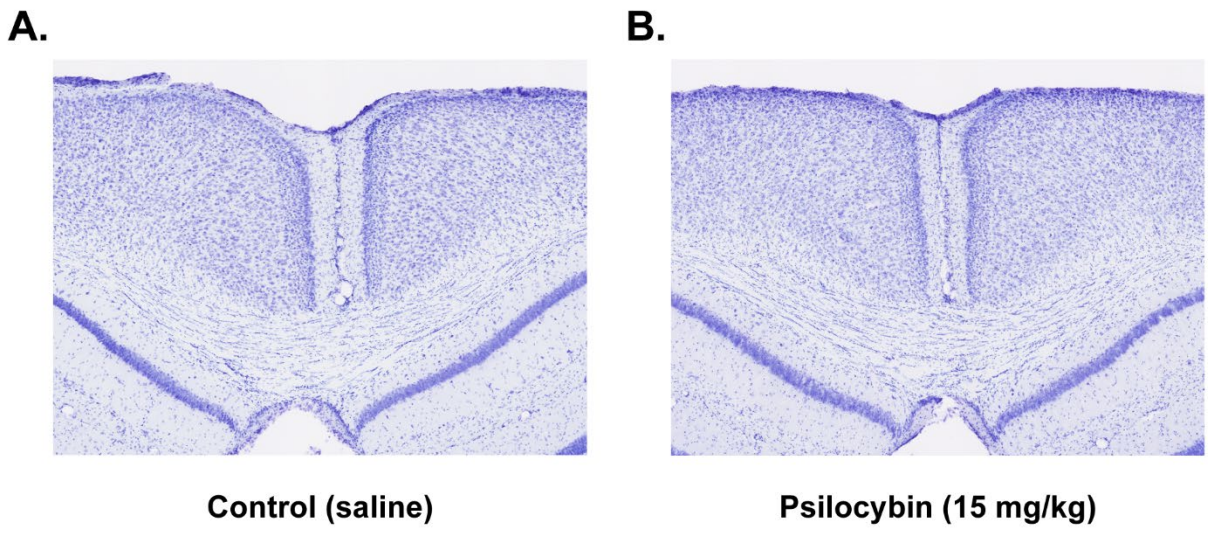

Fig. 5.1. Examples of histological images. Coronal sections (40 μm) of mouse brains stained with Cresyl Violet. The images show the retrosplenial cortex (-2.5 AP) in mice treated with saline (A) and psilocybin (B; 15 mg/kg).

Secondly, the amphetamine administration protocol used is not a typical "drug sensitization" paradigm. These protocols are usually characterized by intermittent administration, followed by a challenge session (Paulson and Robinson, 1995; Gulley and Stanis, 2010; Fordahl et al., 2016). However, the sensitization challenge test was outside of the scope of the current work, and the drug protocol was designed to expose the mice to a prolonged amphetamine treatment to induce a withdrawal effect, which allowed me to assess ibogaine's impact during this critical time. Furthermore, the task is not a classic "drug seeking" task, meaning that animals do not need to employ navigational choices to get the drugs. Lastly, various previous reports have found an increase in locomotion in amphetamine-treated mice (Robinson and Kolb, 1999), but I did not observe any changes in the speed of the animals. These caveats notwithstanding, the present work provides important insights into the cortical neural dynamics associated with chronic drug administration because, to our knowledge, this is one of the first reports on the effects of amphetamine in the RSC at the cellular level.

Reports of ibogaine having the ability to mitigate addictive behaviors and drug self-administration in rodents (Glick et al., 1991; Sershen et al., 1992b; Sershen et al., 1994) have motivated our investigation into the amphetamine-ibogaine signaling dynamics in the cortex. However, I was unable to determine a clear ameliorating effect of ibogaine in the amphetamine-treated animals in our spatial encoding measures. There are several potential explanations for this finding. The chronic amphetamine could have physiological effects which could render the RSC less susceptible to the effects of ibogaine. Alternatively, there is the possibility that the ameliorating effects of the psychedelic are not distinguishable in the RSC. Ibogaine might exert a stronger effect in executive areas which inform the RSC, such as the PFC and HPC. These possibilities have been discussed in Chapter 4. Further research aimed at uncovering the cellular

and functional effects of psychedelics on neural encoding is necessary in order to determine their mechanism of action and, ultimately, their therapeutic potential.

5.9 CONCLUSION

Rodent models can provide us with valuable insights into the effects of psychedelics at the cellular level, and how the evoked changes in neural activity and other features correlate with altered behavioral output. The present work aimed to do just that, using 2-photon imaging, a method that allowed me to record the activity of hundreds of neurons simultaneously in the mouse cortex, while the animals are performing a task that relies on cognitive processes that can be distorted by psychedelics.

Most of the hypotheses posited in the thesis introduction were validated, but a distinction must be made regarding the acute and long-term effects.

Hypothesis 1: Psychedelics will corrupt encoding of RSC place encoding. The data supports the hypothesis. Both ibogaine and psilocybin lower the spatial encoding measures (mutual information, trial-to-trial correlation) while on board.

Hypothesis 2: Psychedelics will disrupt functional connectivity among single units in RSC. This hypothesis is supported by the lower clustering coefficient values of the correlation matrices for neurons recorded within an hour of psychedelic administration.

Hypothesis 3: Psilocybin and ibogaine will show similar effects on RSC activity despite differences in their molecular structure and pharmacology. Both psychedelics have similar effects on behavior, location encoding, and functional connectivity measures. Ketanserin blocked these effects for psilocybin, suggesting that they are primarily due to 5-HT_{2A}R activation.

Hypothesis 4: Chronic amphetamine administration will reduce SNR of place encoding in RSC neurons. The RSC did exhibit a reduction in the signal to noise ratio of the spatial encoding with chronic amphetamine at both 1 and 24 hours after drug administration.

Hypothesis 5: Psychedelics will have long-term effects to improve SNR in mice treated with chronic amphetamine. We did not observe any prolonged effects in any of our measures, including no improving effect of ibogaine for amphetamine-treated mice. Therefore, the data does not support this hypothesis.

Regarding hypothesis 5, the literature that informed the formulation of the hypothesis suggested that I would find a significant interaction between the two drugs. The lack of a positive effect does not necessarily disprove the hypothesis. Possible explanations include that either the task or the brain region chosen were not sensitive enough to reveal the relevant effects. The robust, reliable, and replicable effects of both psychedelics on information processes in the RSC cause me to believe that this cortical area is an appropriate target to study these substances. In retrospect, the task chosen may not have been the best task to achieve a positive result. Future work in this field would benefit from drug seeking task, in which the animals perform for drug self-administration in a particular environment. This would allow testing whether this affects the RSC encoding of space after ibogaine washes out of the system.

Overall, the data presented in this doctoral thesis suggests that cognitive maps are disrupted by psychedelic compounds. Beyond the direct contribution to the research literature investigating how psychedelic drugs alter cognition, these results generate several interesting new questions to explore with future research. One such question is whether the loss of information encoding was due to a dissociative effect (were the animals 'disengaged' from the task). A way to

investigate this could be by giving the mice drugs that sedate but are not psychedelic (e.g. benzodiazepine). Secondly, ibogaine is known to act upon several types of receptors in the brain. A systematic analysis using antagonists in order to determine which one has the strongest influence on the RSC spatial encoding could help determine ibogaine's mechanism of action on cognitive processes. Thirdly, if psychedelics bias the RSC towards a more egocentric navigational system, would exposing the mice to an unfamiliar spatial learning task requiring flexible strategies impair the animals' performance beyond latency? The possibilities these questions create, along with the results presented in this thesis indicate that investigating the neural correlates of psychedelic drugs can be a powerful tool for shaping and testing our understanding of the neural system: "[…] these molecules can be used to probe the links between neurochemistry and neural computation across multiple layers of neuroanatomy and phenomenology" (Swanson, 2018).

5.10 REFERENCES

Alexander, A.S., Place, R., Starrett, M.J., Chrastil, E.R., and Nitz, D.A. (2023). Rethinking retrosplenial cortex: Perspectives and predictions. *Neuron* 111(2)**,** 150-175. doi: https://doi.org/10.1016/j.neuron.2022.11.006.

Andersen, K.A.A., Carhart-Harris, R., Nutt, D.J., and Erritzoe, D. (2021). Therapeutic effects of classic serotonergic psychedelics: A systematic review of modern-era clinical studies. *Acta Psychiatrica Scandinavica* 143(2)**,** 101-118. doi: https://doi.org/10.1111/acps.13249.

Arroyo-García, L.E., Tendilla-Beltrán, H., Vázquez-Roque, R.A., Jurado-Tapia, E.E., Díaz, A., Aguilar-Alonso, P., et al. (2020). Amphetamine sensitization alters hippocampal neuronal morphology and memory and learning behaviors. *Molecular Psychiatry*. doi: 10.1038/s41380-020-0809-2.

Atasoy, S., Roseman, L., Kaelen, M., Kringelbach, M.L., Deco, G., and Carhart-Harris, R.L. (2017). Connectome-harmonic decomposition of human brain activity reveals dynamical repertoire re-organization under LSD. *Scientific Reports* 7(1)**,** 17661. doi: 10.1038/s41598-017-17546-0.

Barnett, L., Muthukumaraswamy, S.D., Carhart-Harris, R.L., and Seth, A.K. (2020). Decreased directed functional connectivity in the psychedelic state. *NeuroImage* 209**,** 116462. doi: https://doi.org/10.1016/j.neuroimage.2019.116462.

Baumann, M.H., Rothman, R.B., Pablo, J.P., and Mash, D.C. (2001). In vivo neurobiological effects of ibogaine and its O-Desmethyl metabolite, 12-Hydroxyibogamine (noribogaine), in rats. *Journal of Pharmacology and Experimental Therapeutics* 297(2)**,** 531-539.

Beggs, J.M., and Plenz, D. (2003). Neuronal avalanches in neocortical circuits. *The Journal of Neuroscience* 23(35)**,** 11167. doi: 10.1523/JNEUROSCI.23-35-11167.2003.

Behrens, T.E.J., Muller, T.H., Whittington, J.C.R., Mark, S., Baram, A.B., Stachenfeld, K.L., et al. (2018). What is a cognitive map? Organizing knowledge for flexible behavior. *Neuron* 100(2)**,** 490-509. doi: https://doi.org/10.1016/j.neuron.2018.10.002.

Brys, I., Barrientos, S.A., Ward, J.E., Wallander, J., Petersson, P., and Halje, P. (2023). 5-HT2AR and NMDAR psychedelics induce similar hyper-synchronous states in the rat cognitive-limbic cortex-basal ganglia system. *Communications Biology* 6(1)**,** 737. doi: 10.1038/s42003-023-05093-6.

Calder, A.E., and Hasler, G. (2023). Towards an understanding of psychedelic-induced neuroplasticity. *Neuropsychopharmacology* 48(1)**,** 104-112. doi: 10.1038/s41386-022-01389-z.

Cameron, L.P., Tombari, R.J., Lu, J., Pell, A.J., Hurley, Z.Q., Ehinger, Y., et al. (2020). A non-hallucinogenic psychedelic analogue with therapeutic potential. *Nature*. doi: 10.1038/s41586-020-3008-z.

Carhart-Harris, R.L., Erritzoe, D., Williams, T., Stone, J.M., Reed, L.J., Colasanti, A., et al. (2012). Neural correlates of the psychedelic state as determined by fMRI studies with psilocybin. *Proceedings of the National Academy of Sciences* 109(6)**,** 2138-2143. doi: 10.1073/pnas.1119598109.

Carhart-Harris, R.L., and Friston, K.J. (2019). REBUS and the anarchic brain: Toward a unified model of the brain action of psychedelics. *Pharmacological Reviews* 71(3)**,** 316. doi: 10.1124/pr.118.017160.

Carhart-Harris, R.L., Muthukumaraswamy, S., Roseman, L., Kaelen, M., Droog, W., Murphy, K., et al. (2016). Neural correlates of the LSD experience revealed by multimodal neuroimaging. *Proceedings of the National Academy of Sciences* 113(17)**,** 4853-4858. doi: 10.1073/pnas.1518377113.

Catlow, B.J., Song, S., Paredes, D.A., Kirstein, C.L., and Sanchez-Ramos, J. (2013). Effects of psilocybin on hippocampal neurogenesis and extinction of trace fear conditioning. *Experimental Brain Research* 228(4)**,** 481-491. doi: 10.1007/s00221-013-3579-0.

Chang, H., Esteves, I.M., Neumann, A.R., Sun, J., Mohajerani, M.H., and McNaughton, B.L. (2020). Coordinated activities of retrosplenial ensembles during resting-state encode spatial landmarks. *Philosophical Transactions of the Royal Society B* 375(1799)**,** 20190228.

Chen, G., Wei, X., Xu, X., Yu, G., Yong, Z., Su, R., et al. (2021). Methamphetamine Inhibits long-term memory acquisition and synaptic plasticity by evoking endoplasmic reticulum stress. *Frontiers in Neuroscience* 14. doi: 10.3389/fnins.2020.630713.

Cho, J., and Sharp, P.E. (2001). Head direction, place, and movement correlates for cells in the rat retrosplenial cortex. *Behavioral neuroscience* 115(1)**,** 3.

Chrastil, E.R., Sherrill, K.R., Hasselmo, M.E., and Stern, C.E. (2015). There and back again: Hippocampus and retrosplenial cortex track homing distance during human path integration. *Journal of Neuroscience* 35(46)**,** 15442-15452.

Cooper, B.G., and Mizumori, S.J.Y. (1999). Retrosplenial cortex inactivation selectively impairs navigation in darkness. *NeuroReport* 10(3).

Crombag, H.S., Gorny, G., Li, Y., Kolb, B., and Robinson, T.E. (2005). Opposite effects of amphetamine self-administration experience on dendritic spines in the medial and orbital prefrontal cortex. *Cerebral Cortex* 15(3)**,** 341-348. doi: 10.1093/cercor/bhh136.

Dearnley, B., Jones, M., Dervinis, M., and Okun, M. (2023). Brain state transitions primarily impact the spontaneous rate of slow-firing neurons. *Cell Reports* 42(10).

Du, Y., Li, Y., Zhao, X., Yao, Y., Wang, B., Zhang, L., et al. (2023). Psilocybin facilitates fear extinction in mice by promoting hippocampal neuroplasticity. *Chinese Medical Journal***,** 10.1097.

Epstein, R.A., Patai, E.Z., Julian, J.B., and Spiers, H.J. (2017). The cognitive map in humans: Spatial navigation and beyond. *Nature Neuroscience* 20(11)**,** 1504-1513. doi: 10.1038/nn.4656.

Fadahunsi, N., Lund, J., Breum, A.W., Mathiesen, C.V., Larsen, I.B., Knudsen, G.M., et al. (2022). Acute and long-term effects of psilocybin on energy balance and feeding behavior in mice. *Translational Psychiatry* 12(1)**,** 330. doi: 10.1038/s41398-022-02103-9.

Fordahl, S.C., Locke, J.L., and Jones, S.R. (2016). High fat diet augments amphetamine sensitization in mice: Role of feeding pattern, obesity, and dopamine terminal changes. *Neuropharmacology* 109**,** 170-182. doi: https://doi.org/10.1016/j.neuropharm.2016.06.006.

Friston, K. (2010). The free-energy principle: a unified brain theory? *Nature Reviews Neuroscience* 11(2)**,** 127-138. doi: 10.1038/nrn2787.

Fukushiro, D.F., Mári-Kawamoto, E., Aramini, T.C.F., Saito, L.P., Costa, J.M., Josino, F.S., et al. (2011). Withdrawal from repeated treatment with amphetamine reduces novelty-seeking behavior and enhances environmental habituation in mice. *Pharmacology*

Biochemistry and Behavior 100(1), 180-184. doi: https://doi.org/10.1016/j.pbb.2011.08.015.
Gable, R.S. (2004). Comparison of acute lethal toxicity of commonly abused psychoactive substances. *Addiction* 99(6), 686-696. doi: https://doi.org/10.1111/j.1360-0443.2004.00744.x.
Gassaway, M.M., Jacques, T.L., Kruegel, A.C., Karpowicz, R.J., Li, X., Li, S., et al. (2016). Deconstructing the iboga alkaloid skeleton: Potentiation of FGF2-induced glial cell line-derived neurotrophic factor release by a novel compound. *ACS Chemical Biology* 11(1), 77-87. doi: 10.1021/acschembio.5b00678.
Ghitza, U.E., Zhai, H., Wu, P., Airavaara, M., Shaham, Y., and Lu, L. (2010). Role of BDNF and GDNF in drug reward and relapse: A review. *Neuroscience & Biobehavioral Reviews* 35(2), 157-171. doi: https://doi.org/10.1016/j.neubiorev.2009.11.009.
Gilbert, C.D., and Sigman, M. (2007). Brain states: Top-down influences in sensory processing. *Neuron* 54(5), 677-696. doi: https://doi.org/10.1016/j.neuron.2007.05.019.
Girn, M., Roseman, L., Bernhardt, B., Smallwood, J., Carhart-Harris, R., and Nathan Spreng, R. (2022). Serotonergic psychedelic drugs LSD and psilocybin reduce the hierarchical differentiation of unimodal and transmodal cortex. *NeuroImage* 256, 119220. doi: https://doi.org/10.1016/j.neuroimage.2022.119220.
Glick, S.D., Maisonneuve, I.M., and Szumlinski, K.K. (2000). 18-Methoxycoronaridine (18-MC) and Ibogaine: Comparison of antiaddictive efficacy, toxicity, and mechanisms of action. *Annals of the New York Academy of Sciences* 914(1), 369-386.
Glick, S.D., Rossman, K., Steindorf, S., Maisonneuve, I.M., and Carlson, J.N. (1991). Effects and aftereffects of ibogaine on morphine self-administration in rats. *European Journal of Pharmacology* 195(3), 341-345. doi: https://doi.org/10.1016/0014-2999(91)90474-5.
Gobbo, F., Mitchell-Heggs, R., Tse, D., Al Omrani, M., Spooner, P.A., Schultz, S.R., et al. (2022). Neuronal signature of spatial decision-making during navigation by freely moving rats by using calcium imaging. *Proceedings of the National Academy of Sciences* 119(44), e2212152119. doi: doi:10.1073/pnas.2212152119.
Golden, C.T., and Chadderton, P. (2022). Psilocybin reduces low frequency oscillatory power and neuronal phase-locking in the anterior cingulate cortex of awake rodents. *Scientific Reports* 12(1), 12702. doi: 10.1038/s41598-022-16325-w.
Gulley, J.M., and Stanis, J.J. (2010). Adaptations in medial prefrontal cortex function associated with amphetamine-induced behavioral sensitization. *Neuroscience* 166(2), 615-624. doi: https://doi.org/10.1016/j.neuroscience.2009.12.044.
Halberstadt, A.L., Koedood, L., Powell, S.B., and Geyer, M.A. (2011). Differential contributions of serotonin receptors to the behavioral effects of indoleamine hallucinogens in mice. *Journal of psychopharmacology* 25(11), 1548-1561.
Hashemnia, S., Euston, D.R., and Gruber, A.J. (2020). Amphetamine reduces reward encoding and stabilizes neural dynamics in rat anterior cingulate cortex. *eLife* 9, e56755. doi: 10.7554/eLife.56755.
He, D.-Y., McGough, N.N.H., Ravindranathan, A., Jeanblanc, J., Logrip, M.L., Phamluong, K., et al. (2005). Glial cell line-derived neurotrophic factor mediates the desirable actions of the anti-addiction drug ibogaine against alcohol consumption. *The Journal of Neuroscience* 25(3), 619. doi: 10.1523/JNEUROSCI.3959-04.2005.

Helsley, S., Dlugos, C.A., Pentney, R.J., Rabin, R.A., and Winter, J.C. (1997). Effects of chronic ibogaine treatment on cerebellar Purkinje cells in the rat. *Brain Research* 759(2)**,** 306-308. doi: https://doi.org/10.1016/S0006-8993(97)00365-X.

Hindley, E.L., Nelson, A.J.D., Aggleton, J.P., and Vann, S.D. (2014). The rat retrosplenial cortex is required when visual cues are used flexibly to determine location. *Behavioural Brain Research* 263**,** 98-107. doi: https://doi.org/10.1016/j.bbr.2014.01.028.

Holmes, S.E., Scheinost, D., Finnema, S.J., Naganawa, M., Davis, M.T., DellaGioia, N., et al. (2019). Lower synaptic density is associated with depression severity and network alterations. *Nature Communications* 10(1)**,** 1529. doi: 10.1038/s41467-019-09562-7.

Iaria, G., Chen, J.-K., Guariglia, C., Ptito, A., and Petrides, M. (2007). Retrosplenial and hippocampal brain regions in human navigation: Complementary functional contributions to the formation and use of cognitive maps. *European Journal of Neuroscience* 25(3)**,** 890-899. doi: https://doi.org/10.1111/j.1460-9568.2007.05371.x.

Iorgu, A.-M., Vasilescu, A.-N., Pfeiffer, N., Spanagel, R., Mallien, A.S., Inta, D., et al. (2023). Psilocybin does not induce the vulnerability marker HSP70 in neurons susceptible to Olney's lesions. *European Archives of Psychiatry and Clinical Neuroscience*. doi: 10.1007/s00406-023-01699-3.

Jefsen, O.H., Elfving, B., Wegener, G., and Müller, H.K. (2021). Transcriptional regulation in the rat prefrontal cortex and hippocampus after a single administration of psilocybin. *Journal of Psychopharmacology* 35(4)**,** 483-493. doi: 10.1177/0269881120959614.

Karege, F., Perret, G., Bondolfi, G., Schwald, M., Bertschy, G., and Aubry, J.-M. (2002). Decreased serum brain-derived neurotrophic factor levels in major depressed patients. *Psychiatry Research* 109(2)**,** 143-148. doi: https://doi.org/10.1016/S0165-1781(02)00005-7.

Kiang, M., Farzan, F., Blumberger, D.M., Kutas, M., McKinnon, M.C., Kansal, V., et al. (2017). Abnormal self-schema in semantic memory in major depressive disorder: Evidence from event-related brain potentials. *Biological Psychology* 126**,** 41-47. doi: https://doi.org/10.1016/j.biopsycho.2017.04.003.

Koob, G.F., and Le Moal, M. (2001). Drug addiction, dysregulation of reward, and allostasis. *Neuropsychopharmacology* 24(2)**,** 97-129.

Koskela, M., Bäck, S., Võikar, V., Richie, C.T., Domanskyi, A., Harvey, B.K., et al. (2017). Update of neurotrophic factors in neurobiology of addiction and future directions. *Neurobiology of Disease* 97**,** 189-200. doi: https://doi.org/10.1016/j.nbd.2016.05.010.

Lebedev, A.V., Kaelen, M., Lövdén, M., Nilsson, J., Feilding, A., Nutt, D.J., et al. (2016). LSD-induced entropic brain activity predicts subsequent personality change. *Human Brain Mapping* 37(9)**,** 3203-3213. doi: https://doi.org/10.1002/hbm.23234.

Li, Y., Kolb, B., and Robinson, T.E. (2003). The location of persistent amphetamine-induced changes in the density of dendritic spines on medium spiny neurons in the nucleus accumbens and caudate-putamen. *Neuropsychopharmacology* 28(6)**,** 1082-1085. doi: 10.1038/sj.npp.1300115.

Lima da Cruz, R.V., Moulin, T.C., Petiz, L.L., and Leão, R.N. (2018). A single dose of 5-MeO-DMT stimulates cell proliferation, neuronal survivability, morphological and functional changes in adult mice ventral dentate gyrus. *Frontiers in Molecular Neuroscience* 11(312). doi: 10.3389/fnmol.2018.00312.

Liu, W., Ge, T., Leng, Y., Pan, Z., Fan, J., Yang, W., et al. (2017). The role of neural plasticity in depression: from hippocampus to prefrontal cortex. *Neural Plasticity* 2017**,** 6871089. doi: 10.1155/2017/6871089.

Lladó-Pelfort, L., Celada, P., Riga, M.S., Troyano-Rodríguez, E., Santana, N., and Artigas, F. (2018). Effects of hallucinogens on neuronal activity. *Behavioral Neurobiology of Psychedelic Drugs,* eds. A.L. Halberstadt, F.X. Vollenweider & D.E. Nichols. (Berlin, Heidelberg: Springer Berlin Heidelberg), 75-105.

Ly, C., Greb, A.C., Cameron, L.P., Wong, J.M., Barragan, E.V., Wilson, P.C., et al. (2018). Psychedelics promote structural and functional neural plasticity. *Cell Reports* 23(11)**,** 3170-3182. doi: https://doi.org/10.1016/j.celrep.2018.05.022.

Mandillo, S., Rinaldi, A., Oliverio, A., and Mele, A. (2003). Repeated administration of phencyclidine, amphetamine and MK-801 selectively impairs spatial learning in mice: a possible model of psychotomimetic drug-induced cognitive deficits. *Behavioural Pharmacology* 14(7).

Mao, D., Molina, L.A., Bonin, V., and McNaughton, B.L. (2020). Vision and locomotion combine to drive path integration sequences in mouse retrosplenial cortex. *Current Biology* 30(9)**,** 1680-1688.e1684. doi: https://doi.org/10.1016/j.cub.2020.02.070.

Marton, S., González, B., Rodríguez-Bottero, S., Miquel, E., Martínez-Palma, L., Pazos, M., et al. (2019). Ibogaine administration modifies GDNF and BDNF expression in brain regions involved in mesocorticolimbic and nigral dopaminergic circuits. *Frontiers in Pharmacology* 10(193). doi: 10.3389/fphar.2019.00193.

Mash, D.C., Kovera, C.A., Pablo, J., Tyndale, R.F., Ervin, F.D., Williams, I.C., et al. (2000). Ibogaine: Complex Pharmacokinetics, concerns for safety, and preliminary efficacy measures. *Annals of the New York Academy of Sciences* 914(1)**,** 394-401. doi: https://doi.org/10.1111/j.1749-6632.2000.tb05213.x.

McDonald, R.J., Hong, N.S., Atwood, A., Tyndall, A.V., and Kolb, B. (2021). An assessment of the functional effects of amphetamine-induced dendritic changes in the nucleus accumbens, medial prefrontal cortex, and hippocampus on different types of learning and memory function. *Neurobiology of Learning and Memory* 180**,** 107408. doi: https://doi.org/10.1016/j.nlm.2021.107408.

McDonald, R.J., Hong, N.S., Germaine, C., and Kolb, B. (2023). Peripherally-administered amphetamine induces plasticity in medial prefrontal cortex and nucleus accumbens in rats with amygdala lesions: implications for neural models of memory modulation. *Frontiers in Behavioral Neuroscience* 17. doi: 10.3389/fnbeh.2023.1187976.

Michaiel, A.M., Parker, P.R.L., and Niell, C.M. (2019). A hallucinogenic Serotonin-2A receptor agonist reduces visual response gain and alters temporal dynamics in mouse V1. *Cell Reports* 26(13)**,** 3475-3483.e3474. doi: https://doi.org/10.1016/j.celrep.2019.02.104.

Moldavan, M., Solomko, E.F., Grodzinskaya, A.A., Storozhuk, V.M., and Lomberg, M.L. (2000). Neurotropic effect of extracts from the hallucinogenic mushroom Psilocybe cubensis (Earle) Sing.(Agaricomycetideae). In vitro studies. *International Journal of Medicinal Mushrooms* 2(4).

Molinari, H.H., Maisonneuve, I.M., and Glick, S.D. (1996). Ibogaine neurotoxicity: A re-evaluation. *Brain Research* 737(1)**,** 255-262. doi: https://doi.org/10.1016/0006-8993(96)00739-1.

Muthukumaraswamy, S.D., Carhart-Harris, R.L., Moran, R.J., Brookes, M.J., Williams, T.M., Errtizoe, D., et al. (2013). Broadband cortical desynchronization underlies the human

psychedelic state. *The Journal of Neuroscience* 33(38)**,** 15171-15183. doi: 10.1523/jneurosci.2063-13.2013.
Nelson, A., and Killcross, S. (2006). Amphetamine exposure enhances habit formation. *Journal of Neuroscience* 26(14)**,** 3805-3812.
Nordquist, R.E., Voorn, P., de Mooij-van Malsen, J.G., Joosten, R.N.J.M.A., Pennartz, C.M.A., and Vanderschuren, L.J.M.J. (2007). Augmented reinforcer value and accelerated habit formation after repeated amphetamine treatment. *European Neuropsychopharmacology* 17(8)**,** 532-540. doi: https://doi.org/10.1016/j.euroneuro.2006.12.005.
North, A., Swant, J., Salvatore, M.F., Gamble-George, J., Prins, P., Butler, B., et al. (2013). Chronic methamphetamine exposure produces a delayed, long-lasting memory deficit. *Synapse* 67(5)**,** 245-257. doi: https://doi.org/10.1002/syn.21635.
O'Hearn, E., and Molliver, M.E. (1993). Degeneration of purkinje cells in parasagittal zones of the cerebellar vermis after treatment with ibogaine or harmaline. *Neuroscience* 55(2)**,** 303-310. doi: https://doi.org/10.1016/0306-4522(93)90500-F.
O'Keefe, J., and Nadel, L. (1978). *The Hippocampus as a Cognitive Map.* Oxford: Clarendon Press.
Palhano-Fontes, F., Andrade, K.C., Tofoli, L.F., Santos, A.C., Crippa, J.A.S., Hallak, J.E.C., et al. (2015). The psychedelic state induced by ayahuasca modulates the activity and connectivity of the default mode network. *PloS one* 10(2)**,** e0118143-e0118143. doi: 10.1371/journal.pone.0118143.
Palhano-Fontes, F., Barreto, D., Onias, H., Andrade, K.C., Novaes, M.M., Pessoa, J.A., et al. (2019). Rapid antidepressant effects of the psychedelic ayahuasca in treatment-resistant depression: A randomized placebo-controlled trial. *Psychological Medicine* 49(4)**,** 655-663. doi: 10.1017/S0033291718001356.
Patai, E.Z., and Spiers, H.J. (2021). The versatile wayfinder: Prefrontal contributions to spatial navigation. *Trends in Cognitive Sciences* 25(6)**,** 520-533. doi: 10.1016/j.tics.2021.02.010.
Paulson, P.E., and Robinson, T.E. (1995). Amphetamine-induced time-dependent sensitization of dopamine neurotransmission in the dorsal and ventral striatum: a microdialysis study in behaving rats. *Synapse* 19(1)**,** 56-65. doi: 10.1002/syn.890190108.
Pink-Hashkes, S., van Rooij, I., and Kwisthout, J. (2017). "Perception is in the details: A predictive coding account of the psychedelic phenomenon", in: *CogSci*.
Pryazhnikov, E., Mugantseva, E., Casarotto, P., Kolikova, J., Fred, S.M., Toptunov, D., et al. (2018). Longitudinal two-photon imaging in somatosensory cortex of behaving mice reveals dendritic spine formation enhancement by subchronic administration of low-dose ketamine. *Scientific Reports* 8(1)**,** 6464. doi: 10.1038/s41598-018-24933-8.
Rangel-Barajas, C., Estrada-Sánchez, A.M., Barton, S.J., Luedtke, R.R., and Rebec, G.V. (2017). Dysregulated corticostriatal activity in open-field behavior and the head-twitch response induced by the hallucinogen 2,5-dimethoxy-4-iodoamphetamine. *Neuropharmacology* 113**,** 502-510. doi: https://doi.org/10.1016/j.neuropharm.2016.11.001.
Robinson, T.E., and Kolb, B. (1999). Alterations in the morphology of dendrites and dendritic spines in the nucleus accumbens and prefrontal cortex following repeated treatment with amphetamine or cocaine. *European Journal of Neuroscience* 11(5)**,** 1598-1604. doi: https://doi.org/10.1046/j.1460-9568.1999.00576.x.
Rodríguez, P., Urbanavicius, J., Prieto, J.P., Fabius, S., Reyes, A.L., Havel, V., et al. (2020). A single administration of the atypical psychedelic ibogaine or its metabolite noribogaine

induces an antidepressant-like effect in rats. *ACS Chemical Neuroscience* 11(11)**,** 1661-1672. doi: 10.1021/acschemneuro.0c00152.
Sakashita, Y., Abe, K., Katagiri, N., Kambe, T., Saitoh, T., Utsunomiya, I., et al. (2015). Effect of psilocin on extracellular dopamine and serotonin levels in the mesoaccumbens and mesocortical pathway in awake rats. *Biological and Pharmaceutical Bulletin* 38(1)**,** 134-138.
Schep, L.J., Slaughter, R.J., Galea, S., and Newcombe, D. (2016). Ibogaine for treating drug dependence. What is a safe dose? *Drug and Alcohol Dependence* 166**,** 1-5. doi: https://doi.org/10.1016/j.drugalcdep.2016.07.005.
Sershen, H., Hashim, A., Harsing, L., and Lajtha, A. (1992). Ibogaine antagonizes cocaine-induced locomotor stimulation in mice. *Life Sciences* 50(15)**,** 1079-1086. doi: https://doi.org/10.1016/0024-3205(92)90344-O.
Sershen, H., Hashim, A., and Lajtha, A. (1994). Ibogaine reduces preference for cocaine consumption in C57BL/6By mice. *Pharmacology Biochemistry and Behavior* 47(1)**,** 13-19. doi: https://doi.org/10.1016/0091-3057(94)90105-8.
Shao, L.-X., Liao, C., Gregg, I., Davoudian, P.A., Savalia, N.K., Delagarza, K., et al. (2021). Psilocybin induces rapid and persistent growth of dendritic spines in frontal cortex in vivo. *Neuron* 109(16)**,** 2535-2544.e2534. doi: https://doi.org/10.1016/j.neuron.2021.06.008.
Sharp, F., Butman, M., Wang, S., Koistinaho, J., Graham, S., Sagar, S., et al. (1992). Haloperidol prevents induction of the HSP70 heat shock gene in neurons injured by phencyclidine (PCP), MK801, and ketamine. *Journal of Neuroscience Research* 33(4)**,** 605-616.
Sherrill, K.R., Erdem, U.M., Ross, R.S., Brown, T.I., Hasselmo, M.E., and Stern, C.E. (2013). Hippocampus and retrosplenial cortex combine path integration signals for successful navigation. *The Journal of Neuroscience* 33(49)**,** 19304. doi: 10.1523/JNEUROSCI.1825-13.2013.
Suzuki, Y., Jodo, E., Takeuchi, S., Niwa, S., and Kayama, Y. (2002). Acute administration of phencyclidine induces tonic activation of medial prefrontal cortex neurons in freely moving rats. *Neuroscience* 114(3)**,** 769-779. doi: https://doi.org/10.1016/S0306-4522(02)00298-1.
Swanson, L.R. (2018). Unifying theories of psychedelic drug effects. *Frontiers in Pharmacology* 9**,** 172.
Tagliazucchi, E., Carhart-Harris, R., Leech, R., Nutt, D., and Chialvo, D.R. (2014). Enhanced repertoire of brain dynamical states during the psychedelic experience. *Human Brain Mapping* 35(11)**,** 5442-5456. doi: 10.1002/hbm.22562.
Takahashi, N., Kawamura, M., Shiota, J., Kasahata, N., and Hirayama, K. (1997). Pure topographic disorientation due to right retrosplenial lesion. *Neurology* 49(2)**,** 464-469.
Tian, Z., Dong, C., Fujita, A., Fujita, Y., and Hashimoto, K. (2018). Expression of heat shock protein HSP-70 in the retrosplenial cortex of rat brain after administration of (R,S)-ketamine and (S)-ketamine, but not (R)-ketamine. *Pharmacology Biochemistry and Behavior* 172**,** 17-21. doi: https://doi.org/10.1016/j.pbb.2018.07.003.
Tolman, E.C. (1948). Cognitive maps in rats and men. *Psychological Review* 55(4)**,** 189-208. doi: 10.1037/h0061626.
Treccani, G., Ardalan, M., Chen, F., Musazzi, L., Popoli, M., Wegener, G., et al. (2019). S-Ketamine reverses hippocampal dendritic spine deficits in Flinders sensitive line rats

within 1 h of administration. *Molecular Neurobiology* 56(11), 7368-7379. doi: 10.1007/s12035-019-1613-3.
Tylš, F., Páleníček, T., Kadeřábek, L., Lipski, M., Kubešová, A., and Horáček, J. (2016). Sex differences and serotonergic mechanisms in the behavioural effects of psilocin. *Behavioural Pharmacology* 27(4), 309-320.
Ubl, B., Kuehner, C., Kirsch, P., Ruttorf, M., Diener, C., and Flor, H. (2015). Altered neural reward and loss processing and prediction error signalling in depression. *Social Cognitive and Affective Neuroscience* 10(8), 1102-1112. doi: 10.1093/scan/nsu158.
van Groen, T., and Wyss, J.M. (1992). Connections of the retrosplenial dysgranular cortex in the rat. *Journal of Comparative Neurology* 315(2), 200-216. doi: https://doi.org/10.1002/cne.903150207.
van Groen, T., and Wyss, J.M. (2003). Connections of the retrosplenial granular b cortex in the rat. *Journal of Comparative Neurology* 463(3), 249-263. doi: https://doi.org/10.1002/cne.10757.
Varley, T.F., Carhart-Harris, R., Roseman, L., Menon, D.K., and Stamatakis, E.A. (2020). Serotonergic psychedelics LSD & psilocybin increase the fractal dimension of cortical brain activity in spatial and temporal domains. *NeuroImage* 220, 117049. doi: https://doi.org/10.1016/j.neuroimage.2020.117049.
Vinh, N.X., Epps, J., and Bailey, J. (2010). Information theoretic measures for clusterings comparison: Variants, properties, normalization and correction for chance. *The Journal of Machine Learning Research* 11, 2837-2854.
Wacongne, C., Labyt, E., van Wassenhove, V., Bekinschtein, T., Naccache, L., and Dehaene, S. (2011). Evidence for a hierarchy of predictions and prediction errors in human cortex. *Proceedings of the National Academy of Sciences* 108(51), 20754. doi: 10.1073/pnas.1117807108.
Wilson, M.A., and McNaughton, B.L. (1993). Dynamics of the hippocampal ensemble code for space. *Science* 261(5124), 1055. doi: 10.1126/science.8351520.
Wojtas, A., Bysiek, A., Wawrzczak-Bargiela, A., Szych, Z., Majcher-Maślanka, I., Herian, M., et al. 2022. Effect of psilocybin and ketamine on brain neurotransmitters, glutamate receptors, DNA and rat behavior. *International Journal of Molecular Sciences* [Online], 23(12).
Wolbers, T., and Büchel, C. (2005). Dissociable retrosplenial and hippocampal contributions to successful formation of survey representations. *Journal of Neuroscience* 25(13), 3333-3340.
Wolbers, T., Wiener, J.M., Mallot, H.A., and Büchel, C. (2007). Differential recruitment of the hippocampus, medial prefrontal cortex, and the human motion complex during path integration in humans. *Journal of Neuroscience* 27(35), 9408-9416.
Wong, S.A., Thapa, R., Badenhorst, C.A., Briggs, A.R., Sawada, J.A., and Gruber, A.J. (2016). Opposing effects of acute and chronic d-amphetamine on decision-making in rats. *Neuroscience*. doi: http://dx.doi.org/10.1016/j.neuroscience.2016.04.021.
Wood, J., Kim, Y., and Moghaddam, B. (2012). Disruption of prefrontal cortex large scale neuronal activity by different classes of psychotomimetic drugs. *The Journal of Neuroscience* 32(9), 3022-3031. doi: 10.1523/jneurosci.6377-11.2012.
Yates, J.W., Meij, J.T.A., Sullivan, J.R., Richtand, N.M., and Yu, L. (2007). Bimodal effect of amphetamine on motor behaviors in C57BL/6 mice. *Neuroscience Letters* 427(1), 66-70. doi: https://doi.org/10.1016/j.neulet.2007.09.011.

Yu, J.Y., Liu, D.F., Loback, A., Grossrubatscher, I., and Frank, L.M. (2018). Specific hippocampal representations are linked to generalized cortical representations in memory. *Nature Communications* 9(1)**,** 2209. doi: 10.1038/s41467-018-04498-w.

Zeifman, R.J., Wagner, A.C., Watts, R., Kettner, H., Mertens, L.J., and Carhart-Harris, R.L. (2020). Post-psychedelic reductions in experiential avoidance are associated with decreases in depression severity and suicidal ideation. *Frontiers in Psychiatry* 11(782). doi: 10.3389/fpsyt.2020.00782.

Zhang, G., Cinalli, D., and Stackman Jr, R.W. (2017). Effect of a hallucinogenic serotonin 5-HT2A receptor agonist on visually guided, hippocampal-dependent spatial cognition in C57BL/6J mice. *Hippocampus* 27(5)**,** 558-569. doi: https://doi.org/10.1002/hipo.22712.

Zhang, J., Qu, Y., Chang, L., Pu, Y., and Hashimoto, K. (2019). (R)-Ketamine rapidly ameliorates the decreased spine density in the medial prefrontal cortex and hippocampus of susceptible mice after chronic social defeat stress. *International Journal of Neuropsychopharmacology* 22(10)**,** 675-679. doi: 10.1093/ijnp/pyz048.

Zhuk, O., Jasicka-Misiak, I., Poliwoda, A., Kazakova, A., Godovan, V.V., Halama, M., et al. (2015). Research on acute toxicity and the behavioral effects of methanolic extract from psilocybin mushrooms and psilocin in mice. *Toxins* 7(4)**,** 1018-1029.

5.11 SUPPLEMENTARY INFORMATION

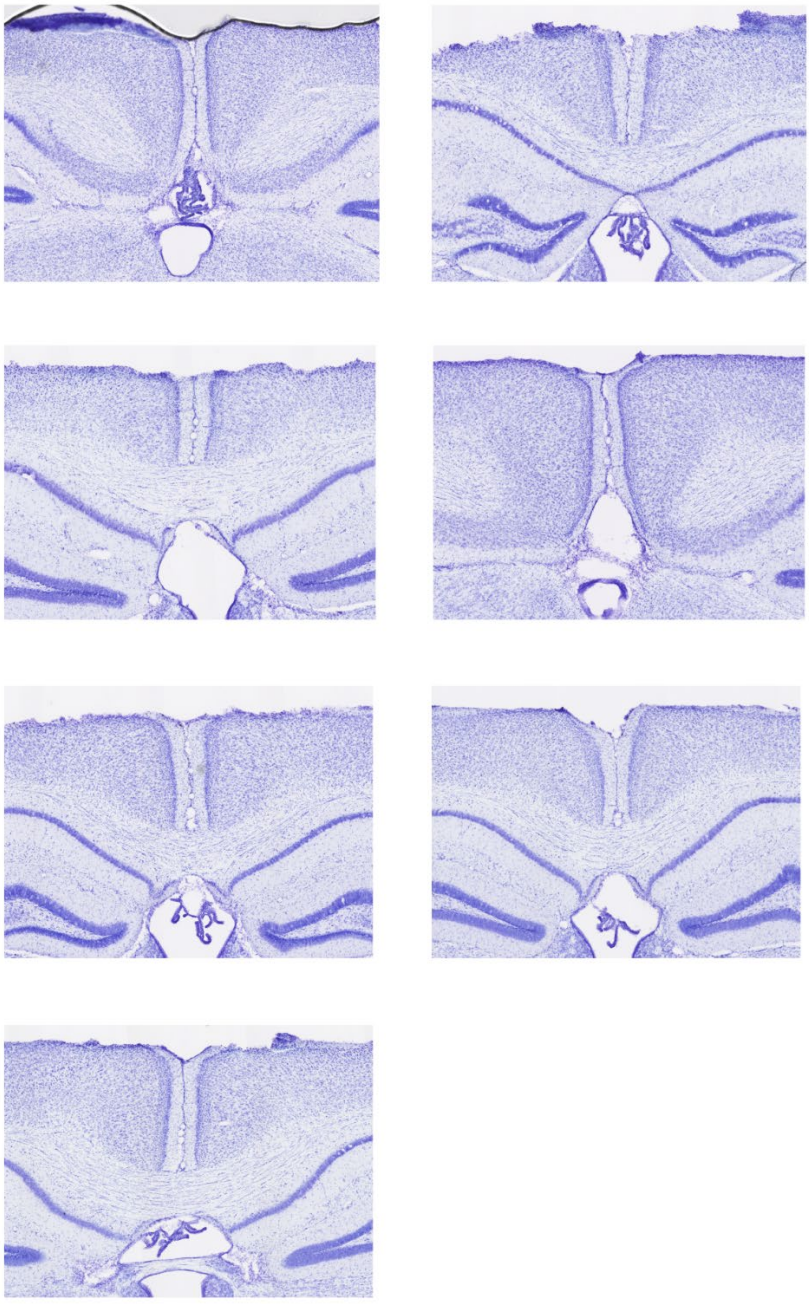

Supplemental Fig. 5.2: Coronal sections of the RSC of animals treated with psilocybin. Each panel is representative of one of the 7 animals in the psilocybin group. Sections range from -1.5 to -2.8 AP.

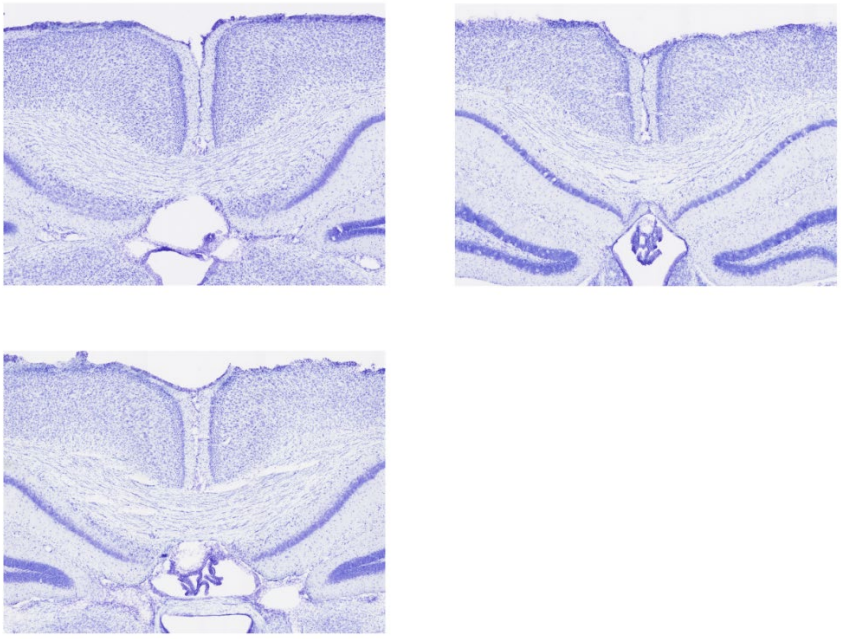

Supplemental Fig. 5.3: Coronal sections of the RSC of animals treated with saline. Each panel is representative of one of the 3 animals in the control group. Sections range from -1.7 to -2.4 AP.